Authors In This Issue

R. P. Heuer (p. 824). From the University of Pennsylvania he received degrees of B. S., Ch. E. and Ph.D., after which he joined the U. S. Bureau of Mines as chemical engineer. He has worked as metallurgist for the Chase Metal Works; as instructor in chemistry at his alma mater; and is now vice-president in charge of research at the General Refractories Co., Philadelphia, living at Bryn Mawr. He is an AIME member.

M. A. Fay (p. 824). After graduating from Pennsylvania State College with a B.S. in Ceramics, he joined the staff of the Bethlehem Steel Co. as research engineer, and from 1943 for three years he worked at the Sparrows Point plant as ceramic engineer. In 1946 he became ceramic engineer for the General Refractories Co. at Philadelphia and now lives in Penn Valley. He is an AIME member and presented a paper: "Mechanism of Wear of Open Hearth, Silica Brick Roofs."

S. Epstein (p. 830), research engineer at Bethlehem Steel Co., Bethlehem, Pa., received a B.S. in Chemistry in 1918 from the City College of New York, after which he joined the Bureau of Standards staff for 11 years. For another 11 years he was associated with the Illinois Steel Co. In 1930 he went to Battelle Memorial Institute and since 1936 has been with Bethlehem Steel. He is an AIME member and enjoys golf.

J. W. Frame (p. 830), after getting his B.S. in Metallurgical Engineering from Missouri School of Mines and Metallurgy, and his M.S. from Lehigh, joined Bethlehem Steel Co. in 1938 as assistant metallurgist at Lackawanna. In 1946, he became research engineer for Bethlehem Steel Co., at Bethlehem. Prior to graduation, he worked summers for Carnegie-Illinois Steel Corp., in Duquesne and South Works. An AIME member, this is his first attempt as far as papers for AIME is concerned.

A. E. Reinhard (p. 835), a Hoosier, attended Wiley High School at Terre Haute and the Rose Polytechnic Institute from which he received a B.S. in Mechanical Engineering. His career includes service in the mechanical and electrical dept. of the Wheeling Steel Corp., after which he became superintendent of the open hearth and bessemer dept. of the Youngstown Sheet & Tube Co. He is now superintendent of steel production of the Great Lakes Corp., Detroit, where he lives. He is an AIME member, a devotee of Isaac Walton, and enjoys golf and baseball.

W. G. McDonough (p. 838) is a native of Homestead, Pa., and spent his entire working career with the National Tube Co., with the exception of two years at the Aliquippa Plant of the Jones & Laughlin Steel Corp., and the Indiana Harbor plant of the Youngstown Sheet & Tube Co. He is now superintendent of the Open Hearth and Bessemer Dept., National Tube Co., at McKeesport, Pa., where he also resides. He reports no particular hobby, enjoying golf, fishing, swimming, bowling, motoring, and church activities.

Francis B. Foley (p. 845) came from Germantown, near Philadelphia, and attended Girard

R. P. Heuer

M. A. Fay

S. Epstein

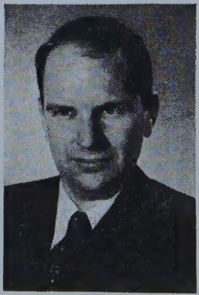

J. W. Frame

Journal of METALS

Published to provide a continuing, authoritative, and up-to-date record of technologic, engineering, and economic progress in all branches of the metals industry by the

Metals Branch
American Institute of Mining and Metallurgical Engineers, Inc.
29 West 39th Street, New York 18

o o o

THOMAS E. LLOYD
Manager of Publications
Editor, Journal of Metals

o o o

JAMES A. STANGARONE
Advertising Manager

o o o

HAROLD N. UNDERHILL, DOROTHY G. GARRETT, MARGARET BAGG, RUTH L. GARRETT, ***Assistant Editors;*** **GRACE PUGSLEY,** ***Production Manager;*** **WALTER J. SEWING,** ***Assistant.***

o o o

OFFICERS, AIME

D. H. McLaughlin — *President*
A. B. Kinzel — *Vice President*
Philip Kraft — *Vice President*
R. W. Thomas — *Vice President*
C. H. Benedict — *Vice President*
C. V. Millikan — *Vice President*
Andrew Fletcher — *VP & Treasurer*

o o o

AIME STAFF

E. H. Robie — *Secretary*
H. A. Maloney — *Asst. Treasurer*
E. J. Kennedy, Jr. — *Asst. Secretary*
Ernest Kirkendall — *Asst. Secretary*
H. Newell Appleton — *Asst. to Secretary*

o o o

Technical Publications Committee

F. B. Foley — *Chairman*
E. J. Kennedy, Jr. — *Secretary*

o o o

Auxiliary Publications Committee

O. B. J. Fraser — *Chairman, IMD*
Michael Tenenbaum — *Chairman, ISD*
Philip T. Stroup — *Chairman, EMD*

o o o

Publications Advisory Committee

J. B. Austin, F. N. Rhines, C. D. King, John D. Sullivan, Fred P. Peters, A. W. Schlechten, Frank T. Sisco, M. Tenenbaum, Felix Wormser

o o o

The AIME Publishes:
Mining Engineering
Journal of Metals
Journal of Petroleum Technology

VOL. 188, NO. 6 JUNE, 1950

COVER

The latest development in gold plate bonding is this special protective atmosphere press-type bonding furnace. Assembled ingots, of base metal between two layers of gold, are pressed while being heated and then repressed in the cooling chamber by hydraulic presses built into the furnace. This unique furnace is in use at Metals & Controls Corp., General Plate Div., Attleboro, Mass.

FEATURES

Authors in This Issue 802
Engineering Employment Service 806
Journal of Metals REPORTER 811
It's Everyone's Business 812
Drift of Things 814

NEWS

Directors' Meeting 815
Section Activities 817
Coming Events 818
Personals 819
Membership 821
Manufacturers' News 822

TECHNICAL ARTICLES

The All-Basic Openhearth — R. P. Heuer, M. A. Fay 824
Vanadium Treated Deep Drawing Quality Steel — S. Epstein, H. J. Cutler, J. W. Frame 830
Oxygen Jets Through the Open Hearth Backwall — A. E. Reinhard 835
Setting Ladle Nozzles — W. G. McDonough 838
Aluminum Foil-Luminate Gasket 839
Clay Graphite Brick for Ladle Linings — E. B. Snyder 840
New Mold Coatings — J. J. Golden 842
1949 Ore Imports at Record High 844

TRANSACTIONS

Factors Affecting Deformation and Rupture of Metals at Elevated Temperatures — F. B. Foley 845
Oxygen in Liquid Open Hearth Steel Oxidation During Tapping and Ladle Filling — T. E. Brower, J. W. Bain, B. M. Larsen 851
Thermodynamic Relationships in Chlorine Metallurgy — H. H. Kellogg 862
A Survey of Thermodynamics of Copper Smelting — R. Schuhmann, Jr. 873
Activation Energy for Recrystallization in Rolled Copper — B. F. Decker, D. Harker 887

TECHNICAL NOTE

Thermal Segregation: A Mechanism for the Segregation of Hydrogen in Steel — G. Derge, E. E. Duncan 884
Twin Relationships in Ingot of Germanium — W. C. Ellis 886
Metallographic Re-evaluation of the Indium-Zinc Eutectic Composition — S. C. Carapella, E. A. Peretti 890
Slip Markings in Chromium — E. S. Greiner 891

Published the first day of each month by the American Institute of Mining and Metallurgical Engineers, Inc., 29 West 39th Street, New York 18, N. Y. Telephone: PEnnsylvania 6-9220. Subscription $8 per year for non-AIME members in United States and North, South and Central America; $9, foreign; $6 for AIME members, or $4 in combination with a subscription to *Mining Engineering* or the *Journal of Petroleum Technology*. Single copies, 75 cents; special issues, $1.50 . . . The AIME is not responsible for any statement made or opinion expressed in its publications. . . . Copyright 1950 by the American Institute of Mining and Metallurgical Engineers, Inc. . . . Registered cable address, AIME New York . . . Indexed in Engineering Index, Industrial Arts Index and Chemical Abstracts . . . Reentered as second-class matter Sept. 21, 1949, at the post office at New York, N.Y., under the Act of March 3, 1879.

Authors In This Issue

R. P. Heuer (p. 824). From the University of Pennsylvania he received degrees of B. S., Ch. E. and Ph.D., after which he joined the U. S. Bureau of Mines as chemical engineer. He has worked as metallurgist for the Chase Metal Works; as instructor in chemistry at his alma mater; and is now vice-president in charge of research at the General Refractories Co., Philadelphia, living at Bryn Mawr. He is an AIME member.

R. P. Heuer

M. A. Fay (p. 824). After graduating from Pennsylvania State College with a B.S. in Ceramics, he joined the staff of the Bethlehem Steel Co. as research engineer, and from 1943 for three years he worked at the Sparrows Point plant as ceramic engineer. In 1946 he became ceramic engineer for the General Refractories Co. at Philadelphia and now lives in Penn Valley. He is an AIME member and presented a paper: "Mechanism of Wear of Open Hearth, Silica Brick Roofs."

M. A. Fay

S. Epstein (p. 830), research engineer at Bethlehem Steel Co., Bethlehem, Pa., received a B.S. in Chemistry in 1918 from the City College of New York, after which he joined the Bureau of Standards staff for 11 years. For another 11 years he was associated with the Illinois Steel Co. In 1930 he went to Battelle Memorial Institute and since 1936 has been with Bethlehem Steel. He is an AIME member and enjoys golf.

S. Epstein

J. W. Frame (p. 830), after getting his B.S. in Metallurgical Engineering from Missouri School of Mines and Metallurgy, and his M.S. from Lehigh, joined Bethlehem Steel Co. in 1938 as assistant metallurgist at Lackawanna. In 1946, he became research engineer for Bethlehem Steel Co., at Bethlehem. Prior to graduation, he worked summers for Carnegie-Illinois Steel Corp., in Duquesne and South Works. An AIME member, this is his first attempt as far as papers for AIME is concerned.

J. W. Frame

A. E. Reinhard (p. 835), a Hoosier, attended Wiley High School at Terre Haute and the Rose Polytechnic Institute from which he received a B.S. in Mechanical Engineering. His career includes service in the mechanical and electrical dept. of the Wheeling Steel Corp., after which he became superintendent of the open hearth and bessemer dept. of the Youngstown Sheet & Tube Co. He is now superintendent of steel production of the Great Lakes Corp., Detroit, where he lives. He is an AIME member, a devotee of Isaac Walton, and enjoys golf and baseball.

W. G. McDonough (p. 838) is a native of Homestead, Pa., and spent his entire working career with the National Tube Co., with the exception of two years at the Aliquippa Plant of the Jones & Laughlin Steel Corp., and the Indiana Harbor plant of the Youngstown Sheet & Tube Co. He is now superintendent of the Open Hearth and Bessemer Dept., National Tube Co., at McKeesport, Pa., where he also resides. He reports no particular hobby, enjoying golf, fishing, swimming, bowling, motoring, and church activities.

Francis B. Foley (p. 845) came from Germantown, near Philadelphia, and attended Girard

Authors In This Issue

College. His career has been principally as metallurgist for the Midvale Co., Philadelphia, which he began in 1905 and continued until 1917. He taught at the University of Minnesota, and followed this with research work for the Bureau of Mines, and collaboration with the late Dr. Henry Marion Howe. In 1926 he returned to the Midvale Co. as director of research. In 1949 he became consulting metallurgist for the International Nickel Co., at Bayonne, N. J. He became a member of the AIME in 1919 and last February was elected a Director. He is currently Chairman of the Institute's Technical Publications Committee. He has prepared numerous technical papers for AIME. His home is in Philadelphia.

A. E. Reinhard

T. E. Brower

T. E. Brower (p. 851). His career has been entirely in the laboratory of the U. S. Steel Corp. since his graduation from Lehigh University in 1930 with a B.S. in Metallurgy and a professional degree of Metallurgical Engineering in 1936. He was born in Little Silver, N. J., and attended the Red Bank, N. J., High School. For nine years from 1935 he worked in the Donora Works of the American Steel & Wire Co., and in 1944 returned to his present job as associate physical chemist at U. S. Steel Co.'s plant in Kearny. He is an AIME member, has written several papers for the Institute, and three Open Hearth Proceedings papers on oxygen in liquid open hearth steel. He likes to study and collect antiques, and to putter in his garden at Red Bank.

B. M. Larsen

B. M. Larsen (p. 851) is physical chemist and supervisor of Process Research at the U. S. Steel Corp., Kearny, N. J. After graduating from the University of Washington with an M.S. in 1922, having previously a B.S. from the University of Wisconsin, he became assistant metallurgist for the U. S. Bureau of Mines. After five years he was called to his present position and lives in Elizabeth, N. J. He was born in Woodford, Wis., and attended the Cumberland, Wis., High School. In 1938 he became an AIME member and in 1948 received its Robert W. Hunt Award. He has presented a large number of technical papers to the Institute and has authored and edited the *Blast Furnace and Open Hearth Proceedings*. He likes music, and enjoys outdoor life—mountain climbing, sailing and gardening.

H. H. Kellogg

Herbert H. Kellogg (p. 862) claims Brooklyn, N. Y., as his birthplace, where he attended Erasmus Hall High School. From the School of Mines at Columbia University he received degrees of B.S. and M.S. His career has been entirely in the teaching profession, beginning as assistant professor of mineral preparation at Pennsylvania State College and continuing as assistant professor of mineral engineering in the School of Mines at Columbia, where he is now working. He is also consultant to various companies on flotation and surface-chemical problems. He has been an AIME member since 1940 and at present is chairman of the Committee on Physical Chemistry of Extractive Metallurgy of the Extractive Metallurgy Division of the Institute. He has contributed four Transactions articles to the AIME. His home is in Pailsades, N. J., and he enjoys reading and music, as well as aquatic sports.

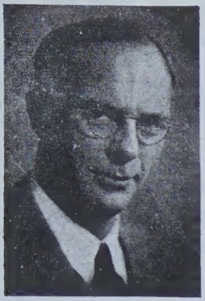

David Harker

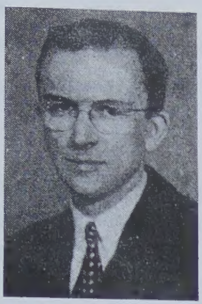

E. S. Greiner

G. Derge (p. 884) has been on the staff of the Metals Research Laboratory and professor of Metallurgical Engineering at Carnegie Institute of Technology since he received his Ph.D. from Princeton University in 1934. Amherst College gave him an A.B. in 1930. He was born in Lincoln, Neb., and attended Warren Senior High School in Warren, Ohio. As an AIME member, he has contributed to its Transactions. The fly rod and the hoe are implements of his hobbies around his home in Pittsburgh.

W. C. Ellis (p. 886) was born in Dundee, N. Y., and attended high school there. From the Rensselaer Polytechnic Institute at Troy he received degrees of Ch.E. and Ph.D. Since 1927, he has been a member of the technical staff of the Bell Telephone Laboratories at Murray Hill, N. J. His home is in Maplewood, N. J.

David Harker (p. 887). Born in the city by the Golden Gate, he attended the C. L. Williams Institute. From the University of California he received a B.S. in 1928 and in 1936 a Ph.D. from the California Institute of Technology. Beginning his career as research assistant with the Atmospheric Nitrogen Corp., he followed with service as associate in chemistry at Johns Hopkins University and research associate and head of the Crystallography Div. of the General Electric Co. at Schenectady, N. Y.

Earl S. Greiner (p. 891) attended high school at Lebanon, Pa., where he was born. From Carnegie Tech, Lehigh and Columbia he received degrees of B.S., M.S. and Ph.D. He is a member of the technical staff of the Bell Telephone Laboratories, Inc., at Short Hills, N. J.

* Long running tests of ferritic and austenitic steel steam pipe are in progress. Using superheated steam at 1050° F under 2000 lb pressure, both types have been tested in an expansion loop where they were worked back and forth more than 4000 times at higher stresses than boiler code limits, or the equivalent of starting a boiler every other day for 20 years. No ruptures occurred. To induce thermal shock, 10 gal of water at 635° F were injected into the pipes 100 times without rupture.

* France is spending some $80,000 in reviving the sponge iron kiln of the U.S. Bureau of Mines, at Laramie, Wyoming. Shipments of about 500 tons of French low-grade ore are being made to the plant for experiments in making iron as good as Krupp-Renn metal, but without the sulphur.

* The recent French proposal of a Franco-German pool of Steel and Coal, to be placed under a joint high authority which other European countries including those in the East, specifically those under the Soviet sphere of influence, are free to join, may be the opening wedge for Russia in its continuous effort to drive out American occupation of Western Germany. While far from a reality, the program smacks of Soviet influence.

* Weirton Steel Co. unveiled its new electrolytic tinning line at Weirton, W.Va., the largest and fastest line yet built. The line will operate at strip speeds up to 2500 ft per min.

* Climax Molybdenum Co. is planning to engage in mining and processing uranium-vanadium ores on the Colorado Plateau. A mill will be built at Grand Junction, Colo. for processing from 50 to 100 tons of ore per day. Minerals Engineering Co., Grand Junction, a new corporation in which Climax will have an interest, will supply some of the ore, and some will come from properties leased from the Atomic Energy Commission.

* A program of establishing nationwide standards of operator performance covering a variety of simple work operations has embraced more than 150 companies. By rating time studies and time study methods, the aim is to develop standards for such operations that will be uniform throughout industry.

* A new oil specification, Mil 2104 to replace 2-104B oils, is being considered by the Army Ordnance Dept. The oil is a compromise between gasoline engine and Diesel requirements. Trend in military engine design to lightweight, high-output, compact dimensions has played a part in the development of the specification.

* A new development in the production of clad metals, particularly gold clad, is the pressure bonding furnace. Two presses are incorporated in the atmosphere controlled furnace, one for pressing the clad package as it approaches the melting point of the solder or joining material and the other for holding the package under compression during cooling. (See Front Cover.)

* A British technical team reporting on the American forging industry concludes productivity is four times greater in America than in Great Britain, because of the "fullest possible machine utilization." Cost per piece in Britain is about twice that in America for forgings.

It's Everyone's Business

OUTSTANDING of the activities offered by technical societies are the Open Hearth, Electric Furnace, Blast Furnace and regional technical conferences of AIME, which fill a void in the presentation of technical information. The JOURNAL OF METALS, or any publication, while presenting the latest in technical information, leaves little opportunity for rebuttal from the reader except in the form of a letter. But the conferences permit the listener to stand up and object—ofttimes rather picturesquely—to statements of the speaker. On the other hand, the listener can bring home to the audience points that the speaker overlooked, either because of lack of time or lack of similar experiences. These may have a definite and far reaching bearing on the subject.

The recent Open Hearth and Blast Furnace Conferences at Cincinnati and the New England Regional Conference at Providence, were both typical of this situation. In reading the stenotype reports of the discussions after the papers had been presented, it was obvious that these audiences—and professional audiences they were—contributed heavily to the presentations. Thus, it bears repeating that AIME conferences are more than an opportunity to meet friends. They add to the reservoir of technical development and practices.

In this issue, several of the papers at the Cincinnati meetings are presented. The lead paper, "The All-Basic Openhearth," is an excellent discussion of years of research into both European and American practice. The reasons for extraordinarily long furnace campaigns in Europe are developed, and the differences in practice between European and American operators are described. Likewise, the use of vanadium in the manufacture of deep drawing steel sheet, another paper included in this issue, brings out some of the important aspects of the manufacture of this huge tonnage item.

British Auto Show

Speaking of deep drawing steel sheet is a reminder of the automobile industry. It may be recalled the British recently held an all-British motor car exhibit in New York City, at which practically all British automobile styles were on exhibit, and British salesmen—or call them what you may—were taking orders for these cars.

Those who visited the show went away wondering how many cars were sold. The low pressure selling methods, as contrasted to methods of American motor car distributors, netted £1,100,000, or about $3,080,000 worth of orders. The British feel, according to the *London Economist,* that there is a real market in the United States for two types of British cars, the small car and the sports car, neither of which is made in the United States.

The British motor car industry has set up a bogie for itself of 1 pct of the U. S. automobile market, or about 40,000 to 50,000 cars a year. Attainment of this will probably depend upon the British automobile industry establishing itself as the main supplier of these two comparatively specialized types of cars.

Price-wise, the British are not in bad shape on these cars. There is the prospect of American competition in the small car field. The Nash 5-passenger Rambler, costing about $1800, is the first to come into this field. Lower priced lines may be in the offing. The cheapest British car shown, the Ford Anglia, costs $1003, while the Austin A40 costs $1480, the Morris Minor, $1250, and the Hillman Minx, $1495. The British are in the slot on deliveries, not being able to augment deliveries to the U. S. for at least two months. Specification requirements of American authorities also give them some trouble. To up production, British carbuilders are faced with another problem, the limitation of supplies of steel sheet. Thus, while the lovely American dollar goes begging for a home, immediate prospects of Britain getting it through the export of automobiles poses almost insurmountable home problems. One possibility is to cut the supplies of cars to overseas markets in the sterling areas, and this cure might be worse than the illness.

Ingot Mold Coatings

J. J. Golden, of Carnegie-Illinois Steel Corp.'s Gary Works describes two ingot mold coating materials on p. 842, that are now being tried. It seems this is quite a controversial subject at the moment, and other companies might do well to heed the work being done. Harold J. Walker, of Republic Steel's Warren District, also has been in on investigations of mold coatings, and work done by Republic was photographed and the movies shown at the Open Hearth Conference. Mr. Walker indicated that a variety of materials had been tried, including powdered pitch; graphite and aluminum powder suspended in water, molasses or in a resin base solvent; salt water; powdered sugar; fuel oil; tar; and petroleum residue, but tar remained the best suited for the work.

While tar is the old favorite and accepted generally as the best mold coating material, it does have the objectionable characteristic of strong fumes and odors. Here is where the union steps in with the demand for better working conditions. Some solution to the problem will be forthcoming.

Mr. Golden points out that *Darmold* and *Hydropaste* have been tried extensively, and Darmold at this point seems the best substitute for tar. Mr. Walker described Republic's work with petroleum residue, with the result that there was an increase in surface preparation cost of semi-finished product of about 28 pct. However, with proper application it produces a coating comparable to tar, but it raises several problems. It has high viscosity at low temperature, requires a low mold temperature for uniform coatings of the proper thickness, and gets foamy in case of rain.

The
Drift of *Things*

. . . . as followed by *Edward H. Robie*

ON our last trip, we noticed this sign in a restaurant window: "Moderate Prices — Reasonably Clean Food." We still regret that we did not stop in there for a meal. In this age of exaggerations, when the tendency is always to reach up into the heights of the superlative and pull down the ultimate in language, it is indeed a relief to find such a temperate and no doubt fair statement of what is offered. It smacks of the good old days. In our hall at home we have an old clock, made by Gilbert at Winchester, Mass., and in large letters inside the case it says "Warranted Good." Not perfect, or the best ever made, but just honestly good.

Our experience has been that if something is reasonably good, or done reasonably well, one should not complain too much. We can remember back when copper ore was treated on tables and vanners and the recovery was sometimes as low as 60 pct; that was not very good but now it is well beyond 90 pct—not perfect but certainly nothing to be ashamed of and not much territory is left for future improvement in this respect. Extraction of ore and coal from mines is only reasonably good; pillars are still left. We shall never get everything out. A substantial portion of crude oil remains in the ground when a field is abandoned, but still modern recovery practices are much better than they used to be. They will never be perfect. Nor will any process ever get 100 pct recovery of high-grade gasoline from crude oil, but marvelous progress has been made. Of course, we should still strive for perfection, even knowing that it will never be attained.

Years ago one of our sons was chided for not living up to his capabilities in school, and getting "A's". "Mother," he finally said, "why can't you be satisfied with "B's" and let me be myself?"

St. Lawrence Seaway

Discovery of huge deposits of iron ore beyond the borders of the United States and current importation of some 900,000 bbl of oil per day have spurred proponents of the St. Lawrence Seaway to increased activity. Hearings have been going on before the House Public Lands Committee, with many Government officials, prominent industrialists, and farmers urging approval of the project. Until recent years United States iron ore and associated steel interests were generally against the idea, but with the present depletion of Lake Superior high-grade ores they have changed their views and now will welcome foreign ore supplies economically delivered to steel centers at and near Great Lakes ports. Congressional hearings ended on May 10. Opponents of the plan did not appear, for it has been decided not to take action at the present session of Congress.

The Seaway really has been under construction, in one way or another, for generations. Already accomplished is a channel 32½ ft deep from the Atlantic to Montreal, 1000 miles inland. A channel generally 25 ft deep is available also from Duluth to Ogdensburg, N. Y., a distance of 1250 miles. The present proposal, which dates from 1941, is to build a 120-mi canal 27 ft deep from Ogdensburg to Montreal, and to deepen to 27 ft existing waterways. The project would take seven years and cost $800,000,000. Power available for the United States would be 1,098,000 hp. Estimated traffic has risen greatly in recent years, the latest guesses being from 57 to 84 million long tons a year.

The desirability of the project is by no means universally admitted. Proponents' arguments fall into three main categories: 1—Addition of needed and cheap transportation, 2—needed and cheap power, and 3—utility in case of war. Opponents have counter arguments on each of these counts. The railroads and present transportation facilities complain of the tax-free status of the seaway project and point out the loss to established facilities that would result. Further, the facilities proposed could not be used for five months of the year, and 27 ft is too shallow for 91 pct of ocean shipping. The private power interests bring forth the usual arguments against power development by the Government. They deny that there is a shortage of power in the Northeast, affirm that the proposed development would take care of only 10 pct of New York State's power needs, and say that a substantial portion of the power that it is proposed to generate could be obtained much more cheaply by further development at Niagara Falls. Opponents say that nothing is more susceptible of damage in wartime than a canal, and that any installations along our northern borders would be right out in the front trenches, so to speak, when an airborne attack comes over the North Pole.

The magazine, *Civil Engineering,* has published two excellent articles on the subject, one in November, 1949, favoring the project, telling something of its history, and giving details of the proposed St. Lawrence development; and another in March 1950, marshaling the arguments of the opponents. Because of the importance of the subject to the mineral industries, AIME members would do well to apprise themselves of the pros and cons.

37 Years Ago

From the Bulletin of the AIME, June 1913: "In view of the great and increasing importance attached to radium and radium deposits, members are urged to communicate to the Secretary any information they may have as to deposits containing radioactive minerals." They still are only substitute "uranium" for "radium".

Meaning of AIME

AIME means different things to different people. To Mrs. Marie M. Beatty, secretary to the superintendent of the Waukegan Township Secondary Schools, Waukegan, Illinois, who writes enquiring what scholarships we have available, it means "American Institute of Mining and Metallurgical Engravers."

aime NEWS

AIME Proposes Bylaw Amendments Regarding Members and Elections

Following the recommendation of the AIME Board of Directors, several amendments to the Bylaws of the Institute will be voted upon at the meeting of the Board on June 21.

Members—Qualifications and Elections

In Article I, Sec. 8, insert the italicized word in the second sentence as follows: "A *full-time* student in good standing. . ."

Nomination and Election of Directors and Officers

Revise the first six paragraphs of Article XI, Sec. 1, of the Bylaws to read as follows:

Sec. 1. A ticket of nomination for nine candidates, each to serve a three-year term as Director, of whom one shall also be designated as President-elect, and two as Vice-President, shall be prepared annually by a Nominating Committee. In 1951 the Nominating Committee shall also select, as one of the nine Directors, a President to take office in February 1952. The President-elect shall automatically become President at the end of his first year of service, and thereafter shall serve one year as Past President.

Sec. 2. The Nominating Committee, of which no member shall at the same time be on the Board, shall consist of eighteen members. Eleven of these (with an alternate for each if desired) shall be selected by the Council of Section Delegates prior to November 1. Two other members shall be chosen by the Mining Branch Council, and one each by the Metals and Petroleum Branch Councils, respectively, (each with alternates if desired) prior to Nov. 1. The other three members, one of which shall be designated by the Board to act as chairman, shall be appointed by the President, with the approval of the Board, at the November meeting of the Board. If necessary, the President of the Institute shall also have the power to appoint a sufficient number to the Nominating Committee, at the November meeting of the Board, to bring the personnel of the committee to the authorized total of eighteen.

The names and addresses of the Nominating Committee shall be published in the December issues of the monthly journals. A meeting of the Nominating Committee shall be held during the week of the Annual Meeting at the place where that meeting is held. This committee shall proceed to the naming of a ticket. In selecting candidates the committee shall be guided by such rules of procedure as may from time to time be established by the Board, provided, however, that of the eight directors in addition to the President-elect, five shall be apportioned on the basis of geographical districts established by the Board. The basis of the selection of the remaining three shall be at the discretion of the Committee.

The ticket thus prepared shall be transmitted to the Secretary of the Institute in time to be submitted to the Board of Directors not later than at its June meeting, and shall be published in the July issues... (continuing in the sixth paragraph as in the present text of Sec. 1).

Sec. 2 to be renumbered as Sec. 3.

AIME Changes Admissions Procedures, Affecting Student and Junior Members

Changes in the handling of AIME applications will increase the efficiency of processing and reduce such expenses. Among other things, each journal will hereafter print only the names of those applicants for membership who are employed in the activities covered by the journal in question. Readers of each journal are urged to review these lists promptly as published.

Distinction between Student Chapters and Affiliated Student Societies was removed by the AIME Board of Directors. All recognized student groups are now Student Chapters, whether or not all members are Student Associates.

No further applications will be accepted for Junior Membership from anyone who has passed his 30th birthday when the application is received. Also Junior Members must change status to Associate Member or Member, and pay the $20 initiation fee (in $5 annual installments, if desired) by the time they have reached their 33rd birthday.

An exception has been made in the case of veterans of World War II who have attended college immediately following discharge from the service. They may apply for Junior Membership, even if over 30 years old, for a period of three years following receipt of a Bachelor's or professional degree, or after completion of schooling, if no degree is earned.

AIME Revises Book Prices

Effective June 1, a new price list for AIME books will take effect. Copies may be obtained from Institute headquarters. One price will be set for each book published by the AIME. From this list price, members, Student Associates, and public libraries will be allowed a discount of 30 pct for as many copies as they may wish. Dealers will be given a 20 pct discount. Transactions volumes ordered a year in advance, at the same time dues are paid, are subject to a 50 pct discount.

Transaction volumes 1 to 183, inclusive, if in stock, are listed at $5 each. Other books will be sold at previous nonmember prices, except: "The Porphyry Coppers," $3; "Industrial Minerals and Rocks," $7; "Seventy-five Years of Progress in the Mineral Industry," $5; and "Nonferrous Rolling Practice," $4.

AIME Budget Set at $477,500

Prospective income for AIME, according to the 1950 budget approved by the Board of Directors at the April 21 meeting, was set at $477,500, and expenditures were set at $477,450. Two main increases in income will come from dues and advertising in the AIME's three journals. The higher rate of dues will add to revenue, but more new members are expected this year than in 1949.

Open Hearth a Annu

Erle G. Hill, director of metallurgy and development at Wheeling Steel Corp., Wheeling, W. Va., and chairman of the National Open Hearth Conference, congratulates William A. Greene, metallurgical engineer, Kaiser Steel Corp., Fontana, Calif., recipient of the McKune Award for his paper, "The Effect of Hot Metal on Open Hearth Production."

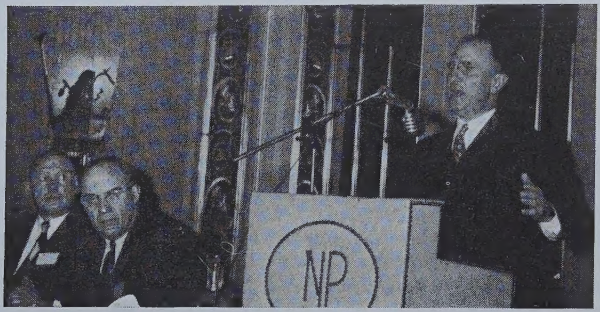

W. W. Sebald, president of Armco Steel Corp., speaker at the Fellowship Dinner, addressed the group on "Pocketbook Economics," belabored Government participation in local enterprises and called on industry to point out the fallacies and pitfalls of such practices. Seated to Mr. Sebald's right are H. M. Griffith of the Steel Co. of Canada and Dr. H. K. Work, Chairman of the Iron and Steel Division AIME and director of the research division, College of Engineering, New York University.

OPEN HEARTH—BLAST FURNACE FELLOWSHIP DINNER

April 11, Netherland Plaza Hotel, Cincinnati

ast Furnace nferences

Vernon W. Jones, superintendent of steel production, Armco Steel Corp., and Robert S. Bower, Covington, Ky., spark-plugged the Open Hearth and Blast Furnace Conference arrangements. Mr. Jones is chairman of the Local Committee on Arrangements, and Mr. Bower is chairman of the Southern Ohio Location Section and also the Fellowship Dinner subcommittee.

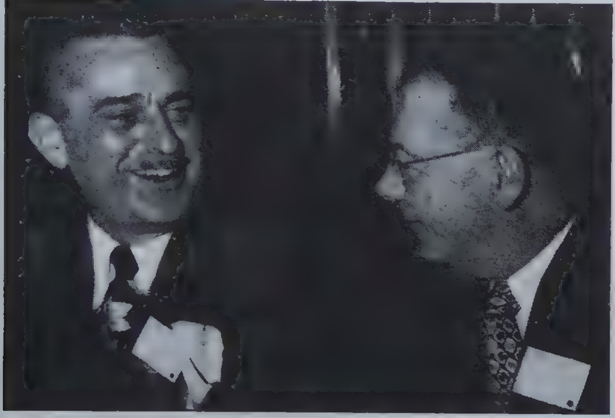

T. F. Plimpton, superintendent of the Blast Furnace Dept., Inland Steel Co., and chairman of the Blast Furnace, Coke Oven and Raw Materials Committee.

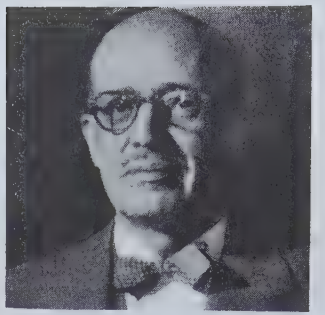

K. C. McCutcheon, assistant to the vice-president, Armco Steel Corp., was elected chairman of the Blast Furnace, Coke Oven and Raw Materials Committee.

H. M. Griffith, works manager of Steel Co. of Canada, Hamilton, Ont., was elected chairman of the National Open Hearth Committee.

SECTION ACTIVITIES

Blast Furnace Smelting Subject of April Chicago Section

"Current Problems in Blast Furnace Smelting" were discussed by T. L. Joseph, of the University of Minnesota and the Minnesota Institute of Technology, at the April 5 meeting of the Chicago Section, AIME. Professor Joseph placed particular emphasis on the ore supply in the Minnesota range and from graphs showed that there should be no drop off in steel production because of the increase in population and the demand for steel items. He touched on the agglomeration problems and what was needed to supply a better basis for appraising innovations in furnace practice.

Practical Aspects of Statistical Quality Control by W. S. Oliver

Soon after Eli Whitney introduced the concept of interchange of parts there arose a need for statistical control in the production of parts. In the ensuing years increase in production has brought increased pressure on inspection—so much so that total inspection is no longer possible and it is now a question of how much inspecting shall be done. This leads to the present day development of scientific methods of statistical quality control by harnessing the laws of chance to production.

Engineering, production and inspection are very closely allied. A little removed from them is accounting, and still further, customer relations. In this chain, according to Walter S. Oliver, of the Timken-Detroit Axle Co., speaking to the Detroit Section, AIME on Apr. 17, statistical quality control is the connecting link. Although the underlying principles are based upon the higher mathematics of probability, the formulations have been brought to a level where ordinary arithmetic will suffice for practical application. The methods of statistical quality control are now widely used in all fields of industry and agriculture.

Measurement of parts can be divided into two classes, those measurements whose variations from the specification is within the range of the normal frequency-distribution curve (normal), and those whose variations is outside this range (abnormal). A plot of the measurement versus observations made will be characterized by high peaks and low valleys for the abnormal condition. The specification is devised from either experience or experiment. Statistical quality control is based upon examination of the causes of abnormal variation, and the operation is "put under control" by adjusting the material, machine, or personnel so as to bring the variation in measurement of the parts to lie within the range of the normal frequency-distribution curve. Mr. Oliver gave examples of the application of statistical quality control to operations at Timken-Detroit Axle Co., where savings in inspection time and scrap rejects were obtained in machining, forging, and heat treating operations.

Mr. Oliver showed how statistical quality control is expanding in scope and how more scientific methods of inspection are being introduced into production schedules.

Physics of Metals Discussed by Hollomon at Detroit Meeting

In a paper on the physics of metals before the Detroit Section of the AIME on Mar. 20, John Hollomon, of General Electric, described the adoption of the phenomena associated with metal behavior to the solution of fundamental problems. He gave a few examples of the use of simple metals in the solution of simple problems, the first of which was surface tension. The driving force for grain growth is surface energy. Dr. Hollomon showed how the surface tension of solid copper had been measured. It is in the order of 380 ergs per sq cm. Surface tension governs not only grain growth and recrystallization, but also plays a part in the precipitation of a phase out of the matrix, since it takes surface energy for the formation of a new surface.

Surface energy also plays a part in the spheroidization of carbides, which in turn affects the rate at which a steel tempers. The rate of diffusion is related to surface energy. Diffusion may proceed through the bulk of the metal, through the grain boundary, or along the surface. Experimental data indicate that diffusion is slowest through the bulk, intermediate at the grain boundary, and most rapid along the surface. Dr. Hollomon cited data to show the degree of supercooling that could be obtained before solidification occurred.

Chilean Steel Mill Scheduled For Full Operation By End of June

Chile's first integrated steel plant blew in its blast furnace during the first week in May, and the entire plant will be in operation sometime in June.

Koppers Co., Inc., which furnished supervisory assistance in construction and engineering of the new Chilean plant erected for the Pacific Steel Co., of Chile, near Concepcion, pushed the first coke during the week of Apr. 17 from a new battery of 57 coke ovens which Koppers designed and built. The coke battery, of the latest Koppers-Becker underjet design, is capable of producing 1100 tons of coke per day. The blast furnace is designed to produce 700 tons of iron per day.

Mills for finishing a wide variety of flat-rolled and merchant products at Concepcion have been in operation for some time, using semi-finished steel shipped from the United States. With the completion of the coke ovens and the blast furnace, Pacific Steel Co., of Chile now will have a completely integrated plant, making finished steel products from Chilean ore.

Work on the mill was inaugurated late in 1947 and has been pushed to completion at a cost in excess of $70,000,000. In addition to the coke ovens, a blast furnace, and finishing mills, the plant has an open hearth furnace, a bessemer converter, an electric furnace, and auxiliaries for handling tar, light oils, and gas.

1949 Acid Steel Production Down

The Acid Open Hearth Research Assn. announced the total tonnages of acid open hearth steel melted for the year 1949 for both ingots and castings was 866,614 tons.

Of this total 46.4 pct was in the form of ingots and 53.6 pct in castings. The tonnages previously reported were: 1944—2,107,493 tons, 1945—1,542,724 tons, 1946—1,132,199 tons, 1947—1,257,673 tons, and 1948—1,267,177 tons.

Proposed for Membership—Metals Branch AIME

Total AIME membership on Mar. 31, 1950, *was* 16,397; *in addition* 4037 *Student Associates were enrolled.*

ADMISSIONS COMMITTEE

E. C. Meagher, Chairman; Albert J. Phillips, Vice-Chairman; George B. Corless, Lloyd C. Gibson, Ivan A. Given, P. Malozemoff, Richard D. Mollison, and John Sherman.

Institute members are urged to review this list as soon as the issue is received and immediately to wire the Secretary's office, night message collect, if objection is offered to the admission of any applicant. Details of the objection should follow by mail. The Institute desires to extend its privileges to every person to whom it can be of service but does not desire to admit persons unless they are qualified.

In the following list C/S means change of status; R, reinstatement; M, Member; J, Junior Member; AM, Associate Member; S. Student Associate.

California
Los Angeles—Crow, Paul E. (M).

Connecticut
Hamden—Treciokas, V. Paul. (R,C/S—S-J).

District of Columbia
Washington—Lang, Elmer T. (M).

Illinois
Chicago—Bauman, Paul J. (AM). Cassel, Carl E. (AM). Marshall, Richard H. (R,C/S—S-M). McDonough, Austin E. (M). Reynolds, Harry W. (J).
Joliet—West, Howard F. (M).
Park Ridge—Bryce, John T. (C/S—AM-M).

Indiana
East Chicago—Bennett, Patrick S. (J).
Gary—Danielson, Robert J. (M).

Michigan
Wyandotte—Reinhard, Adolph E. (M).

Minnesota
Minneapolis—Yoon, Tong S. (AM).

Missouri
St. Louis—Marshall, John N. (M).

Montana
Anaconda—Holderreed, Francis L. (C/S—J-M).

New Mexico
Hurley—Lockart, Charles L. (C/S—S-J).

New York
Albany—Doyle, Nicholas E., Jr. (J).
Brooklyn—Brennan, John P. (J).
Merrick—Pitler, Richard K. (C/S—S-J).
New York—Weimer, David G. (J).

Ohio
Berea—Cooper, Anthony L. (C/S—S-J).
Euclid—Howald, Thomas S. (C/S—AM-M).
Sciotoville—Frecka, James H. (M).
Springfield—Selle, Joseph B. (R,C/S—S-M).
Warren—Walker, Harold J. (M).

Pennsylvania
Lewistown—Callinan, Edward E. (M).
Pittsburgh—Adams, Louis W., Jr. (R,C/S—J-M). Ferree, Jay Wesley. (M). Kaufman, Hershel E. (R,C/S—J-M). Longenecker, Lee S. (M). Palmer, Kenneth W. (M). Protheroe, Alfred W. (AM).
Sewickley—Hannigan, Harry W. (C/S—S-J).

Rhode Island
Kingston—Mairs, Kenneth H. (C/S—J-M).

Tennessee
Oak Ridge—Vagi, Julius J. (C/S—S-J).

Utah
Murray—Norman, Edgar C. (M).

Virginia
Richmond—Timberlake, Richard C. (J).

Brazil
Volta Redonda—Azevedo, Renato Frota R. (C/S—J-AM).

Peru
La Oroya—Robinson, David A. (C/S—S-J).

England
Brighton—Hubbard, Arthur Edward. (M).

Holland
Eindhoven—Van Santen, Jan Heinrik. (M).

New Products, Services and Information...

Products and services recently announced are described here. Also, new free literature published by producers serving the metalworking industry is listed.

For further information on any product or for copies of the free publications, fill in the coupon below and send it to the Journal of Metals.

1—CLAD METAL TUBING

Seamless tubing of Rosslyn Metal, copper core with stainless steel surfaces, is announced by the *American Cladmetals Co.* The copper permits swift heat and cold transfer while the stainless steel surfaces provide hardness, resistance to corrosion, and ease of cleaning. The size range is expected to be from ⅜ to 1½ in. OD and from 0.020 to 0.78 in. wall thickness.

2—ELECTRON MICROSCOPE

Announcement has been made by the *RCA Co.* of a Universal Electron Microscope for use by research institutes and industrial organizations that require the versatility of a larger instrument and want the ultimate in electron microscopy. It is a greatly simplified table model only 30 in. high and sells for less than $6000. It has permanent magnetic lenses, requiring no stabilization circuits and controls. It magnifies up to 50,000 diam by photographic enlargement, with direct magnification ranging up to 6000 diam.

3—BALANCES

The Christian Becker Laboratory Balances manufactured by the *Torsion Balance Co.,* have been redesigned to eliminate corner posts, minimizing reflections and focusing light where needed. Quicker readings are possible with the scientifically positioned, constant-eye-level, dial and vernier, larger numerals.

4—FLOW METERS

A new type of mercury manometer flow meters is manufactured by the *Fischer & Porter Co.,* that requires no pressure-tight bearings or stuffing boxes. They use the F&P magnetic clutch, or the F&P impedance-bridge electric transmitter, which has three times the power of previous similar devices. They are available in several models. Catalog 37 will be sent on request.

5—VISCOSITY METERS

Viscosity measurements without the need for calculations are now possible by the use of the new Fisher Electroviscometer, manufactured by the *Fisher Scientific Co.* It is useful for testing such widely diversified materials as glycerin, water, and any liquids of the free-flowing Newtonian type. The Electroviscometer will supply universal exchange of results and experimental data because of facility of translation into centipoise units.

Journal of Metals
29 West 39th St.
New York 18, N. Y.

June

Please send me

More Information ☐
Free Literature ☐
Price Data ☐

on items indicated.

1	2	3	4	5	6	7	8	9	10
11	12	13	14	15	16	17	18	19	20
21	22	23	24	25	26	27	28	29	30
31	32	33	34	35	36	37	38	39	40

Name .... Title..................
Company ....
Street ....
City and Zone .... State...............

6—HUMIDITY CONTROLS

An instrument to record and control humidity is announced by the *Weston Electrical Instrument Corp.* Two pens operate on a circular 10-in. chart, simultaneously recording the dry-bulb temperature and the wet-bulb depression. The flow of the humidifying agent, moisture, steam or oil fog, is regulated by a valve which is operated by the control instrument.

7—OPTICAL PROJECTORS

An instrument to measure readings in increments of ten-thousandths of an inch in two planes at 90° and to provide contour and/or front-surface projection is available from *Stocker & Yale.* This optical projector has all the features required of a measuring instrument despite its small size, being portable and costing $595. It is available in standard magnifications up to 120 diam. The screen is 6 in. square and made of textolite.

8—RUST PREVENTIVE

A corrosion and oxidation resistant coating of particular interest to all metal producers and fabricators is *End-O-Rust* made by *End-O-Rust, Inc.* It resists 2000 hr of salt spray, caustic soda, ammonia, sulphuric, nitric, acetic, hydrochloric acids, and long periods on structural elements subject to temperature ranges of zero to 100°; and is quick drying.

9—STAINLESS TUBING

A free-machining welded stainless tube is made by the *Carpenter Steel Co.* for products that demand corrosion resistance combined with ready machinability. It is recommended for parts that must be fabricated by threading, turning, reaming, and drilling, and for intricate or difficult-to-machine parts where smooth surfaces are required. It is available in rounds or shapes from ¼ to 4½ in. OD and in all standard wall thicknesses; and is less costly than other type 303 tubing.

10—DIESEL ENGINES

A new heavy-duty diesel engine in the 195 to 375 hp range is announced by *Ingersoll-Rand Co.* This TS diesel can be made portable but is not automotive. It is a four-cycle, 7 in.-bore, 8½ in. stroke, single-acting engine with a weight of about 30 lb per hp, and a fuel consumption of 0.40 lb per hp-hr. Cylinders are provided with replaceable, wet-type liners and individual heads with overhead valves and intake and exhaust valve-seat inserts.

11—BLAST CLEANERS

A bench blast cabinet for cleaning small parts such as automobile pistons, dies, tools, castings, etc., is made by the *W. W. Sly Mfg. Co.* This portable cabinet will operate on the compressed air supplied by a standard 5 hp, 2-stage compressor, and requires space of 14 in. x 18 in.

12—SILVER BRAZING ALLOY

A silver alloy for brazing ferrous, nonferrous and dissimilar metals comes in 5 oz packets of Easy-Flo

45, produced by *Handy & Harman*. The packets contain a 5-oz coil of 1/16 in. wire (approximately 330 lineal in.), instructions for use, especially for repair and maintenance crews in small shops and in those doing experimental work.

13—RUST PRIMER

Brooklyn Varnish Mfg. Co. announces an anti-corrosive primer for corroded iron and steel to be known as "Tuf-on-Rust." It is a pretreatment for ferrous metals in removing oil, grease, rust and scale, etc., and dries in 4 hr for recoating. It can be applied by brush or spray and is recommended for use on projects where weather, water and corrosion resistance are required.

14—SPRAY NOZZLE

A new spiral nozzle for wide angle sprays, designed by the *Bete Fog Nozzle Co.* for low flow rates, requires extremely low pressures. It will produce fine and uniform drop sizes with a 180° umbrella spray pattern of wide coverage. It is available in two sizes, for ½ to 2 gpm and for 1½ to 4 gpm capacities.

15—FLAME CUTTING TRACER

An electronic tracing device called an "electric eye," a flame-cutting machine, is now manufactured by *Joseph T. Ryerson & Son, Inc.* It speeds the oxy-acetylene cutting of highly intricate and irregular shapes from steel plate and permits cuts unobtainable with other mechanized flame cutters, such as parts having sharp corners, narrow slots, etc.

16—WELDING ELECTRODE

A new low amperage electrode for welding light gage steel is Steel-Tectic marketed by the *Eutectic Welding Alloys Corp.* Extremely thin gage steel can now be metallic arc-welded. Because of this smaller size—3/32-in. diam—one bead can be welded over another in continuous passes, without stopping to chip or brush slag, except on the final pass. It can be used where electrodes of AWS specifications E6010, 6011, 6012, and 6013 are applicable.

17—MANHOLE LADDERS

Aluminum Co. of America has perfected aluminum manhole steps and ladder rungs for municipal and industrial installations, forged from high strength aluminum alloys. Three sizes are featured, adaptable to concrete, brick, or concrete block wall construction. The non-sparking characteristic of aluminum is particularly advantageous where explosive gases or dust may be present.

18—TIME-DELAY RELAYS

New type AM pneumatic time-delay relays, with adjustable delay from 0.2 to 200 sec, are available from the *Westinghouse Electric Corp.* A large graduated dial permits delay adjustment throughout this range for general industrial timing functions. They are available as open or enclosed units.

The All-Basic Open Hearth . . . European and American

by R. P. Heuer

and

M. A. Fay

An objective examination of basic open hearth practice of European and American steel producers shows how improvements in these practices can be made by consideration of the techniques of producers of both continents. The first part of this two part article covers comparable operating practices; furnace bindings, bottoms, back and front walls; and silica and basic roof construction.

REPORTS of 3000 heat roof-life records on all-basic open hearth furnaces in European steel plants have focused attention on European roof designs, refractories and general practices in an effort to determine whether those methods might suggest improvements for all-basic open hearths in America. No clear picture of European open hearth practice that might be compared with American practice has been presented. However, with only the available data, some comparisons of individual procedures are practical.

Because of the complex nature and interrelationship of all open hearth procedures, the scope of a study of European practice as compared with American practice cannot be limited to only one field. Therefore, this article, although primarily concerned with basic roof construction, necessarily contains information on combustion practice, furnace designs, and other related subjects.

The fundamental differences in European and American open hearths are caused by varying demands for amounts and qualities of steel; by various available raw materials and fuels; and by different delegation of responsibility to operators and engineers, function of outside engineering companies, etc.

Demand for steel in Europe is less than in the United States. Further, a substantial portion of the steel is produced in equipment other than open hearth furnaces. These conditions de-emphasize the importance of the open hearth and open hearth shops have few furnaces of small capacity.

Open hearth furnace repairs per year are relatively few. This makes it impractical to employ steadily large maintenance crews to do this work quickly. Thus, furnace rebuilds require long down periods and hot repairs are as few as possible.

Some plants maintain spare open hearth furnaces and many schedule each operating furnace for a weekly repair period of short duration. At such times workers are available and hot repairs are made. With this type of operation, all open hearth constructions are designed and all refractories are selected to obtain the ultimate length of repair-free life. This means that walls are generally thicker, water cooling is used discretely and many basic refractories are used.

The analyses of European steels vary more than in most American plants. Many alloy steels, even chrome steels normally made in electric furnaces in America, are made in basic open hearth furnaces in Europe. With demand for quantities of individual special steels small, the small furnaces are well suited to the demand.

The service conditions imposed on refractories by such metallurgical practice are extremely severe. Often tapping temperatures are higher than is common practice in America. Temperatures of over 3200° F on the roofs have been observed. These things have encouraged the wider use of basic refractories, particularly basic main roofs.

The chief differences in raw materials in America and Europe are in pig iron or hot metal and in fuels. Where U. S. has relatively large quantities of low sulphur—low phosphorous hot metal, European operators have little or no hot metal. Where hot metal is available, it is frequently high in phosphorous and not well suited for open hearth. Liquid fuels are used predominantly in U. S. and they use gaseous fuels almost exclusively.

Because of the available amounts and condition of much of the blast furnace iron, there are many plants that operate open hearths in all cold charge of scrap and pig iron or even scrap and coke. Others blow the blast furnace iron in basic bessemers to remove phosphorous and carbon, then charge it into open hearths in a duplex operation. Still others treat the hot metal in

---

R. P. Heuer is vice-president and M. A. Fay is ceramic engineer of General Refractories Co., Philadelphia. This paper was presented at the AIME Open Hearth Conference, Apr. 10 to 12, in Cincinnati.

active mixers similar to tilting open hearths, where carbon, silicon, and some phosphorous are removed before charging it into open hearths.

Thus, open hearth operations vary from 100 pct cold charge to 100 pct hot charge within one plant. Because of this, the wide variation in reported heat times, tons per hour figures, etc., by various investigators is not surprising. Full data as to operating procedures are needed for clear understanding.

Where hot metal is available in Europe, some variation of duplex operation appears to be preferred. More operating data are available on operations of this sort and it is on such furnaces that the extremely long roof life campaigns of all-basic roofs have been made. Basic refractories generally, and particularly basic roofs, are well suited for duplex operation with its relatively small fluctuations of operating temperature. The majority of furnaces operating on such practice in Europe are of all-basic construction.

Less information is available on cold charge operations in Europe, although more plants operate on cold charge than on hot metal. The preferred charge is about 75 pct scrap and 25 pct pig iron, although some plants operate on 100 pct scrap plus coke. The life of furnaces operated on cold charge practice with both basic and silica refractories more nearly approximates the service obtained in this country than does furnace life of duplex operations.

The large majority of European furnaces are fired with low Btu content gases. Producer gas and mixed (coke oven and blast furnace) gas are most widely used. Some higher Btu content gases —straight coke oven gas or natural gas—are available at some plants, and a few furnaces are fired with liquid fuel. Some oil or pitch is also used for carburetting the flame of the higher Btu content gases in some cases. On liquid fuel fired furnaces, usually no steam is used for atomizing the fuel, this being done mechanically so that the combustion control of the liquid fuel furnaces is virtually the same as on gas fired furnaces.

This dependence on gaseous fuels in Europe has had tremendous effect on their open hearth designs. Port design, furnace lines, gas and air flow patterns, etc., are extremely important in gas fired furnaces. In contrast, on American liquid fuel fired furnaces, such considerations have been somewhat neglected, control of the fuel jet having been considered sufficient.

In Europe, fuels generally are more costly than in America. This is reflected in furnace design and construction. Insulation of furnaces is much more complete, even front wall piers being insulated in some plants. In many instances, the entire furnace except for the roof is steel plated to minimize air infiltration. Basic main roofs have been partially insulated to reduce heat losses.

The difference in organization of work in American and European plants is partly the result of the smaller size of the European plants and partly by preference. Since the smaller plants cannot afford to employ the large maintenance crews, they employ graduate engineers who supervise and watch over furnace designs and construction. With the greater time allowance for furnace rebuilds, more attention is paid to engineering detail, careful masonry construction, good workmanship, and theoretical considerations. The operators run the furnaces and supply data to the engineers, but have little or no authority as to changes of furnace design or construction.

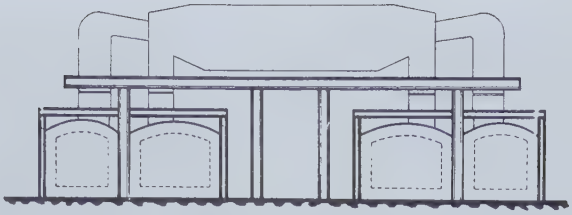

Fig. 1—Steel support of the Maerz furnace.

Often work is let out to outside furnace designing firms who may provide construction labor. Such firms usually conduct research work, investigating refractories, construction, combustion principles, and other related subjects.

With such arrangements, available materials and their best use is studied. Furnace design is used as a tool not only to improve furnace production, combustion and other operating characteristics, but to provide best construction for individual refractories.

This discussion has outlined major factors which cause differences in American and European open hearth practices and furnaces. In general, most conditions imposed on the European plants—low heat value gas fuels, large scrap charges, etc.—would be considered detrimental to best operations here. An examination of the construction and refractories used in the European furnaces, and their comparison with American practices help explain how they may tend to offset such conditions.

Most new open hearth furnaces in Europe are built with the slag pockets entirely separated from the furnace ends. The furnace proper and the ends are carried by a special steel framework. Fig. 1 shows such a construction on a Maerz design preheated gas fired furnace. This construction eases the load on the slag pocket brickwork and contributes to ease of repair work. It permits the use of portable sections in the furnace ends.

Bottoms of European furnaces are similar to many American bottoms. They usually consist of fireclay brick adjacent to the pan, a subhearth of basic brick, and a working hearth of rammed or burned in basic grain refractories. Bottom repair and fettling are done by hand. It appears that bottoms are replaced more frequently than in American practice.

Refractories used are burned magnesite brick and magnesite grains, or in many cases burned dolomite instead of the magnesite grains. Tarred dolomite is sometimes rammed in to form the bottom. Maintenance material is largely burned dolomite, although some grain magnesite is used. There is no apparent advantage in this practice over conventional American practices.

Back walls of virtually all European basic furnaces are vertical and built of basic materials. However, they are thicker at the bottom than at the top, so that the inner face is sloped. The walls are much thicker than in American furnaces, sometimes as much as 3 ft thick. The courses of brick in the wall are frequently tipped downward from inner to outer faces to provide greater stability, as shown in fig. 2. The brick are laid tight against a steel backing plate to provide additional support and prevent air infiltration. The back wall is maintained by normal fettling.

Front walls are similar to back walls. They usually include in addition, water cooling in the door jamb sections. With the backing plate behind the brickwork, it is virtually impossible to repair such walls from outside the furnace so that the great thickness of the walls and water cooling are needed. The front wall is maintained by fettling and by spooning refractory grains onto the front wall piers. By these means, it is possible to extend the life of both front and back walls, usually for the entire main roof campaign.

Campaigns of 1200 heats are not unusual in duplex operations under basic roofs. However, about 500 heats life for front walls is a more average condition. Life of 250 heats is considered short for front walls and probably could be obtained frequently from silica front walls.

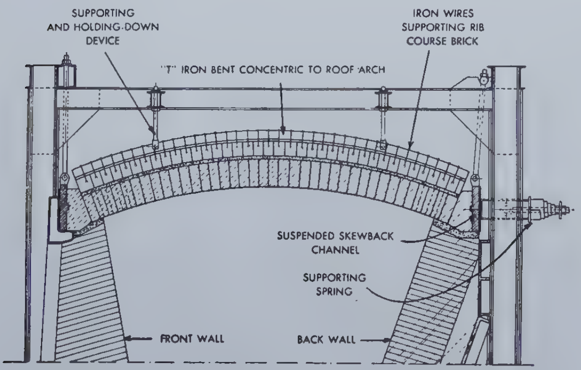
SUPPORTING AND HOLDING-DOWN DEVICE
IRON WIRES SUPPORTING RIB COURSE BRICK
"T" IRON BENT CONCENTRIC TO ROOF ARCH
SUSPENDED SKEWBACK CHANNEL
SUPPORTING SPRING
FRONT WALL
BACK WALL

Fig. 2—General arrangement of the suspended arch on a European all-basic furnace.

Refractories in both front and back walls are burned chrome-magnesite brick on the hot face, backed up with similar brick of poorer quality, and fireclay or silica brick adjacent to the steel backing plate. Backup materials are used to reduce costs. The burned chrome-magnesite brick used in the exposed positions are similar to the burned chrome-magnesite brick made by several American manufacturers. In the few competitive trials of such European and American brick, no significant difference in service has been observed. It seems likely that the chemically-bonded, steel-plated, magnesite-chrome brick that give best service in many American furnaces might give better service in European furnaces as well.

Upon comparison, it appears that present American practice for both front walls and back walls is far better for the existing conditions. Heavy front and back walls not only would cut down furnace capacities, but would be difficult to replace except at cold shutdowns.

Silica roofs on European furnaces are almost identical with American roofs. Ribbed roofs are most common, but occasionally roofs are laid up with key shaped brick instead of the wedge shaped brick commonly used here. Little patching is done, the furnaces being operated carefully to protect the roofs.

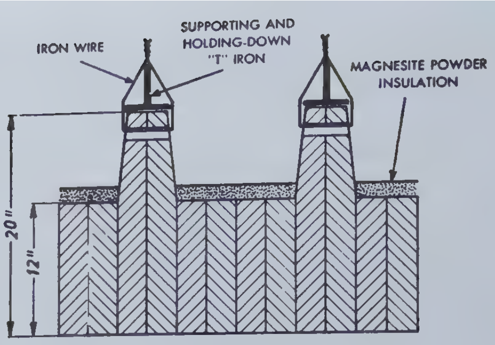
IRON WIRE
SUPPORTING AND HOLDING-DOWN "T" IRON
MAGNESITE POWDER INSULATION
20"
12"

Fig. 3—Longitudinal section of a European all-basic roof.

Roof life with silica roofs shows wide variation. Larger numbers of heats than is common in America are general. Roof life of 250 to 500 heats is not uncommon in either hot or cold metal operations. With many gaseous fuels, however, refractory life is longer than with liquid fuels and furnaces are designed to promote longest possible roof life.

The quality of European silica refractories, although not as good as the best American silica brick, is comparable with that of much of American production. Many brick made for steel plant use contain sand additions to decrease the alumina content to about 1 pct. The ratio of cost of these brick to the cost of basic materials is not widely variant from that in the United States. Thus, the greater preference for basic refractories in Europe is not based to any great extent on cost differentials or quality differences that are radically different from those found in America.

Basic roofs are more common in continental Europe than in the United Kingdom. In Great Britain, the all-basic furnace is still in the development stage. Several different designs are undergoing tests. In continental Europe, basic roof designs are fairly well standardized. One of the most commonly used constructions is the Radex roof, named after the Radex-E brick made by the Austrian American Magnesite Co. This design will be used as the basis for the following

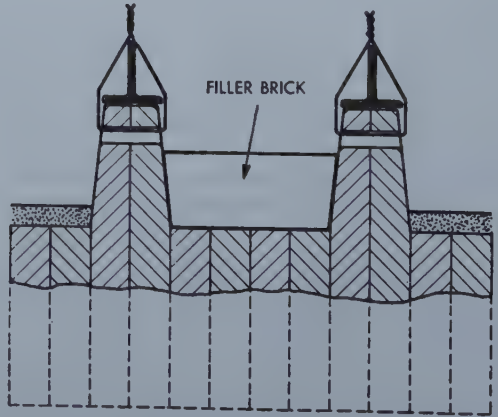

Fig. 4—Arrangement of filler brick between rib courses for patching European all-basic roof.

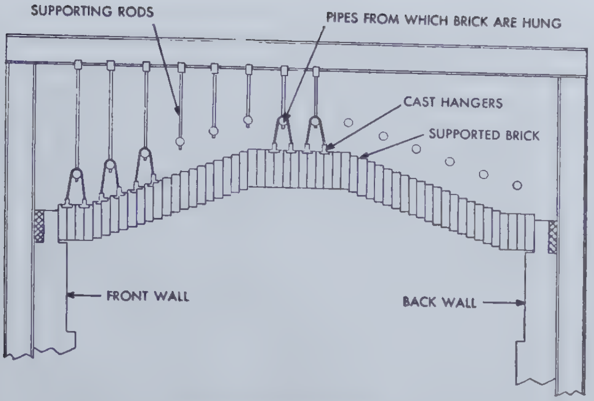

Fig. 5—Brick arrangement in the first American suspended basic roof.

illustrations and sketches made by the Maerz Furnace Co., a subsidiary company of the brick producing concern.

Fig. 2 shows the Radex roof. This design consists of a combination of sprung and suspended constructions with frequent holding down devices on the outside of the roof, which determine the roof contour.

The steel superstructure for such roofs is simple. "T" shaped steel members bent concentric to the desired arch shape are fastened to the rigid furnace binding so they cannot move. The skewback channels are also hung from the binding. The front skewback channel is placed directly against the front buckstays, but the rear skewback channel is held a few inches away from the rear buckstays by large helical springs. These springs are sufficiently strong to support the entire weight of the roof.

Ribbed construction is used and the rib brick are tied to the steel "T" irons by iron wires, as shown in fig. 3. The valleys are fully sprung. In earlier designs, special shapes were used so that the valley courses were keyed between the ribs and supported by them. This construction was expensive and has been eliminated, the bonding between adjacent brick being depended upon to support sprung valley courses. Key shaped brick now normally are used for both rib and valley courses. The ribs are usually two courses, about 5 to 6 in. wide. The valleys are usually four courses and about 10 to 12 in. wide. About 1 in. of magnesia powder insulating material is sometimes used on top of the valley courses.

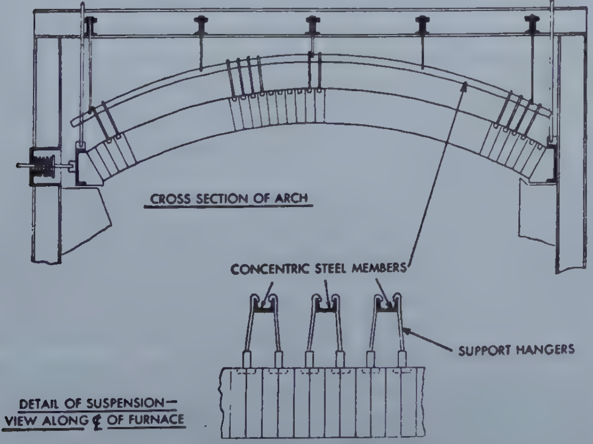

Fig. 6—Arrangement of an American radially suspended roof.

No expansion joints are left in the roof. Steel sheets are inserted in all joints running across the roof, and steel mesh or screen is used in joints running along the furnace. The absorption of the oxide product of this steel by the brick is expected to provide some expansion relief.

With this arrangement of steelwork, replacement of brick in the roof as a patch is difficult. Therefore, the only provision for patching is a supply of special shaped arch filler brick designed to fit between the external portions of the rib courses, as shown in fig. 4. Some reports indicate that the arch brick must be cut to fit the individual valley sections on the job.

In the development of this design, trials of fully sprung roofs and sprung roofs with external steel jackets were tried before the including suspension designs were evolved. It is apparent that the use of suspension was essential to the success of the construction.

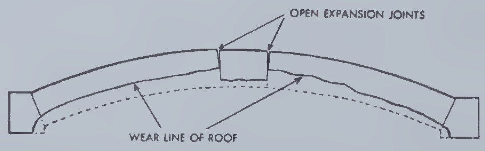

Fig. 7—Wear pattern of a basic arch, resulting from the shearing stresses set up by expansion joints.

Before evaluating merits of the Radex roof, it is necessary to review the development of basic roofs in America to establish the essential requirements of a basic roof design for American operations. American basic roof designs are still in the development stage and existing roofs do not necessarily incorporate all desirable design features. However, enough experience has been obtained on American furnaces to indicate the essential features of basic roof designs.

First attempts at suspended basic roofs for metallurgical furnaces in America were made in the copper industry. Suspended arch companies, refractories manufacturers, and plant operators were involved in this development. The development of suspended designs in America is illustrated by sketches and diagrams from drawings engineered by the M. H. Detrick Co., Chicago.

Fig. 5 illustrates the first suspended design used. Rectangular tile were hung vertically from pipes, which in turn hung from the steel superstructure, the desired contour being achieved by corbelling the brick. This design worked successfully on many copper industry furnaces and is still used. However, in the open hearth, it was unsatisfactory because the corbelled sections wore rapidly.

Such construction caused shearing stresses to be applied to all corbelled brick. Basic refractories are relatively weak at elevated temperatures and usually will break or tear if excessive or unbalanced stresses are exerted upon them.

They are not sufficiently strong to withstand the stresses set up by such construction in an open hearth roof.

Two steel companies made trials of a succession of such roofs with various basic refractories. Both were unsuccessful and discontinued their work. It was obvious that a design that included a true arched roof was essential.

Fig. 6 shows the arch that was developed. This is the radial roof, the brick and their hangers lying along radii of the arch. In this construction, a curved steel member concentric with the desired arch is hung from the furnace binding. From it by means of hanger castings the brick are suspended. The brick are partially supported by the skewbacks, but only enough to hold them in desired positions. Most of the weight is carried by the suspension.

Originally the skewbacks for such arches were fixed on the buckstays, but later the rear skewback was suspended and moved towards the furnace centerline, being supported laterally by springs. Most experience on American all-basic furnaces has been obtained under arches of this design.

Such arches showed marked improvement in life over previous designs. However, as they became thin, they exhibited a tendency to rise and buckle, eventually necessitating roof patches even though the bricks patched were sufficiently thick to endure considerable further service. The springs were applied to the rear skewback to correct these conditions, but while they decreased the action, the rising and buckling of thin sections of the roof continued.

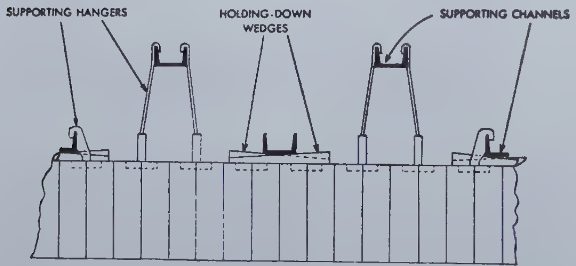

Fig. 8—Arrangement of hold down devices on an American basic roof.

When such action occurs, pressure is applied to the hot faces of the basic brick. This is detrimental in the corbelled construction and probably causes accelerated wear here also. However, patching normally is required because of the complete loss of mechanical stability of the structure.

The chief cause of this rising and buckling action appears to be growth of the roof resulting from oxidation of the steel plates in the cooler part of the joints. The volume of the plate oxide is approximately three times as great as that of the original steel. This oxide can be absorbed by the brick material and this action takes place rapidly near the hot end of the brick. However, near the cold end of the brick, absorption of the oxide is low unless considerable pressure is applied across the joint. That the oxides will be absorbed by the basic brick at lower temperatures has been demonstrated in rotary cement kilns where basic linings with plates in the joints are laid up without any provision for expansion or growth. After service at comparatively low temperatures, the plates are completely oxidized and are totally absorbed. Thus, growth of the roof can be stopped in two ways; first by decreasing the amount of metal present, and second by increasing the pressure applied across the joints.

Trials of various amounts of metal in the joint have not been concluded and have not yielded definite results. Somewhat less metal than has been common will likely prove more desirable. The presence of a certain amount of metal is essential to refractory life, and it cannot be completely eliminated.

The effect of pressure on the joints in inhibiting roof growth has been shown in recent trials. The original radial roof had fixed skews and provided for thermal expansion only by means of expansion joints. This roof rose off the hangers shortly after the start of its campaign. However, it yielded one of the best results obtained to date. To prevent the rising action, springs were applied to the rear skewback and only low pressure was supplied. The roof as a whole did not rise off its hangers until the allowed skewback movement was completely taken up, but local buckling still continued. Subsequently, more skewback movement was allowed. As a result, growth of the roof increased. Recently on one furnace on which spring pressures have been increased so that about 10 psi is applied to the arch, roof growth has been materially decreased. Further tests with varied pressures have been proposed to determine optimum conditions.

With pressures applied across the arch, it is not possible to provide for thermal expansion by expansion joints. The expansion must be taken up by springs on the skewbacks. This is advantageous because expansion joints coupled with plate oxidation cause shearing stresses to be set up in the brick, with resulting accelerated wear.

Expansion joints in service frequently close only at the hot face. Thus, any pressure applied to the brick is carried only at or near the hot face. Meanwhile, with the cold end of the joint being open, the roof brick are apt to be relatively loose near the joint and plate oxidation without absorption proceeds rapidly. This places the brick adjacent to the expansion joint in shear. As soon as one brick breaks, a corbelled condition results and the next adjacent brick is placed under shearing stress. The end result of such action is shown in fig. 7, which shows the wear pattern of a basic port roof recently observed.

Accelerated roof wear can occur from expansion joints regardless of whether they run across or along the arch. This was demonstrated by a series of campaigns on one basic furnace during which the longitudinal expansion allowance was increased with each consecutive rebuild. Roof life decreased in almost directly inverse proportion. Expansion allowances in this direction now have been decreased drastically. It appears that longitudinal expansion allowance should be no more than 1 pct and should occur as many small joints rather than as a few large ones. Since it is not practical to provide thermal expansion relief by springs along the length of the roof as is done across the arch, it does not seem advisable to eliminate all expansion joints in this direction.

Since it is necessary to increase pressures on the joints and to decrease or eliminate expansion allowance to improve performance, some provision for holding the roof down to the desired contour by external means must be provided. Ribbed construction would stiffen the arch to the buckling forces acting across the arch, but would not resist forces acting along the arch. Also, the extra cost of the longer rib brick and the increased wastage of unused brick at the end of a campaign tend to make this practice uneconomical. It is necessary to use external bracing or holding devices that will maintain both roof contour and position. Present American designs incorporate such provisions.

Fig. 8 illustrates the features of the most advanced present designs. This arrangement consists of a radial roof to which hold down devices have been added and other improvements have been made. The hold down is achieved by dropping alternate concentric curved supporting members to a position about 1 in. away from the brick where they are fixed in place. Wedges are inserted between the brick and the supporting member, each wedge being along a joint and in contact with eight brick. Thus, alternate groups of four courses each (14 in. along the roof) are held in fixed position.

With this construction, roof patching can be accomplished. Even the held down brick are accessible for replacement if adjacent brick that are not held down are knocked in.

Skewback suspension and support should be altered from existing arrangements in this design. Best design would include springs on both front and backskews to minimize movement of individual brick. However, because of difficulties entailed in supporting door frames on the front wall, interference with charging machine movements, etc., the spring support is confined to the rear skewback. Since the hold down devices will maintain the roof in a fixed contour, expansion of the roof cannot move the skew horizontally without slippage in the joints. Movement should be allowed in a tangential direction at the skew point. This can be done by moving the suspension point of the skewback channel to a position along the radius of the arch to the skew point and by canting the spring to the tangential position. Fig. 9 shows a preferred design.

These arrangements satisfy virtually all requirements of the basic refractories. Pressure is kept away from the hot face and is distributed evenly. If oxidation growth occurs, the resulting increased pressures will affect only the cold ends of the brick where they are amply strong to withstand the stresses set up. Such construction should yield excellent results.

Summarizing the foregoing, the most essential design features for basic roofs in American practice are: 1—Adequate suspension of all the brick in the roof. 2—A true arched contour. 3—External bracing of the roof which will prevent deformation of the arch. 4—No expansion joints across the roof and less than 1 pct expansion allowance along the length of the roof to be provided in small increments. 5—Spring skewback support which allows movement tangential to the arch. 6—Skewback support springs of sufficient strength to provide pressures approaching those normal in sprung arches. 7—Provision for hot patching of the roof.

In considering European roof designs on the basis of these essentials, several shortcomings of the European designs are evident. Suspension arrangement of such designs probably are not strong enough to carry the weight of American roofs. The skewback arrangement does not allow the best movement. No provision for hot patching of the roof is allowed.

In other respects, European designs meet the requirements of American practice. To their advantage, installation cost would be less than that of American designs because of the lighter steelwork and absence of hanger castings. However, this would be more than offset by higher repair costs.

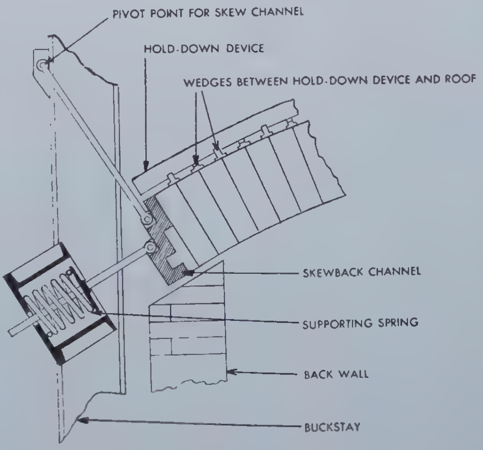
PIVOT POINT FOR SKEW CHANNEL
HOLD-DOWN DEVICE
WEDGES BETWEEN HOLD-DOWN DEVICE AND ROOF
SKEWBACK CHANNEL
SUPPORTING SPRING
BACK WALL
BUCKSTAY

Fig. 9—Preferred skew arrangement and support for American basic roofs.

In general, it appears that being faced with similar problems, American and European engineers have arrived at answers that are almost identical in engineering principles, but American designs are better suited to American practices.

Part II of this article will appear in the July issue of Journal of Metals.

Vanadium Treated, Non-Aging, Rimming Steel

For Deep Drawing Quality Sheet

by S. Epstein,
H. J. Cutler and J. W. Frame

FOR many years sheet steel for drawing has been made of rimming steel and most drawing sheet is still so made. One of the main advantages of rimming steel is its very good surface. Ordinary rimming steel has a serious drawback, however, in being subject to aging during storage. Such aging may be the cause of increased hardness, reduced drawability, and the formation of stretcher strains in the drawn part.

To obviate aging aluminum-killed steel came into use for deep drawing sheet about 15 years ago. This steel is killed by adding to the molten steel about 4 or 5 lb of aluminum per ton of steel. Sheet made of such aluminum-killed steel is non-aging. Properly skin-rolled sheet of this sort will not show stretcher strains in drawing, even after the longest storage periods; nor will there be an increase in hardness. The non-aging aluminum-killed steel has excellent deep drawing properties. Despite the large addition of aluminum the interior of sheet made from such steel is surprisingly free of aluminum-oxide inclusions.

The surface of aluminum-killed steel sheet, however, is not as good as that of rimming steel sheet. The poor surface of aluminum-killed steel seems to be caused by aluminum-oxide inclusions, which form at the outer surface of the ingot as the steel is poured and solidifies. Surface defects caused by such aluminum-oxide inclusions may not only mar the appearance of the drawn part but also may be a cause of breakage.

Because of this serious disadvantage of aluminum-killed steel, a way was sought of making a rimming non-aging steel. Vanadium combines readily with nitrogen and does not act as a strong deoxidizer, and by its use steel can be rendered non-aging without killing. Vanadium proved a weak deoxidizer, not much stronger than manganese, but it has a strong affinity for nitrogen. Thus, the addition of about 0.05 pct vanadium, or about 1 lb per ton of steel, to rimming steel does not deoxidize the steel enough to affect the rimming action. Yet sheet made from such vanadium-treated rimming steel can be completely non-aging.

The vanadium-treated non-aging steel rims perfectly, has the good surface characteristic of rimming steel, and has good deep drawing properties. Over 100,000 tons of vanadium-treated sheet steel have been produced. Every heat of this steel rimmed perfectly, without a single exception. The vanadium-treated steel has been used for some of the toughest deep drawing jobs, such as in the fabrication of most difficult automobile front fenders. However, the bulk of it has been applied on deep drawing jobs of medium severity.

To explain better the use that may be made of vanadium-treated deep drawing steel, the difference between deep drawing steel delivered as sheets and in coils must be understood. In recent years there has been an increase in demand by sheet consumers for sheet steel in coil form. Many customers want drawing sheet delivered in coils because these can be blanked with less handling than separate sheets and because the blanks can be better spaced and fitted-in so as to reduce scrap loss.

The poorer surface of aluminum-killed steel is a greater drawback when the steel is delivered in coils. Processed as sheets, individual defective sheets can be rejected during mill inspection and the prime material can be shipped. In the case of coils, however, a defective portion of the coil can not be rejected and the rest of the coil shipped. A whole coil either must be rejected or shipped. Since many coils of aluminum-killed

---

S. Epstein and J. W. Frame are research engineers, and H. J. Cutler is engineer of tests for Bethlehem Steel Co.

This paper was presented at the 1950 Open Hearth Conference of the Iron and Steel Div., AIME, at Cincinnati.

steel contain some steel with poor surface it is impossible to reject all such coils. A greater amount of surface defects in coils of aluminum-killed steel than in coils of rimming steel must be expected.

The good surface of vandadium-treated rimming steel, therefore, becomes especially advantageous when the steel is shipped in coil form. As a consequence most vanadium-treated steel now being made is processed and shipped as coils.

The high cost of vanadium makes it necessary to utilize the product of the whole ingot for deep drawing, including the top cuts. It has seemed preferable not to risk using these top cuts on the toughest jobs.

On the jobs of medium severity on which the bulk of the vanadium-treated steel has been applied, such as automobile hood tops, quarter panels, and some front fenders, vanadium steel has made an excellent record. On these jobs it previously had been found necessary to use aluminum-killed non-aging steel. The vanadium-treated rimming non-aging steel gave appreciably lower breakage rejections in these stampings than either our Bethlehem's aluminum-killed steel or that of competitors. This was probably the result of the better surface of the vanadium-treated steel. There is, of course, a large tonnage in these deep drawing jobs of medium severity.

In making the vanadium steel the same open hearth practice is used as for ordinary rimming steel for deep drawing except that 1 lb of vanadium per ton of steel is added in the ladle. The rimming action in the molds is controlled with small aluminum additions, just as with ordinary rimming steel.

In the slabbing mills the same yields are obtained as in ordinary rimming steel, that is about 85 pct yield, and the same amount of conditioning by scarfing is given the vanadium steel. For the same final gage of the deep drawing sheet the vanadium steel can be hot rolled to a thicker hot band than aluminum-killed steel. This is a marked advantage, especially in wider sheets. The thicker hot band gives less surface to be pickled and is easier for the hot mill to handle. The reason the thicker hot band can be used with the vanadium steel is that the amount of cold reduction with aluminum-killed steel must be held under 50 pct to get the desired coarse as-annealed grain; whereas with rimming vanadium-treated steel, it is possible to get a satisfactory as-annealed grain with cold reductions of as much as 60 pct.

To obtain the desired grain structure after cold reducing and annealing in ordinary rimming steel and in aluminum-killed steel, it is advisable to cool the hot band rapidly with water sprays as it emerges from the finishing stand, and to coil it cold or under about 1200°F. With the vanadium-treated steel, it was discovered that the best grain structure after annealing is obtained by finish rolling the hot band at a high temperature of over 1600°F, and then coiling it hot, or above approximately 1400° F.

Vanadium costs $2.90 per lb so that the addition of a pound of vanadium per ton of steel adds $2.90 to the ingot cost, or approximately $4.50 to the cost of the finished product, since the yield of prime product is only about 2/3 of the ingot weight. This high cost of the vanadium in vanadium-treated steel as against the much lower cost for the aluminum in aluminum-killed steel may be made up, however, by: 1—The better slab yield in the vanadium steel than in aluminum-killed steel; 2—Less surface conditioning, 3—Using a thicker hot band; and, above all, 4—Lower rejections for poor surface during inspection of the finished product.

Table I—Additions to Vanadium-Treated Rimming Non-aging Steel

Addition	Where Added	Amount Added Per ton of Steel
Ferromanganese, 80 Pct	Furnace	3.6 lb
Ferromanganese, 80 Pct	Ladle	About 7 lb
Silicomanganese, 67 Pct	Ladle	1.4 lb
Ferrovanadium, 52 Pct	Ladle	2.0 lb (1 lb vanadium)
Sodium Fluoride	Mold	1 oz
Shot Aluminum	Mold	Varied to control rimming action, usually about ½ oz

A somewhat less obvious point in favor of the vanadium steel is that a greater percentage of prime deep drawing sheet can be obtained from a given ingot tonnage with vanadium-treated steel than with aluminum-killed steel. Under the particular conditions at Bethlehem Steel Co., this increase in prime deep drawing product is about 8 pct. The difference between the cost of vanadium-treated steel and aluminum-killed steel will vary from plant to plant, depending on such factors as 1—whether or not the aluminum-killed steel is hot topped; 2—the facilities for rapid charging after stripping (the surface of aluminum-killed steel appears to be more sensitive to injury because of long "time-out" after stripping); 3—whether the top slabs of aluminum-killed steel are diverted to applications other than deep drawing steel, 4—on the type and amount of slab conditioning used on aluminum-killed steel, and 5—on the facilities for cold coiling after hot rolling the hot band. In many cases the cost of the vanadium steel will be no more than that of aluminum-killed steel, and it may even be substantially less. The fact is that aluminum-killed steel is much more expensive to make than many steel mills probably realize.

There is little consistency about the surface of aluminum-killed steel. After a run of passable surface there may be an epidemic of bad surface, with the rejections of the finished product running as high as 20 pct. The bad surface of aluminum-killed steel was recognized from its inception and it has not been overcome yet. Such recourses as pouring through splash cylinders, adding special fluxes such as cryolite in the mold, special mold coatings, and entirely skinning and pickling the slab have been found to be relatively ineffective. On the other hand, vanadium rimming non-aging steel provides, in large measure, a solution to this problem.

As has been stated, open hearth melting practice for the vanadium-treated steel is the same as that of ordinary rimming steel for drawing, except for the addition of the vanadium.

Table I shows additions made to the molten vanadium-treated steel. The ferromanganese additions conform to usual practice and are intended to give a manganese content in the finished steel of about 0.3 pct. The silicomanganese addition is not a special requirement, but it was part of the practice before vanadium treatment was started and was left unchanged. No adverse effects have been found on either the rimming action or on the cleanliness from this use of silicomanganese instead of aluminum. It is, however, more common to use the latter.

There has been no adverse effect on cleanliness from the ferrovanadium addition. The ferrovanadium is added to the ladle after the ferromanganese and silicomanganese additions, so as to obtain the optimum recovery of vanadium. This recovery has averaged about 65 pct. Ladle additions are made after about 1/3 of the heat has been tapped.

The small mold addition of sodium fluoride, the same as in ordinary rimming steel, is made to improve rimming action. For controlling this about ½ oz of shot aluminum in the mold per ton of steel usually is required on vanadium-treated steel. This amount of aluminum averages only slightly less than with ordinary rimming steel. Most excellent rimming action invariably has been obtained on the vanadium-treated steel.

For full non-aging properties, a residual vanadium content of about 0.03 pct should be obtained. With appreciably less than this, poor non-aging quality may occur. This residual content of 0.03 pct will be obtained by adding 1 lb of vanadium per ton of steel, with a recovery of vanadium of 65 pct.

In hot rolling vanadium-treated steel it has proved desirable, when wishing to get as soft steel as possible, to finish the hot band at a high temperature—over 1600°F—and then coil it hot—at about 1400°F—without cooling with water sprays along the runout table.

Fig. 1 illustrates the effect on the as-annealed grain size of the vanadium-treated steel coiled cold and coiled hot. After cold coiling the as-annealed structure shows fine grain near the surface. After hot coiling, the as-annealed grain structure at and near the surface comes out coarser and the steel consequently is softer.

Fig. 1—After coiling cold, vanadium-treated steel has finer as-annealed grain size at the surface, shown in upper area of A. After coiling hot, the as-annealed grain size at the surface is coarser, about the same size as in the interior area, as shown in B. (100x)

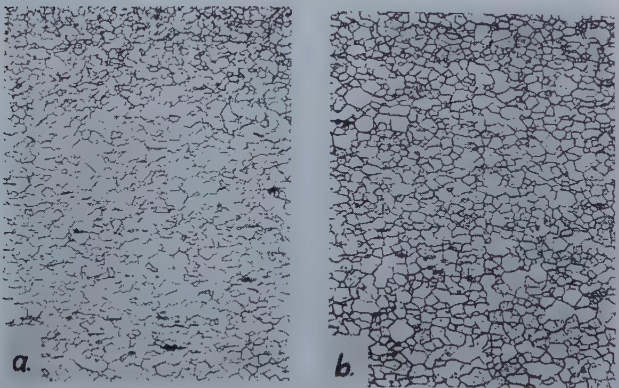

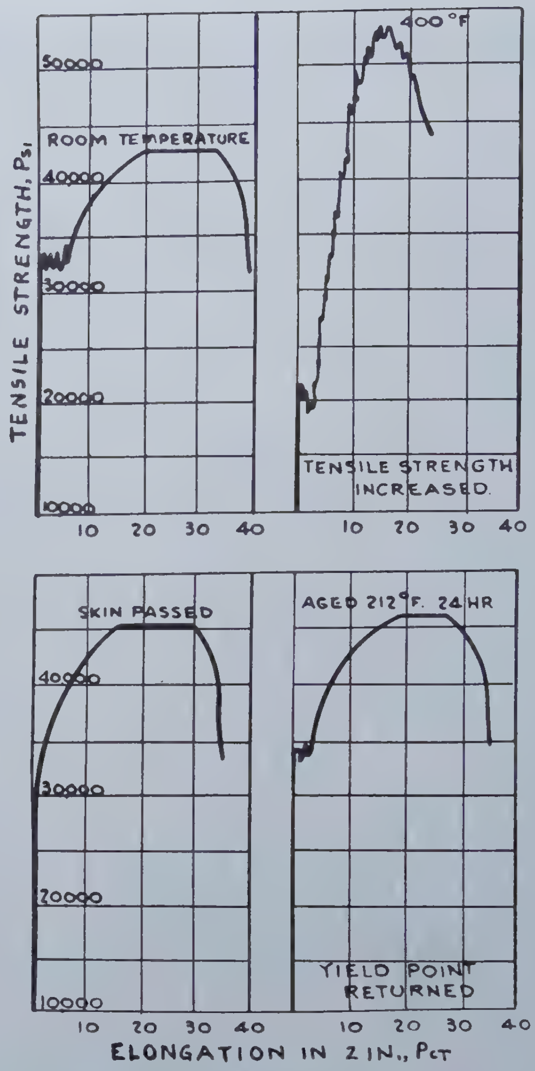

Ordinary Rimmed Steel

Fig. 2—Stress-strain curves for

The vanadium-treated rimming steel is fully as non-aging as the aluminum-killed steel. One of the most convenient and accurate ways of distinguishing between aging and non-aging steel is to determine the tensile strength at room temperature and at the so-called "blue heat" temperature of about 400°F. Aging steel has a considerably higher tensile strength at 400°F than at room temperature, whereas non-aging steel has a considerably lower tensile strength at 400°F than at room temperature.

The difference between aging and non-aging steel, as manifested by tests at 400°F is shown in the upper half of fig. 2. The ordinary rimming steel being an aging steel shows a much higher tensile strength at 400°F whereas the aluminum-killed and the vanadium-treated steels, being non-aging, show a lower tensile strength at 400°F. In regard to this characteristic of non-aging steel, the vanadium-treated steel behaved exactly as the aluminum-killed steel.

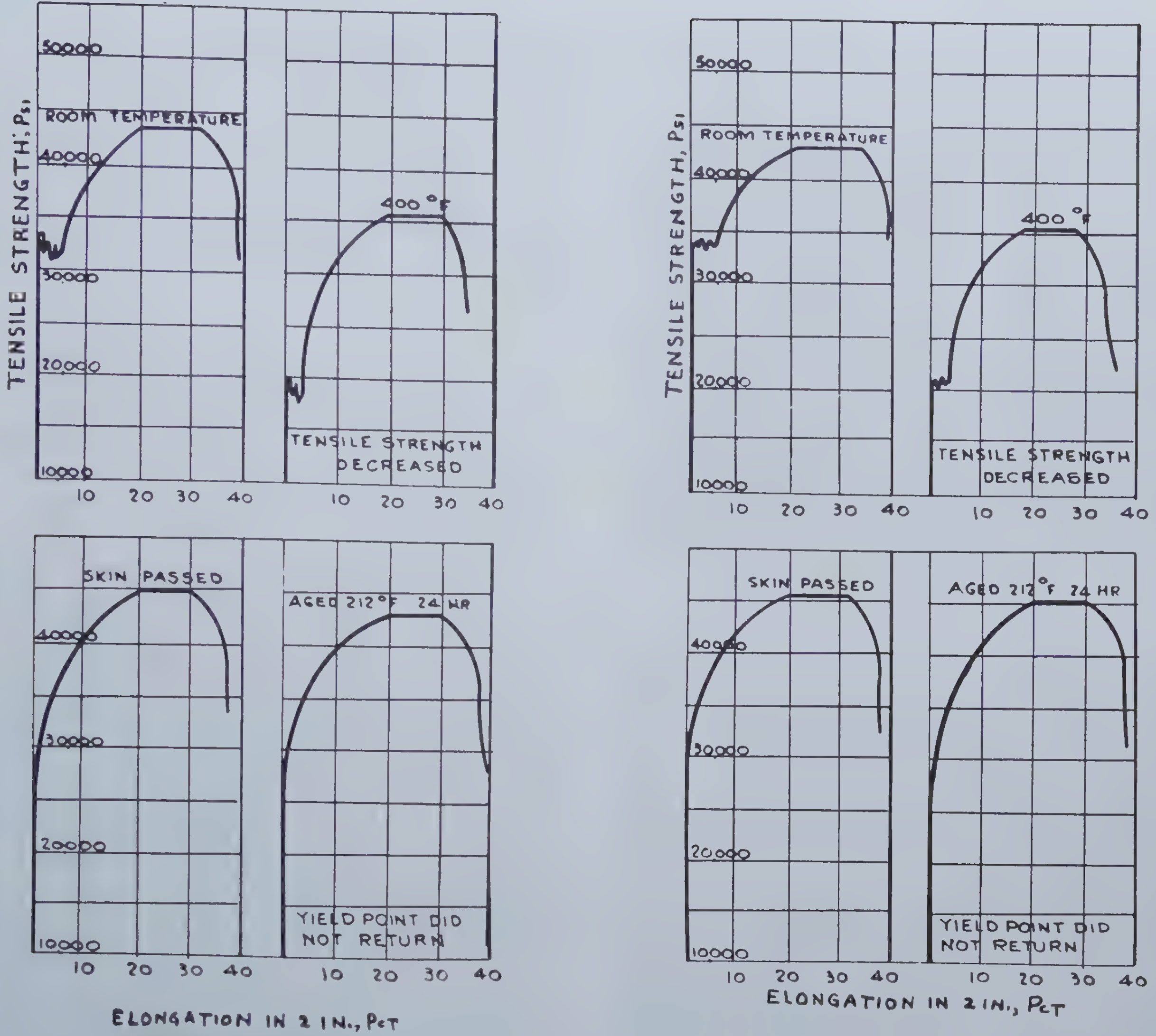

Aluminum Killed Steel

Vanadium Treated Rimmed Steel

aging and non-aging steels.

The tensile test results in the lower half of fig. 2, these tests having all been made at room temperature, manifest the aging phenomenon not by the increase in tensile strength at 400° F but by the return of the yield point after skin rolling and aging at 212° F. The ordinary rimming aging steel, which shows a higher tensile strength at 400° F, shows a return of the yield point upon accelerated aging at 212° F after skin rolling. The non-aging steels, which show a lower tensile strength at 400° F, do not show a return of the yield point upon accelerated aging at 212°F after skin rolling. In such steel, aging will not cause the reappearance of stretcher strains after skin passing, even after the most prolonged storage periods. In this respect also, the vanadium steel is fully as non-aging as the aluminum-killed steel.

In fig. 3 tensile samples are shown of aging and non-aging steel tested at room temperature and at 400° F. In samples tested at room temperature, there is practically no difference between the ordinary rimming steel aging sample and the two non-aging samples; all three samples showing about the same high ductility. In the samples tested at 400° F, however, the two ordinary rimming steel aging samples look quite different from the two non-aging samples, the aging samples showing much lower ductility.

The difference between the tensile strength at room temperature and at 400° F has been termed the *aging index*. Table II shows typical hardness and tensile properties of aging and non-aging steel and also typical *aging indexes*. It will be observed that the ordinary rimming aging steel has a plus *aging index* (+8000 psi), indicating that the tensile strength at 400°F is 8000 psi higher than at room temperature. The non-aging steels each have a minus *aging index* (—7000 psi), indicating that the tensile strength is 7000 psi lower than at room temperature. A minus aging index as large as—7000 psi indicates fully non-aging steel.

The vanadium-treated rimming steel has this large minus *aging index*, just as large as the fully aluminum-killed steel. The Rockwell B hardnesses and the elongations in the tensile test of the vanadium-treated steel are likewise the same as in the fully aluminum-killed steel.

The high cost of vanadium makes it necessary

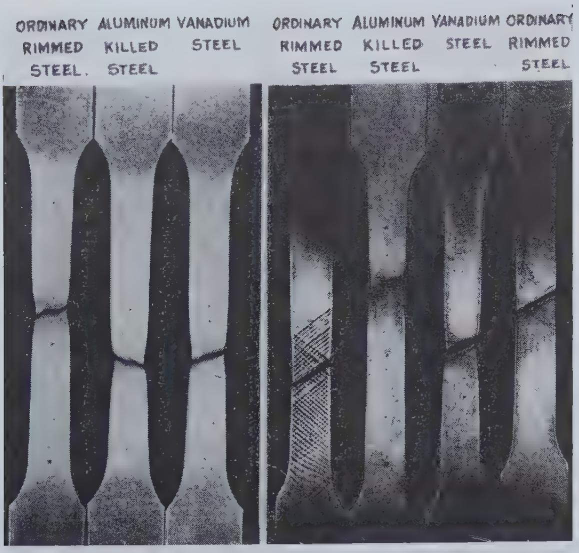

Fig. 3—Appearance of samples of aging and non-aging steels tested at room temperature (left) and at 400°F. (right).

to utilize the product of the whole ingot of vanadium-treated steel for deep drawing purposes, including the top cuts. Data comparing the composition and properties of top and bottom cuts of vanadium-treated steel are, therefore, of interest.

Table III shows representative average analyses from 160 top and bottom cuts of 80 ingots from 20 heats of vanadium-treated steel. The full slab yield from the ingot is 85 pct, the top crop being 9 pct, the bottom crop 4 pct, and the scaling loss 2 pct. These ingots were divided into three equal cuts—top, middle, and bottom cuts. Samples for analysis were taken from the finished sheets, from the top and from the bottom cuts from the midway position in the sheet, between the edge and center. The sheet to represent each cut was selected at random.

Table II—Typical Hardness and Tensile Properties

	Ordinary Rimming Steel	Aluminum-Killed Steel	Vanadium-Treated Rimming Steel
Hardness, Rb	40	40	39
Yield Strength, Psi	26,000	24,200	24,500
Tensile Strength, Psi	43,200	44,500	43,300
Elongation in 2 in., Pct	41	42	42
Aging Index, Psi	+8,000	—7,000	—7,600

As may be seen in table III, there was no significant difference in the average analyses in carbon, manganese, and vanadium between the top and bottom cuts. The average analyses for sulphur from the top cuts were somewhat higher than average analyses from the bottom cuts. However, the sulphur contents in the top cuts were not unduly high.

Table III—Difference in Composition Between Top Cuts and Bottom Cuts of Vanadium Steel*

Analysis, Pct	Top Cuts	Bottom Cuts
Carbon	0.05	0.05
Manganese	0.27	0.27
Sulphur	0.029	0.025
Vanadium	0.034	0.035

* Average analyses from midway between edge and center of sheet from 160 top and bottom cuts of 80 ingots from 20 heats of vanadium-treated steel.

Table IV presents data on the properties and performancé of sheet from top cuts and bottom cuts of a heat of vanadium-treated steel. This was a 135-ton heat and the sheet product of the whole heat, including the entire product of the top cuts, was used for drawing a difficult front fender. In this heat each ingot was divided into only two cuts, a top cut and a bottom cut.

There was very little difference between the composition and properties of the top and bottom cuts. In regard to performance, the amount of breakage was somewhat higher on the top cuts than on the bottom cuts, but considering the severity of the job performance of the top cuts was satisfactory.

The properties shown in tables II and IV were obtained after processing as sheets. When processing as coils, the properties may not be quite as good. However, excellent performance, both with regard to low breakage and freedom from stretcher strains, of a large tonnage of vanadium-treated steel in jobs of medium severity indicates that vanadium-treated steel in coil or sheet form is applicable to such jobs, and the top cuts as well as the bottom cuts can be utilized.

Table IV—Composition, Properties, and Performance of Top and Bottom Cuts of Vanadium Steel.*

	Composition, Pct									
	Top Cuts					Bottom Cuts				
	C	Mn	S	P	V	C	Mn	S	P	V
PROPERTIES:	0.05	0.29	0.030	0.006	0.044	0.04	0.26	0.026	0.006	0.037
Hardness, Rb			37					35		
Yield Strength, Psi			27,850					27,650		
Tensile Strength, Psi			44,500					43,550		
Elongation in 2 in. Pct			42					43.5		
Aging Index, Psi			—5800					—7700		
PERFORMANCE:										
Breakage in One of the Most Difficult Front Fender Stampings, Pct			3.4					1.7		

---

* Average analyses, hardness, tensile and aging properties, and performance of 0.045 in. gage sheet from the top and bottom cuts of an entire heat of vanadium-treated steel.

Oxygen Jets Through the Open Hearth Backwall

by A. E. Reinhard

An experimental program was undertaken early in 1947 by Great Lakes Steel Corp., to determine the value of oxygen in open hearth steel production and to devise a means of oxygen introduction into the bath for carbon removal. This oxygen introduction had to: 1—Offer no interference with the normal flow of materials across the charging floor, 2—serve as an efficient tool during the refining period, 3—be operated easily and efficiently by the furnace operator, namely the first helper, requiring no additional furnace crew members, 4—be of such a design as to be an integral part of furnace equipment requiring a minimum of maintenance.

With these aims in mind, the Engineering Dept. of the company designed and constructed a system utilizing water-cooled, high-velocity jets, developed with the Linde Air Products Co., which has functioned quite satisfactorily.

Each of the four 250-ton furnaces in the No. 2 Shop has two water-cooled jets on individual motorized injector mechanisms above the platform at the rear of the furnace, mounted so that the jets can be introduced through a water-cooled port in the backwall to a position over the bath opposite Nos. 2 and 4 charging doors, respectively, midway between front and backwall. Location of the jets is as shown in fig. 1.

Oxygen of 99.5 pct purity is supplied by a Driox plant to all furnaces in the shop by a 6-in. main, from which 4-in. lines feed individual regulator stations at each furnace. From this point, a 2½-in. line leads through a quick opening solenoid valve, operated from the control board, to a point near the front of each injector mechanism where a 1½-in. flexible, high-pressure hose connects. This hose carries oxygen to the hose entrance at the rear of the jet. A bypass arrangement around the solenoid valve is provided so that a reduced oxygen flow through the jet prevents possible plugging of the jet nozzle when positioning over the bath. A safety, hand valve in the oxygen line, located at the end of the 2½-in. pipe and opened just prior to operation, permits the bypass to function.

The jet itself is about 20 ft long, made up of an 18 ft length of 4½-in. OD seamless steel tubing through which runs concentric pipes carrying oxygen and cooling water to a replaceable, nozzled, copper head. This head is brazed to the entry end of the jet tube. The jet head, preferred after considerable experimentation, is 12 in. long × 4½ in. OD at its junction point with the jet-tube, tapering to 4¼ in. OD at its rounded nose. A 17/32-in. (0.531-in.) diam. hole, drilled at a 45° angle to the longitudinal axis of the jet head and at a point along the taper behind the nose, serves as the nozzle. This injects oxygen from the underside of the jet head when in position over the bath. Detail of the jet, in a cutaway cross-section, is shown in fig. 2. Oxygen pressure at the jet for the recommended flow rate of 30,000 cu. ft per hr is 140 to 160 psi.

Cooling water, both supply and return, is carried through 2-in. lines and 2-in. flexible hose at a pressure of 20 to 25 psi. The flexible hose section of the water system parallels that of the oxygen supply system providing freedom of jet movement. Under operating conditions, this cooling method has proved quite adequate as the temperature of return water is only slightly higher than that of the service supply.

The jet and its injector mechanism, mounted at the rear of the furnace, with the jet in its retracted position, is shown in fig. 3. A safety platform, not shown, is provided at each jet for safe maintenance. It extends out over the pit sufficiently to permit servicing the rear of the installation. The backwall port, the jet and its manner of suspension, the motorized traversing mechanism and limit switches, and the trough arrangement supporting the flexible hoses feeding the jet can be seen. Movement of the jet is controlled from the rear of the furnace and from an operating board on the charging floor. The

---

A. E. Reinhard is Superintendent of Steel Production at Great Lakes Steel Corp., Detroit. This paper was presented at the 1950 Open Hearth Conference of the Iron and Steel Div., AIME, at Cincinnati.

approximate 15° angle at which the jet enters the furnace and approaches the bath is shown in fig. 3. When coupled with the 45° nozzle angle incorporated into the jet head used, oxygen stream to the bath is provided with an angle of incidence of 60° from horizontal or 30° from normal. The path of the oxygen stream is inclined toward the furnace frontwall. Also evident in this installation is the adequate platform space behind the furnace so that no appreciable interference is experienced with pit operations.

A certain amount of experimentation has been necessary with flow rates, position relative to the bath, number and size of nozzles, jet head design, stage of heat, slag condition, and furnace operation to provide an efficient refining tool of minimum hazard to the furnace and operators and requiring minimum maintenance. Trials, carried out at medium carbon levels, the first jet head used was of goose neck design having a thread-in, divergent nozzle of 17/32-in. throat designed to operate at an oxygen flow rate of 20,000 cu. ft per hr.

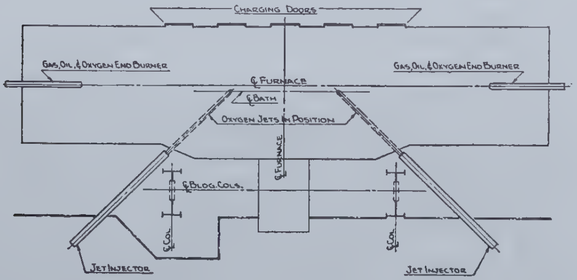

Fig. 1—Location of the open hearth oxygen jets in use at Great Lakes Steel Corp.

Excessive burning out of the nozzle plus inability to penetrate the bath brought about a simultaneous change involving an increased flow rate to 30,000 cu. ft per hr and a single straight-walled, drilled-out nozzle 17/32-in. diam. With the increased velocity of the oxygen stream through the straight-walled nozzles, nozzle burn outs were minimized and penetration was satisfactory.

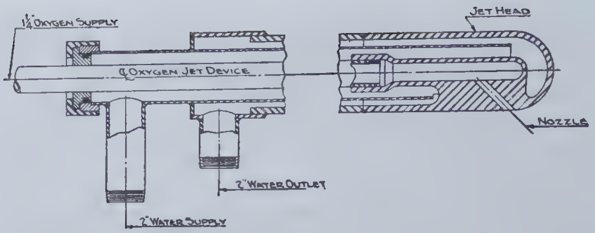

Fig. 2—The jet is 4½ in. seamless tube carrying concentric pipes for oxygen and water for cooling. The head of the jet is copper, which is brazed to the entry end of the tube.

Two jets, operating in this manner at a height of 6 to 8 in. above the slag, efficiently directed oxygen through the slag to the interface, quickly creating a carbon boil over the entire bath. With optimum flow rate and nozzle size determined, the evolution of the jet head to the design now in use, shown in fig. 4, consisted of streamlining to facilitate cleaning and retraction from the furnace. Fig. 2 shows the same jet head in cross section as an integral part of the jet.

Trials have been made also with multiple-nozzle jet heads positioned above and immersed in the slag, as with the single hole design described. Difficulties again were experienced with nozzle burn out and decreased efficiency because of the lack of penetration. No advantage in minimizing splash was realized with the multiple-nozzle design over the single-hole jet head.

Initially, oxygen injection periods were restricted to starting, at bath carbons of 0.30 to 0.40 pct or less. The purpose was to accomplish as much as possible without risking considerable refractory damage. Experience has shown since that limiting starting carbons to that range has proved optimum practice for the No. 2 Shop, which makes soft and low alloy grade heats charged to melt-in at 0.45 pct carbon.

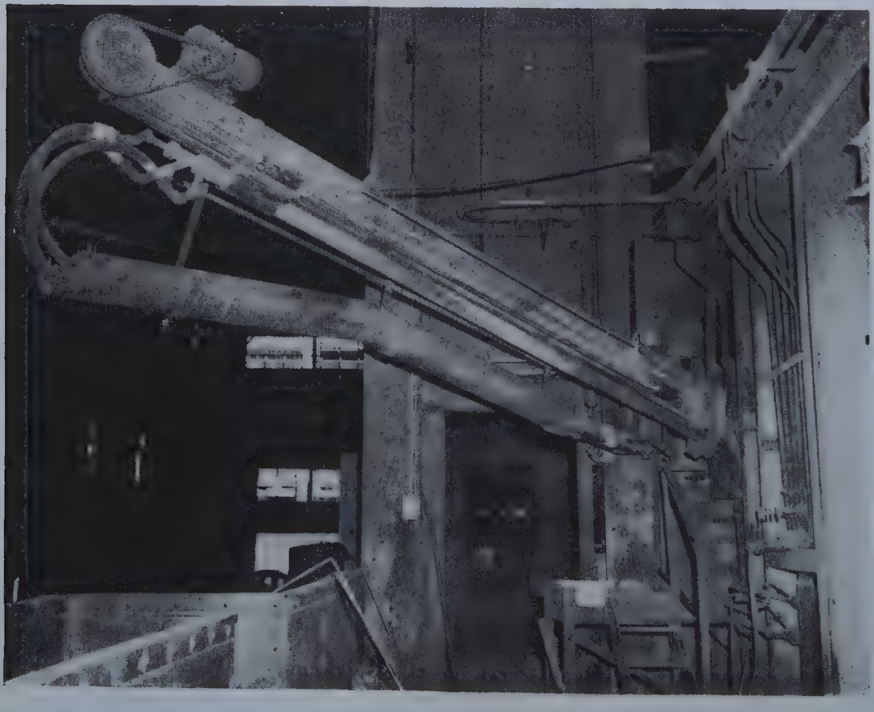

Fig. 3—The jet and injector mechanism mounting at the rear of the furnace. This arrangement permits complete control of the injector mechanism either from the rear of the furnace or from a control panel in front.

With all or nearly all the lime up, and at least partially in solution at the start of the jet period, a rapid shaping up of the slag is possible. This is equally as advantageous as the speed with which bath carbon can be reduced. Water cooled jets permit the operator to continue firing his furnace and maintain slag temperature and fluidity, thereby taking full advantage of bath agitation and increased bath temperature in slag conditioning. Splashing under the jets is greatly reduced when injecting through an open slag, and free passage of the gaseous reactants is permitted without creating a foamy condition. The volume of combustion gases passing through the furnace, with continued firing, assists in protection of the roof by carrying fine particles and fumes to the furnace ends. The jet practice, as outlined, enables the operator to use bath oxygen for rapid decarburization with slag condition keeping pace, so that when tapping-carbon is approached the heat is ready for the melter.

The time from the end of jet period to tap is approximately 30 min, employing the practice described. The creamy tapping slag desired is attained quickly by the addition of small amounts of fluorspar. This reduces the thickened condition usually existing at the end of the jet period. Bath temperature is usually sufficient to eliminate the need of additional time to attain tapping temperature.

Although general practice is to employ two jets simultaneously, each using oxygen at 30,000 cu. ft per hr when bath carbon is within range or lower, there are variations in practice that should be mentioned. Heats melting in at carbons over 0.40 pct are ored down to the preferred range before using jets. Heats melting in at carbons under 0.20 pct usually are worked with a single jet. On occasion, when only one jet is available for usage, heats are worked with jet oxygen and feed ore in conjunction.

Table I

Bath and Slag Changes Resulting from Use of Oxygen

	Bath Analysis, Pct					Slag Analysis, Pct
	C	Mn	P	S	FeO	FeO
Start of Jet O_2*	0.42	0.17	0.057	0.036	0.122	14.25
After 30 min Jet O_2	0.11	0.12	0.014	0.030	0.254	22.58
20 min after O_2 period	0.08	0.10	0.008	0.027	0.338	23.25

*—Oxygen at 60,000 cu. ft per hr through two jets, 30,000 cu. ft per hr through each jet.

Operation of this jet installation has not required the addition of any men to the individual furnace crews. One maintenance man employed on each turn services the four furnaces; operating the regulator stations and inspecting the equipment in the interests of safety. Operation of the mechanized jets is handled by the first helper. There are two manual operations involved; the opening of the backwall-port door and a safety hand-valve in the oxygen line between the quick opening valve and the jet. Switches controlling the movement of the jets and the opening and closing of the flow valves are located on the furnace board. Positioning of the jets over the bath usually is done from the control panel by sighting through an opened charging door.

Fig. 4—Considerable experimentation with jet heads resulted in the choice of this single-hole type.

To determine rates of carbon elimination, chemical analyses were run on series of samples taken just prior to, immediately after and 20 mins. after jet oxygen periods. This latter test approximated the observed time necessary, after shut off, for the induced bath action to subside. Averaged carbon removal rates, starting at the level of 0.30 to 0.40 pct carbon and reducing to 0.08 pct, for the several jet practices were determined as follows:
1—Two jets, each at 30,000 cu. ft per hr, 1.00 point per min; 2—One jet at 30,000 cu. ft per hr with ore, 0.85 point per min; and 3—One jet at 30,000 cu. ft per hr, 0.65 point per min.

Typical of the changes brought about in both slag and steel are the analyses shown in table I, determined on tests taken as indicated on a low alloy heat.

The efficiency of the two jet operation, based on the assumption that the volume of oxygen injected entirely accounts for the carbon removed, is estimated to be in the range of 80 to 85 pct.

Oxygen consumption by jets, for a four furnace operation producing 511 heats over a four month period, averaged 45 cu. ft of oxygen per net ton of ingots. Jets were used singly or in pairs on 60 pct of the heats in this group, the balance melting in such that jets were not needed or advisable.

Maintenance of the jets and associated equipment has not been unduly excessive. The usual care required in the employment of equipment using high purity oxygen is necessary and, when properly carried out, insures adequate life of hoses, piping, valves, and other equipment. The service life of the replaceable jet heads now in use has been about 100 hr, providing optimum practice is employed. Oxygen flow rates less than the desired 30,000 cu. ft per hr per jet adversely affect the degree of penetration achieved and induce rapid nozzle burn out.

Setting Ladle Nozzles

by W. G. McDonough

THE various practices used by the steel industry for setting pouring nozzles in steel ladles can be classified under two general descriptions: (1—Where the nozzle is set from the inside of the ladle, after the lining is cool, and (2—Where facilities are incorporated for removal and replacement of the nozzle from the outside of the ladle bottom while the lining is still hot. A variation of the latter method has been in continuous use for many years at National Works, National Tube Co., on both 60-ton bessemer ladles and 185-ton open hearth steel ladles.

The practice consists of the use of a removable nozzle plate, which is detached from the bottom of the ladle permitting the old nozzle to be broken out. The new nozzle, after being plastered with mud, is inserted into the nozzle brick opening and the nozzle plate is replaced and keyed into position. After sealing the nozzle hole with mud and securing a sand plate over the hole in the nozzle, the ladle is ready for use. The entire interval from the time of finish pouring the last heat to the time the ladle is ready for the next heat is only 12 to 15 min.

The illustration shows a cross section of the nozzle arrangement with the stopper and nozzle in position. Surrounding the nozzle is a well brick, below which is a sleeve brick that rests on the ladle shell. A 2-in. extended removable nozzle plate is keyed to the bottom of the ladle by key bolts extending through the shell. The bottom face of the nozzle plate is provided with lugs into which a sand plate is inserted and secured by small sand plate wedges.

The nozzle in use at National Works is 14¼ in. long, although any length nozzle may be used by varying the depth of the nozzle plate or by altering the depth of the well. The diameter of the nozzle is 7 in.

The well brick consists of two equal sized halves that form a square when placed together, measuring 18 x 18 in.; the well depression is 16 in. diam and 3 in. deep with an additional 3-in. high shoulder at the bottom of the 7¼-in. diam well. The sleeve brick is a one piece refractory block 12 in. square, 5 in. thick, and has a 7¼-in. diam hole.

The nozzle plate may be either cast or fabricated, but fabricated plates are less expensive to make. The plate is secured to the bottom of the ladle by three 1-in. bolts which have slots for the insertion of small keys to hold the nozzle plate in position.

The sand plate is nothing more than a 9 x 18 in. piece of ¼-in. flat steel plate, rounded on one end to facilitate sliding into the lugs in the nozzle plate. It has a ¾-in. hole in the opposite end for inserting a hook to pull it out when opening up the heat. The small wedges, inserted between the nozzle plate lugs and the sand plate, secure the plate into position.

The operations in changing a nozzle on a 185 ton open hearth ladle start with the time the used stopper is knocked out of the ladle until the ladle is opened up to pour the succeeding heat. The gooseneck is sledged to drop the stopper

---

W. G. McDonough is Superintendent of the Open Hearth and Bessemer Dept., of the National Works of National Tube Co. This paper was presented at the 1950 Open Hearth Conference of the Iron and Steel Div., AIME, at Cincinnati.

from a used ladle; the keys are knocked out of the plate bolts; and the nozzle plate is pried off.

A short bar, having a right angle hook on the working end, is inserted into the nozzle hole to break out the old nozzle. After the old nozzle is completely removed, the inside surface of the opening is cleaned out and any rough places are smeared with mud by hand.

The new nozzle, smeared all over with mud, is inserted into the ladle. This mud is made by grinding 24 parts white plastic clay with 5 parts graphite, and mixing to a consistency of soft putty. The nozzle, after being covered with about 1 in. of mud, is inserted into the nozzle opening in the ladle.

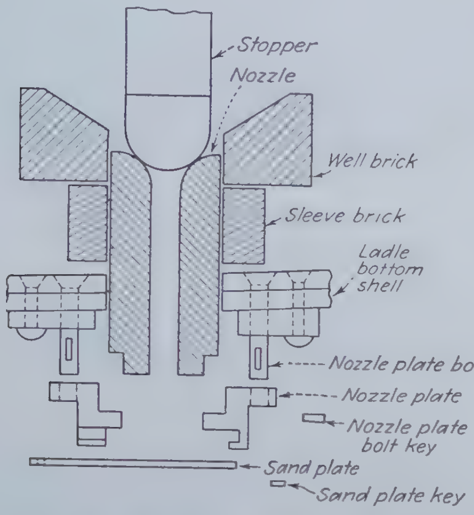

Cross section of nozzle arrangement showing stopper and nozzle in position.

After the mudded nozzle has been pushed half way in by hand, the nozzle plate is placed on the end of the nozzle. The holes in the plate are lined up with the bolts in the bottom of the ladle, and the plate is tapped simultaneously on either side to drive it into final position. The small keys are driven into the slots in the nozzle bolts to secure the plate fast to the bottom of the ladle. To insure against leaks through the nozzle, the end of the nozzle hole is smeared with mud before inserting the sand plate.

The sand plate, inserted endwise through the three small lugs on the base of the nozzle plate, is keyed into position by driving wedge pins between the lugs and the plate.

Just prior to setting the stopper, a small scoop of white sand is poured into the well from the edge of the ladle. Just enough is used to fill the hole in the nozzle and form a light cushion for the stopper head. The sand prevents steel from entering the nozzle hole before the heat is opened up.

The advantages of this method of changing nozzles are several. Ladles need be out of service only 12 to 15 min between pours to change nozzles. Furnace time often can be saved by tapping into a hot ladle instead of recarburizing the heat with hot metal and holding it in the furnace to gain temperature. A light ladle skull may be melted out by using the hot ladle immediately on the next heat.

No work is required inside hot ladles. Fewer ladles are required, because of the short delay time between heats. Hazards of climbing in and out of hot ladles are eliminated.

In the 20 years this method of setting nozzles has been in use at National Works, cases have been rare where trouble was encountered from steel breaking out around the nozzle.

Aluminum Foil-Laminate Gasket

A NOVEL and interesting gasket material has been developed, based on an aluminum-foil laminate bonded with a special synthetic resin, as reported in an article in *Light Metals* for February, 1950. According to the purpose for which the gasket is to be used, the thickness of the individual foils employed will vary from 0.00394 to 0.0005 in. The total thickness of the laminated mass may vary at will, but, for the majority of purposes, 1/32 in. appears to be most effective. Unless a different thickness is specified, all gaskets are cut from this gage.

The properties of the foil laminate are such that not only may it readily be cut to shape with shears or tinsnips, but, even in the mass production of particular gaskets, it required only the simplest and cheapest of tools.

In use, its capacity for plastic deformation is such that it will readily take up all surface forms against which it is bolted, including machining marks. A gas-tight seal is thus assured. In this regard, the plastic adhesive also plays a part, for, under pressure, some slight exudation occurs at the cut edges and, under the influence of heat, hardening of the resin occurs. This bonds the edges together and furthermore seals the laminate against penetration by gas under pressure. A further valuable service performed by the synthetic-resin bond occurs in those situations where chemical attack of the outer surface of the foil may occur, as, for example, in marine engines. Here, even though the outer layer of foil be entirely removed, for example, by the action of salt water, progress of attack tends largely to be inhibited by the varnish-like film adhering to the following sheet.

Plexeal aluminum-foil-laminate gaskets, made by Plexeal, Ltd., Haddenham, England, may be used for all purposes where normal gasket materials are required, on marine engines, water-cooled engines, air-cooled engines, compressors, steam installations, and the like. In the case of smaller internal-combustion engines, experience appears to have shown that the use of aluminum-foil packs for the cylinder-head gasket actually promotes more efficient running, inasmuch as heat dissipation is facilitated by the presence of the mass of high-conductivity metal.

Plexeal gaskets are manufactured in standard forms, or the uncut material is obtainable in the form of sheets, measuring 18 x 7 in., 28 x 9 in., or 35 x 9 in.

Clay Graphite Brick for Ladle Refractories

by Ernest B. Snyder

IN an attempt to increase the life of open hearth steel ladles tests were conducted late in 1948 and 1949 with fired clay-graphite brick bands in the top section of the ladles. The bricks used in all but one of these tests contained about 20 pct graphite and 80 pct clay and they were fired in a reducing atmosphere to prevent oxidation of the graphite. Ladle life at the Steubenville Open Hearth Shop, Steubenville, Ohio, of the Wheeling Steel Corp., had decreased about 20 pct in the previous 3 years. An increase in the oxide content of slides and the possibility of the increase in the percentage of heats in the lower carbon groups were believed to have attributed to this decrease in ladle life.

The low carbon heats normally carry a higher oxide slag. Many of these high oxide slags, ranging from 45 to 50 pct iron oxide, cut out from 2 to 4 in. of the regular clay ladle brick around the top of the ladle in a single heat. The lining in the lower parts of the ladle is subjected to these corrosive slags as the heat is teemed.

In the first test, a complete band of clay-graphite brick was installed in the top 3 ft of the ladle, the brick being laid up with dip joints of clay-graphite mortar. In a second group of tests, the 3 ft band was installed on the furnace side and extended around one-half to two-thirds of the circumference of the ladle. The remainder of the top section was installed with regular ladle brick. In a third test, the clay-graphite brick were installed in a 3 ft band covering approximately two-thirds of the ladle circumference. Alternate brick in this band were regular clay ladle brick. In the fourth series of tests, a clay-graphite brick was used which contained approximately 15 pct instead of 20 pct graphite.

The results of the first test with the complete band of clay-graphite brick in a 3 ft section around the top of the steel ladle were very encouraging. The ladle was used for one special low carbon heat, four semi-special heats and several regular heats. Normally a ladle would not be used for more than one semi-special heat after a special low carbon heat usage. The total life on this ladle showed a 50 pct increase over the present average. No patching was required in the top section after the special low carbon heat. The only objection to the use of these brick was that the high oxide slags reacted with the graphite in the brick causing a violent boil. This violent boiling action started as the slag covered the brick during tap. As the ladle filled up, large quantities of slag were thrown over the sides. Although the boil had subsided to some extent by the time the ladle reached the pouring platform, the reaction was still sufficient to throw fingers of slag over the side of the ladle. Fig. 1 shows this reaction as the heat was being poured.

The results of the second group of tests using partial bands of clay-graphite brick were satisfactory from the standpoint of increased ladle life. In two trials the ladle was used for three special low carbon heats and several regular heats. The total life was as good or better than the shop average. All of the ladles with partial bands showed increased ladle life even though they were used for more special heats than normal. It was rather hard to believe that the partial bands of clay-graphite brick would give comparable life to the ladle with a complete band. However, it

---

Ernest B. Snyder is Refractories Engineer, Wheeling Steel Corp., Steubenville, Ohio. This paper was presented before the 1950 Annual Open Hearth Conference, of the Iron and Steel Div., at Cincinnati..

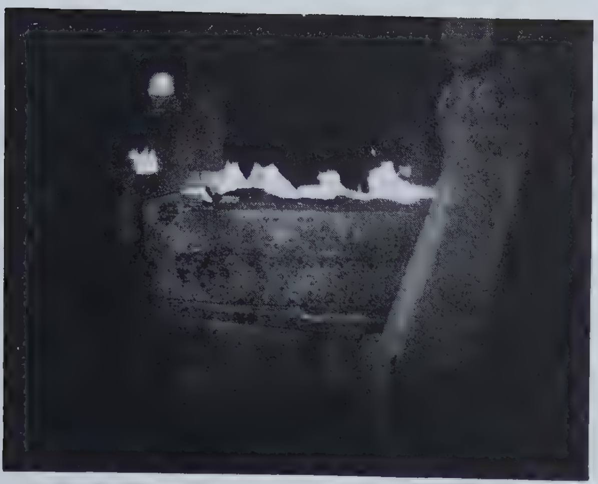

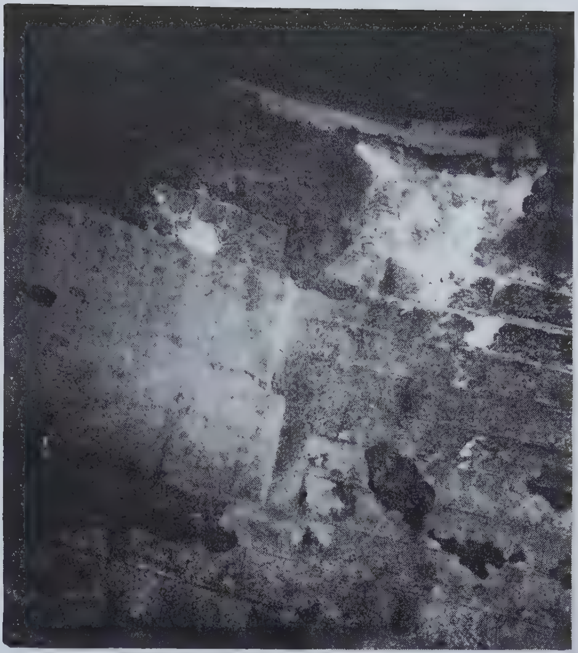

Fig. 1 (above)—Reaction between the slag and the graphite in the clay-graphite brick panel of the ladle was violent and caused slopping.

Fig. 2 (right)—The panel of clay-graphite brick of the photo shows very little erosion after several heats, as compared with surrounding regular clay ladle brick.

was noted that the clay ladle brick used in the top section on the pouring platform side of the ladle did not cut out as much as would be expected with similar types of heats. Fig. 2 shows the clay-graphite brick panel after several heats. The clay ladle brick on the right showed very little more wear than the clay-graphite panel on the left. The photograph shows that slag and metal did not adhere to the clay-graphite panel; and it was noted that there was no severe cutting in this section of the lining and the stopper rod sleeves did not erode as rapidly when using clay-graphite brick bands as with regular clay ladle brick linings. Two explanations were advanced for this phenomenon: 1—The reaction of iron oxide in the slag with graphite lowered the oxide content of the slag layer near the brick lining. Slag tests proved that the iron oxide in the slag dropped over 8 pct in these ladles. 2—The reaction, being endothermic, lowered the temperature of the slag and thus lowered its reactivity.

Although the use of partial bands of clay-graphite brick on the furnace side of the ladle gave good ladle life and eliminated the hazard of splashing slag on the steel pourers, the reaction was great enough to throw large quantities of slag into the pit at the furnace.

The partial band of alternate clay-graphite and regular clay ladle brick was installed to reduce the intensity of the reaction. This ladle was used for two regular heats and one special low carbon heat. The amount of reaction was reduced but an inspection of the lining after the low carbon heat stopped this test immediately. The clay brick had been cut out 2 to 2½ in. deeper than the adjacent clay-graphite brick. As in previous tests, the clay ladle brick opposite this panel showed little wear. Apparently the boiling action on the clay-graphite brick had speeded up the erosion of the clay brick between them by continually renewing the slag in contact with the brick or the localized reducing effect of the graphite contributed to this rapid wear.

The results of the fourth group of tests using panels of clay-graphite brick containing approximately 15 pct graphite did not decrease the amount of reaction.

From data obtained in tests with fired clay-graphite brick in a steel ladle, the following conclusions can be drawn: 1—The fired clay-graphite brick resists high oxide slags extremely well. Their reaction with these slags in an open hearth steel ladle apparently reduces the oxide content and chills the slag, thus reducing the amount of erosion of the clay ladle brick lining. 2—The violent reaction between the slag and the graphite in the brick may rule out their use for steel ladles in shops where high oxide slags are common, unless some development is made that will reduce this reaction, or a shield is used on the side of the ladle. One low carbon open hearth shop has reported good results with this brick and they have not had the objectionable reaction. Some electric furnace shops also report successful tests. 3—The reaction occurs between the slag and graphite only. The reaction has no effect on the steel analysis. Numerous checks gave definite proof that if there was no carbon pickup on any type of heat. 4—A panel of these brick, 2½ to 3 ft high and extending around one-half to two-thirds of the ladle circumference, is as effective as a complete panel. 5—The clay-graphite brick is giving satisfactory service for special uses such as pig machine runners, blast furnace splasher plates, etc. This type of brick may find many important uses in a steel plant and plans have been made to carry out further tests to determine its possibilities.

Acknowledgments

The author thanks Wheeling Steel Corp. for permission to publish this paper, and the open hearth personnel at the Steubenville shop who helped with this investigation.

New Mold Coatings

by J. J. Golden

ALTHOUGH controversy exists regarding the merits of coated vs. uncoated molds, it is generally accepted that coated molds are superior to uncoated, from the standpoints of both steel quality and mold life. Gary Works of Carnegie Illinois Steel Corp., as well as many other steel plants, have been using byproduct tar to coat ingot molds for many years with very satisfactory results from the quality, mold life, and cost viewpoints. However, heavy fumes are given off during the coating or dipping of molds with tar and during the pouring of steel in tar coated or tar dipped molds.

Because of this fuming, Gary Works currently is engaged in an extensive testing program to evaluate the relative merits of several mold coating materials, with the ultimate purpose of obtaining a mold coating which does not give off fumes and which approaches tar in performance and cost. The two most promising materials used to date are **Darmold** and **Hydropaste.** Darmold is a colloidal graphite solution resembling a heavy black paint which, when applied to hot molds, leaves a rather light appearing, dull gray coating, quite unlike tar in appearance. Hydropaste is a non-inflammable paste consisting of flake aluminum and binder, and resembles cold water paint in character and consistency when mixed with water. A mold temperature of between 200° and 400°F is desirable for applying either Darmold or Hydropaste. Both materials are superior to tar for coating cold molds. With mold temperatures above 450°F, neither material appears to adhere in sufficient quantities, and a non-uniform coating usually is obtained.

The initial experience with Darmold revealed that although the fumes were not as heavy as those from tar, they possessed a disagreeable, somewhat nauseating odor. The supplier remedied this condition to a considerable extent in later shipments by alterations in processing. No objectionable fumes are produced during the coating of molds with Hydropaste. However, the aluminum flake in Hydropaste has a tendency to settle out after being mixed with water. Consequently it requires, in addition to special equipment for initial mixing with water, constant agitation up to and during the actual mold coating operation. The main advantage of Darmold over Hydropaste is that it can be used direct from the supplier in the manner that tar is now used; or, to reduce the cost, it can be diluted with up to 20 pct water. Both materials must be kept warm, which is also true for tar. Recently, 7500 gal of Darmold were received by tank car and on arrival were unloaded into a special tank car equipped with steam coils and a circulating pump. The Darmold was diluted with 20 pct hot water and will remain in the tank car until used.

The initial service trials with Darmold and Hydropaste indicated that neither material is suitable for application with present type tar applicators because of the difference in consistency and viscosity of these materials as compared with tar. Gary Works developed, and has been using for a number of years, a portable electrically-driven, spinner type, tar sprayer for coating molds shown in figs. 1 and 2.

The apparatus has a spinner unit with spiral vanes which is driven at 575 rpm by a vertical shaft electric motor. Tar flows to the spinner unit when a needle valve, controlled by a solenoid, is open. This arrangement functions auto-

---

Mr. Golden is Superintendent, steel production and central mills Carnegie-Illinois Steel Corp., Gary, Ind. Third paper was presented at the 1950 Open Hearth Conference of the Iron and Steel Div., AIME, Cincinnati, Ohio.

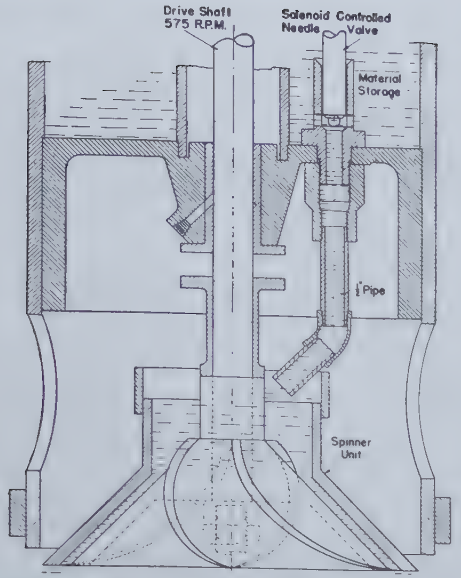

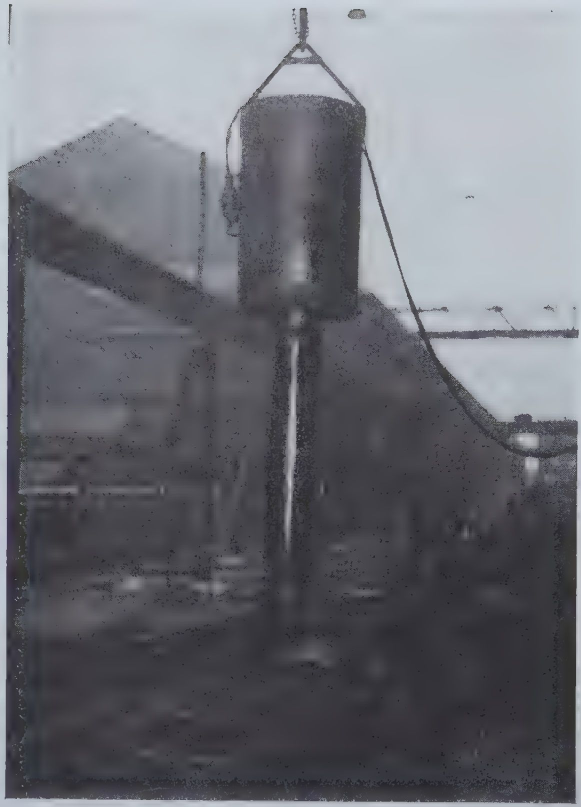

Fig. 1—(Right) This portable type tar sprayer is used for coating ingot molds. By a control arrangement tar is permitted to flow only while the sprayer is being lifted inside the mold.

Fig. 2—(Above) The tar sprayer is an electrically driven spinner type. Tar flows to the spinner unit when a needle valve is open as shown in this detailed drawing.

matically and permits tar to flow to the spinner unit only while the sprayer is being lifted inside the mold by the crane. Molds coated with Darmold or Hydropaste, using the spinner type sprayer, were unsatisfactory in that a steaky, beady, non-uniform coating was obtained, and material consumption was excessive.

In view of the higher material cost of Darmold and Hydropaste as compared with tar, it became evident that an apparatus capable of applying the thinnest possible uniform coating, consistent with acceptable quality performance, was necessary if these materials were to be used on a comparative cost basis with tar. Subsequently, a compressed air applicator was developed, and this unit currently is coating approximately twice as many molds with the same volume of material as was possible with the spinner type sprayer.

This apparatus is essentially the same in appearance and operation as the spinner type tar sprayer, excepting it has a stationary type nozzle in place of the spinner unit, as shown in fig. 3. The material is atomized by compressed air instead of being forced out by centrifugal action of the spinner. Compressed air at about 25 to 30 psi is supplied from a service line. Eventually, it may be possible to install an air compressor in the top of the unit, thereby eliminating the disadvantage of the present ground-to-unit air hose connection.

Table I

Rail Steel
Quality Performance Surface Defects

Coating Material	No. Rails Inspected	Ratio of Defective Rails, Darmold to Tar
Darmold	13 649	1.110:1
Tar	6 833	
Hydropaste	5 090	1.182:1
Tar	6 857	

Gary Works is fortunate in having what are considered ideal facilities for comparing quality performance of various mold coating materials. The Gary rail mill produces railroad rails direct from ingots without intermediate heating or surface conditioning. Table I shows the data obtained from two separate production runs of rail steel. For each run, two new sets of molds were put in service and each set used exclusively for one type of mold coating material. Surface quality performance for the product from both the Darmold and Hydropaste coated molds was somewhat inferior to that of tar.

Table II

Billet and Slab Product
Quality Performance, By Grades

Grade	Coating Material	Ingot Tons	Ratio of Surface Rejections, Darmold to Tar
Rimmed	**Darmold**	18 117	1.135:1
	Tar	12 377	
Semi-killed 0.30 Pct. C	**Darmold**	15 689	0.359:1
	Tar	8 113	
Killed-steel 0.30 Pct. and Over C	**Darmold**	3 128	0.968:1
	Tar	1 462	
Total	**Darmold**	36 934	0.865:1
	Tar	21 952	

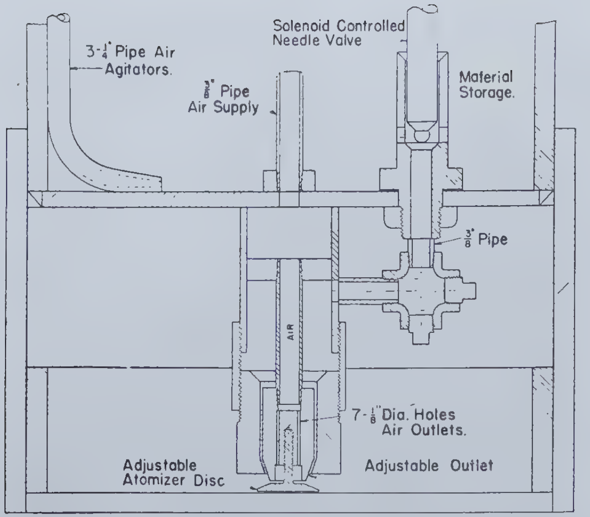

Fig. 3—A new type mold coating apparatus, developed to apply a thin uniform coating, uses a compressed air applicator.

The data in tables II and III show surface quality performance of Darmold vs. tar coated molds for billet and slab product. A comparison by grades of steel is shown in table II while in table III the data have been rearranged to show quality performance by type of product. The overall results of this comparison indicate a slight advantage for Darmold coated molds.

The case of semi-skilled steels under 0.30 pct carbon, the product from the Darmold coated molds definitely was superior to the product from tarred molds. In view of the critical nature of this grade with respect to surface quality, lower surface rejections from the product of Darmold coated molds were not expected, but nevertheless were gratifying.

Table III

Comparative Cost, Mold Coatings

Material	Cost Ratio
Virgin Tar	1.000
Graphite	1.250
Hydropaste	3.333
Darmold	5.000

Comparative mold coating costs, based on current market prices, are shown in table IV. Graphite has been included in the comparison because an extensive service trial with this material is scheduled in the near future. Preliminary experience with graphite has indicated that mold coating costs will not exceed appreciably that of tar. Quality performance data for graphite vs. tar coatings are not available.

Inasmuch as the present program for obtaining a satisfactory mold coating substitute for tar will not be completed for some time, quality performance and mold coating cost comparisons are not regarded as conclusive and may be subject to revisions at a later date. However, based on experience to date, it can be stated that with respect to quality and mold life, Darmold and Hydropaste appear to compare favorably with tar for coating molds. Unfortunately, mold coating costs with either are substantially greater than with tar. Darmold is readily adaptable to present equipment at Gary, while Hydropaste requires special mixing equipment and constant agitation to maintain the desired consistency. Providing the contemplated experiments with graphite mold coatings show acceptable quality performance, this material will be attractive from a cost viewpoint. However, similar problems of mixing and agitation as encountered with Hydropaste are anticipated.

Table IV

Billet and Slab Product, Quality Performance, By Product

Product	Coating Material	Ingot Tons	Ratio of Surface Rejections, Darmold to Tar
Slab	**Darmold**	13 466	0.950:1
	Tar	9 978	
Billet	**Darmold**	23 488	0.835:1
	Tar	11 974	
Total	**Darmold**	36 934	0.865:1
	Tar	21 952	

1949 Iron Ore Imports at Record High

IMPORTS of foreign iron ore were greater in 1949 than in any previous year, with receipts totaling 8,300,000 net tons from 18 countries, the American Iron and Steel Institute reports. This total represents an increase of 22 pct. over 1948, when imports totaled 6,800,000 net tons. In 1947 about 5,492,000 tons were delivered, and in 1946 the imports totaled 3,085,000 tons. The largest supplies came from Sweden, Chile, and Canada.

Simultaneously, steel companies have been active in exploring and developing large ore deposits in South America, in exploring the Quebec-Labrador iron range, and in constructing facilities for shipment of ore from Liberia. This extension of ore supply lines has been taken to supplement domestic ores, particularly while research proceeds toward the economical use of the taconite and low grade ores abounding in the Lake Superior region.

Estimates of the capital investment required in the taconite program place the cost at $15 to $20 per ton of annual capacity for producing taconite concentrates. Thus, at least $300,000,000 must be invested to make 20,000,000 tons of taconite concentrate yearly. If the steel industry were to replace the present Lake Superior natural ore supply with a taconite supply alone, it would be faced with a capital investment in iron ore facilities of upward of $1,250,000,000 at today's costs.

Factors Affecting Deformation and Rupture of Metals at Elevated Temperatures

Howe Memorial Lecture

by **Francis B. Foley**

IT is with an unusual degree of personal satisfaction that I find myself in a position to pay tribute to the memory of Henry Marion Howe. One could not have spent any length of time in the presence of Dr. Howe without profiting intellectually. I do not hesitate to say that my years of association with him were the most stimulating of all my years of metallurgical study. He always impressed one with his own eager search for knowledge. Never dependent on the written word alone he sought information from anyone whose opinion he valued. His ability to piece together bits of apparently conflicting data from various sources so as to build up a logical hypothesis was unique. A small slight man with the intellect of genius he would have gone to the top in any endeavor he undertook and it was fortunate for metallurgy that its study attracted him as it did. Howe was a modest man. I like to recall an incident which left a lasting impression with me. The laboratory in his home, "Green Peace," was in the basement and access was by way of stairs leading down from his secretary's room. In using these stairs my attention was attracted many times to an ordinary cardboard shoe box which reposed on the shelf above the landing. It was crudely labeled on its side in black ink "Vanity Box." My curiosity was aroused to the point that I finally asked his secretary what it was. With some amusement she took the box from its shelf on the stairway, opened it and showed me its contents—numerous letters, from the foremost men of science of every civilized country throughout the world, commending his "Metallography of Steel and Cast Iron." I recall that in reply to one who thought there was not enough of Howe's own researches in his book he wrote, "Primarily I am a writer, secondarily an investigator."

Howe wrote to make his readers think. No one ever strove harder than he to be right but above all, whether his viewpoint proved ultimately to be right or wrong, he was always content if by his stand, he provoked a reader to take the next step along the path to greater knowledge. I doubt that he was ever afraid to be wrong for he was always secure in the thought that his effort was guided by a sincere search for the truth. One continually searching for truth is entitled to occasional excursions up the wrong alley. A glance backward to the metallurgical confusion of some thirty to forty years ago, or need one go back so far, provides convincing proof of what a host of companions one may have in a common acceptance of ideas which the future will prove to be wholly untenable.

Well over a hundred years have passed since investigators have interested themselves in the effect of increasing the temperature of iron and steel on their mechanical properties. We are told by Charles Walrand[1] in "Industrial Annals" for June 11, 1822, that bend tests, conducted in a Russian steel works of Prince Demidoff, on steel bars "highly heated" and bent during cooling became brittle when bent at an iris blue color. He concluded, "That when steel is heated to a temperature between 473°F and 662°F the mettle was more brittle between these limits than at a much lower or at a much higher temperature." It was a curious bit of information recognized as true to this day and still not explained satisfactorily. In 1878 Charles Houston in Annales de Mines associated this brittleness with an increase in tensile strength at 572°F.

When this relatively low temperature is exceeded it is recognized that steel becomes weaker as temperature is increased up to the melting point, where no strength of practical importance remains. It is easy to believe, in fact it goes without saying, that this weakening as the temperature of a metal is increased is the result of the motion of the atoms making up the metal, a motion which itself is evidence of the temperature increase. However, if we are considering iron or steel we find that this decrease in strength is not a steady one, for, besides the increase in strength just referred to, one comes to a temperature, the critical temperature, where results of tests indicate the metal to be extremely weak and then as temperature increases to become sensibly stronger again. This apparent anomaly was made the subject of the first Howe Memorial Lecture, delivered by Albert Sauveur in 1924. It may be of interest to review these findings of Sauveur. He used two methods of investigation. One involved the twisting of bars. The bars were heated in an

---

FRANCIS B. FOLEY, Member AIME, is Consulting Metallurgist, Research Department, International Nickel Co., Bayonne, N. J.

AIME New York Meeting, Feb. 1950.
TP 2866 CE. Manuscript received March 15, 1950.

This page of Transactions AIME is a continuation from p. 796.
The missing pages appeared in Journal of Metals.

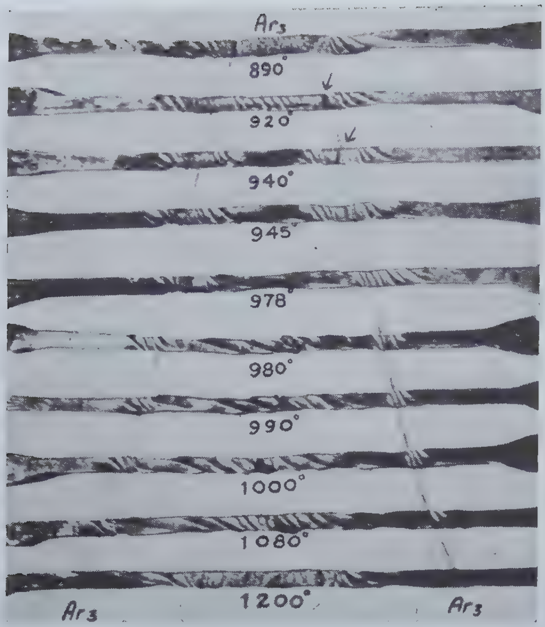

Fig. 1—Hot twist tests.
(*Sauveur.*)

electric furnace to a maximum temperature at mid-length and with one end held fast the other end was turned by means of a crank, twisting the bar. By twisting electrolytic iron at some ten to fifteen temperatures between 600°C (1112°F) and 1200°C (2192°F) Sauveur showed this region of easy twisting to occur consistently at the transformation temperature from alpha to gamma on heating and from gamma to alpha during cooling (fig. 1). This type of test has been reproduced many times since by other investigators with the same characteristic result. Fig. 2 shows the result of twisting a bar of Silcrome valve stem steel of 3.5 pct silicon, 8.5 pct chromium. At two points along the length of the bar, where the temperature attained, 1600°F, was that at which the steel transformed from alpha to gamma iron, the twists are very close together indicating a low order of resistance to torsion.

Sauveur's other test consisted of heating test bars to 1100°C and pulling them in tension during cooling to determine the tensile strength developed at each temperature at which they were broken. His results appear in fig. 3. Note here the extraordinary dip towards very low values when the bars were broken while the maximum temperature corresponded to the Ar_3 transformation from gamma to alpha.

Sauveur considered two possible explanations of this phenomenon. One was that, at its highest temperature of stability, alpha iron was weaker than gamma at its lowest temperature, and the other, that the weak condition results from the transformation itself. His inclination was to accept the latter explanation with which one finds little difficulty in agreeing for, to the kinetic energy normally associated with the temperature of testing is added the atomic movement incident to the assumption of new relative positions of the atoms bent on assuming a new crystalline orientation.

Phase change, such as that observed in iron and steel, is only one source of added atomic movement conducive to a decrease in resistance to applied mechanical stress. Grain growth accompanying the heating of metals is a source of another such atomic activity. It is a generally recognized fact that the path of rupture, at high temperature, is through the grain boundaries of metals and that, at low temperatures, rupture takes place as a rule, through the body of crystals. Nearly forty years ago Beilby proposed the vitreous amorphous cement hypothesis to account for this characteristic behavior of metals and his ideas gained a considerable amount of endorsement. Briefly stated, the idea, as it applies to grain boundaries, was that crystals were joined together by atoms in a random orientation constituting an amorphous condition in which the properties of the grain boundaries partook of those of an undercooled liquid, lacking crystallinity. Like glass it was weak and mobile when hot but strong and rigid when cold. The precise condition of grain boundary metal is still not known but considerable is known about its behavior.

When metals in certain conditions are heated their crystals grow. Offhand it would be difficult to say why crystals grow but one may assume that were the energy levels throughout the mass, particularly at grain boundaries, such as to permit equilibrium, or the maintenance of the *status quo*, there would be no grain growth. The fact that grains grow is evidence that such conditions do not prevail.

It can be shown, in fact it has been experimentally demonstrated, that grain growth occurs by the robbing of one crystal, atom by atom, by its neighbor. It is commonly held that the large crystals in a structure of mixed sizes of crystals, are the robbers and the small crystals the victims. There are some however who will contend that the little ones are the aggressors, growing at the expense of the bigger ones. One might argue that were the big ones to consume the little ones, the ultimate grain size would always be larger than the largest initial grain. On the other hand, with the smaller grains eating away at the big ones, an intermediate size is likely to be attained after which further increase in size is likely

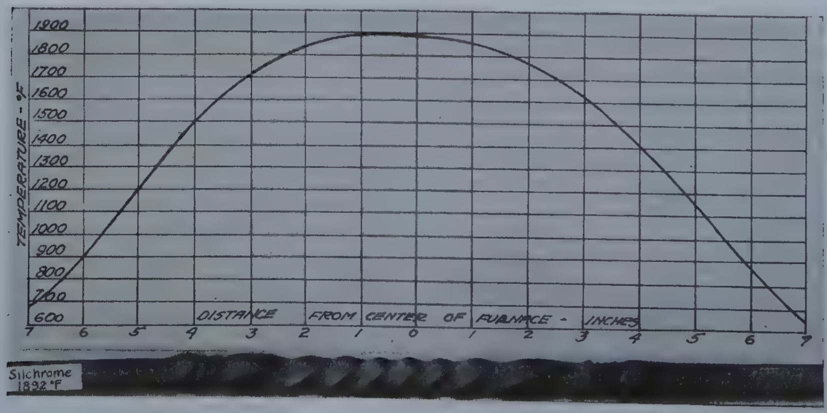

Fig. 2—Twist test of an 8.5 pct Cr, 3.5 pct Si steel.

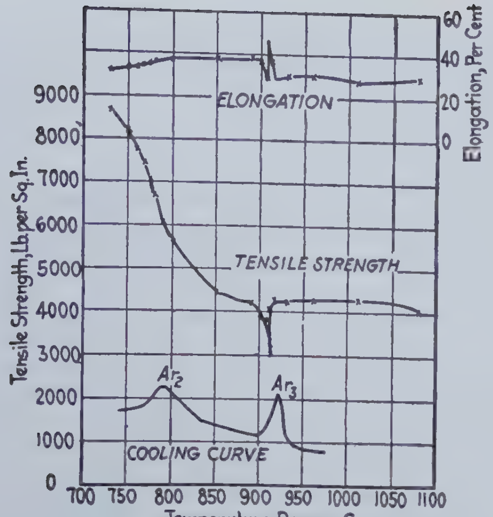

Fig. 3—Tensile tests of Norway iron under differential heating.
(Sauveur.)

to be a slow process. The question arises as to what governs the movement of grain boundary atoms, the atoms themselves or the family of atoms as a whole making up the individual crystals. Are the grain boundary atoms rugged individuals determining, as units of the crystal, whether to stay with their present orientation or to swing into that of the neighboring atom; or are they controlled by the combined crystallizing force of the crystal as a whole, which holds them in their proper place while the neighboring crystal exerts a force tending to pull them into its family? One is inclined to this latter view for, were all the crystals of exactly the same size, each composed of exactly the same number of atoms it is likely that no grain growth would occur. A difference in size, however small, is indicated as a prerequisite of grain growth and such a difference is inevitably present. It is easy, if one accepts this view, to accept the idea that the large crystals grow at the expense of the smaller ones, with rapid change occurring when crystals differ greatly in size and slow change proceeding as grain size becomes uniform. As temperature increases smaller differences in grain size give rise to more rapid grain growth activity because the increased kinetic activity renders coercion by small differences in crystallizing energy easier.

In any event one visualizes the region of grain boundaries as one in which adjoining crystals contend for boundary atoms. The grain boundary is thus in motion in heated metal undergoing grain growth, sometimes moving rapidly, sometimes imperceptibly. At any instant of time one conceives a location—the boundary itself—where the atoms have lost allegiance to their former family but have not yet come under complete influence of their new host. Moving towards the crystal center the bonds become stronger between atoms until the maximum strength of the lattice is established within the main body of the crystal.

This concept and some of its consequences may appear clearer by reference to fig. 4. The sketch represents a section comprised of a number of crystals and particularly the large crystal *A* and the smaller one *B*. Set up on these two crystals are coordinates, the abscissa representing distance from the centers to the grain boundaries and the ordinate representing stress. The region of greatest atomic instability is represented on the crystals by the black border, the next more stable bonding by the cross hatched area, a still more stable region by the adjoining shaded portion, and the ultimate in atomic stability at the temperature by the white area within the crystals. The relative resistance to deformation of the various regions in the crystals is indicated by the curve plotting stress against distance from center to boundary of the crystals. A stress *L* represents the strength of the stable region within the crystal. Such a stress would deform the entire grain with considerable incident deformation. A suddenly applied load considerably higher than *L* would rupture much more quickly and with a great amount of attendant permanent deformation. A load L_1 would ultimately produce rupture accompanied by less extensive deformation since permanent deformation would occur only in the cross hatched and blackened-in region—little occurring, if any at all, in the clear and in the adjoining shaded region. Finally a quite low stress L_{11} produces rupture in a longer period of time with a very low order of deformation since permanent deformation would be confined to the region of junction of the grains. Conceivably a low enough stress would result in a deformationless fracture after a very long period of time.

This relationship of limited deformation with failures resulting from the application of low loads over long periods of time and of a high order of deformation with failures resulting from the application of rapidly applied overloads is well recognized. Out of many examples of this phenomenon may be cited the results of tests by Avery, Cook, and Fellows[2] of a cast ferrous alloy of 25 pct Cr 12 pct Ni. A logarithmic plotting of time to rupture and of stress producing rupture against percentage of elongation is shown in fig. 5. A load of 8000 psi breaks this metal in 1070 hr at 1400°F with an elongation of only 1 pct, whereas 25,000 psi breaks it in 2½ hr at the same temperature with an elongation of 7.8 pct. At 1800° fracture in about 485 hr produces about 5 pct elongation but with a greater stress fracture occurs in 1.7 hr with nearly 22 pct elongation. Effects of rate of deformation of aluminum have been discussed by Hanson in his 1939 Institute of Metals Lecture. According to Jeffries,[3] fracture of copper wire in 1 min under a stress of

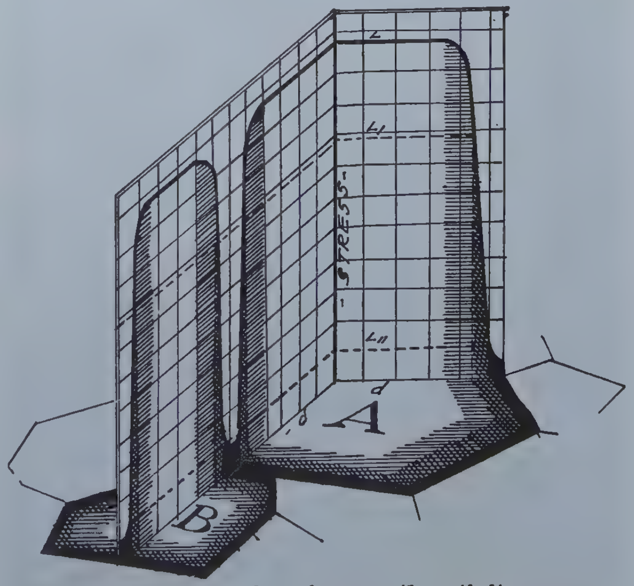

Fig. 4—Influence of grain growth activity on resistance to deformation within crystals at elevated temperatures.

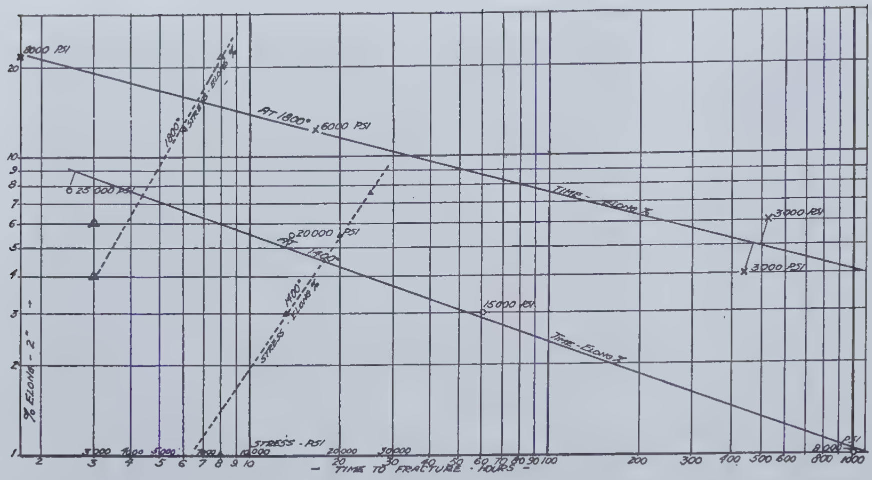

Fig. 5—Relationship of elongation to fracture time of C 0.32, Ni 11.5, Cr 25.9, N 0.16 castings.

(Avery, Cook, and Fellows.[2])

710 psi at 1742°F (950°C) resulted in an intercrystalline, brittle fracture whereas fracture in 5 sec under a load of 2500 psi at the same temperature was transcrystalline and ductile.

If the energy be very great and its application extremely rapid even a notoriously brittle material may behave in an extraordinarily ductile manner. Only recently Clark and Bruckner[4] experimented with the use of shaped charges employing the "Monroe effect" (the principle of the bazooka of World War II) to produce holes in very hard rock. The cone used for shaping the charge was of cast iron, of the structure in fig. 6, with a base 6 in. in diameter, a 45° apex angle and a 3/16-in. wall thickness. Recovery of the collapsed cone showed it to have deformed from the outlined conical form to the slug shown in fig. 7. Microexamination showed this brittle metal to have undergone the deformation indicated in fig. 8. The time required for the complete deformation of this cast iron cone was of the order of 10 or 15 microsec, the velocity of detonation of the blasting gelatine having been 26,200 fps. Leaving to the physicists the explanation of effects such as temperature generated by friction and pressure effects, one recognizes in this the effect of the application of very great energy over an extraordinarily short period of time. Certainly the constituent atoms of this metal were all set into motion by the very rapidly developing gas pressure of the explosive so that the metal attained some high temperature. The phenomenon gives a useful point approaching zero time in our time to rupture-elongation plotting. The shape of the slug is the product of the environment. By controlling the environmental conditions and with sufficient speed, though perhaps considerably less than five miles per second, might one very rapidly produce brittle materials in a desired wrought form?

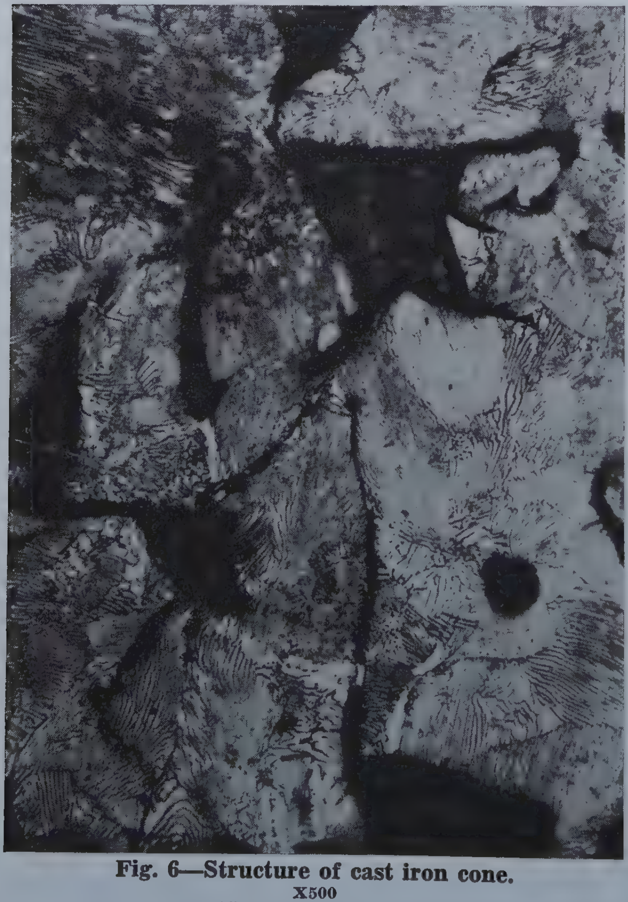

Fig. 6—Structure of cast iron cone.
X500
(Clark and Bruckner.)

While the crystals of metals are growing rapidly there is great atomic movement at the grain boundaries which, like all atomic movement, lowers the resistance of the metal to deformation while under the influence of energy applied externally. When metal is cold worked its hardness, and strength, undergo a change. Cold deformation is a common method of increasing strength at room temperature. When metal that has been cold worked is heated it recrystallizes and at some temperature of heating, which is higher the lower the amount of cold deformation, rapid grain growth occurs. If the metal be stressed at such a temperature of rapid grain growth it is found to be weaker and, while the amount of cold deformation which does not result in rapid grain growth at a given temperature may strengthen the metal, as it does at room temperature, the process of grain growth may reduce the strength to below that of the metal had it not been cold worked at all. This is illustrated in fig. 9, the work of Zschokke.[5] The room temperature tensile strength of his tungsten, titanium bearing 18 Cr 8 Ni stainless steel was steadily increased from 42,670 psi to 87,450 psi by cold working it 35 pct. When tested at elevated temperatures there is no such steady increase in strength. For each testing temperature there is an optimum amount of cold working for strengthening. When that amount of cold working is exceeded the elevated temperature strength decreases. At 1112°F (600°C) the highest creep strength, 48,360 psi, resulted from cold working about 10 pct. After 35 pct of cold elongation the creep strength at 1112°F was only 9960 psi compared with 24,890 psi without any cold working. Cold working in excess of about 15 pct is sufficient to decrease the creep resistance of this metal at temperatures of 1112°F (600°C) on up to 1382°F (750°C). The reason for this reduction in strength seems clear. For each of the temperatures of testing there is an amount of cold deformation that leads to rapid grain growth. Cold working of a lesser degree does not result in grain growth. Consequently the lower amounts of cold deformation have a strengthening effect and the higher amounts a weakening one because grain growth involving considerable atomic movement is going on at the testing temperature *while the mechanical stress is being applied.* The same effect would not be expected were the cold worked pieces first subjected to the temperature of test for a period of time without stressing, so that grain growth could be completed, and then loaded. It is the combination of recrystallization activity, the temperature, and the stress that results in the weakened condition. It is the same type of weakening as that shown by Sauveur in his tensile and in his twisting tests.

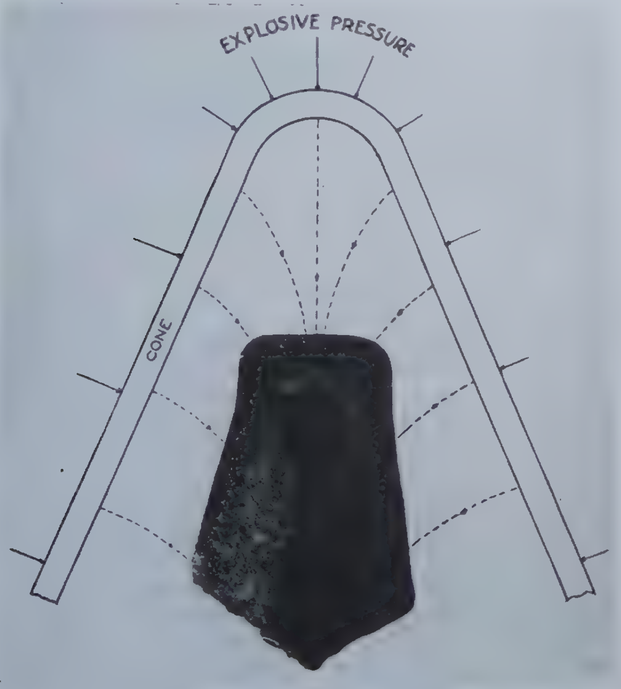

Fig. 7—Slug produced from cast iron cone.
X1¼
(*Clark and Bruckner.*)

Stresses capable of deforming the entire crystal with high elongation do not necessarily cause rupture to occur through the crystal nor is intercrystalline fracture necessarily an indication of brittleness or of low ductility. Considerable deformation of the body of the crystal may be observed before rupture at high temperatures. Fig. 10 shows the region immediately in back of and in a plane normal to the fracture of a specimen of 18 Cr 8 Ni broken at 1500°F. The deformation of the crystals themselves and parting of the grain boundaries where they lie normal to the applied stress are clearly evident with fracture occurring between the grains. The brittle type of fracture is produced when failure occurs in grain boundaries with little or no deformation of the crystals themselves.

During the early period of what may be called modern metallurgy the influence of the chemist was apparent in the search for a chemical reason for the variations in the mechanical properties of metals, particularly of steel, at ordinary temperatures. Metallurgists have come more and more to realize that the mechanical properties of metals are the result of the structure or of what may be called the architecture of metals and that it is only through their effects on the structure that chemical elements play a part. Their specific effects reside in their chemical properties that confer on metals resistance to chemical attack. It is not a difficult matter to carry this general conception into the region of elevated temperatures. To be sure the chemical properties of alloying elements become more important at high temperatures because chemical reactions are speeded up as temperature increases so that, for example, resistance to oxidation in air, which at ordinary temperatures may not present a serious problem in corrosion, becomes of very great importance. Structure, however, still remains the predominant factor in mechanical strength.

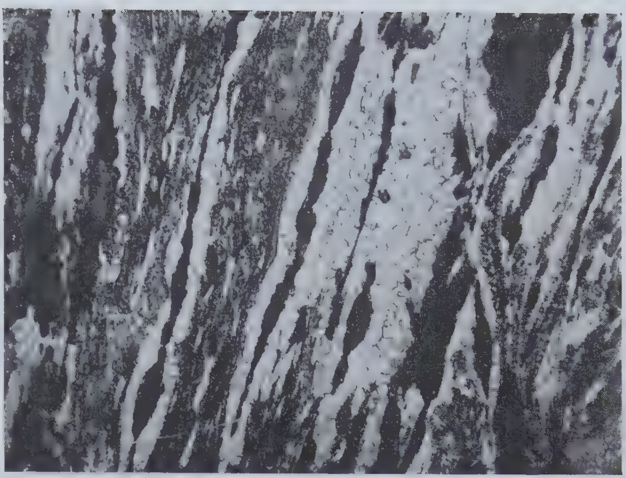

Fig. 8—Structure of cast iron slug.
X500. Reduced approximately one quarter in reproduction.
(*Clark and Bruckner.*)

The effect of atomic movement resulting from the application of energy in the form of heat in lowering the resistance of metals to deformation under the influence of energy mechanically applied is well known but the magnitude of the effect is not the same on the different elements. If the coefficients of thermal expansion at 20°C of the body-centered cubic, face-centered cubic, and close-packed hexagonal metallic elements be plotted against their melting points, it is observed, as shown in fig. 11, that as the coefficient decreases the melting temperature becomes higher. Evidently the tendency of the

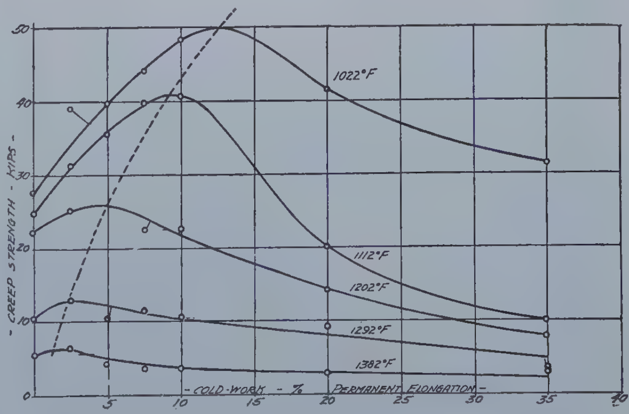

Fig. 9—Effect of cold deformation on creep strength at various testing temperatures.
C 0.11, Mn 1.03, Si 0.82, Cr 18.2, Ni 8.7, Mo 0.03, W 0.82, Ti 0.32. Annealed 1922°F—water.
(*Zschokke.*)

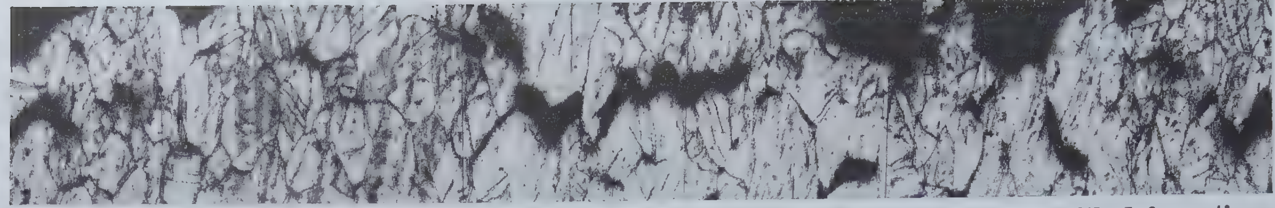

Fig. 10—Fracture of 18-8 at elevated temperature showing intercrystalline rupture along with deformation.

atoms of some elements to resist separation under the influence of heat is greater than that of others. In the formation of some solid solutions the constituent elements tend to retain this characteristic of resisting separation under the influence of heat so that it is observed that additions of metals of low coefficient, such as tungsten, molybdenum, tantalum, and columbium, have a strengthening effect. An exception is noted, of course, in the case of certain nickel-iron alloys of the Invar type where magnetostriction affects the coefficient of expansion below the Curie temperature of the alloy.

Criteria, with respect to structural effects on mechanical properties, change as temperature increases. The association of fine grain with hardness and strength at ordinary temperatures gives place to its association with weakness and flow at high temperatures. The strong body-centered alpha iron of hard steel becomes a weak structure and the soft dutile face-centered gamma iron becomes the strong structure at elevated temperatures. Fig. 4 offers an explanation of the association of low ductility with long-time failure under low loads at elevated temperatures and it also supplies a reason for the lower strength of small crystals at high temperature. The conclusion is quickly reached in a glance at this sketch that were the metal made up entirely of crystals of the size of *B* it would contain much less of the high strength structure represented by the clear area than were it made up of crystals of the size of *A*. At ordinary temperatures the black and the shaded areas would disappear since no grain growth activity occurs. This condition of grain size stability would exist up to the temperature at which effective grain growth sets in.

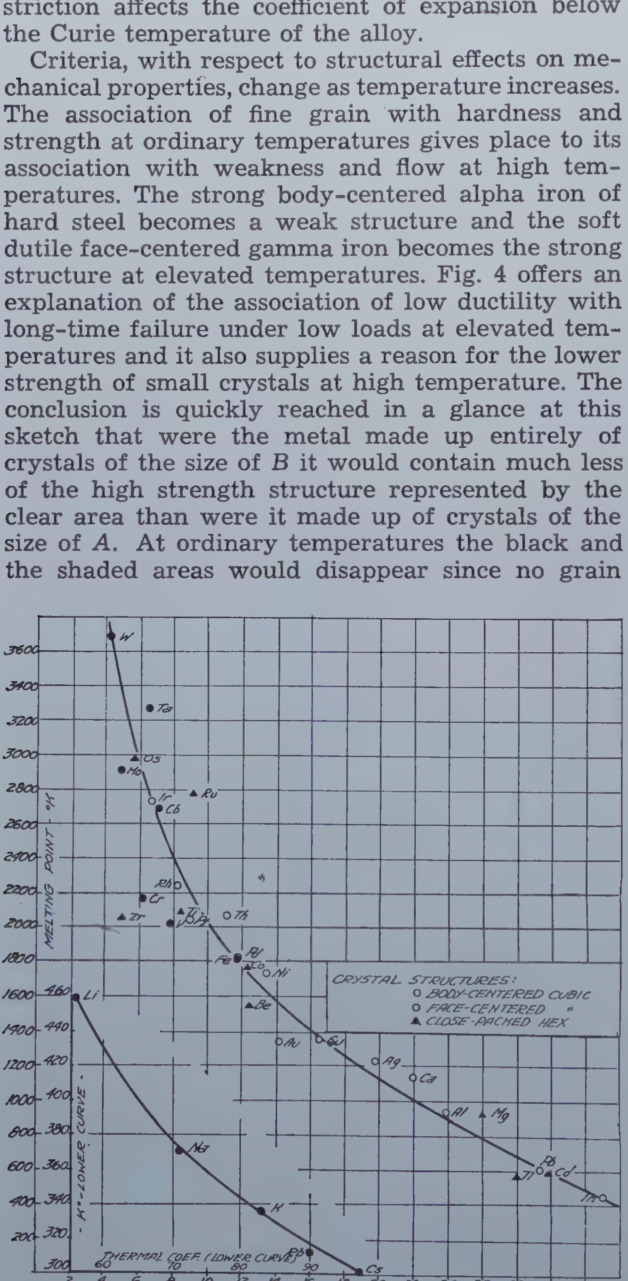

Fig. 11—Relationship of melting points of metallic elements to their coefficients of thermal expansion at 20°C, (10^{-6} per degree C).

There is no evidence to prove that the ultimate in grain size results in the ultimate to be attained in resistance to deformation at elevated temperatures excepting perhaps for a stable solid solution or a pure metal. The presence of two or more stable phases undoubtedly improves elevated temperature strength. The word stable is used advisedly, for when the formation or solution of one of the phases or a change in form, such as spheroidization, occurs while the metal is subjected to a mechanical stress resistance is lowered.

It is difficult to consider the effect of grain size on strength apart from the effect of grain growth at temperatures where grain growth is normally an active factor. No doubt a fine grain size would be stronger at elevated temperatures than a coarse one were the grain boundaries no more active than at normal temperatures. It is therefore reasonable to conclude that it is not small grain size *per se* that produces weakness at high temperatures but rather the activity of the boundary atoms engaged in grain growth. A metal composed of grains grown at a temperature of, say, 2100°F, is thus stronger at 1600°F than is the same metal when it is composed of small grains grown at, say, 1400°F. However, the finer grained of two different metals may be the stronger at a given temperature if it happens to be the more resistant to grain growth at that temperature.

The recounting of the effects of the various factors considered on the resistance of metals to deformation and fracture at elevated temperatures may appear here to have been rather oversimplified. The picture drawn has been one of metallic systems in a disturbed state varying from near stability to great activity, from rigidity to fluidity, from strength to weakness. Other pictures may be drawn from other points of view.

May I then close with a quotation which Howe, with so much greater grace and appropriateness, borrowed from the sayings of Tyndall: "Right or wrong, a thoughtfully uttered theory has a dynamic power which operates against intellectual stagnation; and even by provoking opposition is eventually of service to the cause of truth."

References

[1] *Jnl.* Franklin Inst. **69**, 257-266.

[2] Howard S. Avery, Earnshaw Cook, and J. A. Fellows: Engineering Properties of Heat-resistant Alloys. *Trans.* AIME (1942) **150**, 383.

[3] Z. Jeffries: Effect of Temperature, Deformation, and Grain Size on the Mechanical Properties of Metals. *Trans.* AIME (1919) **60**, 474.

[4] George B. Clark and Walter H. Bruckner: Behavior of Metal Cavity Liners in Shaped Explosive Charges. *Trans.* AIME (1948) **176**, 527: *Met. Tech.* (Aug. 1947) TP 2158.

[5] H. Zschokke: *Brown Boveri Milleilunger.* **33**, No. 9, 227-233.

Oxygen in Liquid Open-Hearth Steel—Oxidation During Tapping and Ladle Filling

by T. E. Brower, J. W. Bain and B. M. Larsen

A mass of circumstantial evidence is presented to indicate that the main source of alloy losses in open-hearth tapping is oxidation by air, with the steel apparently reacting with an amount of oxygen equivalent to about 30 times its own volume of air. The effect is erratic from heat to heat, depending largely on turbulence and distance of free fall of the stream of liquid metal.

THIS paper reports another phase in a general study of oxidation in the open-hearth, various aspects of which have already been discussed in previous papers.[1, 2, 3] It is based on experiments conducted on commercial, basic open-hearth furnaces at various times when opportunity offered, beginning about 1938, in an attempt to determine the mechanism and measure the amount of air oxidation during the flow of the tapping stream through the air into a ladle. This effect is closely connected, not only with alloy losses and control of chemical analysis, but possibly with various questions regarding inclusion content and steel quality and with a true picture of the deoxidation of steel in general. Thus it is believed that discussion of a large part of the results to date may be of assistance to others who are studying problems related to deoxidation or to steel cleanliness and quality.

The literature reveals that strangely little attention has been devoted specifically to the effect of pouring steel through open air. Bardenheuer and Henke[4] in 1939, in a paper devoted largely to overall losses of manganese in the basic open-hearth, reported that for a number of heats tapped into a tilted ladle held just beneath the runner so that the maximum distance of drop of the stream through the air was held to less than about 30 in., there was in most cases almost no loss of manganese from furnace to ladle. Hultgren,[5] in 1945, showed that in high-carbon basic electric steel deoxidized in the furnace and containing no large inclusions as it left the furnace, large silicate inclusions, often rich in manganese oxide, were present in samples dipped from the pool in the ladle; also that the rise in content of large inclusions (above 0.01 mm diam) was greater when the metal stream was made to spray or flow in a turbulent manner.

Our interest in this phase of oxidation in the open-hearth was first aroused by a study of alloy efficiencies on ladle additions. The frequency curves of manganese efficiency (net recovery of metal added in ladle) given in fig. 1 are of interest in this connection. Lowest, and also most variable (47 to 95 pct), recovery was in low-carbon heats having no coal additions to the ladle, progressing upward to a maximum average and least variable (82 to 97 pct) recovery in high-carbon heats killed with aluminum and silicon. Both coal additions and higher carbon contents in the tap stream, as well as additions of silicon and aluminum, help to lower the amount of manganese loss. But the most interesting point is the amount of manganese oxidized in many heats tapped at 0.50 to 1.00 pct carbon. It has been shown in a previous paper[3] that the amount of oxygen in the tap stream in such heats is very small, usually below 0.01 pct, too small to oxidize any appreciable amount of manganese. Also, the fact that manganese should be oxidized at all in a metal solution containing such more stable oxide-forming elements as aluminum and silicon is an indication of some rather intense oxidizing effect such as could be caused by reaction with the air during ladle filling.

Oxygen Balances from Tap Stream to Teeming Stream: Data in the form of alloy efficiencies, such as those shown in fig. 1, are not a proper measure of such a general oxidation effect. Having available

---

T. E. BROWER, Member AIME, J. W. BAIN, and B. M. LARSEN, Member AIME, are associated with the Research Laboratory, U. S. Steel Corp. of Delaware, Kearny, N. J.

AIME St. Louis Meeting, Feb. 1951.

TP 2872 C. Discussion (2 copies) may be sent to Transactions *AIME before Aug. 1, 1950. Manuscript received Jan. 26, 1950.*

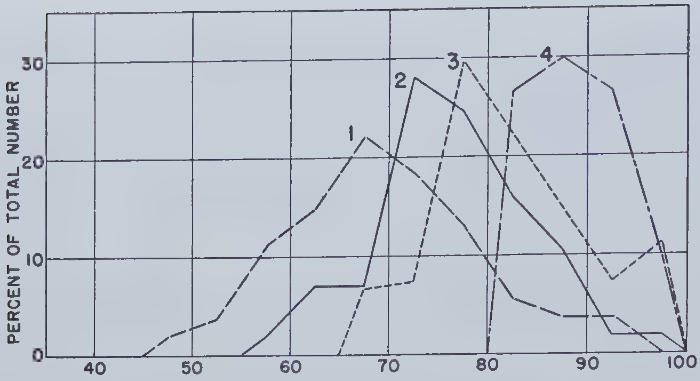

Fig. 1—Distribution curves of net efficiency or recovery of manganese added in ladle in four groups of open-hearth heats, as follows:

Curve 1.	54 heats without coal, 0.08 to 0.14 C at tap, rimmed or capped.
Curve 2.	57 heats with coal, 0.06 to 0.15 C at tap, rimmed or capped.
Curve 3.	27 heats without coal, 0.06 to 0.12 C at tap, Al, Si killed.
Curve 4.	30 heats with and without coal, 0.50 to 1.00 C at tap, Al, Si killed.

a rather accurate method[1] of sampling to obtain the analysis of tapping and teeming streams, including dissolved oxygen content, it seemed logical to attempt an approximate alloy and oxygen balance between these two steps in the steelmaking process. We could not hope to measure the amount of iron lost, but from data on the total weight of metal, the amount of carbon, manganese, silicon, etc. added to the ladle, and the composition of samples taken from tap stream and teeming stream,* we could measure the loss of all solute elements and obtain their oxygen equivalents, assuming negligible losses by vaporization.

As an example of such calculations, which have been made on more than 200 heats of various grades of steel, we give averaged results for a group of 8 heats of 0.53 to 0.67 C, Si-Al killed, fine-grain open-hearth steel. All weights are expressed in pounds per ton of steel tapped. In addition to manganese, silicon, and aluminum (2.01 lb per ton of Al average), an average of 0.90 lb per ton of graphite was added in the ladle. Additions were analyzed and weighed with some extra care and the total weight of ingots, butts, and pit scrap or skulls was measured as accurately as was practicable. The loss of alloys between tap and teeming streams averaged as follows:

	Lb per ton
Mn	1.62
C	0.31
Si	0.88
Al	0.94

The above metal losses, converted into oxygen equivalents as MnO, CO, SiO_2, and Al_2O_3 are as follows:

	Lb per ton
O_2 equivalent of Mn loss	0.47
O_2 equivalent of C loss	0.41
O_2 equivalent of Si loss	1.00
O_2 equivalent of Al loss	0.84
Total	2.72

The dissolved oxygen, however, dropped from 0.009 pct in the tap stream to 0.002 pct in the teeming stream, representing an oxygen contribution of 0.14 lb per ton.

	Lb per ton
Total oxygen equivalent of solute losses	2.72
Change in dissolved oxygen	0.14
Apparent oxygen from external sources	2.58

In these heats of fine-grained steel, apparently, only a few percent of the losses of alloys can possibly be due to reaction with that oxygen which is dissolved in the steel as it leaves the furnace. The large remaining loss could conceivably be due in part to vaporization or if, as seems very probable, it is nearly all oxidation loss, it could also be partly due to reaction with the furnace slag. If, as the authors believe, it is essentially all the result of air oxidation, this means that the liquid steel and the alloys added, in the above average of 8 fine-grain heats, have somehow come into contact with an amount of oxygen equivalent to about 146 cf of air per ton of metal, or about 33 times the volume of the liquid metal itself, all this in the 8 to 15 min of flow of the tap stream down the runner and in its tumbling rather violently into the ladle below.

We can observe certain qualitative indications of such an effect. The high temperature of the liquid steel surface and the transparency of air to radiant energy cause sharp temperature gradients and an obviously violent rising and eddying flow of air around the stream and into and out of the ladle. A layer of oxide scum something like an inch thick can be seen to rise up and cover most of the ladle pool surface before the slag flow begins. Repeated bursts of flame occur from gases rising out of the pool, which must contain carbon monoxide. As discussed in a later section, we find evidence of great turbulence and much breaking up of the falling stream and of air carried down into the ladle pool by such a stream of metal. However, experimental conditions prevent a direct quantitative confirmation of such an oxidation. We cannot measure the iron loss, nor separate and weigh the scum on the ladle pool nor the CO gas evolved. Thus the simplest presentation is perhaps to give the data on the assumption that the unaccounted-for loss of the solute elements is an approximately accurate measure of air oxidation and to let the reader judge as to the reasonableness of the picture thus outlined.

A few clues result from the distribution and amount of solute losses in various grades of steel as tabulated in table I below, where enough heats are averaged in each group to eliminate largely the variability from one heat to another. The proportion of the apparent total oxidation effect which is due to reaction with oxygen dissolved in the tap stream is larger in the low-carbon steels, though even here there is three to four times as much oxidation from external sources, presumably air. Also total loss and oxidation are greater in those grades to which more silicon, aluminum, or chromium are added in addition to the manganese. This may be caused by more unmeasured iron loss in the low-carbon grades, especially the open steels, also by more total reaction with the air when more of the easily oxidizable elements are present. Although somewhat less manganese is lost in those grades in which more silicon and aluminum are present, the fact that manganese loss is high even in these grades is an indication of a "strong" oxidation effect such as would result from a bessemer-type reaction with air. Addition of coal or graphite causes larger carbon losses, and it seems likely that a part of this increased loss may be due to carbon granules of low density being blown up into the air above by rising air currents. There is, however, a small but definite measured carbon loss even in heats in which the carbon could only have been oxidized directly out of the iron solution. This is again an indication of direct oxidation by air; enough is known of the carbon reaction to make it very unlikely that any appreciable amount of this carbon oxidation could be caused by the furnace slag under these conditions. The losses in general strongly suggest a general oxidation of all the elements in solution as well as of the iron itself (much of this oxidized iron might be reduced again before mixing with the final ladle slag) such as would result only from direct reaction with oxygen present at high activity in the atmosphere.

---

* Average of 2 or 3 samples taken before middle ingot to avoid effect of ladle slag reaction on last 1 or 2 ingots.

Compared to air, the tap slag is only mildly oxidizing to both the tap stream and the alloyed metal in the ladle. Also, it normally comes out only with the last one-third or less of the steel and flows on top with no great amount of mixing into the ladle pool. Thus it would seem reasonable to assume that slag oxidation after tap is only a minor factor.* This assumption is fairly well substantiated by the comparisons in table II below, which includes the oxidation effect in heats with furnace tap slag kept off the ladle compared with normal practice heats and also heats made with a tilted ladle, all the heats being of low-carbon steel, tapped open.

Heat A was tapped from a tilting furnace, with the taphole stopped off sufficiently to prevent any slag flow ahead of the steel; the furnace was tipped back quickly with some steel remaining on the hearth so that only a very small amount of slag followed the metal. Heat B was tapped from a stationery furnace, but through a slag-separating box; here again only a small amount of furnace slag, and that only at the end of the tap, entered on top of the ladle. Col. 3 shows the average alloy loss equivalents for 5 similar low-carbon (0.06 pct or below) rimming heats tapped in the normal manner with slag flowing into the ladle during the later part of the tapping period; the total net oxidation which is unaccounted for is essentially the same as in the heats in which practically no slag tumbled into the ladle.

Table I. Distribution and Amount of Solute Losses in Various Grades of Steel

	Capped and Rimmed		Semi-killed	Si-killed	Fine-grain	Fine-grain	Alloy
	0.03-0.13C	0.10-0.26C	0.11-0.30C	0.05-0.10C	0.53-0.67C	0.25-0.80C	0.40-0.60C
No. heats averaged	55	22	11	25	8	6	7
Coal or graphite to ladle	none	coal	coal	none	graphite	coal	graphite or coal
	Lb per Ton of Steel						
Mn loss	2.27	2.23	2.21	1.50	1.62	1.92	2.00
C loss	0.17	0.65	0.38	0.10	0.31	0.73	0.56
Si loss	0.05	0.08	0.67	2.01	0.88	0.73	0.97
Al loss	0.18	0.04	0.32	0.29	0.94	0.71	0.94
Cr loss							0.76
Total alloy losses	2.67	3.00	3.58	3.90	3.75	4.09	5.23
Total oxygen equiv. of alloy losses	1.13	1.67	2.20	3.09	2.72	2.98	3.61
Decrease in oxygen in solution	0.27	0.36	0.46	0.78	0.14	0.24	0.22
Apparent air oxidation	0.86	1.31	1.74	2.31	2.58	2.74	3.39

Table II. Comparison of Oxidation Effect in Heats with Normal Practice Heats and Heats Made with Tilted Ladle Oxygen Balances—Lb O_2 per Ton of Steel

	Slag-separated Heats		Avg. of 5 Normal Tap Heats Comparable to A and B	Tilted Ladle Heats		
	A	B		C	D	Avg. of 7 Similar Heats
Oxygen equiv. of Mn lost	0.84	0.44	0.74	0.75	0.61	0.54
Oxygen equiv. of C lost	0.25	0.11	0.25	0.14	0.21	0.27
Oxygen equiv. of Si lost	0.07	0.90	0.08	0.08	0.10	0.08
Oxygen equiv. of Al lost	0.33	0.34	0.24			0.10
Oxygen equiv. of total alloy losses	1.49	1.79	1.31	0.97	0.92	0.99
Net change in dissolved oxygen	—0.50	—0.90	—0.32	—0.52	—0.44	—0.43
Apparent oxygen from external sources	0.99	0.89	0.99	0.45	0.48	0.56

---

* Except with respect to the top layer of steel which can react with slag all through the teeming period and produce the well-known falling off in manganese or residual aluminum contents in the last ingot in many heats, especially when a thick layer of slag remains on the ladle metal.

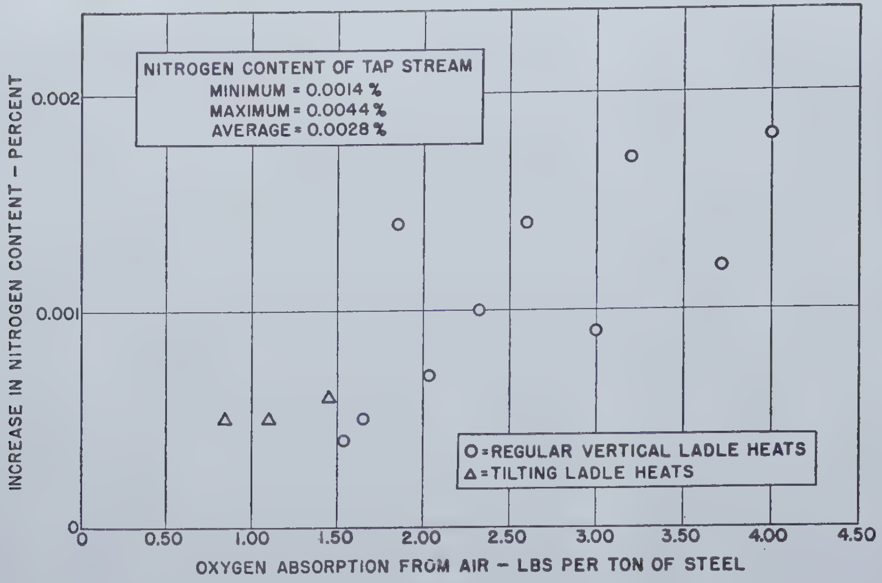

Fig. 2—Air oxidation vs. nitrogen increase between tap stream and teeming stream.

The last three columns give the corresponding data for two individual heats, and for one average of 7 heats, all of low-carbon open steel as in the first three columns; here, the ladle was tilted and held under the runner during the tap so that the metal stream never fell more than 12 to 18 in. through the air to the sidewall or the pool of metal in the ladle; furnace slag was allowed to accompany the latter part of the metal into the ladle in the normal manner. The only different condition present in these tilted-ladle heats was the smaller fall and less violent tumbling of the tap stream into the ladle pool.

There is perhaps no significance in the various individual loss items in table II, but the difference in total external oxidation between the first three and the last three columns is large enough to be significant. Whereas the elimination of mixing between furnace slag and ladle metal had almost no effect, the decreased fall and violence of drop of metal stream into ladle pool reduced the oxidation effect to about half the average level for normal practice, in these low-carbon heats. Similar differences in other heats and for different grades are shown in the discussion later in this paper. It is very difficult to explain such an effect by any mechanism other than the predominance of air oxidation, not only by reaction of air with exposed liquid surface, but apparently also by actual mixing of air down into the ladle pool, as will be discussed later.

Nitrogen Absorption During Ladle Filling: Preliminary nitrogen analyses on samples from: (1) furnace bath just before tap; (2) tap stream off the end of the runner, and (3) pouring stream at the platform gave very close agreement between samples (1) and (2) but a definite increase in nitrogen from (2) to (3). Due to a probable higher energy barrier to reaction and the limited solubility of nitrogen in the liquid metal, one would expect very much less reaction with nitrogen than with oxygen during tap. Nevertheless, if this alloy loss during tapping and ladle filling is essentially a matter of air oxidation, one would expect some degree of correlation between oxygen and nitrogen absorption. Nitrogen analyses were made therefore on tapping and teeming samples from a group of heats selected to cover a wide range of calculated values for total air oxidation, with results shown in fig. 2. The ordinate in this figure is the increase in percent nitrogen from tap stream to teeming stream. As indicated on the figure, the actual nitrogen contents in tap stream samples varied from 0.0014 to 0.0044 pct. Considering possible errors in differences between such small nitrogen contents, the points indicate a surprisingly good approach to a linear relationship between nitrogen and oxygen absorption, thus giving us another independent effect tending to confirm the reality of such a surprising amount of reaction between atmosphere and liquid metal.

Another somewhat related indication was derived from the observation that rimming action was more sluggish in a group of rimmed heats tapped into a tilted ladle with only 12 to 18 in. of free fall into the pool and only about half as much air oxidation as in normal tapping practice. In table III, averaged data on seven such heats are compared with ten normal-tap rimming heats which gave almost the same average carbon and oxygen contents in the tap stream. The reduced turbulence in the tilted ladle gave a 46 pct reduction in "external" oxidation, which showed up mainly in an increased recovery of manganese; however, this also seemed to leave a decreased amount of oxygen in the steel at the platform. The $\Delta[O]$ values (the excess of oxygen in solution above the value for equilibrium with the carbon at 1 atm pressure) are nearly the same in the tap stream in both groups, but after the turbulence of ladle filling is over, the quieter tilted-ladle heats show only about half as much excess oxygen in the stream entering the molds. Only by the use of extra sodium fluoride and less aluminum in the molds was reasonably good rimming action obtained on these heats, in spite of a slightly lower average aluminum addition to the ladle.

Flow of Air with Falling Streams into a Liquid Pool: The rate of reaction between exposed surfaces of liquid metal and oxygen diffusing through a postulated air film might be calculated on the assumption that all oxygen molecules reaching the metal surface would react, but the results would be uncertain, even perhaps in order of magnitude. The effective air-film thickness at temperatures of 2850° to 2950°F, the true area and time of exposure of liquid surface together with other possible unknown aspects of the reaction all tend to discourage such a calculation. One can guess that the rate would be relatively high because of the probable steep temperature gradient in air next to the liquid surface, but it is still difficult to accept a surface reaction with air to the extent of as much as 30 to 50 times the liquid-metal volume, in view of the short exposure of such a massive tap-stream and ladle-pool surface. Also, the probable degree of variability in surface exposure would not appear sufficient to explain the wide range in amount of air oxidation indicated by the points in fig. 2.

We were thus led to suspect that bubbles of air are carried down into the ladle pool by the falling tap stream. In some laboratory studies of water streams falling into a glass tank from a reservoir with a bottom outlet simulating a ladle nozzle, it was found that the entrapment of bubbles into the pool was too rapid for visual observation or for recording by a motion picture camera operating at 4 to 6 times the normal speed. This finally led to pictorial records made with a high-speed camera at 1000 to 2500 frames per second so as to enlarge the time scale 75 to 150 times. Such studies led to the following conclusions:

Table III. Comparison of Low-carbon Rimmed Heats

	Avg. of 10 Non-Tilting Ladle Heats	Avg. of 7 Tilting Ladle Heats	Difference
Lb O_2 per ton equivalent to Mn loss	0.84	0.54	
Lb O_2 per ton equivalent to C loss	0.28	0.27	
Lb O_2 per ton equivalent to Si loss	0.06	0.08	
Lb O_2 per ton equivalent to Al loss	0.15	0.10	
Total lb. O_2 per ton equivalent	1.33	0.99	
Net change in dissolved O_2*	—0.30	—0.43	
Lb O_2 per ton from air	1.03	0.56	0.47 or 45.7 pct reduction
Mn loss lb per ton	2.87	1.86	1.01
C loss lb per ton	0.21	0.20	
Si loss lb per ton	0.06	0.07	
Al loss lb per ton	0.17	0.11†	0.06
Total loss lb per ton	3.31	2.24	1.07
Avg. lb per ton Mn added in ladle	6.5	7.7	
Mn efficiency of ladle addition, pct	55.5	76.9	21.4
[C] in tap stream, pct	0.066	0.068	
[O] in tap stream, pct	0.060	0.056	
[O] equilibrium with C, pct	0.034	0.033	
Δ [O] above equilibrium, pct	0.026	0.023	
[C] in teeming stream, pct	0.079	0.088	
[O] in teeming stream, pct	0.045	0.034	
[O] in equilibrium with C, pct	0.028	0.025	
Δ [O] above equilibrium, pct	0.017	0.009	0.008

* O_2 in tap stream minus O_2 in teeming stream.

† Two heats did not have aluminum addition, average for remaining five was 0.15.

1. Smooth streams of constant, or nearly constant, diameter seem to carry no bubbles into a pool, even with rather long distances of free fall.

2. Any such free-falling stream is unstable, however, tending eventually to break up into drops, with a transition of increasing waviness between smooth cylindrical stream and separate drops. Because of the instability in such a stream, any eddy or vortex within the liquid, or any disturbance of smooth flow by obstacles, sudden turns, etc. all tend to accelerate the development of roughness in the falling liquid stream. All these effects seem to be even more marked in liquid mercury than in water, due, perhaps, to higher surface tension.

3. It is the impact of a wave or other roughness in the stream surface which pushes the pool aside and permits the entrapment of a volume of the air being pulled along adjacent to the stream surface; this entrapped volume is then carried down into the pool as a shower of smaller bubbles.

4. Such bubbles, once carried down into the pool, are prevented from rising out immediately by circular eddies set up within the pool by the falling stream.

This effect can be seen best by viewing the high-speed motion picture records, but the enlargements of two frames from one such record, shown here in figs. 3*a* and 3*b*, will serve as an indication. Fig. 3*a* shows a wave in the stream just about to enter the pool, which contains at the moment only scattered

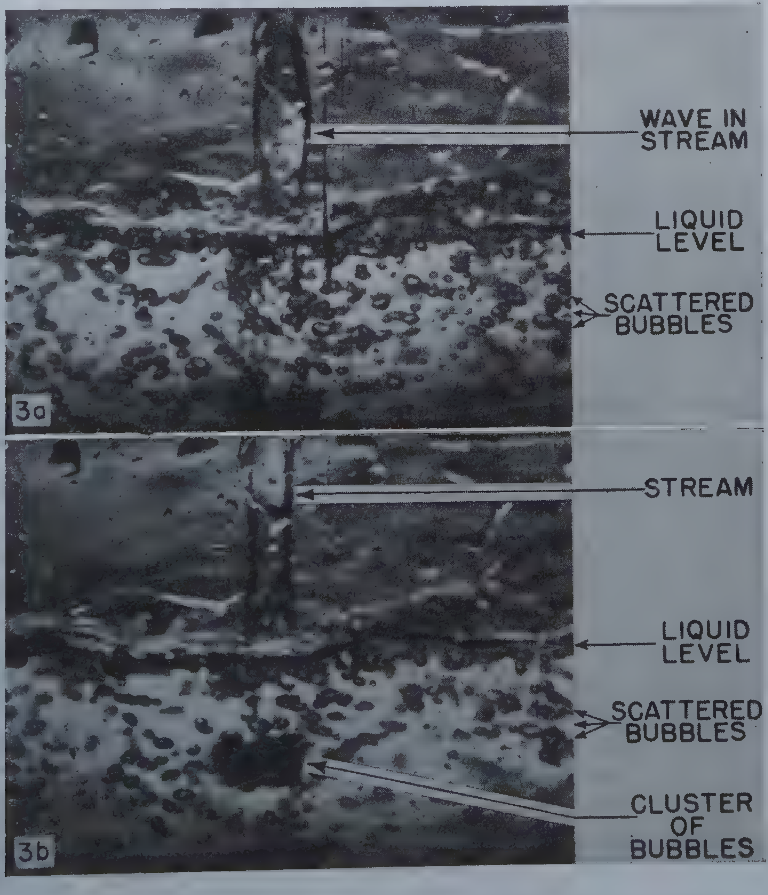

Fig. 3—Enlarged frames from high-speed motion picture of falling water stream entering pool.

a. Wave in stream just entering pool.
b. About 0.015 sec later than 3*a*, showing mass of bubbles carried into pool with impact of wave.

bubbles but none entering with the stream; fig. 3*b* shows the shower of bubbles present in the pool near the stream a very small fraction of a second later, after the impact of this wave on the pool surface. Similar photographs of liquid mercury which in this case include only the stream and the pool surface, showed that wavy streams carry air bubbles down into the pool of this much heavier liquid.

The density of liquid steel is intermediate between water and mercury; its viscosity is rather close to that of water and its surface tension more nearly like that of mercury. Similar high-speed picture records were made during the tapping of several commercial open-hearth heats. Figs. 4*a*, 4*b*, and 4*c* are again enlarged frames from motion picture records showing tap stream and ladle pool, on three such heats; here again, the original records viewed in slow motion, made in natural color in some cases, show the effects much more clearly. Fig. 4*a* serves at least to indicate the surface character of what, by comparison, would be called a relatively smooth tap stream; even under best average conditions the stream surface, as shown here, has rather rough contours, indicating turbulent flow. Fig. 4*b* illustrates the rougher contours of what would be called a relatively heavy surging or pumping tap stream; at this particular instant of flow, the stream is divided into almost completely separate portions. Reasoning by analogy from the above observations on falling water streams, one would expect a considerable transport of bubbles down into the ladle pool, even with the relatively smooth stream of fig. 4*a*, but that this transport would be much greater with a rougher stream such as in 4*b*, which difference was actually observed in these heats. In 4*c* is shown a flame burst, presumably from burning CO, indicating the escape of bubbles comprising mainly nitrogen and carbon monoxide, from the pool after

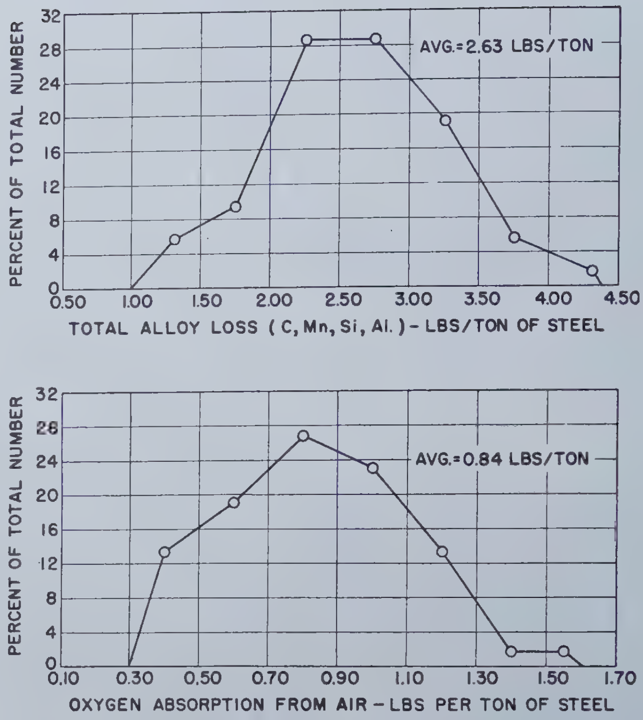

Fig. 5—Distribution curves of total alloy loss and calculated oxygen absorption in pounds per ton of steel—based on 52 heats of 0.03 to 0.13 C capped and rimmed steel, tapped into regular vertical ladle.

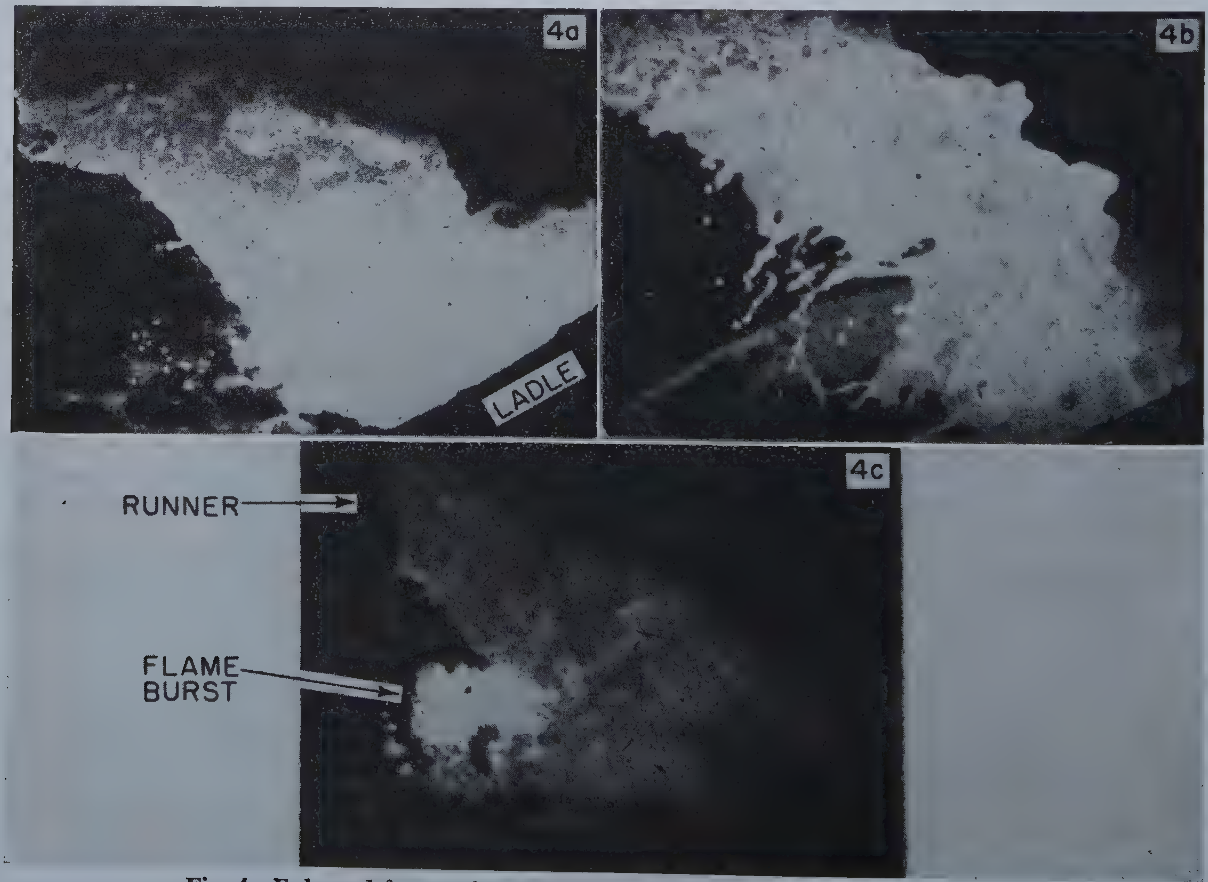

Fig. 4—Enlarged frames from high-speed motion pictures of tap streams entering ladle pool on three open-hearth heats.

a. Relatively smooth tap stream.
b. More turbulent tap stream with rougher contours.
c. Flame burst from pool near tap stream; duration of burst about 0.01 sec.

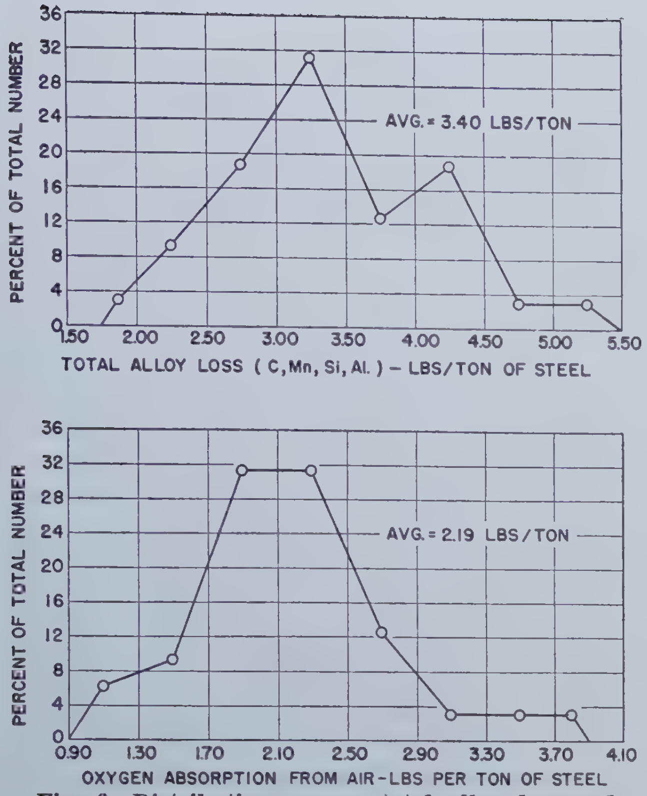

Fig. 6—Distribution curves, total alloy loss and calculated oxygen absorbed from air—32 heats of 0.08 to 0.68 C silicon-killed, coarse grain, tapped into vertical ladle.

having been carried under as air bubbles by the falling stream.

Variability in Oxidation Losses During Tap in Normal Shop Practice: Even ordinary visual observation gives rather good indications that turbulence and exposure to air are quite variable from one heat to another in normal open-hearth tapping practice. Irregularities inside the taphole or in the runner near the taphole exit are probably responsible for surging and waviness in the stream; however, such extreme conditions as spraying or pumping of the stream may be in part related to other factors such as gas evolution back inside the taphole. Occasionally, a tap stream may appear smooth, flowing like a viscous fluid such as tar or honey, but this condition is rather exceptional and may vary through degrees of turbulence to really violent taps when pumping, spraying, and billowing of the stream are present all together.

Therefore, on the assumptions: (1) that air oxidation is the main, or at least a major factor determining alloy losses, and (2) that area and amount of reaction at exposed liquid surface as well as amount of air entrained in the ladle pool would increase with degree of turbulence in the tap stream, we would logically expect a wide variability in alloy losses, as indeed was indicated by the plant data on manganese recovery from ladle additions shown in fig. 1. However, the true variability in pounds per ton of steel in both total alloy loss and the calculated amount of air oxidation are shown for normal tapping practice more accurately by the frequency curves in figs. 5 and 6. Fig. 5 is derived from 52 heats of low-carbon (0.03 to 0.13 pct) open steels, showing a variability of at least 4 to 1 in apparent air oxidation. Fig. 6 is based on 32 heats of coarse-grained silicon-killed steel varying from 0.08 to 0.68 pct in carbon content; alloy losses in this case average somewhat higher, the variability of about 3 to 1 in ratio being about the same in pounds per ton of steel as in the lower carbon heats.

The word "deoxidation" has always been a rather ambiguous term in steelmaking parlance. Actually the normal process of tapping and adding alloys in the ladle is a combination of oxidation and deoxidation which nearly always results in some net decrease in oxygen content between tapping and teeming streams. The loss in any one solute element is presumably due in part to reaction with oxygen in solution in the tap stream as well as with oxygen coming from external sources, which we are assuming to be the atmosphere in this discussion. If we make the somewhat arbitrary assumption that the net decrease in dissolved oxygen is divided among the various alloy additions in the ratio of their relative losses, we can derive approximate values for the losses of any given metal which is due to "air oxidation only." The frequency curves of fig. 7 are obtained from such values, in this case for manganese loss; the solid curves show the range of total manganese losses, the dashed curves show the loss "from air oxidation only." In the higher carbon killed-steel heats shown by the upper curves, the dissolved oxygen is small and is shared among other alloys, so that the range and variability in manganese loss from "air oxidation alone" is almost the same as the total loss. In the low-carbon open steel heats shown by the lower curves, about 25 pct of the manganese loss is counted as resulting from the oxygen in the tap stream, but the variability is seen to be nearly all due to oxygen from external sources.

These curves indicate a variability range of from 0.16 to 0.18 pct Mn apparently due to variable "external oxidation" during tap. This variable may be considered as almost entirely out of control of the

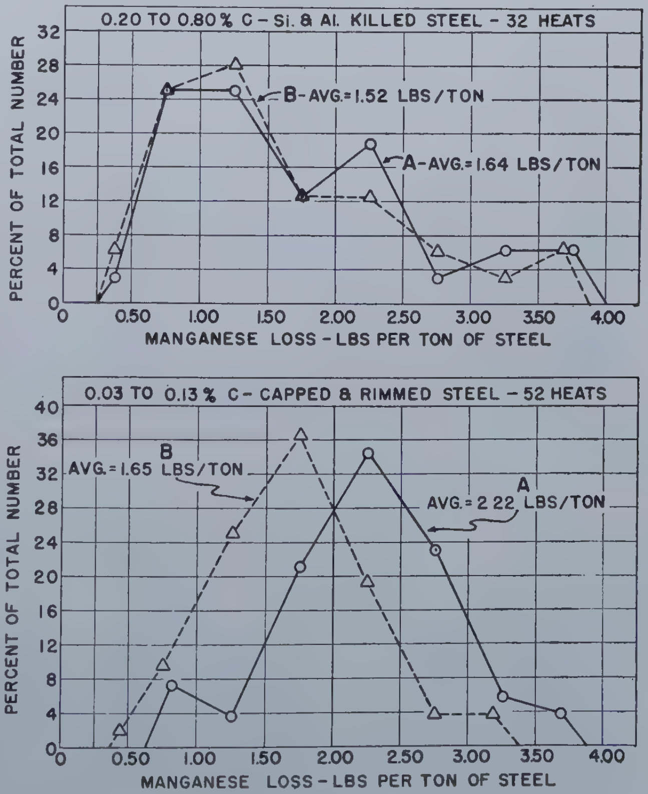

Fig. 7—Distribution curves of manganese loss—regular vertical ladle.

A. Total loss from air oxidation plus oxygen dissolved in tap stream.
B. Loss from air oxidation only.

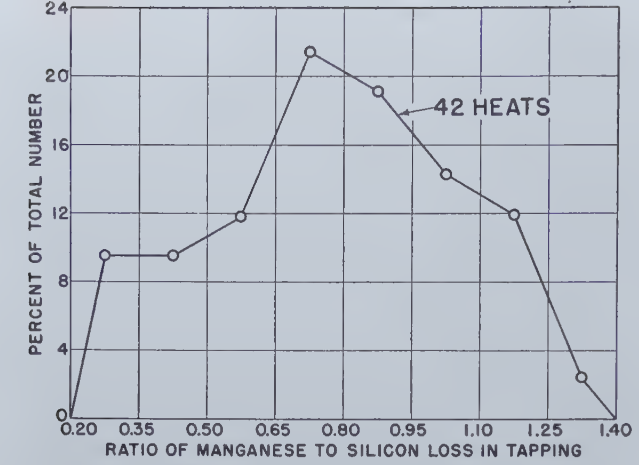

Fig. 8—Distribution curve of ratio between manganese and silicon losses during tap into normal vertical ladle—based on 42 heats of 0.08 to 0.18 C, silicon-killed.

furnace operators under normal conditions of furnace operation, so that even with the most accurate analyses and weights, the melter cannot be expected to regulate the manganese content within a range of less than about 20 points. This is a typical instance of the lack of close control of composition in general which is inevitable in nearly all present practices for handling steel from furnace to ingot mold.

Silicon losses show a similar variability in normal practice. The relative amounts of manganese and silicon losses obtained in any one heat also vary widely in their ratio; even among heats of the same grade of steel in one shop the manganese loss is sometimes larger, very often much smaller than the silicon loss, in pounds per ton of steel. This is illustrated by the frequency curve of fig. 8, derived from data on 42 heats of silicon-killed steel, all within 0.08 to 0.18 pct carbon and with aluminum additions to the ladle around 0.5 lb per ton or below; the variation here of 6 to 1 in the ratio probably covers most of the heats of a given grade, although in this case three heats with Mn/Si loss ratios of 2.5, 2.5, and 3.6 were not included since they were so far out of the range covered in fig. 8. Briefly, we may say that erratic oxidation effects seem to be inherent in normal furnace tapping practice, probably due to erratic mixing conditions and the "strong" oxidizing effect of oxygen from air.

Experiments on Some Methods of Reducing Air Oxidation: In view of the practical difficulties in handling liquid steel at 2800° to 2950°F, only a few of the simpler methods of minimizing this oxidation effect have been tried up to the time of this writing. The simplest idea which might occur to anyone considering the problem would be to surround the stream and ladle pool with a reducing or neutral atmosphere. A number of heats were tapped with a stream of small coal, from 25 to 75 lb total weight, fed until slag began to flow, on the tap stream near the taphole, the coal flowing on the metal down the runner and into the ladle. A few heats were also made with a large number of tiny streams of heavy oil flowing on the steel along the length of the runner. In either case, the hope was to form reducing gases which might be carried along by the moving metal surface. These efforts were a complete failure, giving no reduction in total loss of manganese, silicon, and aluminum. In the heats fed with coal, the total carbon loss was somewhat higher, which was to be expected.

In another group of silicon-killed heats, large additions of calcium-silicon alloy, substituting for part, or all, of the ferrosilicon normally used, were made in various ways. The alloy was placed all on the bottom of the ladle, or fed at various intervals to the ladle during tap, or, by selecting fine-sized pieces, was fed on the tap stream in the runner over the whole tapping period. Counting in the oxygen required to oxidize the calcium, the total oxidation effect was larger on these heats than in a comparison group deoxidized with ferrosilicon. Silicon loss was about the same in both groups, manganese loss was appreciably lower in the Ca-Si-treated group, and with the oxygen equivalent to the change of the calcium metal to CaO omitted, the total apparent external oxidation in these heats was lower by about 20 pct. In spite of the higher specific gravity of calcium vapor or CaO fume, it was quite apparent that a violently eddying layer of air was carried down with the tap stream, easily displacing the fume-filled gases over the pool in the ladle. In general, manganese recovery can be improved rather consistently by feeding a stream of small-sized silicon or other similar alloy on the tap stream in the runner. However, total air oxidation is not reduced and, in fact, is likely to be somewhat increased by such practice. It merely tends to decrease manganese loss at the expense of a larger silicon loss.

The failure to reduce air oxidation in these tests is interesting mainly because it illustrates the violent eddying caused by the steep temperature gradient which makes it practically impossible to prevent air from being swept into intimate contact with all exposed liquid metal surfaces.

Since with a stream of any given turbulence, the larger the distance of free fall into the ladle pool, the greater should be the tendency to break up and

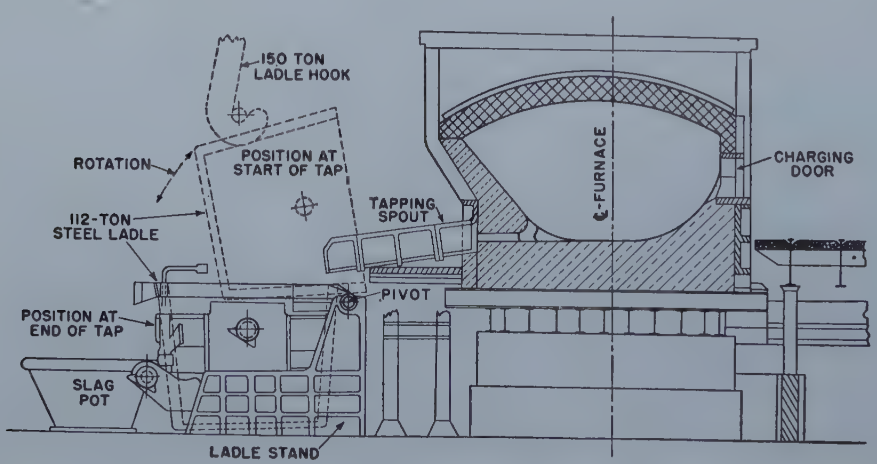

Fig. 9—Tilting ladle.

(South Works, Carnegie-Illinois Steel Corp.)

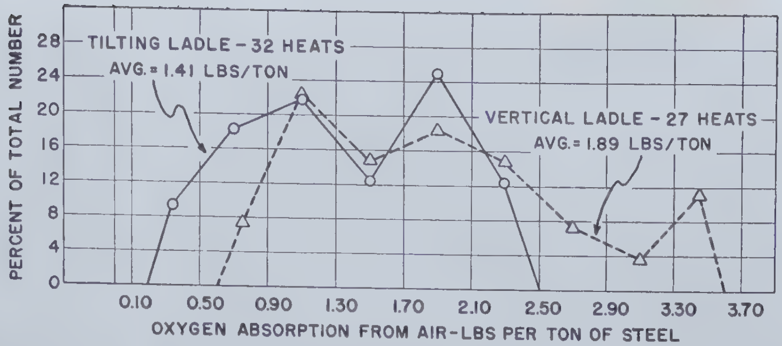

Fig. 10—Distribution curves of oxygen absorption from air for taps into vertical and tilting ladles—both groups of heats are similar composites of rimmed, semikilled, and killed steels.

carry in more air bubbles, a few preliminary taps were made in which the craneman held the ladle initially almost horizontal just under the runner and lowered it during tap only fast enough to prevent overflow, so that free fall of the tap stream to the side of the ladle lining or the pool was held to below about 18 to 20 in. In contrast to the negative results mentioned above with reducing gases, this decrease in distance of free fall lowered the air oxidation to around half the usual value (see table II above). However, the safety problem and the skill required for such a tilting operation with the ladle crane made desirable a tilting-ladle arrangement such that any required number of experimental heats could be run off with a minimum of disturbance to normal shop operations.

Such an arrangement is shown in the sketch of fig. 9; this involves a special ladle stand designed to support both normal and tilting ladles, and a special ladle with four extra castings attached to the shell. Two of these form a pivoting point at the top of the vertical extensions to the ladle stand, the other two engaging the main hoist hooks on the ladle crane. The dashed lines show the ladle position at the beginning of tap; a gradual lowering during tap until the filled ladle rests in the normal way on the stand maintains less than about 15 in. of free fall of tap stream, and the ladle is then picked up in the normal manner for transfer to the pouring platform.

As far as we could judge, this technique, which was successfully used on some 40 to 50 heats, altered nothing but the distance of free fall of stream, at least to any large extent. The total effective exposure of liquid surface to air was probably not decreased; there was less falling stream surface but a somewhat larger average area of ladle-pool surface which was also situated more favorably for contact with moving air in the tilted ladle. It is therefore very probable that any effect on amount of air oxidation is essentially due to less breaking up of the free-falling stream so that a decreased amount of air bubbles was carried into the ladle pool. The frequency curves of fig. 10 show the distribution of oxygen absorbed from air per ton of steel for 32 heats into the tilting ladle and for a comparable group of 27 heats tapped into the usual vertical ladle. Both groups include rimmed, semikilled and killed steels, but all heats were made in one shop and the comparison group of vertical ladle heats was selected to eliminate as much as possible any average differences in other known variables. On the average, the tilting ladle reduced the amount of apparent air oxidation by 25 pct and also reduced the spread in air oxidation between different heats in the group.

From visual observation of the tap stream, helped out by the high-speed moving pictures (see fig. 4) it soon became obvious that: (1) even relatively "smooth" tap streams were quite possibly turbulent enough to carry air bubbles into the ladle pool in either tilting or vertical ladle; (2) there were large differences in stream turbulence between heats in both groups; and (3) these differences, even as judged by ordinary visual observation, had an obvious effect on the amount of alloy losses. These effects are illustrated by the frequency curves of fig. 11. In these observations, the visual estimate of relative stream roughness is only a rough criterion but is probably adequate for such statistical comparisons. The general trend is toward a reduction in alloy loss with less turbulence and spraying of the tap stream

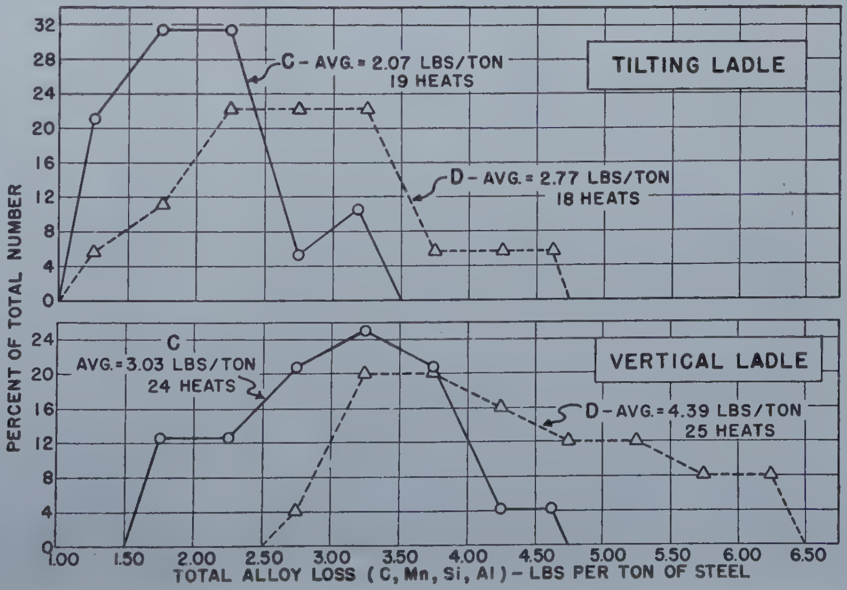

Fig. 11—Distribution curves of total alloy loss in groups with different degrees of roughness of the tap stream for both tilting ladle and normal vertical ladle. Composite of rimmed, semikilled and killed steels in each group.

C. **Smooth to slight surging.**
D. **Heavy surging and pumping.**

in both the tilting ladle heats (12 to 18 in. of free fall) and those tapped in the normal way into a ladle standing vertical (5 to 10 ft of free fall of stream); as in fig. 10 for oxygen absorption, the total alloy losses here in fig. 11 again show the effect of the shorter distance of stream fall.

In general, it is difficult to account for such behavior on any assumption other than that of variable amount of mixing and reaction with the oxygen of the atmosphere. No correlation has been observed between tap time and these calculated amounts of air oxidation. Apparently, oxidation can proceed very rapidly so that the effectiveness of mixing with air is the controlling factor. Some more recent data have been obtained on heats from tilting furnaces in which the rate of tap-stream flow is generally higher, but in which there is also a more turbulent and violent impact of the stream on the ladle pool. Six of these heats averaged close to 3.0 lb external oxygen absorption per ton of metal, with a few heats above the maximum of the distribution range for vertical ladle heats in fig. 10.

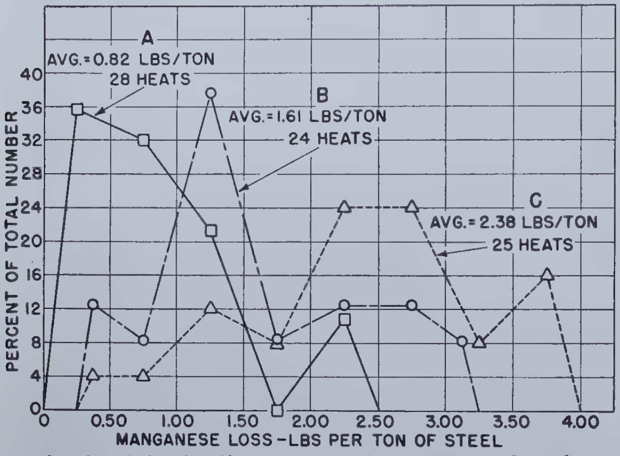

Fig. 12—Distribution curves of manganese loss for groups with various tap stream conditions—composites of rimmed, semikilled and killed steels.

A. Smooth to moderate surging — tilting ladle.
B. Smooth to slight surging — vertical ladle.
C. Heavy surging and pumping — vertical ladle.

Reduction of Manganese Losses in Tapping Practices: Relative losses of individual alloys in tapping show no consistent trends, the most definite being that aluminum losses are less variable and much less affected by tapping conditions than those of either manganese or silicon. A very small saving in average aluminum recovery in fine-grained heats was obtained with the tilting ladle practice, for example. In partial agreement with the results of Bardenheuer and Henke,[4] a few heats with the tilting ladle gave practically zero loss of manganese, but this was not at all consistent. Under present conditions of potential manganese supply for our steel industry, any possible saving in manganese loss happens to be of special importance. In fig. 12 are shown the distributions of manganese loss for three groups of heats, each group a composite of rimmed, semikilled and killed steels.

Group A includes nearly all the tilting ladle heats, with only those having definitely turbulent or spraying tap streams omitted. Group B includes heats from normal tapping practice in which the tap streams appeared smooth or with only a very moderate degree of turbulence. Group C includes heats from normal practice all having turbulent, pumping or spraying tap streams. These groups of about 25 heats are not large enough to give regular frequency distribution, but the average manganese losses of 0.82, 1.61, and 2.38 lb per ton, respectively, are probably close to what might be expected in larger groups.

These results indicate that merely with much improved taphole practice and tapping procedures such as would give consistently smooth-flowing tap streams, an average saving of around 0.4 to 0.5 lb manganese per ton might be obtained, perhaps a little more. (The writers' somewhat limited observations would indicate that really smooth-flowing tap streams are more the exception than the rule in typical shop practice.) Although the total potential saving of manganese is around 2 lb per ton by elimination of all air oxidation, we are not likely to devise any very practicable method for such elimination in the near future. However, a combination of smooth tap-stream flow in nearly all heats with some method such as the tilting ladle which would result in a minimum free fall of the tap stream would appear to give an average decrease in manganese loss of around 1.0 lb per ton of steel. Since this would probably be accompanied by around 0.7 lb of increased silicon recovery and perhaps 0.05 lb less aluminum loss, the cost savings in alloys should materially reduce any probable increase in operating cost involved in such practices.

It should be remembered that any such reduction in manganese loss in tapping is entirely independent of any saving through increased recovery in the metal in the furnace bath before tap.

Oxidation Effects and Steel Quality: We have no definite evidence at this time of any correlation between "air oxidation" and "steel quality," and in any case would prefer not to complicate the present discussion with this subject and with the vague and contradictory evidence regarding it to be found in the literature. A few brief comments may be helpful, however. Seams, inclusion streaks, and certain surface defects have in various papers been associated with "deoxidation practices," with erosion or chemical attack on refractories, with precipitation of nonmetallics during freezing, and with furnace charge materials or refining practices. The writers feel that clear-cut evidence is lacking for practically all the various viewpoints, probably because we still lack fundamental knowledge about the mechanism and controlling factors in the formation of precipitates or emulsified nonmetallics in the liquid metal.

There are definite indications of some kind of relationship between the oxidation effects involved in normal tapping practices and inclusions in the metal. In killed heats, the 3 to 9 lb of manganese, silicon, and aluminum oxides formed by oxidation per ton of metal in the ladle amounts to approximately 0.4 to 1.0 pct in terms of liquid metal volume. A very large majority of these oxide particles rise quickly to the surface of the ladle pool, forming a scum which mixes with the rest of the ladle slag. In the molds, an additional amount of oxide material tends to rise out and form a scum on ingot tops. This scum quite often carries occluded or partially dissolved fragments eroded from refractories, but is more normally a rather homogeneous material with a composition which tends either to agree with that which would be predicted from the relative amounts of loss of the various alloy additions by oxidation in the ladle, or deviates from this predicted composition in a manner consistent with variable rising rates of particles of variable composition and physical state. This scum is sometimes partly entrained in the surface layers of the ingot to give surface or subsurface defects, or it may sink down into the shrinkage cavity during freezing to give certain pipe or blowhole defects. Some data on analysis of inclusions extracted from the final steel again suggest the same ladle oxidation products as the main source, suggesting that these inclusions are chiefly those emulsified oxide or silicate products of (mainly) air oxidation which did not float out in either ladle or mold.

On the other hand, the preliminary indications were that final steel cleanliness or various indexes of defects or "quality" had little or no relationship to the relative total amount of air oxidation in the ladle. The dirt left in the steel is hardly ever more than a very small percentage of the total amount formed by oxidation and occasional refractory erosion. It seems probable therefore that other, still unknown, factors are dominant in this general problem, and that there is some critical factor which largely determines the degree of fineness or emulsification in the liquid metal, of at least part of the large amount of oxidation products formed in all present steelmaking practices. We therefore merely wish to indicate here the belief that the problem is essentially an unsolved one at this writing. It seems reasonable to conclude, however, that the air oxidation during tapping is one major, though probably not the decisive, factor in this general problem of steel cleanliness and quality.

Discussion of Results and Conclusions: In addition to its possible relationship with the control of steel quality in general, this oxidation effect appears to result in an extra cost of 20 to 50 cents per ton through alloy losses and is the main variable which limits our present degree of control of composition within specifications for any given grade of steel. Although the practical or complete elimination of the effect would be very desirable, this appears to be a very difficult problem, at least in quantity production, and any complex or expensive method of handling the steel out of the furnace would probably not be justifiable. The main purpose here is to describe what happens and the main factors which appear to influence the amount of oxidation. More frequent piping of tap holes, or some new taphole and tapping practices, and some innovation, such as the tilting ladle which would limit the fall of tap stream in the air, appear to promise a marked reduction in variability and are at least worth consideration. Any resultant lowering in manganese loss would be especially helpful under present conditions.

The following conclusions summarize results to date:

1. Although direct and conclusive evidence is not yet available, the writers believe that there is very good circumstantial evidence for reaction with air as the main source of alloy loss in tapping and ladle filling. The metal stream appears to react with an amount of oxygen equivalent to 20 to 30 or more volumes of air per volume of metal, forming 3 to 9 lb per ton, or 0.4 to 1.0 pct by volume of oxides.

2. Along with the oxidation, 0.001 to 0.002 pct of nitrogen is absorbed between tap stream and teeming stream. Rimming action seems to be increased in open steels due to a higher $\Delta[O]$ or excess of dissolved oxygen above carbon equilibrium in the teeming stream.

3. The mechanism of air oxidation appears to include not only the violent convection flow of air over the exposed liquid metal surfaces but also an actual carrying of air bubbles down into the liquid metal pool in the ladle. Such entrainment of bubbles appears to occur at the instant of impact on the pool of waves or other irregularities in the metal stream surface. Turbulence and waviness in stream and impact velocity both tend to increase with distance of free fall through the air.

4. Results tend to indicate that because of the high activity of atmospheric oxygen, the resultant oxidation is independent of the time factor and speed of tap, since it is controlled in amount essentially by the turbulence and violence of tap and the degree of exposure and mixing with air.

5. Also because of this strongly oxidizing effect of air, and the erratic mixing conditions in normal ladle filling and alloy additions, not only aluminum and silicon but also carbon, chromium, and manganese are oxidized, and the total amounts and the relative ratios between different alloy losses are variable and erratic between heats of one grade in the same shop practice. This variability (at least 4 to 1 in total alloy loss) is the main factor rendering close control of composition difficult in present steelmaking practices.

6. The most immediately practicable methods of limiting this effect would seem to be: (*a*) control of taphole contour and opening-up and tap-stream flow in general to give consistent smoothness of flow, and (*b*) decrease in distance of free fall through air from runner to ladle pool. There are promising indications that such conditions could result in a saving in manganese of somewhere between 0.4 and 1.0 lb. per ton of steel. Since this should be accompanied by corresponding savings in silicon and chromium and would be independent of, and in addition to, any manganese savings in the furnace bath before tap, it would appear to be worth serious consideration.

Acknowledgments

Any study of this kind, conducted largely on commercial open-hearth furnaces, depends chiefly on the willing help and cooperation of plant personnel. We are indebted to South Works, Johnstown Works, and Vandergrift Works, Carnegie-Illinois Steel Corp., Donora Works, American Steel and Wire Co., and National Works, National Tube Co., especially to members of the engineering, metallurgical, and open-hearth departments of South Works. For the high-speed photographic studies of stream flow, we are indebted to R. A. Buchanan of this Laboratory.

References

[1] T. E. Brower and B. M. Larsen: The Occurrence of Oxygen in Liquid Open-hearth Steel—Sampling Methods. *Trans.* AIME (1945) **162**, 712-722.

[2] T. E. Brower and B. M. Larsen: Oxygen in Liquid Open-hearth Steel—Oxygen Content During the Refining Period. *Trans.* AIME (1947) **172**, 137-163; *Met. Tech.* (Sept. 1946) TP 2035.

[3] T. E. Brower and B. M. Larsen: Oxygen in Liquid Open-hearth Steel—Effect of Special Additions, Stirring Methods and Tapping. *Trans.* AIME (1947) **172**, 164-175; *Met. Tech.* (Oct. 1946) TP 2076.

[4] P. Bardenheuer and G. Henke: Avoidance of Manganese Losses in the Siemens-Martin Process. *Mitt. K.-W. Inst. Eisenforsch.* (1939) **21**, 243-260.

[5] A. Hultgren: The Origin of Silicate Inclusions in Basic Electric Steel of High Carbon Content. *Jernkont. Annal.* (1945) **129**, 633-671.

Thermodynamic Relationships in Chlorine Metallurgy

Equations representing the standard free energy of formation as a function of temperature, for thirty metallic chlorides, are presented and plotted on a free-energy vs. temperature diagram. The use of these data for calculations on reduction of metallic chlorides, refining of metals with chlorine, and chlorination of metallic oxides and sulphides is illustrated.

by Herbert H. Kellogg

'CHLORINE metallurgy' has attracted metallurgists for more than a century because the unusual properties of the metallic chlorides—low melting point, high volatility, and ease of formation from the oxides—make possible many useful extractive processes. Interest in chlorine processes is undergoing a renaissance due to present availability of chlorine at relatively low prices, and to recent advances in technology.

During the present century there have accumulated a considerable number of reliable values of the thermodynamic constants for the metals and their chlorides. These data permit the calculation of free-energy equations for many metallurgically important reactions. Consideration of free-energy values makes possible certain predictions of the direction and extent of a given reaction, as well as the effect of temperature, pressure, and composition upon the result. Reaction rate, although not predictable from free-energy data, is usually sufficiently great at elevated temperatures that diffusion of the reactants and products to and from the zone of reaction determines the actual rate. Thus, if the free-energy indication is favorable, the chances are good that a high temperature metallurgical reaction will proceed at a reasonable rate, if adequate provision for rapid diffusion has been made.

HERBERT H. KELLOGG, Member AIME, is Assistant Professor of Mineral Engineering, School of Mines, Columbia University, New York.

AIME New York Meeting, Feb. 1950.

TP 2869 D. Discussion (2 copies) may be sent to Transactions *AIME before July 30, 1950. Manuscript received Oct. 13, 1949; revision received Jan. 18, 1950.*

This paper presents standard free-energy equations for a number of metallic chlorides, based on data which are scattered throughout the literature. The equations are presented in a form that simplifies their use, and typical examples are given of the application of free-energy data to metallurgical processes.

Free Energy of Reaction

The free-energy change (ΔG) of a reaction is the true measure of the "driving force" of the reaction under a given set of conditions, and this is related to the standard free-energy change (ΔG°) of the reaction as follows:

For the reaction:

$$bB + cC = dD + eE$$

$$\Delta G = \Delta G^\circ + RT \ln \frac{A_D{}^d \cdot A_E{}^e}{A_B{}^b \cdot A_C{}^c} \qquad [1]$$

where A_i = activity of constituent (i)
T = absolute temperature, °K
R = gas constant

The criterion of a spontaneous reaction from left to right, at constant temperature and pressure, is a negative value for the free-energy change (ΔG). The standard free energy of the reaction is equal to the free energy of the reaction when all the reactants and products are at unit activity, since under these conditions the second term on the right-hand side of eq 1 is equal to zero.

The concept of activity is treated fully in many textbooks on chemical thermodynamics[1] and in a recent article by Chipman.[2] Briefly, the activity (A_i) of a constituent (i) is a measure of the reactivity of this constituent relative to its reactivity in some arbitrary standard state. For liquids and solids the standard state most often used is the pure liquid or solid constituent. Thus the activity of a pure liquid or solid in a metallurgical reaction is equal to unity. Gases under moderate pressure and at elevated temperatures behave very nearly as 'ideal gases,' and the standard state is chosen as the gas at 1 atm pressure. The activity of an ideal gas is therefore equal to its partial pressure, and this relation is sufficiently exact for real gases in most metallurgical reactions. For a liquid or solid solution there is in general no simple way to express the activity of a constituent as a function of its concentration, and activity must be determined by experiment. A few solutions follow a so-called 'ideal' behavior, and if the pure constituent is chosen as the standard state, the activity of a constituent in an ideal solution becomes equal to its mol fraction.

When a reaction reaches a state of thermodynamic equilibrium at constant temperature and pressure, ΔG becomes equal to zero and eq 1 reduces to:

$$\Delta G^\circ = -RT \ln \left[\frac{A_D{}^d \cdot A_E{}^e}{A_B{}^b \cdot A_C{}^c}\right] \text{ equilibrium} \qquad [2]$$

The brackets surrounding the activity term are used to emphasize that each of the activities is an activity under equilibrium conditions—not just any arbitrarily assigned value. The bracketed term is the equilibrium constant (K) of the reaction. Eq 2 makes possible the calculation of equilibrium activities for a given reaction, if ΔG° is known at the desired temperature.

The standard free-energy equations presented in this paper were calculated from the fundamental thermodynamic values of enthalpy of formation at 298°K ($\Delta H^\circ{}_f$), standard entropy at 298°K ($S^\circ{}_{298}$), heat capacity as a function of temperature (Cp), and enthalpies of transition, fusion, vaporization, and sublimation for the various constituents. Where possible the data reported in the recent "Selected Values of Chemical Thermodynamic Properties," published by the Bureau of Standards,[3] were used. A large number of data came from the publications of K. K. Kelley[4-7]* and a few values of ΔH°_f came from Bichowsky and Rossini.[9] The method of calculation of ΔG° from these data can be found in any textbook on chemical thermodynamics.[1]

In a few cases the standard entropy (S°_{298}) of the metallic chloride was not available in the literature, and rather than omit an important substance from consideration, the entropy was estimated by one of the empirical methods available. These estimated entropies are probably reliable to ± 2 entropy units. The error introduced into the free-energy equations, as a result of the uncertainty in the entropy, is small at low temperature but becomes appreciable as the temperature is increased. In some cases the heat-capacity data were estimated, but the error introduced into the free-energy equations by this procedure is by no means as serious as that from an inaccurate entropy value. Whenever data were estimated the resulting free-energy equations have been clearly designated as approximate. Some indication of the reliability of each equation will be found in the appendix where the equation for each of the lines on figs. 1 and 1*A* is given along with the sources of the data for each chloride.

Extreme accuracy is not claimed for any of the equations in this paper. Particularly at high temperatures the errors are probably large in some cases, and the values should be considered provisional. Only with the aid of much more experimental evidence on high temperature equilibrium, and by painstaking analysis of the data can the accuracy of the equations be increased. Maier[10] has performed such a service for the chromium chlorides, and as a result these equations are probably more reliable than most of the others reported in this paper. Despite the provisional character of many of the free-energy equations, their usefulness for preliminary calculations in development problems and in the teaching and understanding of extractive metallurgical processes is very great.

One further limitation of the free-energy equations should be pointed out. The thermodynamic constants for a great many chlorides of lower or higher valence state than the normal chlorides are not available, and these chlorides have been omitted from consideration. In many metallurgical processes these other chlorides may play the predominant role, and the free-energy equations reported in this paper would be insufficient to predict their behavior. A recent patent[11] affords an example of a process for refining aluminum which makes use of the normally unstable compound AlCl.

Standard Free-energy vs. Temperature Diagram

H. J. T. Ellingham[12, 13] has performed an important service for the literature on extractive metallurgy by his recent publications in which he has given the standard free energies of metallic oxides and sulphides as functions of temperature and related these to practical problems in smelting and refining. The method of presentation of data used by Ellingham has been adopted in this paper. A brief discussion of the characteristics of a standard free-energy vs. temperature diagram follows:

In figs. 1 and 1*A*, the standard free energies of formation of the metallic chlorides are plotted as functions of the Centigrade temperature. The basis of each equation is 1 g mol of chlorine, rather than the more usual 1 g mol of chloride. Thus the reactions are written:

$$2\ M + Cl_2 = 2\ MCl$$
$$M' + Cl_2 = M'Cl_2$$
$$2/3\ M'' + Cl_2 = 2/3\ M''Cl_3$$

The use of 1 g mol of chlorine as the basis for the equations makes possible the direct visual comparison on figs. 1 and 1*A* of the relative 'affinities' of the metals for chlorine at any temperature. The farther down on the graph the chloride appears (the more negative is the value of ΔG°) the more stable is the chloride. At a given temperature, a metal is able to displace from their chlorides all other metals that appear above it on figs. 1 and 1*A*, provided all reactants and products are in their standard states (for the more practical problem, where the substances are not in their standard states, this relation can be contradicted as will be explained later). The preceding statement is true because if one equation on the graph is subtracted from another, the chlorine will cancel out and the result will be a replacement reaction:

$$\begin{array}{lr} (a) & M + Cl_2 = MCl_2 \\ (b) & M' + Cl_2 = M'Cl_2 \\ \hline (a)-(b)=(c) & M + M'Cl_2 = M' + MCl_2 \\ & \Delta G^\circ_c = \Delta G^\circ_a - \Delta G^\circ_b \end{array}$$

If MCl_2 appears below $M'Cl_2$ on the graphs at a given temperature, then ΔG°_a is a larger negative value than ΔG°_b, and ΔG°_c will also be negative. Since ΔG°_c is negative, reaction c will proceed spontaneously from left to right if all reactants and products are in their standard states, and M will displace M' from $M'Cl_2$.

The curves on figs. 1 and 1*A* form a quantitative 'affinity series' for the metallic chlorides that is valid for the temperature range 0° to 2000°C. The relatively unstable chlorides of the noble metals appear on the upper part of fig. 1, while the very stable chlorides of the alkali and alkaline earth metals are at the bottom of fig. 1*A*; the base-metal chlorides lie between these extremes. The fact that many of the curves cross each other indicates that the stability of the chlorides, relative to each other, changes as the temperature increases. For this reason a single affinity series, valid at one temperature only, is of little use for metallurgical purposes.

The standard free energy of a chemical reaction is related to the standard electrode potential of an electrolytic cell which embodies that reaction, as follows:

$$\Delta G^\circ = -jnE^\circ F \qquad [3]$$

where: E° = standard electrode potential in volts

F = Faraday constant, 96,500 coulombs per mol

n = number of faradays per mol of reaction

j = conversion factor from joules to calories = 0.239

It follows that the ordinate representing standard free energy can also represent the standard electrode potential (E°) if (n) is constant for all of the reactions. When the basis of the free-energy values is 1 g mol of chlorine, (n) will have the constant value

---

* Kelley's most recent revision of heat capacity data[8] was received too late for use in the majority of the calculations.

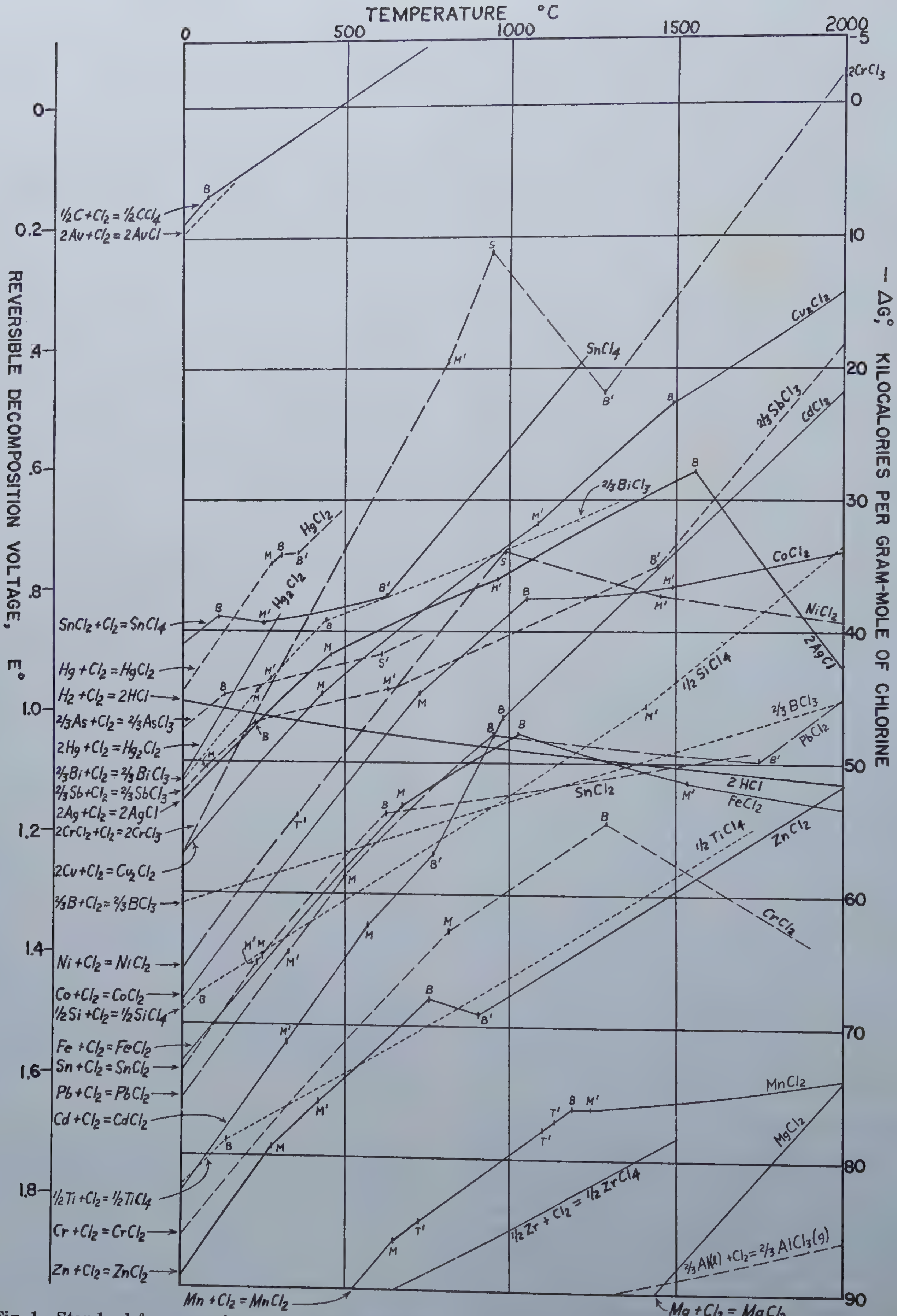

Fig. 1—Standard free energies of formation for metal chlorides as a function of temperature. ΔG° between +5000 and —90,000 cal.

of 2, and figs. 1 and 1A show the ordinate plotted as E° as well as —ΔG°. It is therefore possible to read directly from the figures the 'reversible decomposition voltage' of an electrolytic cell that performs one of the reactions listed.

The standard free energy of a reaction is related

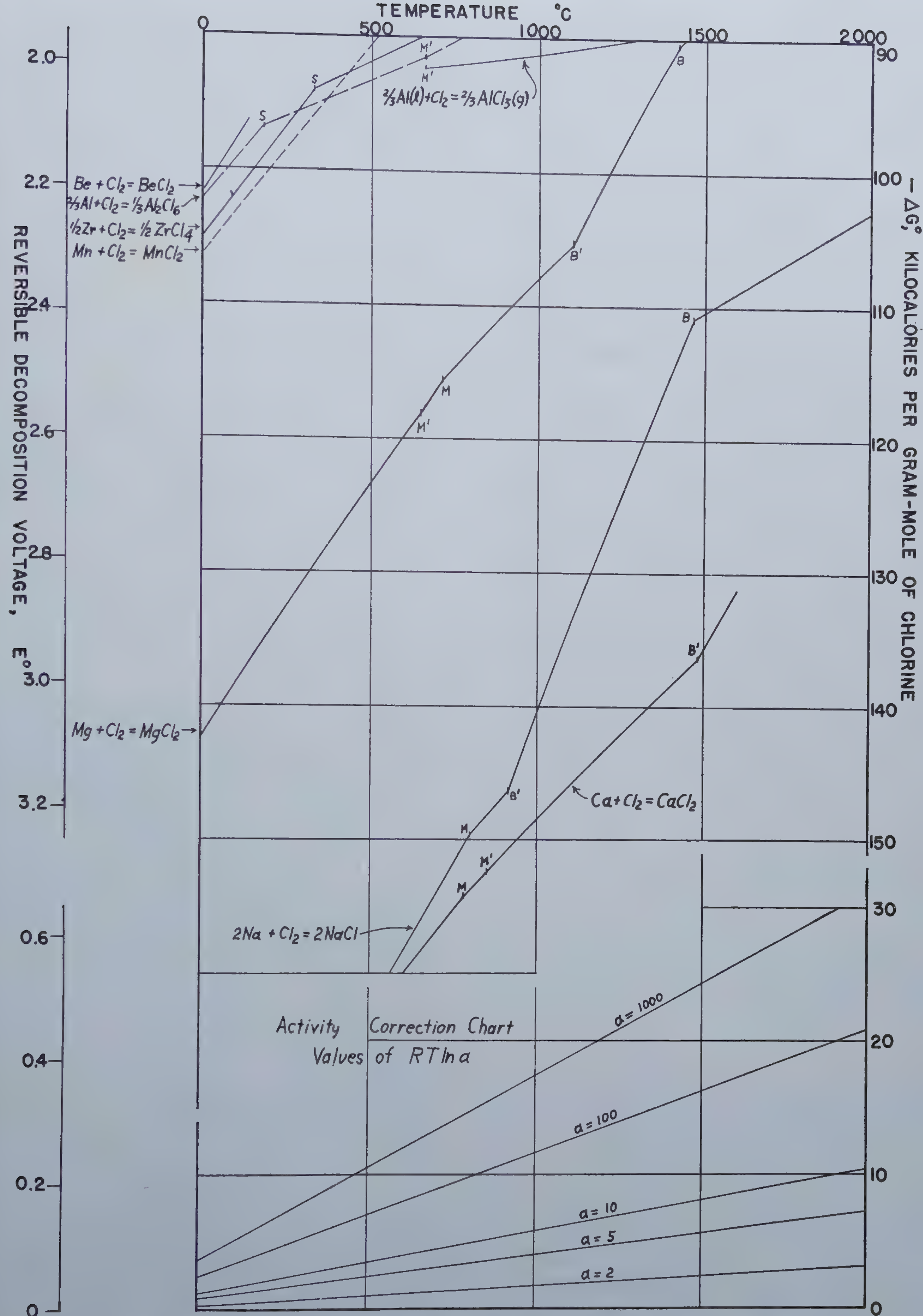

Fig. 1*A*—Standard free energies of formation for metal chlorides as a function of temperature. ΔG° between —90,000 and —160,000 cal.

to the standard enthalpy of reaction (ΔH°) and the standard entropy of reaction (ΔS°) as follows:

$$\Delta G^\circ = \Delta H^\circ - T\Delta S^\circ, \text{ constant temperature and pressure} \quad [4]$$

Since ΔH° and ΔS° change to a minor extent only with a change in temperature (provided the reactants and products undergo no phase changes), a plot of $-\Delta G^\circ$ versus T will result in lines which are very nearly straight and having a slope of $+\Delta S°$. In figs. 1 and 1*A*, $-\Delta G°$ is plotted downwards and the slope of the lines is $-\Delta S°$; a line that slopes upward from left to right has a positive slope but a negative $\Delta S°$. The slight curvature noticeable in some of the lines reflects the small temperature dependence of $\Delta S°$, which results from the differences in heat capacities of the products and reactants.

At all phase-change temperatures (transition, fusion, vaporization, and sublimation) the entropy of the reaction changes abruptly by an amount equal to the entropy of the phase change, and the lines on figs. 1 and 1*A* show sudden 'breaks' at each such temperature. The entropy changes for vaporization and sublimation are usually much greater than for transition and fusion, and the lines have sharper breaks at the points of greater entropy change. When a substance appearing on the right-hand side of the equation (i.e., the metal chloride) undergoes a phase change upon increase in temperature, the entropy of the reaction becomes more positive (or less negative); the slope of the line, therefore, becomes less when such a phase change occurs. A substance on the left-hand side of the equation (i.e., the metal or lower valence-state chloride) will have the reverse effect upon the entropy of the reaction when it undergoes a similar phase change. The 'normal' fusion, boiling, and sublimation temperatures for the chlorides are indicated on figs. 1 and 1*A* by the symbols *M*, *B*, and *S*. The same phase changes for the metal (or lower valence-state-chloride) are denoted by *M'*, *B'*, and *S'*. *T'* refers to the temperature of transition between two crystalline forms of the metal.

In most reactions of practical interest the products and reactants are not in their standard states. In this case the driving force of the reaction is ΔG, rather than $\Delta G°$, and appropriate values of the activities must be used in eq 1 to predict the spontaneity of the reaction. If the activity values are known, the value of ΔG for the reaction can be found graphically by the use of the correction chart at the bottom of fig. 1*A*. As an example of the use of this chart consider the following:

The free energy (ΔG) of the reaction

$$(a) \quad 2\,Ag(l) + Cl_2 = 2\,AgCl\ (l)$$

is desired at 1000°C, when Ag is in a metallic solution at activity 1/1000, chlorine is a gas at 2 atm pressure, and AgCl is a pure liquid. From eq 1:

$$(b) \quad \Delta G = \Delta G° + RT \ln \frac{1}{(1/1000)^2 \times 2}$$

$$(c) \quad \Delta G = \Delta G° - RT \ln 2 + 2\,RT \ln 1000$$

Each of the terms on the right-hand side of (*c*) can be evaluated from figs. 1 and 1*A*. Thus, at 1000°C:

$$\Delta G°_{2AgCl} = -35{,}500 \text{ cal}$$
$$RT \ln 2 = 1{,}750 \text{ cal}$$
$$RT \ln 1000 = 17{,}480 \text{ cal}$$

$$(d) \quad \Delta G_{2AgCl} = -35{,}500 - 1{,}750 + 2(17{,}480) = -2{,}290 \text{ cal}$$

Applications to Chlorine Metallurgy

Hydrogen Reduction: If the curve for the standard free energy of a metallic chloride on fig. 1 lies above the curve for

$$H_2 + Cl_2 = 2HCl$$

at a given temperature, the metallic chloride will be reduced to the metal by hydrogen, provided the substances are in their standard states. A metal whose chloride lies below the 2HCl curve at a given temperature will be converted to the chloride by treatment with HCl (gas) under standard conditions. The curves for most of the chlorides slope upward from left to right and cross the 2HCl curve, thus an increase in temperature makes the free energy of the hydrogen-reduction reactions more favorable. At 2000°C, $\Delta G°$ for the reaction

$$MCl_2 + H_2 = M + 2HCl$$

is negative for all the metallic chlorides on figs. 1 and 1*A* except $CrCl_2$, $ZnCl_2$, $MnCl_2$, $2/3AlCl_3$, $1/2ZrCl_4$, $MgCl_2$, $CaCl_2$, and 2NaCl (and probably $BeCl_2$).

It is not essential that the curve for the standard free energy of the chloride lie above the 2HCl curve in order to effect the reduction of the chloride by hydrogen. If the chloride curve is not too far below the 2HCl curve, the free energy of the reduction reaction can be adjusted to a negative value by maintaining a large activity of hydrogen and a small activity of HCl. An example of such a case is the method of $CrCl_2$ reduction with hydrogen which was developed by Maier for the U. S. Bureau of Mines.[10] This process is operated at 800°C, and fig. 1 shows that at this temperature:

	$\Delta G°_{800°C}$
(*a*) $H_2 + Cl_2 = 2HCl$	$-48{,}350$
(*b*) $Cr(s) + Cl_2 = CrCl_2(s)$	$-63{,}150$
(*c*) $H_2 + CrCl_2(s) = Cr(s) + 2HCl$	$+14{,}800$ cal

The partial pressures of the two gases required to make the reduction reaction spontaneous from left to right are found, in the limiting case, by solving for the equilibrium condition. From eq 2:

$$\Delta G° = -RT \ln \frac{A^2_{HCl} \cdot A_{Cr}}{A_{H_2} \cdot A_{CrCl_2}}$$

The activities of $Cr(s)$ and $CrCl_2(s)$ are unity, since these substances are present in their standard states.

$$RT \ln \frac{P^2_{HCl}}{P_{H_2}} = -14{,}800 \text{ cal at } 800°C\ (1073°K)$$

$$(d) \quad \log \frac{P^2_{HCl}}{P_{H_2}} = -3.017$$

If the total pressure in the reduction system is 1 atm, then:

$$(e) \quad P = 1 = P_{HCl} + P_{H_2}$$

If (*d*) and (*e*) are solved simultaneously, the results are:

$$P_{HCl} = 0.031 \text{ atm}$$
$$P_{H_2} = 0.969 \text{ atm}$$

If the amount of HCl in the reducing gas is kept below 3.1 pct by supplying fresh, dry hydrogen and continuously removing the HCl which is formed, ΔG will be negative and the reduction reaction will proceed spontaneously.

Reduction by Carbon and Methane: Carbon is one of the most useful reducing agents for metallic oxides but is useless as a reducing agent for chlorides. This conclusion is based on the position on fig. 1 of the free energy for the reaction

$$1/2\,C + Cl_2 = 1/2\,CCl_4$$

which lies far above all the curves for the metallic chlorides except AuCl. Carbon has such a low affinity for chlorine that the standard free energy of formation of CCl_4 becomes equal to zero at 475°C, and CCl_4 will decompose into carbon and chlorine above this temperature.

Methane has been reported as a practical reducing agent for the metallic chlorides.[14, 15] However, the use of methane should be considered as an alternative (and perhaps cheap) method of effecting hydrogen reduction of the chlorides. Methane is unstable when heated much above 600°C and decomposes into hydrogen and carbon. The products of the methane reduction of metallic chlorides always contain solid carbon—no carbon chlorides are formed. The hydrogen from the methane combines with chlorine from the metallic chloride to form HCl, as in ordinary hydrogen reduction.

$$(a) \quad 1/2\ CH_4(g) + MCl_2 = M + 2HCl + 1/2C$$

The standard free energy of formation of methane is given in table I.

Table I. Standard Free Energy of Formation of Methane*

$1/2\ C(s) + H_2 = 1/2\ CH_4(g)$

°C	ΔG°
25	—6,070
727	+2,305
1,027	+6,250

* Values from "Selected Values".[8]

The standard free energy for the methane reduction reaction, (*a*), is obtained by subtracting ΔG° for the metal chloride (from fig. 1) and ΔG° for the formation of 1/2 CH_4 (from table I) from ΔG° for 2HCl (from fig. 1). At those temperatures where ΔG° for 1/2 CH_4 is negative, the reducing power of methane is less than that of pure hydrogen, while for positive values of $\Delta G^\circ_{1/2CH_4}$ the reducing power of methane is a little greater than that of hydrogen. A disadvantage of the use of methane is that the reduced metal is contaminated with carbon.

Electrolytic Reduction: The required free energy for the reduction of a metallic chloride may be supplied by electrolysis, instead of employing the free energy involved in the formation of HCl from H_2. Eq 3 gives the relation between the variables involved. The use of electrical energy for reduction has one important advantage over chemical methods—the strength of the reducing action in electrolysis is unlimited, and even a very stable chloride like NaCl may be electrolyzed to produce sodium metal and chlorine gas, if a sufficiently large voltage is employed. For this reason electrolysis of the molten metallic chloride is the principal method for the production of the active metals[16] such as magnesium, sodium, calcium, lithium, and cerium.

For the electrolysis of a pure molten chloride with the formation of chlorine at 1 atm pressure and the pure metal, figs. 1 and 1*A* give directly the 'reversible decomposition potential' for the electrolysis at any temperature, since all substances are in their standard states. If pure liquid $PbCl_2$ is electrolyzed at 500°C, fig. 1 indicates a reversible decomposition potential of 1.27 v.

When the substances involved in an electrolysis are not in their standard states, appropriate activity corrections must be made in order to find the reversible decomposition potential (*E*). *E* is related to *E*° by the relation:

$$E = E^\circ - \frac{RT}{nF} \ln \frac{A_D{}^d \cdot A_E{}^e}{A_B{}^b \cdot A_C{}^c} \qquad [5]$$

where *R* = gas constant expressed as joules per °C per mol.

In most commercial methods for electrolysis of molten chlorides, the electrolyte is a solution of several chlorides—the additions serving the purpose of lowering the melting point and increasing the conductivity. In such a case the activity of the chloride undergoing electrolysis is less than unity and eq 5 must be used to calculate *E*.

The actual cell voltage used for the commercial production of a metal is considerably higher than the reversible decomposition potential for several reasons. The internal resistance of the electrolytic cell causes a voltage drop which may be as much as 5 v in some cases. The electrode reactions may exhibit 'overvoltage' or 'polarization' which adds to the cell voltage. All of these effects are rate phenomena—they depend upon the current density of the electrolysis—and cannot be accounted for by studies of reaction equilibrium.

In a molten solution of two chlorides, such as $PbCl_2$-$ZnCl_2$, electrolysis can be used to obtain a fractional separation of the two metals. The farther apart the curves for the two chlorides appear on figs. 1 and 1*A*, the more successful will be the separation. Drossback[17] was able to obtain close to 100 pct recovery of lead (containing 0.1 pct Zn) from a $PbCl_2$-$ZnCl_2$-NaCl electrolyte at 540°C, by adjusting the cell voltage so that it did not exceed 1.6 v. The zinc could subsequently be reduced by increasing the cell voltage after all the lead was deposited. The possibility of this separation is indicated from the curves on fig. 1. At 540°C:

$$E^\circ \text{ for } PbCl_2 = 1.25 \text{ v}$$

$$E^\circ \text{ for } ZnCl_2 = 1.59 \text{ v}$$

If activity corrections are neglected as a first approximation, then lead should begin to deposit when the cell voltage reaches 1.25 v and pure zinc could not deposit until the cell voltage had been raised above 1.59 v (Drossback's value of 1.6 v includes the voltage drop across the internal resistance of his cell). For a more accurate analysis of the system the activities in the chloride melt would have to be taken into account.

Reduction of Chlorides by Other Metals: Practical use of metal reducing agents for other metallic chlorides is at present the subject of many papers, investigations, and patents.[18–26] Perhaps the most important of these are the production of ductile titanium and zirconium by the reduction of the respective tetrachlorides with magnesium metal.[18, 19] The free-energy relations which indicate the possibility of these reactions are found on figs. 1 and 1*A*. The standard free-energy curve for $MgCl_2$ lies far below that for 1/2 $TiCl_4$ and 1/2 $ZrCl_4$, hence the replacement reaction

$$Mg^\circ + 1/2\ TiCl_4 = 1/2\ Ti^\circ + MgCl_2$$

should proceed readily. The position of the NaCl curve on fig. 1*A* indicates that sodium metal could also be used to reduce zirconium and titanium tetrachlorides, and this reaction formed the basis for the production of titanium at one German plant during the recent war.[26]

Kroll[22-25] has suggested a number of processes for the refining of metal scrap and alloys, which involve reactions of the type:

(*a*) Mn (as solid ferromanganese) + $FeCl_3(l)$ (or $FeCl_2$) = $MnCl_2(l) + Fe(s)$

(*b*) Co (as alloy with Ni°) + $NiCl_2(l) = Ni(s) + CoCl_2(l)$

These reactions are carried out with the alloy in the form of solid powder or turnings and a molten bath of chlorides (NaCl, KCl, etc., are usually added in order to reduce the melting point and the volatility of the other chlorides). The possibilities of these reactions are indicated by the curves on figs. 1 and 1*A*. If the chloride of the metal to be removed from the alloy has a standard free energy which lies far below the standard free energy of the chloride used for purification (as is the case for the Mn-Fe separation in eq *a*), then the success of the process is very likely. However, the substances in such a reaction are not in their standard states, and an accurate prediction from thermodynamic data must consider the activities of each constituent. The activities of the chlorides are less than unity since they are constituents of a solution along with NaCl and/or KCl. The metals in the alloy will also be at less than unit activity if solid solutions or intermetallic compounds are formed.

Refining of Metals with Chlorine: If chlorine gas is bubbled through a molten alloy, the metallic constituent that forms the most stable chloride will react first, thus effecting a purification or refining of the alloy. Such a reaction is the basis of the Betterton process for dezincing of lead,[27] and many similar processes may be predicted from the curves on figs. 1 and 1*A*. The essential requirement for the success of the process is that the standard free-energy curve for the chloride of the metal to be removed should lie as far below that for the chloride of the other metal as possible. All of the substances in such a process are components of either the metallic or chloride solutions, and their activities will be less than unity. Accurate prediction from the thermodynamic data must take into account the activity of each constituent.

As an example of the use of figs. 1 and 1*A*, the Betterton process will be analyzed, since the operating conditions and results are known and it is possible to estimate the activities of all substances present. Table II summarizes the operating conditions and results of the process.

Table II. Betterton Process

Operating temperature	390°C
Analysis of lead to process	about 0.6 pct Zn
Analysis of lead from process	about 0.005 pct Zn
Analysis of chloride crust (after removing prills of lead)	about 2.5 pct Pb, remainder zinc and chlorine.

Zinc reacts with chlorine gas according to the reaction:

(*a*) Zn (liquid, dissolved in Pb) + $Cl_2 = ZnCl_2(l)$

$$\Delta G^\circ_a = -76{,}640 \text{ cal at } 390^\circ\text{C (from fig. 1)}$$

Since lead is present in the system a second reaction is possible:

(*b*) $Pb(l) + Cl_2 = PbCl_2(l)$

$\Delta G^\circ_b = -61{,}550$ cal at 390°C (obtained from fig. 1 by extension of the curve, or from eq 79 in the appendix).

Only reaction (*a*) will proceed to a significant extent because any $PbCl_2$ formed by reaction (*b*) will react with zinc (as long as zinc is present in the system) according to the reaction:

(*c*) Zn (liquid, dissolved in Pb) + $PbCl_2$ (liquid, dissolved in $ZnCl_2$) = $Pb(l) + ZnCl_2(l)$

Since reaction (*c*) = (*a*) — (*b*):

$$\Delta G^\circ_c = -76{,}640 + 61{,}550 = -15{,}090 \text{ cal at } 390^\circ\text{C.}$$

Reaction (*c*) controls the equilibrium between the metal and chloride phases. At the start of the process when the activity of the zinc in the lead is high, the amount of $PbCl_2$ that exists in the chloride phase is small. At the end of the process, considerably more $PbCl_2$ can exist in the chloride phase, since the activity of zinc in the lead has been reduced to a very low value.

In order to check the thermodynamic prediction against the operating results, the expected residual zinc in the lead will be calculated on the assumption that the metal and chloride phases reach equilibrium at the end of the process. Applying eq 2:

$$(d) \quad \Delta G^\circ_c = -15{,}090 = -RT \ln \frac{A_{Pb} \cdot A_{ZnCl_2}}{A_{Zn} \cdot A_{PbCl_2}}$$

Activity of Pb: The final lead is 99.9+ pct, hence $A_{Pb} = 1$, is fully justified.

Activity of $ZnCl_2$: The final chloride phase has a mol fraction of $ZnCl_2$ = 0.983. Muromtsev and Nazarova[28] have shown that $ZnCl_2$-$PbCl_2$ solutions are 'ideal' with respect to $ZnCl_2$ when the mol fraction of $ZnCl_2$ is large. Therefore:

$$A_{ZnCl_2} = \text{mol fraction of } ZnCl_2 = 0.983$$

Activity of Zinc: Lumsden[29] has investigated activities in the lead-zinc system and the use of his equations gives rise to:

$$A_{Zn} = 29\, N_{Zn}$$

where N_{Zn} is the mol fraction of zinc in lead. This relation is approximately valid for very dilute solutions of zinc in lead at 390°C.

Activity of $PbCl_2$: The data of Muromtsev and Nazarova on the vapor pressure of $ZnCl_2$-$PbCl_2$ solutions indicate some departure from ideality for the activity of $PbCl_2$ below mol-fraction 0.7. Rather than make an uncertain extrapolation of their data, it will be assumed that the system is ideal and that the activity of $PbCl_2$ is equal to its mol fraction (0.017). The error involved in this assumption is probably less than a factor of two.

If the activity values are substituted in (*d*):

$$(e) \quad 15{,}900 = RT \ln \frac{(1) \cdot (0.983)}{29\, N_{Zn} \cdot (0.017)}$$

Solving for N_{Zn}:

$$(f) \quad N_{Zn} = 2.1 \times 10^{-5}$$
$$\text{pct Zn} = 0.00066$$

The theory predicts that at equilibrium, if the chloride phase contains 2.5 pct lead (0.017 mol-fraction $PbCl_2$), the residual zinc in the lead phase will be 0.00066 pct. Practice indicates a value of 0.005 pct zinc in the lead. The error is not large and is, in fact, to be expected. When very little zinc remains in the lead, the attainment of equilibrium between the zinc dissolved in the lead and the $PbCl_2$ in the chloride phase will be a very slow process, and the reaction between lead and chlorine will proceed without equilibrium being established with zinc.

Chlorination of Metallic Oxides: Many metallic oxides can be converted to chlorides by heating with chlorine alone:

$$(a)\quad MO + Cl_2 = MCl_2 + 1/2O_2$$

Systems where this reaction is possible can be predicted by a combination of the data on figs. 1 and 1*A* with that reported by Ellingham[12, 13] for the metallic oxides. Reaction (*a*) is the sum of two partial reactions:

$$(b)\ M + Cl_2 = MCl_2 \qquad \Delta G^\circ_b$$
$$(c)\ M + 1/2O_2 = MO \qquad \Delta G^\circ_c$$
$$(a) = (b) - (c)\ MO + Cl_2 = MCl_2 + 1/2O_2 \qquad \Delta G^\circ_a = \Delta G^\circ_b - \Delta G^\circ_c$$

Table III gives values for ΔG°_a at 500° and 1000°C for several metals.

Table III. Chlorination of Oxides by Chlorine Alone*

No.	Reaction (*a*)	ΔG°_a 500°C	ΔG°_a 1000°C
1	$Ag_2O + Cl_2 = 2AgCl + 1/2O_2$	—46,200	
2	$HgO + Cl_2 = HgCl_2 + 1/2O_2$	—31,800	
3	$PbO + Cl_2 = PbCl_2 + 1/2O_2$	—24,100	—25,000
4	$CdO + Cl_2 = CdCl_2 + 1/2O_2$	—21,200	—22,700
5	$Cu_2O + Cl_2 = Cu_2Cl_2 + 1/2O_2$	—15,000	—12,500
6	$MnO + Cl_2 = MnCl_2 + 1/2O_2$	—12,300	— 9,900
7	$NiO + Cl_2 = NiCl_2 + 1/2O_2$	— 9,200	— 6,400
8	$ZnO + Cl_2 = ZnCl_2 + 1/2O_2$	— 8,900	—17,600
9	$SnO + Cl_2 = SnCl_2 + 1/2O_2$	— 8,500	—16,600
10	$FeO + Cl_2 = FeCl_2 + 1/2O_2$	— 7,600	— 5,200
11	$MgO + Cl_2 = MgCl_2 + 1/2O_2$	+ 4,000	+ 6,200
12	$1/3Cr_2O_3 + Cl_2 = 2/3CrCl_3 + 1/2O_2$	+14,300	+18,600
13	$1/2TiO_2 + Cl_2 = 1/2TiCl_4 + 1/2O_2$	+19,000	+15,900
14	$1/3Al_2O_3 + Cl_2 = 2/3AlCl_3 + 1/2O_2$		+ 9,400
15	$1/2SiO_2 + Cl_2 = 1/2SiCl_4 + 1/2O_2$	+24,300	+21,400

* ΔG°_c for oxides was obtained from Ellingham's[13] graph. ΔG°_b for chlorides was obtained from figs. 1 and 1*A*. Refer to these sources for the physical states of the oxides and chlorides at 500° and 1000°C.

ΔG°_a for the chlorination of many of the metallic oxides in table III is negative, and these oxides can readily be converted to chlorides by treatment with chlorine. Maier[30] has reported the chlorination of ZnO and PbO in this manner. The chlorination reactions for MgO, Cr_2O_3, TiO_2, Al_2O_3, and SiO_2 have positive values for ΔG°_a, and the successful use of these reactions is doubtful. It is theoretically possible to make these reactions spontaneous if the products of the reaction are continuously removed as gases and kept at far less than unit activity. Maier[10] reports several attempts of this kind that showed a partial chlorination of Cr_2O_3.

The chlorination of those metallic oxides which show a positive value of ΔG°_a in table III can be effected by the use of chlorine gas and a reducing agent. Carbon, CO, and sulphur have been suggested and used as reducing agents for this purpose. The production of anhydrous magnesium chloride from MgO by treatment with chlorine and coke at 1000°C, was used by Basic Magnesium at Las Vegas during the recent war.[31] Titanium tetrachloride is produced for the Bureau of Mines titanium plant by a similar process.[19]

The effectiveness of a given reducing agent in chlorination can be estimated by combination of the data of table III with the data of table IV, which lists ΔG° for the oxidation of several reducing agents.

Table IV. Reducing Agents for Chlorination

No.	Reaction	ΔG° 500°C	ΔG° 1000°C
1	$C + 1/2O_2 = CO$*	—43,100	—53,670
2	$1/2C + 1/2O_2 = 1/2CO_2$*	—47,270	—47,340
3	$CO + 1/2O_2 = CO_2$*	—51,430	—41,000
4	$1/2S + 1/2O_2 = 1/2SO_2$†	—36,500	—32,200

* Values of ΔG° from Bureau of Standards, Selected Values.[3]
† Values of ΔG° read from Ellingham's graphs.[18]

Any one of the reactions in table IV may be combined with the desired reactions from table III to give the standard free energy of the chlorination reaction when a reducing agent is used. Thus for titanium:

	ΔG° 500°C	ΔG° 1000°C
(Table III) $1/2TiO_2(s) + Cl_2 = 1/2TiCl_4(g) + 1/2O_2$	+19,000	+15,900
(Table IV) $1/2C(s) + 1/2O_2 = 1/2CO_2$	—47,270	—47,340
$1/2TiO_2(s) + 1/2C(s) + Cl_2 = 1/2TiCl_4(g) + 1/2CO_2$	—28,270	—31,440

By use of a reducing agent with chlorine, ΔG° for the chlorination of any of the oxides in table III becomes negative and the chlorination reaction is possible under standard conditions.

HCl can be used to convert metallic oxides to chlorides according to the reaction:

$$(d)\quad MO + 2\,HCl = MCl_2 + H_2O(g)$$

Combination of the data of figs. 1 and 1*A* with Ellingham's values for the oxides[13] and the standard free energy of formation of $H_2O(g)$,[3] makes possible the calculation of ΔG°_d. Values of ΔG°_d are reported in table V. The interpretation of these data is similar to that for the data of table III.

Table V. Chlorination of Oxides with HCl(*g*)*

No.	Reaction	ΔG°_d 500°C	ΔG°_d 1000°C
1	$Ag_2O + 2HCl = 2AgCl + H_2O(g)$	—47,800	
2	$HgO + 2HCl = HgCl_2 + H_2O(g)$	—33,400	
3	$PbO + 2HCl = PbCl_2 + H_2O(g)$	—25,700	—18,400
4	$CdO + 2HCl = CdCl_2 + H_2O(g)$	—22,800	—16,100
5	$Cu_2O + 2HCl = Cu_2Cl_2 + H_2O(g)$	—16,600	— 5,900
6	$MnO + 2HCl = MnCl_2 + H_2O(g)$	—13,900	— 3,300
7	$NiO + 2HCl = NiCl_2 + H_2O(g)$	—10,800	+ 200
8	$ZnO + 2HCl = ZnCl_2 + H_2O(g)$	—10,500	—11,000
9	$SnO + 2HCl = SnCl_2 + H_2O(g)$	—10,100	—10,000
10	$FeO + 2HCl = FeCl_2 + H_2O(g)$	— 9,200	+ 1,400
11	$MgO + 2HCl = MgCl_2 + H_2O(g)$	+ 2,400	+12,800
12	$1/3Cr_2O_3 + 2HCl = 2/3CrCl_3 + H_2O(g)$	+12,700	+25,200
13	$1/2TiO_2 + 2HCl = 1/2TiCl_4 + H_2O(g)$	+17,400	+22,500
14	$1/3Al_2O_3 + 2HCl = 2/3AlCl_3 + H_2O(g)$		+16,000
15	$1/2SiO_2 + 2HCl = 1/2SiCl_4 + H_2O(g)$	+22,700	+28,000

*ΔG° for MCl_2 and 2HCl from figs. 1 and 1A; ΔG° for *MO* from Ellingham[13]; ΔG° for $H_2O(g)$ from Selected Values.[3] Refer to figs. 1 and 1*A*, also Ellingham,[13] for the physical states of the oxides and chlorides at 500° and 1000°C.

Chlorination of Metallic Sulphides: Metallic sulphides can be converted to chlorides by reaction with Cl_2 or HCl in a neutral or reducing atmosphere, according to the reactions:

(a) $MS + Cl_2 = MCl_2 + 1/2S_2$

(b) $MS + 2HCl = MCl_2 + H_2S$

The standard free energy for either of these reactions can be calculated by combination of the data of figs. 1 and 1*A* with Ellingham's[13] data on the metallic sulphides.

$\Delta G°_a$ is a large negative value (—15,000 to —45,000 cal) for the systems HgS-$HgCl_2$, Ag_2S-$2AgCl$, Cu_2S-Cu_2Cl_2, PbS-$PbCl_2$, FeS-$FeCl_2$, CdS-$CdCl_2$, ZnS-$ZnCl_2$, and MnS-$MnCl_2$. $\Delta G°_b$ is a small positive or small negative value for the same systems. Chlorination with HCl is far less energetic than chlorination with Cl_2 because the free energy of formation of H_2S is small and the free energy of formation of 2HCl is large.

Summary

Equations representing the standard free energy of formation as a function of temperature, for a number of metallic chlorides, have been calculated and plotted on a free-energy vs. temperature diagram. The use and advantages of such a diagram have been discussed. The application of the free-energy data to a variety of chlorine processes of interest to extractive metallurgists has been illustrated.

Many other applications of the data given on figs. 1 and 1*A* are possible, but these data do not exhaust the possibilities in chlorine metallurgy. Free-energy equations for many more metallic chlorides and more information on activities in metallic solutions and in chloride melts are necessary for a comprehensive treatment of the subject.

Acknowledgments

The author would have been discouraged long before completion of the calculations, except for the help of Jane Breckwoldt and Mehmet Ali Kaci, research associates in Mineral Engineering, Columbia University. Thanks are due to A. F. Taggart and M. D. Hassialis for criticizing the manuscript.

Appendix

For those who plan to use any of the standard free-energy values of figs. 1 and 1*A*, it may be

Table VI. Summary of Free-energy Relationships for Formation of Metallic Chlorides

$$\Delta G° = a + bT + cT^2 + dT\log T + e \qquad T = °K$$

No.	Reaction	a	b	cx10³	d	e	Range °K
1	$2Ag(s) + Cl_2(g) = 2AgCl(s)$	−61,180	+30.29	−7.51	+0.65		298-728
2	$2Ag(s) + Cl_2(g) = 2AgCl(l)$	−56,420	+75.71	+1.78	−19.86		728-1,234
3	$2Ag(l) + Cl_2(g) = 2AgCl(l)$	−57,050	+35.27		−5.90		1,234-1,830
4	$2Ag(l) + Cl_2(g) = 2AgCl(g)$	+49,380	−101.01		+18.03		1,830-2,273
5	$2/3Al(s) + Cl_2(g) = 1/3\,Al_2Cl_6(s)$	−110,330	+13.76	−8.315	+7.55	$\frac{-0.34 \times 10^5}{T}$	298-453.3
6	$2/3Al(s) + Cl_2(g) = 1/3Al_2Cl_6(g)$	−100,410	−4.53		+4.72		453.3-931.7
7	$2/3Al(l) + Cl_2(g) = 1/3Al_2Cl_6(g)$	−102,030	−3.47		+4.95		931.7-§
8	$2/3Al(l) + Cl_2(g) = 2/3AlCl_3(g)$	−92,360	−8.04	+1.43	+2.28		931.7-2,273
9	$2/3As(s) + Cl_2(g) = 2/3AsCl_3(l)$	−56,090	+80.64		−20.27		298-403
10	$2/3As(s) + Cl_2(g) = 2/3AsCl_3(g)$	−47,720	+9.71		−1.01		403-883
11	$1/6As_4(g) + Cl_2(g) = 2/3AsCl_3(g)$	−52,500	+12.14				883-1,000
12*	$2Au(s) + Cl_2(g) = 2AuCl(s)$	−16,800	+26.1				298-423
13	$2/3B(s) + Cl_2(g) = 2/3BCl_3(g)$	−63,690	+17.66	+0.54	−3.20	$\frac{+0.475 \times 10^5}{T}$	298-2,273
14*	$Be(s) + Cl_2(g) = BeCl_2(s)$	−112,600	+39.6				298-405
15†	$2/3Bi(s) + Cl_2(g) = 2/3BiCl_3(s)$	−60,330	+8.15	−15.885	+11.51		298-505
16†	$2/3Bi(s) + Cl_2(g) = 2/3BiCl_3(l)$	−61,250	+84.53		−19.04		505-544.2
17†	$2/3Bi(l) + Cl_2(g) = 2/3BiCl_3(l)$	−62,650	+83.10		−17.57		544.2-714
18†	$2/3Bi(l) + Cl_2(g) = 2/3BiCl_3(g)$	−44,200	−6.03		+4.61		714-1,600
19	$1/2C(s) + Cl_2(g) = 1/2CCl_4(l)$	−18,560	+70.81		−14.6		298-349.9
20	$1/2C(s) + Cl_2(g) = 1/2CCl_4(g)$	−12,870	+23.93	+0.935	−2.6	$\frac{-0.2925 \times 10^5}{T}$	349.9-1,373
21	$Ca(\alpha) + Cl_2(g) = CaCl_2(s)$	−191,510	+56.77	+0.26	−7.18		298-673
22	$Ca(\beta) + Cl_2(g) = CaCl_2(s)$	−191,400	+50.48	−0.79	−4.77		673-1,055
23	$Ca(\beta) + Cl_2(g) = CaCl_2(l)$	−190,050	+90.00		−18.54		1,055-1,124
24	$Ca(l) + Cl_2(g) = CaCl_2(l)$	−192,580	+94.14		−19.16		1,124-1,760
25	$Ca(g) + Cl_2(g) = CaCl_2(l)$	−233,560	+136.09		−24.91		1,760-1,873
26†	$Cd(s) + Cl_2(g) = CdCl_2(s)$	−93,860	+53.28	−2.48	−4.97		298-594
27†	$Cd(l) + Cl_2(g) = CdCl_2(s)$	−96,620	+79.90		−13.42		594-841
28†	$Cd(l) + Cl_2(g) = CdCl_2(l)$	−93,200	+90.86		−18.56		841-1,040
29†	$Cd(g) + Cl_2(g) = CdCl_2(l)$	−119,190	+130.09		−23.28		1,040-1,253
30†	$Cd(g) + Cl_2(g) = CdCl_2(g)$	−77,120	+24.36				1,253-2,273
31†	$Co(s) + Cl_2(g) = CoCl_2(s)$	−78,860	+59.05	+0.385	−8.45		298-1,000
32†	$Co(s) + Cl_2(g) = CoCl_2(l)$	−74,290	+71.63		−14.04		1,000-1,323
33†	$Co(s) + Cl_2(g) = CoCl_2(g)$	−31,910	−43.0		+12.42		1,323-1,763
34†	$Co(l) + Cl_2(g) = CoCl_2(g)$	−38,390	−27.4		+8.75		1,763-2,273
35	$Cr(s) + Cl_2(g) = CrCl_2(s)$	−95,540	+46.21	−2.815	−4.39	$+0.26 \times 10^{-6}T^3$	298-1,088
36	$Cr(s) + Cl_2(g) = CrCl_2(l)$	−93,140	+114.1	−4.08	−29.74	$-0.33 \times 10^{-6}T^3$	1,088-1,575
37	$Cr(s) + Cl_2(g) = CrCl_2(g)$	−31,540	+0.50	+1.83	−5.54	$-0.16 \times 10^{-6}T^3$	1,575-2,173
38	$2CrCl_2(s) + Cl_2(g) = 2CrCl_3(s)$	−70,200	+40.65	−4.1	+3.3	$+0.33 \times 10^{-6}T^3$	298-1,088
39	$2CrCl_2(l) + Cl_2(g) = 2CrCl_3(s)$	−75,000	−95.1	−17.9	+54.0	$+1.51 \times 10^{-6}T^3$	1,088-1,218
40	$2CrCl_2(l) + Cl_2(g) = 2CrCl_3(g)$	+49,600	−208.3	−6.1	+53.5	$+0.51 \times 10^{-6}T^3$	1,218-1,575
41	$2CrCl_2(g) + Cl_2(g) = 2CrCl_3(g)$	−73,600	+19.0	−1.6	+5.1	$+0.17 \times 10^{-6}T^3$	1,575-2,273
42†	$2Cu(s) + Cl_2(g) = Cu_2Cl_2(s)$	−65,330	+38.76	+1.74	−3.78		298-703
43†	$2Cu(s) + Cl_2(g) = Cu_2Cl_2(l)$	−65,590	+86.31	+1.74	−20.35		703-1,356
44†	$2Cu(l) + Cl_2(g) = Cu_2Cl_2(l)$	−68,170	+54.24		−8.75		1,356-1,763
45†	$2Cu(l) + Cl_2(g) = Cu_2Cl_2(g)$	−31,390	−72.03		+23.72		1,763-2,273
46	$Fe(s, avg.) + Cl_2(g) = FeCl_2(s)$	−82,800	+57.90	+0.59	−9.21	$\frac{+0.245 \times 10^5}{T}$	298-950
47	$Fe(s, avg.) + Cl_2(g) = FeCl_2(l)$	−74,750	+62.63		−13.45		950-1,299
48	$Fe(s, avg.) + Cl_2(g) = FeCl_2(g)$	−29,710	−53.87		+12.83		1,299-1,808
49	$Fe(l) + Cl_2(g) = FeCl_2(g)$	−35,240	−42.76		+10.36		1,808-2,273
50	$H_2(g) + Cl_2(g) = 2HCl(g)$	−43,690	−14.75	−0.155	+3.46		298-2,273
51	$2Hg(l) + Cl_2(g) = Hg_2Cl_2(s)$	−64,350	+66.6		−7.945		298-575
52	$Hg(l) + Cl_2(g) = HgCl_2(s)$	−56,340	+67.32		−10.36		298-550
53	$Hg(l) + Cl_2(g) = HgCl_2(l)$	−54,530	+90.85		−20.15		580-577
54	$Hg(l) + Cl_2(g) = HgCl_2(g)$	−34,670	−7.27		+2.92		577-629.7
55	$Hg(g) + Cl_2(g) = HgCl_2(g)$	−49,360	+24.23				629.7-2,273

§ (See "Sources".)

* Estimated entropy value used. Probable error ±1000 cal at 500°K, ±2000 cal at 1000°K, ±4000 cal at 2000°K.

† Estimated value for Cp used. Probable error less than ±500 cal.

necessary to obtain more accurate values of $\Delta G°$ than can be read from the graphs. For this purpose table VI is included, which lists the empirical equations relating $\Delta G°$ to T, for all of the lines on figs. 1 and 1*A*. The equations are probably valid for one or two hundred degrees above and below the "range" indicated on table VI, except where specifically noted in the following section.

In order that the reader may judge as to the reliability of the standard free-energy values, the following section gives a brief reference to the data used in each calculation.

Source of Thermodynamic Data

1. $AgCl$: $\Delta H°_f$, $S°_{298}$ and for ΔH for fusion and vaporization from Selected Values.[8] Cp values from Kelley.[4, 5]

2. $AlCl_3$: $S°_{298}$, $\Delta H°_f$ from Selected Values.[8] Cp values from Kelley.[5, 8] ΔH for fusion and sublimation from Kelley.[5, 8] $\Delta G°$ vs. T for the dissociation, $Al_2Cl_{6(g)} \rightleftarrows 2\ AlCl_{3(g)}$, from Treadwell and Terebesi.[34] $AlCl_3$ is the predominant form of the gas molecule above melting point of Al, hence eq 8 takes preference over eq 7.

3. $AsCl_3$: $\Delta H°_f$, $S°_{298}$, and ΔH for vaporization and sublimation from Selected Values.[8] Cp values from Kelley.[4, 5] Not valid above 1000°K since $As_4(g)$ dissociates.

4. $AuCl$: $\Delta H°_f$, $S°_{298}$ from Selected Values.[8] $S°_{298}$ for AuCl estimated from Wenner's graph[33] as 25.0 entropy units. ΔCp was neglected. This equation is to be considered tentative.

5. BCl_3: $S°_{298}$ and $\Delta H°_f$ from Selected Values.[8] Cp values from Kelley.[8]

6. $BeCl_2$: $\Delta H°_f$ from Bichowsky and Rossini.[9] $S°_{298}$ for $Be(s)$ and $Cl_2(g)$ from Kelley.[7] $S°_{298}$ for $BeCl_2(s)$ estimated from Wenner's graph,[33] as 16.0 entropy units. ΔCp was neglected. This equation is to be considered tentative.

7. $BiCl_3$: $\Delta H°_f$, $S°_{298}$, and ΔH for fusion and vaporization from Selected Values.[8] Cp for $BiCl_3$ was estimated; Cp for other constituents from Kelley.[4]

8. CCl_4: $\Delta H°_f$, $S°_{298}$, ΔH for vaporization from Selected Values.[8] Cp values from Kelley.[4]

9. $CaCl_2$: $S°_{298}$ for $Ca(s)$ from Kelley;[7] $S°_{298}$ for $CaCl_2(s)$ from Kelley and Moore;[35] $S°_{298}$ for Cl_2 from

Table VI (Continued). Summary of Free-energy Relationships for Formation of Metallic Chlorides

$$\Delta G° = a + bT + cT^2 + dT\log T + e \qquad T = °K$$

No.	Reaction	a	b	cx10³	d	e	Range °K
56	$Mg(s) + Cl_2(g) = MgCl_2(s)$	—154,590	+ 66.34	+ 0.07	— 9.07	$\frac{+0.30 \times 10^5}{T}$	298-923
57	$Mg(l) + Cl_2(g) = MgCl_2(s)$	—156,310	+ 60.26	— 0.68	— 6.17	$\frac{+0.69 \times 10^5}{T}$	923-987
58	$Mg(l) + Cl_2(g) = MgCl_2(l)$	—148,380	+ 73.85		—13.59		987-1,380
59	$Mg(g) + Cl_2(g) = MgCl_2(l)$	—184,140	+116.74		—19.00		1,380-1,691
60	$Mg(g) + Cl_2(g) = MgCl_2(g)$	—134,470	+ 12.74		+ 4.12		1,691-2,273
61	$Mn(\alpha) + Cl_2(g) = MnCl_2(s)$	—116,440	+ 56.57	+ 0.14	— 8.11	$\frac{+0.16 \times 10^5}{T}$	298-923
62	$Mn(\alpha) + Cl_2(g) = MnCl_2(l)$	—110,170	+ 79.53	+ 1.71	—18.61	$\frac{-0.525 \times 10^5}{T}$	923-1,000
63	$Mn(\beta) + Cl_2(g) = MnCl_2(l)$	—109,470	+ 61.98	+ 0.36	—12.55	$\frac{-0.34 \times 10^5}{T}$	1,000-1,374
64	$Mn(\gamma) + Cl_2(g) = MnCl_2(l)$	—107,430	+ 43.56		— 7.00		1,374-1,410
65	$Mn(\Delta) + Cl_2(g) = MnCl_2(l)$	—107,740	+ 43.22		— 6.82		1,410-1,463
66	$Mn(\Delta) + Cl_2(g) = MnCl_2(g)$	— 64,310	— 59.36		+16.21		1,463-1,517
67	$Mn(l) + Cl_2(g) = MnCl_2(g)$	— 68,220	— 54.81		+15.59		1,517-2,273
68	$2Na(s) + Cl_2(g) = 2NaCl(s)$	—197,510	+ 64.18	+ 1.44	— 7.55		298-371
69	$2Na(l) + Cl_2(g) = 2NaCl(s)$	—197,660	+ 37.13	— 3.92	+ 3.91		371-1,073
70	$2Na(l) + Cl_2(g) = 2NaCl(l)$	—189,000	+ 91.77		—18.17		1,073-1,187
71	$2Na(g) + Cl_2(g) = 2NaCl(l)$	—241,060	+170.39		—29.47		1,187-1,738
72	$2Na(g) + Cl_2(g) = 2NaCl(g)$	—134,850	+ 3.76		+ 3.09		1,738-2,273
73	$Ni(\alpha) + Cl_2(g) = NiCl_2(s)$	— 76,680	+ 64.13	+ 1.92	—10.44		298-626
74	$Ni(\beta) + Cl_2(g) = NiCl_2(s)$	— 76,140	+ 47.40	— 0.83	— 4.15		626-1,260
75	$Ni(\beta) + Cl_2(g) = NiCl_2(g)$	— 19,840	— 35.91		+ 7.97		1,260-1,725
76	$Ni(l) + Cl_2(g) = NiCl_2(g)$	— 23,200	— 37.62		+ 9.10		1,725-2,273
77	$Pb(s) + Cl_2(g) = PbCl_2(s)$	— 86,510	+ 50.19	— 2.885	— 4.22		298-600.5
78	$Pb(l) + Cl_2(g) = PbCl_2(s)$	— 87,480	+ 45.8	— 3.895	— 1.84		600.5-771
79	$Pb(l) + Cl_2(g) = PbCl_2(l)$	— 87,810	+114.79		—26.63		771-1,227
80	$Pb(l) + Cl_2(g) = PbCl_2(g)$	— 41,580	— 19.26		+ 4.58		1,227-2,023
81	$Pb(g) + Cl_2(g) = PbCl_2(g)$	— 88,610	+ 19.17				2,023-2,273
82	$2/3Sb(s) + Cl_2(g) = 2/3SbCl_3(s)$	— 62,420	+ 64.98		—11.81		298-346.6
83	$2/3Sb(s) + Cl_2(g) = 2/3SbCl_3(l)$	— 61,620	+ 83.20		—19.90		346.6-494
84	$2/3Sb(s) + Cl_2(g) = 2/3SbCl_3(g)$	— 49,560	— 2.25		+ 2.764		494-903.7
85	$2/3Sb(l) + Cl_2(g) = 2/3SbCl_3(g)$	— 52,230	— 3.24		+ 4.10		903.7-1,713
86	$2/3Sb(g) + Cl_2(g) = 2/3SbCl_3(g)$	— 86,360	+ 29.93				1,713-2,273
87	$1/2Si(s) + Cl_2(g) = 1/2SiCl_4(l)$	— 78,420	+ 70.00		—14.81		298-330.2
88	$1/2Si(s) + Cl_2(g) = 1/2SiCl_4(g)$	— 72,550	+ 14.13	+ 0.435	+ 0.3455	$\frac{-0.2525 \times 10^5}{T}$	330.2-1,683
89	$1/2Si(l) + Cl_2(g) = 1/2SiCl_4(g)$	— 75,960	+ 2.15		+ 4.928		1,683-2,273
90*	$Sn(s) + Cl_2(g) = SnCl_2(s)$	— 84,630	+ 56.97	— 1.95	— 6.61		298-505.1
91*	$Sn(l) + Cl_2(g) = SnCl_2(s)$	— 87,290	+ 79.37		—13.31		505.1-520
92*†	$Sn(l) + Cl_2(g) = SnCl_2(l)$	— 85,800	+ 94.76		—20.04		520-896
93*†	$Sn(l) + Cl_2(g) = SnCl_2(g)$	— 55,480	— 9.76		+ 3.915		896-2,000
94*	$SnCl_2(s) + Cl_2(g) = SnCl_4(l)$	— 50,170	+ 98.58		—26.85		298-386
95*	$SnCl_2(s) + Cl_2(g) = SnCl_4(g)$	— 35,660	— 34.78		+10.18		386-520
96*†	$SnCl_2(l) + Cl_2(g) = SnCl_4(g)$	— 36,710	— 56.46		+18.84		520-896
97*†	$SnCl_2(g) + Cl_2(g) = SnCl_4(g)$	— 66,290	+ 41.66		— 3.22		896-2,000
98	$1/2Ti(s) + Cl_2(g) = 1/2TiCl_4(l)$	— 91,880	+ 76.80		—17.22		298-409
99	$1/2Ti(s) + Cl_2(g) = 1/2TiCl_4(g)$	— 83,830	+ 9.60	+ 0.565	+ 1.13	$\frac{-1.083 \times 10^5}{T}$	409-2,000
100	$Zn(s) + Cl_2(g) = ZnCl_2(s)$	—100,320	+ 54.63	— 2.37	— 5.46		298-548
101†	$Zn(s) + Cl_2(g) = ZnCl_2(l)$	— 98,060	+ 99.42	+ 1.63	—24.11		548-692.7
102†	$Zn(l) + Cl_2(g) = ZnCl_2(l)$	— 98,550	+ 85.56	+ 0.555	—18.72		692.7-1,029
103†	$Zn(l) + Cl_2(g) = ZnCl_2(g)$	— 56,680	— 32.43		+ 7.14		1,029-1,180
104†	$Zn(g) + Cl_2(g) = ZnCl_2(g)$	— 87,770	+ 15.84				1,180-2,273
105	$1/2Zr(s) + Cl_2(g) = 1/2ZrCl_4(s)$	—117,050	+ 72.55	+ 1.065	—12.62	$\frac{+0.755 \times 10^5}{T}$	298-604
106	$1/2Zr(s) + Cl_2(g) = 1/2ZrCl_4(g)$	—100,810	+ 11.14	+ 1.065	— 0.12	$\frac{-0.20 \times 10^5}{T}$	604-1,773

Selected Values.[3] ΔH°_f for $CaCl_2$ from Bichowsky and Rossini.[9] ΔH for fusion vaporization and transition from Kelley.[5, 6, 8] Cp values from Kelley.[5, 8]

10. $CdCl_2$: ΔH°_f, S°_{298}, ΔH for fusion and vaporization from Selected Values.[3] Cp of $CdCl_2$ was estimated; other Cp values from Kelley.[4, 5]

11. $CoCl_2$: ΔH°_f, S°_{298}, from Selected Values.[3] ΔH for fusion and vaporization from Kelley.[5, 7] Cp for $CoCl_2$ was estimated; other Cp values from Kelley.[4]

12. $CrCl_2$: Maier[10] gives ΔG° vs. T for reduction of $CrCl_2$ by H_2 and for vaporization of $CrCl_2$. These equations, combined with eq 50 from table VI were used to calculate eqs 35, 36, 37 of table VI. Maier's equations are probably quite accurate from 1000° to 2000°C.

13. $CrCl_2$-$CrCl_3$: Maier[10] gives ΔG° vs. T for reaction 38 of table VI, also for sublimation of $CrCl_3$, and fusion and vaporization of $CrCl_2$. Combination of these equations yields eqs 39, 40, and 41 of table VI. These equations are probably quite accurate from 1000 to 2000°C.

14. Cu_2Cl_2: ΔH°_f, S°_{298} and ΔH for fusion from Selected Values.[3] ΔH for vaporization of Cu_2Cl_2 from Kelley.[5] Cp for Cu_2Cl_2 was estimated; other Cp values from Kelley.[4]

15. $FeCl_2$: S°_{298}, ΔH°_f and phase change data from Selected Values.[3] Cp values from Kelley,[8] except Cp for Fe (*s*, avg.) which was obtained from Basic Open Hearth Steelmaking.[36]

16. HCl: ΔH°_f from Bichowsky and Rossini.[9] S°_{298} and Cp from Kelley.[4, 7] Values of ΔG° agree with those reported in Selected Values[3] to ± 0.05 pct.

17. Hg_2Cl_2: ΔH°_f, S°_{298} from Selected Values.[3] Cp from Kelley.[4]

18. $HgCl_2$: ΔH°_f, S°_{298} and ΔH for fusion and vaporization from Selected Values,[3] except $S^\circ_{HgCl_2}$ which is from Kelley.[7] Cp values from Kelley.[4, 5]

19. $MgCl_2$: S°_{298} for $Mg_{(s)}$ and Cl_2 from Kelley;[7] S°_{298} for $MgCl_2(s)$ from Kelley and Moore.[35] ΔH°_f from Shomate and Huffman.[37] ΔH for fusion and vaporization from Kelley.[5, 8] Cp values from Kelley.[8]

20. $MnCl_2$: S°_{298}, ΔH°_f and phase change data from Selected Values.[3] Cp values from Kelley.[5, 8]

21. NaCl: ΔH°_f from Bichowsky and Rossini.[9] S°_{298}, ΔH for fusion and vaporization, and Cp values from Kelley.[4–7]

22. $NiCl_2$: ΔH°_f, and S°_{298} from Selected Values.[3] ΔH for fusion and sublimation from Kelley.[5, 6] Cp values from Kelley.[4]

23. $PbCl_2$: ΔH°_f, S°_{298}, and ΔH for fusion and vaporization from Selected Values.[3] Cp values from Kelley.[4, 5]

24. $SbCl_3$: ΔH°_f, S°_{298}, and ΔH for fusion and vaporization from Selected Values.[3] Cp values from Kelley.[4, 5]

25. $SiCl_4$: ΔH°_f, S°_{298}, and ΔH for fusion and vaporization from Selected Values,[3] Cp values from Kelley,[4, 5] except Cp for liquid silicon which was estimated.

26. $SnCl_2$: ΔH°_f, S°_{298}, and ΔH for fusion and vaporization from Selected Values.[3] S°_{298} for $SnCl_2$ was estimated from Wenner's graph[33] as 29.0 entropy units. Cp for liquid and gaseous $SnCl_2$ was estimated; other Cp values from Kelley.[4] These equations are to be considered tentative.

27. $SnCl_2$-$SnCl_4$: ΔH°_f, S°_{298}, and ΔH for vaporization and fusion from Selected Values.[3] S°_{298} of $SnCl_2$ estimated as 29.0 entropy units (see paragraph 26). Cp for liquid and gaseous $SnCl_2$ was estimated; other Cp values from Kelley[4, 5] and Selected Values.[3] These equations are to be considered tentative.

28. $TiCl_4$: ΔH°_f and S°_{298} from Selected Values.[3] ΔH for vaporization and Cp values from Kelley.[4, 5]

29. $ZnCl_2$: ΔH°_f, S°_{298}, and ΔH for fusion and vaporization from Selected Values.[3] Cp for $ZnCl_2$, liquid and gaseous, was estimated; other Cp data from Kelley.[4]

30. $ZrCl_4$: S°_{298}, ΔH°_f and ΔH for sublimation from Selected Values.[3] Cp values from Kelley.[5, 8]

References

[1] O. A. Hougen and K. M. Watson: Chemical Process Principles. Part II. New York. 1947. John Wiley and Sons.

[2] J. Chipman: Disc. Far. Soc. (1948) No. 4, p. 23.

[3] Selected Values of Chemical Thermodynamic Properties. Nat. Bur. Standards. Published in installments beginning March 31, 1947.

[4] K. K. Kelley: U.S. Bur. Mines. *Bull.* 371 (1934).

[5] K. K. Kelley: U.S. Bur. Mines. *Bull.* 383 (1935).

[6] K. K. Kelley: U.S. Bur. Mines. *Bull.* 393 (1936).

[7] K. K. Kelley: U.S. Bur. Mines. *Bull.* 434 (1941).

[8] K. K. Kelley: U.S. Bur. Mines. *Bull.* 476 (1949).

[9] F. R. Bichowsky and F. D. Rossini: The Thermochemistry of Chemical Substances. 1936. New York. Reinhold Pub. Co.

[10] C. G. Maier: U.S. Bur. Mines. *Bull.* 436 (1942).

[11] P. Gross: U.S. Pat. 2,470,305. May 17, 1949.

[12] H. J. T. Ellingham: *Jnl.* Soc. Chem. Ind. (London) (May 1944) 125.

[13] C. W. Dannatt and H. J. T. Ellingham: Disc. Far. Soc. (1948) **4**, 126.

[14] J. Racine: *Bull.* soc. chim. France. (1947) 1075-1077.

[15] J. Racine: *Bull.* soc. chim. France. (1949) 50-53.

[16] C. L. Mantell: Industrial Electrochemistry. (1940). New York. McGraw-Hill Pub. Co.

[17] P. Drossback: z. Electrochem. (1939) **45**, 435-440.

[18] W. J. Kroll: *Trans.* Electrochem. Soc. (1940) **78**, 35-47.

[19] W. H. Waggaman and E. A. Gee: *Chem. Eng. News* (1948) **26**, 377-381.

[20] W. J. Kroll: *Metal Ind.* (London) (Oct. 8, 1948) 283-286; (Oct. 15, 1948) 307-310; (Oct. 22, 1948) 323-325.

[21] H. V. Zeppelin: U.S. Pat. 2,214,211. Sept. 10, 1940.

[22] W. J. Kroll: U.S. Pat. 2,396,792. March 19, 1946.

[23] W. J. Kroll: U.S. Pat. 2,396,793. March 19, 1946.

[24] W. J. Kroll and F. E. Bacon: U.S. Pat. 2,443,253. June 15, 1948.

[25] W. J. Kroll and F. E. Bacon: U.S. Pat. 2,452,665. Nov. 2, 1948.

[26] Anon: *Metal Ind.* (London) (1947) **70**, 363.

[27] J. O. Betterton: AIME (1933). TP 504.

[28] B. A. Muromtsev and L. A. Nazarova: *Jnl.* Gen. Chem. (U.S.S.R.) (1946) **16**, 1767-1776.

[29] J. Lumsden: Disc. Far. Soc. (1948) No. **4**, p. 60.

[30] C. G. Maier: *Eng. Min. Jnl.*-Press (Jan. 13, 1923) p. 51.

[31] C. J. P. Ball: *Trans.* AIME (1944) **159**, 285.

[32] Gross, Campbell, Kent, and Levi: Disc. Far. Soc. (1948) No. 4.

[33] R. R. Wenner: Thermochemical Calculations. New York. McGraw-Hill Pub. Co. (1941) p. 176.

[34] W. D. Treadwell and L. Terebesi: *Helv. Chim. Act.* (1932) **15**, 1053.

[35] K. K. Kelley and G. E. Moore: J.A.C.S. (1943) **65**, 1264.

[36] Basic Open Hearth Steelmaking. AIME, Seeley Mudd Series (1944) p. 360.

[37] C. H. Shomate and E. H. Huffman: J.A.C.S. (1943) **65**, 1625.

A Survey of the Thermodynamics of Copper Smelting

by R. Schuhmann, Jr.

Available thermodynamic data applicable to copper smelting systems are collected and tabulated, and the important gaps are pointed out. A few examples are given of estimations which can be made from the available data. An experimental research program is proposed to supply the thermodynamic data that appear most essential to better quantitative understanding of the chemistry of copper smelting. The proposed program is designed also to shed specific light on the practical problems of slag losses and magnetite behavior.

COPPER smelting, from flotation concentrates to blister copper, is conspicuous among the large scale chemical processes which are conducted with only relatively incomplete knowledge of the physical chemistry involved. For example, no common metallurgy text explains adequately why copper enters the matte phase while iron enters only to the extent that sulphur is left over after satisfying the copper. Explaining this important phenomenon as a manifestation of the greater affinity of sulphur for copper than for iron is unsound because the affinities of copper and iron for sulphur are about the same at smelting temperatures. As will be shown, other affinities are really decisive in the relatively clear-cut separation of copper in the matte.

In contrast, thermodynamic studies have contributed much to our understanding of copper refining, zinc oxide reduction, magnesium production, steelmaking, etc. For each of these processes, the important reactions are clearly recognized, and fair to good quantitative values of the free-energy changes and equilibrium constants are available. Such data have proved to be of constantly increasing practical value in process development and improvement.

Work in other fields has furnished much thermodynamic data applicable to copper smelting systems. In fact, several promising starts have been made in applying such data to specific smelting problems. Kelley[1] made an appraisal of the possibilities of recovering elementary sulphur from low grade matte. His calculations and compilations of thermodynamic data have represented the starting point for much of the work in this field, including the present survey. Huang and Hayward[2] and Aksoy[3] used thermodynamic methods in the study of copper losses in reverberatory slags. Peretti[4] used thermodynamic data in explaining the chemistry of converting. The recent publications of Darken and Gurry[5, 6] and of Darken,[7] dealing with the iron-oxygen and iron-silicon-oxygen systems, respectively, present equilibrium data that are applicable to copper smelting systems. Also additional data were reported recently on the affinity of sulphur for copper, manganese, and iron[8] and on the sulphur pressures of iron-sulphur melts.[9]

The survey presented in this paper was made as the basis for planning an experimental program on the thermodynamics of copper smelting. Few researches on the chemistry of copper smelting have been reported in recent years, so that a reappraisal and coordination of old and new data are essential if further work is to take the directions of maximum value. The experimental program is now in progress, and the plan of attack is outlined at the end of this paper.

Progressive Oxidation and Desulphurization of Copper-bearing Liquid Phases: The chemical activities of sulphur and oxygen are two of the most important thermodynamic yardsticks to be applied to copper smelting processes. Virtually the entire smelting and refining sequence involves a series of systems characterized by decreasing sulphur activity and increasing oxygen activity. In this section, therefore, an attempt is made to define and explain these activities in terms of equilibrium partial pressures of SO_2, S_2, and O_2. Also, estimates of these quantities are presented, the estimates being based largely on calculations presented in a later section of this paper.

The sequence of steps from raw flotation concentrate to fully oxidized copper ready for poling involves progressive and controlled oxidation. Iron is oxidized and enters the slag. Sulphur is oxidized and leaves in the gas. Table I summarizes several important features of this oxidation and desulphurization sequence, starting at the beginning of the matte blow in the converter. The top line gives in order the principal smelting and refining stages up to fully oxidized copper, plus the additional step, not used commercially, of oxidizing all the way to Cu_2O. In the second line are shown the principal copper-bearing liquid phases which characterize the process. Through most of the sequence the copper

---

R. SCHUHMANN, JR., Member AIME, is Associate Professor of Process Metallurgy, Massachusetts Institute of Technology, Cambridge.

AIME New York Meeting, Feb. 1950.

TP 2868 D. Discussion (2 copies) may be sent to Transactions *AIME before July 30, 1950. Manuscript received April 25, 1949; revision received Dec. 5, 1949.*

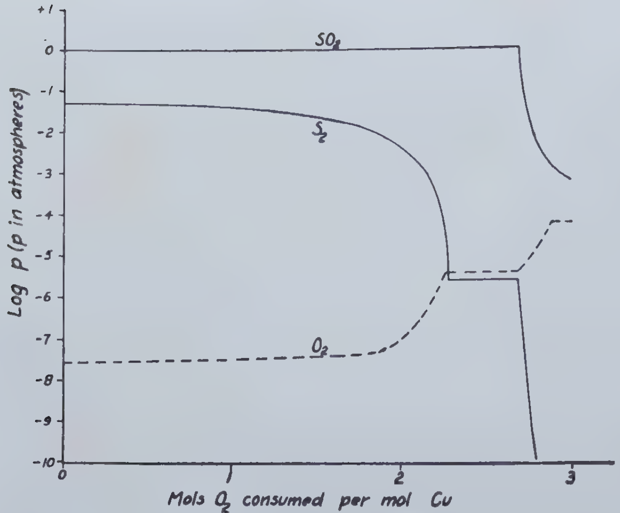

Fig. 1—Estimated equilibrium pressures of SO_2, S_2, and O_2 at 1300°C for converting copper matte and subsequent oxidation of blister to Cu_2O.

is concentrated in one phase at a time, but for part of the white metal-to-blister blow two high-copper phases are present and again during oxidation to Cu_2O two high-copper phases are present simultaneously. The next two lines summarize the stoichiometry of oxidation and desulphurization, emphasizing the fact that from a purely stoichiometric point of view the bulk of the oxidation and desulphurization is in the earlier stages. In the last three lines of table I and in fig. 1 are given estimates of equilibrium pressures of SO_2, S_2, and O_2 at the various stages of the sequence. These estimated equilibrium pressures, discussed in more detail below, are significant as thermodynamic measures of the extent of oxidation and desulphurization; that is, they are measures of the chemical activities of oxygen, sulphur, and sulphur dioxide.

The equilibrium pressures of SO_2, S_2, and O_2 at a given stage may be defined as the partial pressures of these gases in a gas phase that would be in equilibrium with an instantaneous, representative sample of the reacting system withdrawn to a separate container at the same temperature and total pressure and held until equilibrium is reached. In the copper converter these are the partial pressures that would prevail in the gas phase if the blowing were stopped, the converter closed and vented at one atmosphere, and held at constant temperature until equilibrium was reached. By definition, these pressures cannot be measured directly in the system while reactions are in progress since the fact that reactions are occurring is *prima facie* evidence of lack of equilibrium. The distinction between equilibrium conditions and actual process conditions is characteristic of the application of thermodynamics to chemical processes in general, and underlines the fact that equilibrium data describe only limiting conditions within which the process must operate. Furthermore, it should be clearly understood that equilibrium partial pressures and other equilibrium data to be considered subsequently do not constitute a basis for choosing between different reaction mechanisms. Thus, we can talk about equilibrium p_{S_2}, for example, even though S_2 molecules might be of minor or of no importance as reactants when reaction mechanisms are considered.

During converting, SO_2 is evolved rapidly at actual partial pressures which are substantial fractions of 1 atm. If blowing were stopped instantaneously, we would expect at that instant the presence within the converter of some copper oxide, for example, which would continue reacting with sulphides to give additional evolution of SO_2 for a short time after blowing stopped. If the converter were vented at 1 atm, the SO_2-producing reactions would stop when the reactants had been consumed to the point that they were in equilibrium with SO_2 at 1

Table I. Oxidation and Desulphurization of Copper-bearing Liquid Phases

LIQUID PHASES

	Converting					Refining		Overoxidation	
Stage of process	Low grade matte	→	White metal	→	Blister copper	→	Oxygen-saturated copper	→	Cuprous oxide
Copper-bearing phases	← Liquid sulphide →								
				← Liquid metal →					
							← Liquid oxide →		
Cumulative oxygen consumption, mols O_2 per mol Cu	0	2	2.25	2.5	2.75		2.9	3.0	
Residual Sulphur, mols S per mol Cu	2	0.67	0.5	0.25	0.0		(Residual S stoichiometrically negligible, but not nil)		
Estimated equilibrium partial pressures at 1300°C, in atmospheres									
SO_2	1	1		1			10^{-3}		
O_2	2.7×10^{-8}	5.2×10^{-8}		3.4×10^{-6}			4.7×10^{-5}		
S_2	4.5×10^{-2}	10^{-2}		2.7×10^{-6}			1.4×10^{-14}		

Notes: 1. The stoichiometric data are for illustrative purposes only, and were calculated on the assumption that the matte originally consisted of 25 mol pct Cu_2S and 75 mol pct FeS. Oxygen consumptions are theoretical quantities to oxidize Fe to FeO and S to SO_2.
2. Calculations of p_{S_2} and p_{O_2} are presented in the section on "Sample Calculations and Applications of Thermodynamic Data."

Fig. 2 — Equilibrium diagram of system FeO-SiO_2, calculating all iron oxides in liquid to FeO.

Upper figure gives actual amounts of Fe_2O_3 in liquid at liquidus temperature.
(*Bowen and Schairer*[11])

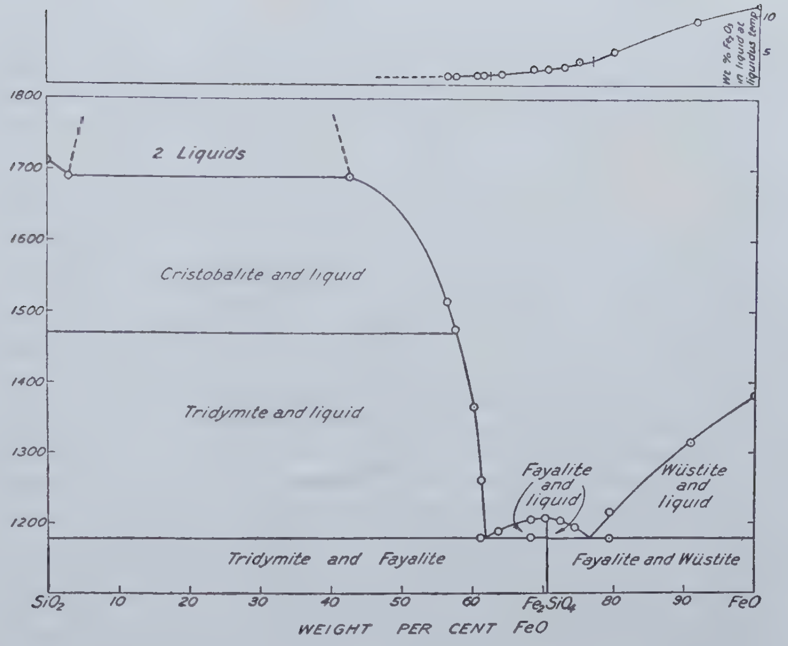

atm. On this basis, then, the equilibrium value of p_{SO_2} for converting is estimated at 1 atm. Another way of making the estimate is to consider equilibrium as the limiting condition of operating the converter so slowly that each mol of oxygen added is allowed to react and reach equilibrium before the next one is blown in. In such equilibrium operation, we know the SO_2 would be produced at pressures of 0.21 atm and greater (for bubbles formed deep in the melt). Accordingly, an equilibrium p_{SO_2} of 1 atm appears of the proper order of magnitude for the converting process, and is so estimated in table I and fig. 1.

The oxidation procedure in fire refining must give equilibrium sulphur dioxide pressures some orders of magnitude below 1 atm. Phillips[10] has analyzed carefully the sulphur-oxygen and other equilibria in liquid copper and has suggested that the sulphur dioxide equilibrium pressure at the end of refining might approach the actual partial pressure in the atmosphere of the refining furnace. He has calculated that this might be from 0.05 to 0.9 mm mercury for various fuels or in the range of 10^{-3} to 10^{-4} atm. These estimates are reflected in the dip of the p_{SO_2} curve at the right of fig. 1.

Equilibrium pressures of S_2 and O_2 cannot be estimated directly from process characteristics, as was done with SO_2, but must be estimated indirectly. The equilibrium pressures of SO_2 and O_2 at a given temperature are related by the equilibrium constant at that temperature for the reaction,

$$\tfrac{1}{2}\, S_2(g) + O_2(g) \rightleftarrows SO_2(g) \qquad [1]$$

which is

$$\frac{p_{SO_2}}{p_{S_2}^{1/2}\, p_{O_2}} = k_1 = 1.8 \times 10^8 \text{ at } 1300^\circ\text{C}^*$$

Thus, if the estimates of p_{SO_2} given above are accepted, a determination of p_{S_2} automatically permits calculation of p_{O_2}, or a determination of p_{O_2} permits calculation of p_{S_2}. The data for p_{S_2} and p_{O_2} in table I and fig. 1 are based on the p_{SO_2} estimates, on k_1, and on thermodynamic data for Cu, Fe, S, and O reactions to be presented in detail later. It is believed that the estimates of equilibrium pressures are correct within one order of magnitude (within a factor of 10).

Conditions in reverberatory smelting are undoubtedly less oxidizing (lower p_{O_2}) than in converting; also formation and evolution of SO_2 are usually secondary so that p_{SO_2} must be somewhat lower than 1 atm. Probably p_{SO_2}, p_{S_2}, and p_{O_2} vary considerably from one reverberatory furnace to another depending on the stoichiometry of the charge, and these variations will be related to magnetite buildup (or digestion), slag losses, and other operating features. However, on the basis of information now available on the chemistry of matte smelting, even an order-of-magnitude estimate of these equilibrium partial pressures hardly seems justified.

Iron Silicate Slags: Iron oxides and silica are the major constituents of most copper smelting slags, while lime, alumina, magnesia, etc., usually are each well under 10 pct. Hence, a first thermodynamic study might well be based on a simple iron silicate system. This idealized slag system has three components, Fe, O, and SiO_2.* As will be shown, looking upon the slag as a binary system (FeO-SiO_2) is a misleading oversimplification because the Fe to O relation is one of the most significant chemical properties of the slag.

Constitution Diagrams: Although the Fe-O-SiO_2 ternary system has not been worked out in detail, many of its important features can be distinguished by study of Bowen and Schairer's[11] FeO-SiO_2 diagram, Darken and Gurry's[6] Fe-O diagram, and Darken's[7] oxygen-pressure vs. constitution data for the Fe-O-SiO_2 system.

Fig. 2, from Bowen and Schairer, represents the system of iron oxide and silica in equilibrium with metallic iron. Even for slags in contact with iron metal, the atomic ratio of O to Fe, $\frac{N_O}{N_{Fe}}$ (after satisfying Si as SiO_2), is not unity as it would be by the formula FeO, but is always greater than unity as Bowen and Schairer's data in the upper portion of fig. 2 show. The slag region is bounded by melt compositions in equilibrium with a separate silica phase on the left, by melts containing no silica on the right, and at lower temperatures, by compositions in equilibrium with fayalite ($2FeO, SiO_2$) and with wüstite (FeO_x). This diagram shows the constitution only of the series of iron silicate slags which, for a given percent SiO_2, are in the lowest state of oxidation. However, as will be shown, there are good grounds for believing that copper smelting slags contain more oxygen (more Fe_2O_3) and represent a much higher state of oxidation than Bowen and Schairer's slags. For example, fig. 2 gives no hint of slag compositions in equilibrium with solid magnetite which are at the other end of the oxidation scale from slags in equilibrium with solid iron.

---

* Equilibrium constants and sources are discussed in more detail later.

* Choice of the components is partly a matter of convenience; we can specify iron silicate slags in terms of FeO, Fe_2O_3, and SiO_2; FeO, Fe_3O_4, and SiO_2; FeO, O and SiO_2; or Fe, O, Si if desired.

By a careful application of the Phase Rule to oxygen-pressure data in the Fe-O-Si system, Darken developed the temperature vs. oxygen-pressure diagram given in fig. 3 (using the experimentally convenient CO_2/CO ratio as a measure of oxygen pressure). Darken's work represents an important step in the understanding of the ternary system, since for the first time the relative positions of the fixed points, univariant curves, etc., are made clear. There remains, of course, much more experimental work to be done before a quantitative model can be made of the ternary constitution diagram.

The information summarized in figs. 2 and 3 and in Darken and Gurry's[6] Fe-O diagram makes possible the construction of a ternary temperature-composition diagram which can be regarded as qualitatively correct. Though void of quantitative significance in several important regions, such a diagram has been constructed by P. J. Ensio and the author and has proved very helpful in the study of iron silicate slags. An isothermal section at 1300°C is shown in fig. 4.

Referring to fig. 4, the homogeneous slag region is bounded by the following curves:

1. Curve *AB*, melts in equilibrium with solid Fe. Position of curve established by Bowen and Schairer.
2. Curve *BC*, melts in equilibrium with wüstite. Composition for point *B* established. Existence of curve *BC* and point *C* shown by Darken, but locations unknown.
3. Curve *CD*, melts in equilibrium with magnetite. Existence of points *C* and *D* and of connecting curve shown by Darken, who indicated also that at higher temperatures point *D* probably is near the straight line connecting Fe_3O_4 and SiO_2.
4. Curve *DA*, melts in equilibrium with silica. Only point *A* is quantitatively established.

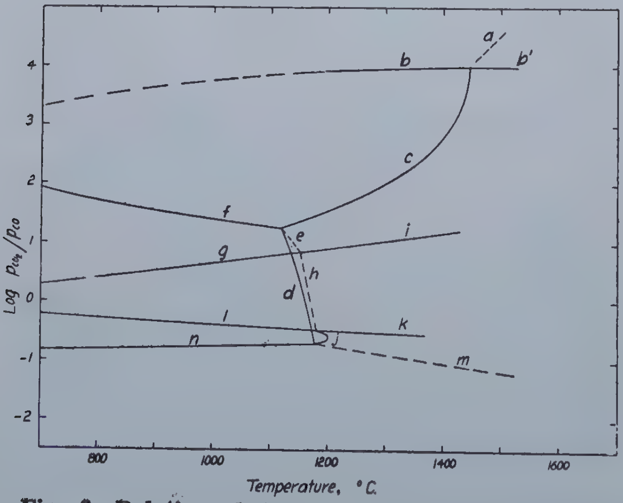

Fig. 3—Relations between gas composition and temperature for univariant equilibria of system Fe-Si-O (*Darken*[7])

a. Hematite, silica, melt
b. Hematite, magnetite, silica
b.' Hematite, magnetite, melt
c. Magnetite, silica, melt
d. Fayalite, silica, melt
e. Magnetite, fayalite, melt
f. Magnetite, fayalite, silica
g. Magnetite, wüstite, fayalite
h. Wüstite, fayalite, melt
i. Magnetite, wüstite, melt
j. Metal, fayalite, melt
k. Wüstite, metal, melt
l. Wüstite, fayalite, metal
m. Metal, silica, melt
n. Metal, fayalite, silica

Small percentages of lime, alumina, other oxides, and of dissolved sulphides in actual slags will modify the picture to some extent, but these effects can be studied best after a clear picture of the constitution of the simpler FeO-Fe_2O_3-SiO_2 melts is obtained. Qualitatively, converter slags are relatively low in SiO_2 and saturated or nearly saturated with Fe_3O_4; hence, in terms of fig. 4 their compositions should fall near curve *CD* and well to the right of point *D*. Reverberatory slags, on the other hand, probably will be well below Fe_3O_4 saturation in most cases and perhaps not too far from the middle of SiO_2-saturation curve *AD*. Though the facts are not yet available, it appears doubtful that any copper smelting slags would approach saturation with solid iron or compositions along *AB*.

Clearly, quantitative experimental determination of the ternary constitution diagram at smelting temperatures is among the first steps to be taken toward the understanding of copper smelting slags. Such an investigation is in progress in the M.I.T. process metallurgy laboratory, using the techniques of quenching and microscopic examination already successfully used by Bowen and Schairer[11] in establishing the constitution diagram given in fig. 2.

Oxygen Pressure of Iron Silicate Slags: Earlier in this paper the equilibrium oxygen pressure was pointed out as one of the thermodynamic variables in the copper smelting system. The magnitude of the oxygen pressure is closely related to slag composition, and in straight iron silicate slags is fixed when the temperature, percent silica and $\frac{N_O}{N_{Fe}}$ ratio are specified.* The fact that the iron in the slag can be present in varying degrees of oxidation means not only that the oxygen pressure of the slag can vary between wide limits, as will be shown, but also that the slag can serve as an important oxygen carrier in the system, releasing large quantities to reducing agents and absorbing large quantities from oxidizing agents. Thus, control of slag composition is an important means of control of oxygen pressure.

Oxygen pressure (p_{O_2}) is quantitatively related to the activities of Fe, FeO, Fe_3O_4 in the slag by means of the equilibrium constants for reactions 2 and 3 below.

$$Fe + \tfrac{1}{2} O_2 \rightleftarrows FeO \qquad [2]$$

$$3FeO + \tfrac{1}{2} O_2 \rightleftarrows Fe_3O_4 \qquad [3]$$

The equilibrium constants k_2 and k_3 are known accurately at smelting temperatures from the data of Darken and Gurry[5, 6] if the activities of iron and its oxides are defined in terms of standard states in the Fe-O system. Accordingly, let us adopt the following standard states for all subsequent calculations:

$a_{Fe(\gamma)} = 1$ for solid γ iron

---

* This follows from the Phase Rule, which shows that a two-phase (gas and slag), three-component (Fe, O, SiO_2) system is completely determined by specifying the values of three independent variables.

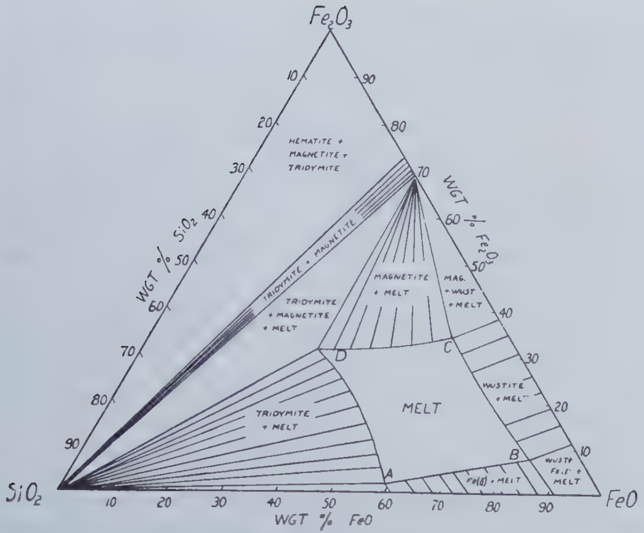

Fig. 4—Semiquantitative equilibrium diagram of system Fe_2O_3-FeO-SiO_2.
Isothermal section at 1300°C.

$a_{FeO(l)} = 1$ for the pure iron oxide melt in equilibrium with solid iron

$a_{Fe_3O_4} = 1$ for pure solid Fe_3O_4

At 1300°C, calculations based on Darken and Gurry's data give:

$$k_2 = \frac{a_{FeO(l)}}{a_{Fe(\gamma)}\, {p_{O_2}}^{1/2}} = 2.1 \times 10^5$$

$$k_3 = \frac{a_{Fe_3O_4}}{{a_{FeO(l)}}^3\, {p_{O_2}}^{1/2}} = 3.1 \times 10^4$$

Darken's oxygen-pressure data in fig. 3 include estimates of oxygen pressure for slags in equilibrium with both magnetite and silica (curve *c*), and for slags in equilibrium with metallic iron and silica (curve *m*). Combination of these estimates with the equations for k_2 and k_3 above and with Darken and Gurry's data for p_{O_2} and a_{FeO} in wüstite[5] leads to the oxygen-pressure diagram in fig. 5, which is calculated for 1300°C to correspond to the ternary diagram in fig. 4. The closed melt area in fig. 5 corresponds to the melt area in fig. 4. Also the boundaries correspond, and for every point representing melt composition in fig. 4 there is a corresponding point within the closed area in fig. 5 representing the values of oxygen pressure and a_{FeO} for that slag composition. Unlike fig. 4, however, the positions of the boundary lines and curves of the melt field in fig. 5 are known quantitatively (except for the shape of the dotted curve).

The outstanding feature of the iron silicate slags brought out by fig. 5 is the tremendous variation in oxygen pressure which can be brought about by changing the composition from slags in equilibrium with metallic iron to slags in equilibrium with magnetite. The maximum oxygen pressure, 2×10^{-6} atm (equivalent in oxidizing power to a gas with CO_2:CO = 100:1), is for melts in contact with both magnetite and silica (point *D*), and the minimum, 3×10^{-12} atm (CO_2:CO about 0.1:1), is for melts in contact with both silica and iron (point *A*), giving a range of variation in p_{O_2} of about 10^6-fold between the extremes. These limiting data emphasize the need for quantitative study of the relation of slag composition to oxygen pressure over the whole range of melt compositions.

Copper-Iron-Sulphur Melts: *Constitution Diagrams:* Fairly complete constitution data are available for the Cu-Fe-S system at smelting temperatures, showing at least approximately the freezing points and composition ranges of the liquid mattes. The available binary diagrams cover the systems Cu-S,[12] Fe-S,[12] Cu_2S-FeS,[13] and Cu-Fe.[12] The portion of the Cu-Fe-S ternary diagram in which the liquid mattes fall was investigated by Reuleaux,[14] from whose work fig. 6 is taken.

The fact that commercial copper mattes tend to be deficient in sulphur compared with mixtures of Cu_2S and FeS has been pointed out frequently in the literature. This deficiency is clearly related to the fact that as the S content approaches stoichiometric equivalence to the Cu and Fe, the partial pressure of sulphur gas from the melt becomes a substantial fraction of an atmosphere.[15] Accordingly, unless the matte is enclosed under pressure or given a protective atmosphere of sulphur, sulphur will escape until the sulphur pressure is reduced to a low value. In the ternary diagram in fig. 6, then, the matte compositions of practical importance lie to the left of the straight line connecting Cu_2S and FeS. The prominent feature of the left-hand portion of the diagram is the miscibility gap or two-phase field extending at smelting temperatures from the Cu-S edge nearly to the Fe-S edge.* Thus, the compositions of or-

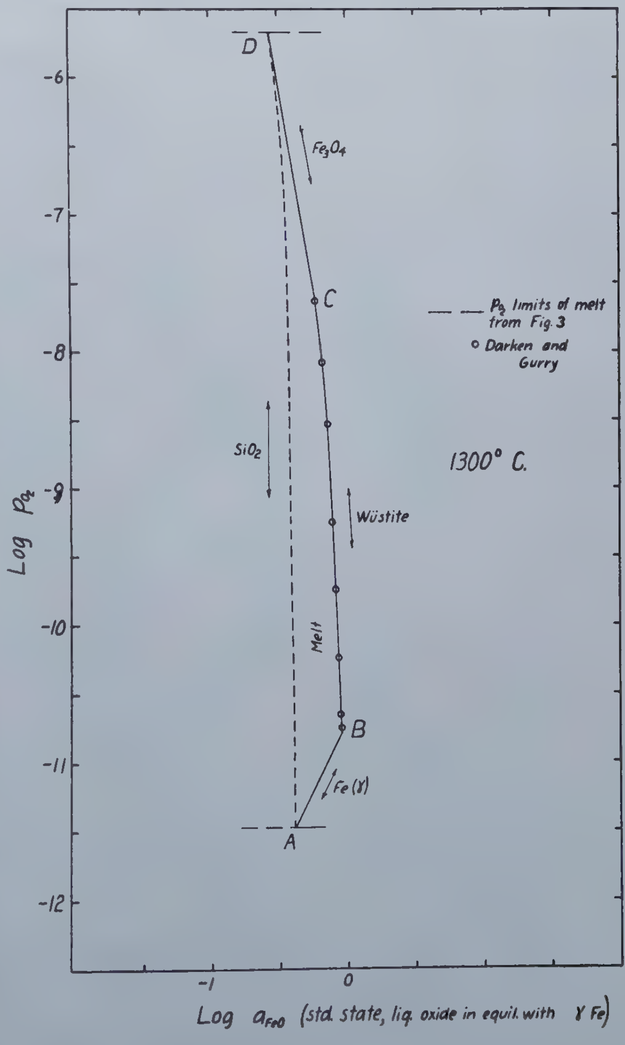

Fig. 5—Activities of FeO and O_2 in iron silicate melts at 1300°C.

---

* Reuleaux's experiments gave the boundary curve of the two-phase field at temperatures just above freezing. At higher temperatures this field will decrease in area.

dinary copper mattes will fall in the narrow, roughly triangular region bounded by (1) the Cu_2S-FeS join, and (2) the high-sulphur boundary curve of the miscibility gap. The shape of the miscibility gap in fig. 6 indicates that high-iron mattes can be obtained with greater stoichiometric deficiencies of sulphur (compared to Cu_2S-FeS mixtures) than high-copper mattes.

Since a given quantity of Cu and Fe in a matte can combine with a variable quantity of sulphur, it follows that mattes can serve as sulphur carriers in the same way as the iron silicate slags of variable $\frac{N_O}{N_{Fe}}$ serve as oxygen carriers. That is, a given matte can take up relatively large quantities of sulphur from a source of higher sulphur pressure or give up relatively large quantities of sulphur to a system of lower sulphur pressure.

Sulphur Pressures of Mattes: For liquid mattes consisting of Cu, Fe, and S the equilibrium sulphur pressure will vary both with composition and with temperature. No sulphur-pressure measurements have yet been reported on ternary Cu-Fe-S melts within the liquid-matte field of fig. 6 to the left of the Cu_2S-FeS join. However, Cox, Bachelder, Nachtrieb, and Skapski[8] recently determined p_{S_2} for melts very close to Cu_2S in composition at temperatures up to about 1250°C. Also, Maurer, Hammer, and Möbius[9] have determined p_{S_2} for Fe-S melts over a wide composition range (0-36.5 pct S). These two sets of data give equilibrium values of p_{S_2} for the reactions:

$$2\,Cu + \tfrac{1}{2}S_2(g) \rightarrow Cu_2S(l) \qquad [4]$$

$$Fe + \tfrac{1}{2}S_2(g) \rightarrow FeS\ (l) \qquad [5]$$

Unfortunately, however, the data for p_{S_2} at various melt compositions do not permit calculation of equilibrium constants for reactions 4 and 5 since the activities of Cu and Fe in these melts are not known quantitatively and in liquid Cu_2S and FeS are probably an order of magnitude or so below unity if pure liquid Cu and solid Fe are taken as standard states of unit activity.

For the subsequent calculations in this paper, equilibrium constants for reactions 4 and 5 will be based on Kelley's extrapolations of lower temperature equilibrium data for reactions of the solid sulphides. Since Kelley's publication, additional experimental data on reactions of the solid sulphides have been published.[8, 9] However, extrapolations of these new data to liquid-matte temperatures lead to equilibrium constants close to those calculated from Kelley's equation, so that revision does not seem justified pending completion of more experimental work at high temperatures. Kelley's data lead to the following values for the equilibrium constants at 1300°C:

$$k_4 = \frac{a_{Cu_2S(l)}}{a_{Cu(l)}{}^2\, p_{S_2}{}^{1/2}} = 760$$

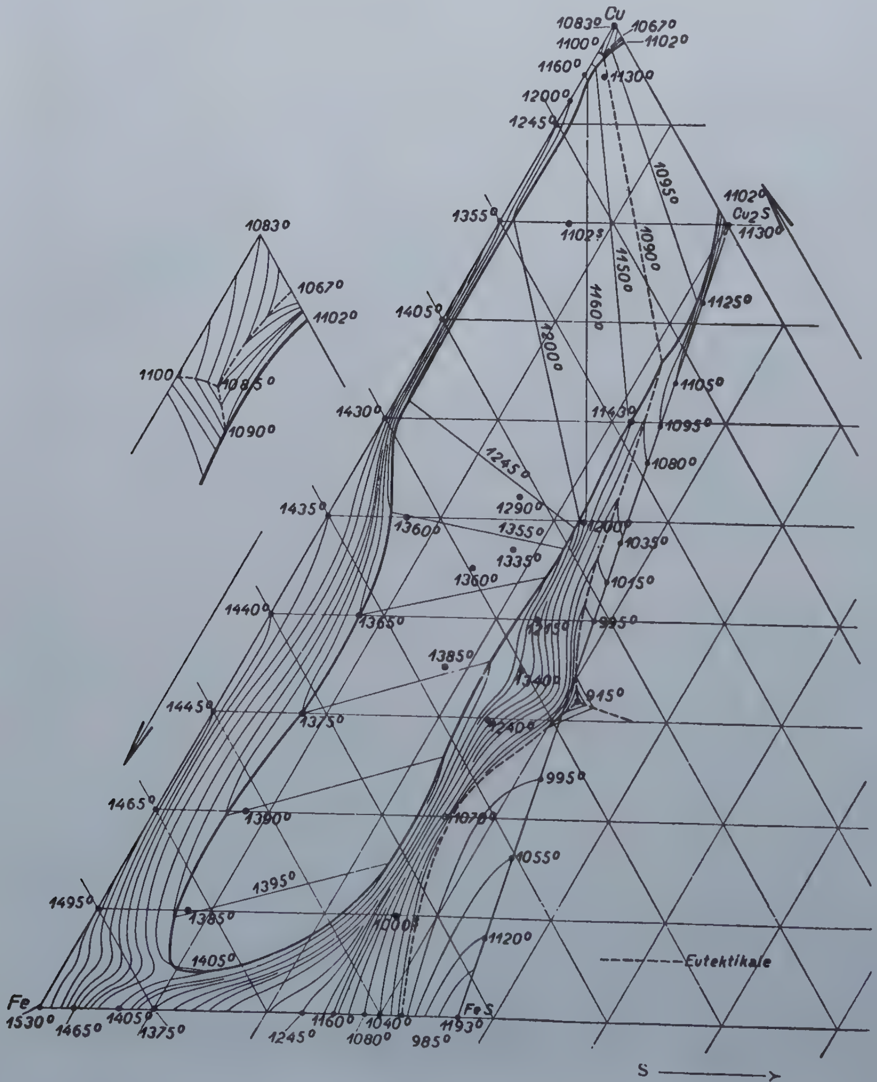

Fig. 6—Constitution diagram for portion of Cu-Fe-S system.

(*Reuleaux*[14])

Contour lines show liquidus temperatures.

$$k_5 = \frac{a_{FeS(l)}}{a_{Fe\,(\gamma)} p_{S_2}{}^{1/2}} = 250$$

In these constants the standard states for the sulphides are the pure liquids, and for Cu and Fe are the pure liquid and solid metals, respectively.

Relative Sulphur and Oxygen Affinities of Copper and Iron: Combination of eqs 4 and 5 gives

$$2\,Cu(l) + FeS(l) \rightarrow Fe(\gamma) + Cu_2S(l) \qquad [6]$$

The equilibrium data for this reaction show the extent to which copper can displace iron from iron sulphide, and thus the equilibrium constant k_6 is a measure of the relative affinities of copper and iron for sulphur. At 1300°C, based on Kelley's data,

$$k_6 = \frac{k_4}{k_5} = \frac{a_{Cu_2S(l)}\ a_{Fe(\gamma)}}{a_{Cu(l)}{}^2\ a_{FeS(l)}} = 3.1$$

The value of k_6 indicates that copper does have a little greater affinity for sulphur than does iron. However, the value is so close to unity that we obviously cannot account for the iron-copper separation in matte smelting on the basis of differences in sulphur affinities of copper and iron.

The possibility of forming Cu_2O during smelting can be appraised, starting with consideration of reaction 7.

$$2\,Cu(l) + \tfrac{1}{2}\,O_2 \rightleftarrows Cu_2O(l) \qquad [7]$$

At 1300°C, Kelley's data give:

$$k_7 = \frac{a_{Cu_2O(l)}}{a_{Cu(l)}{}^2\ p_{O_2}{}^{1/2}} = 160$$

Combining eq 7 with eq 2, and also combining equilibrium constants,

$$Cu_2O(l) + Fe(\gamma) \rightleftarrows FeO(l) + 2\,Cu(l) \qquad [8]$$

$$k_8 = \frac{a_{FeO}\ a_{Cu}{}^2}{a_{Cu_2O}\ a_{Fe}} = 1300$$

The large value of k_8 shows the strong tendency of the reaction to go to the right and shows that iron has a much greater affinity for oxygen than does copper.

Combining eqs 6 and 8 and their equilibrium constants,

$$Cu_2O(l) + FeS(l) \rightleftarrows Cu_2S(l) + FeO(l) \qquad [9]$$

$$k_9 = \frac{a_{Cu_2S}\ a_{FeO}}{a_{Cu_2O}\ a_{FeS}} = 4000$$

Thus reaction 9 has a strong tendency to go to completion. In moderate-grade mattes, a_{Cu_2S} and a_{FeS} must be about the same order of magnitude, so that as a first approximation $\frac{a_{Cu_2S}}{a_{FeS}} = 1$. From fig. 5, a_{FeO} lies between 0.3 and 0.9 in the slag. Inserting these estimates in k_9 and solving for a_{Cu_2O}, we find $a_{Cu_2O} =$ about 10^{-4}. This low value of a_{Cu_2O} is at least of the correct order of magnitude. Thus, the presence of copper oxide in the smelting system at an activity level corresponding to more than about one ten thousandth of the activity of pure liquid Cu_2O will drive reaction 9 to the right, displacing iron from the matte. The relationship expressed by the equilibrium constant of reaction 9 thus accounts in large measure for the clear-cut segregation of copper into the matte in the matte smelting process.

It is clear from the derivation that the relative oxygen affinities of iron and copper play the predominant role rather than the relative sulphur affinities which are not very different from each other.

Application of the Phase Rule to the Ideal Matte-Slag System: The simplest matte-slag system to which the previous discussion is applicable is represented schematically in fig. 7. This system has three phases and five components; hence, according to the Phase Rule it has four degrees of freedom. That is, specification of temperature and three other independent variables completely determines the state of the system at equilibrium (i.e., composition of each phase, activity of each constituent). For example, the following three alternative groups of four variables (or other groups) might be specified:

I	II	III
Temperature	*Temperature*	*Temperature*
a_{FeO}	Pct SiO_2 in slag	p_{O_2}
a_{FeS}	$\frac{N_O}{N_{Fe}}$ in slag	p_{S_2}
p_{SO_2}	Pct Cu in matte	Pct Cu in matte

The choice of independent variables in solving a given problem is a matter of ingenuity and convenience, in utilizing what is known practically about the system and in utilizing the available thermodynamic and stoichiometric relations.

Under some conditions an additional phase may be present in the system; e.g., solid magnetite or solid silica. If either of these solids is present at equilibrium, the system then has only three degrees of freedom; if both are present, the system has only two degrees of freedom.

The limited number of truly independent variables which can be imposed on the ideal matte-slag system at equilibrium is of considerable practical importance. In other words, the *equilibrium* matte, slag, and gas compositions at a given temperature are very intimately related and are not subject to wide independent controls on the part of the metallurgist. If full advantage is to be taken of the independent controls which are possible, it is essential that the fixed thermodynamic relations between activities, partial pressures, temperature, and phase

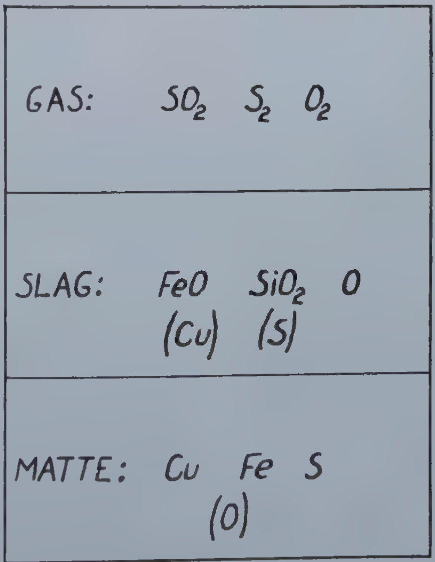

Fig. 7—Ideal matte-slag system.

compositions be clearly recognized, and it is highly desirable that these relations be known quantitatively.

Equilibria in the Matte-Slag System: *Activity-Composition Relations:* Before full use can be made of equilibrium constants such as those already given, experimental determination of the relations between activities and composition must be made for both mattes and slags. The assumptions that activity is directly proportional to concentration (Henry's law for dilute solutions) or is equal to mol fraction (Raoult's law for ideal solutions) appear to have only very limited applicability to mattes and slags.

Complete activity-composition data for Fe-O melts are available from Darken and Gurry's work.[6] These melts, however, contain no SiO_2 and thus represent merely the limiting conditions for slags. Thus, referring to fig. 4 experimental work is needed to find how p_{O_2}, a_{FeO}, and a_{SiO_2} vary with composition within the ternary melt field *ABCD*.

Similarly, very few activity data are available for liquid mattes, and experimental work is needed to find how p_{S_2}, a_{Cu}, a_{Fe}, a_{Cu_2S}, and a_{FeS} vary with composition. For rough estimations, regarding mattes as binary solutions of Cu_2S and FeS and assuming that a_{Cu_2S} and a_{FeS} are equal to the respective mol fractions appear justified pending the availability of experimental data.

Mutual Solubilities: In the previous discussion, the matte has been regarded primarily as a metal-sulphide solution and the slag as an oxide solution. In actuality, however, when the matte and slag are in equilibrium, some Cu_2S and FeS probably will dissolve in the slag and some FeO and Fe_3O_4, perhaps even a little SiO_2, will dissolve in the matte. The solubility of Cu_2S in the slag, and the Cu_2S distribution equilibrium between slag and matte are of primary importance in relation to slag losses and call urgently for laboratory study in simple systems.

Slag-Matte Reactions: Literally dozens of balanced chemical equations can be written for possible slag-matte reactions involving the substances Fe, FeO, Fe_3O_4, FeS, Cu, Cu_2O and Cu_2S present in the matte and slag solutions and S_2, O_2, and SO_2 in the gas phase. Since reaction mechanisms are of secondary consequence in the thermodynamic appraisal of equilibrium relationships, we may work rigorously with any of these equations for which the necessary data happen to be available. However, all the chemical equations for slag-matte reactions that might be composed are not independent of each other; in fact they are mostly algebraic additions and subtractions of each other. Hence, for equilibrium studies it is necessary to consider not all possible reactions but only a few independent reactions. The Phase Rule gives this principle in different language.

The bookkeeping of equilibrium data is greatly simplified by expressing the data in terms of free-energy changes. The standard free-energy change in calories per mol, $\Delta F°$, for any chemical reaction is related to the equilibrium constant k, as follows:

$$\Delta F° = -RT \ln_e k = -4.576\, T \log_{10} k$$

in which R is the gas constant and T is the absolute temperature (°C + 273). Also, $\Delta F°$ is related to the heat of reaction, ΔH, and the standard entropy change ($\Delta S°$) for the reaction:

$$\Delta F° = \Delta H - T\,\Delta S°$$

This relation is useful because *over a relatively narrow range of temperature,* such as the range from the melting point of Cu to 1500°C with which we are most concerned in copper smelting, ΔH and $\Delta S°$ for a given reaction are substantially constant and can be assumed constant without introducing any significant error in equilibrium calculations.

Table II gives ΔH and $\Delta S°$ data for various reactions of interest in the matte-smelting system, from which by use of the relations given above, equilibrium constants can be calculated over the temperature range 1100° to 1500°C. The calculated values of the equilibrium constants at 1300°C (1573°K) are given in the last column. The reactions are in two groups: first, the simple reactions of formation of the oxides and sulphides, and second, the more complex reactions between the various compounds. The data for the second group of reactions are all obtained by algebraic combinations of the data for the reactions of formation. That is, when the chemical equations are added and subtracted algebraically, the values of $\Delta F°$, ΔH, and $\Delta S°$ are also added and subtracted according to the same rules to obtain their respective values for the resulting chemical equation.

The data for the reactions of formation of SO_2 and the iron oxides at smelting temperatures are established with high accuracy. On the other hand, the data for the reactions of formation of Cu_2S, FeS, and Cu_2O are calculated on the basis of low temperature equilibrium results and rough specific-heat estimates, and may prove to be in error when further experiments are made.

The data in table II lead to equilibrium constants in which the activities of the reactants and reaction products must be evaluated with respect to certain specific standard states of unit activity. For the gaseous reactants, activities are given by partial pressures in atmospheres so that the standard states are the pure gases at 1 atm. The standard states for the other reactants are the pure substances in the state of aggregation which is stable over all or most of the temperature range of interest in copper smelting. These standard states are indicated in the chemical equations by the use of the appropriate abbreviations in parentheses. Sometimes it is convenient to retain a given standard state for calculations involving conditions where the given standard state is metastable. For example, FeO(l) is taken in a formal sense as a standard state at temperatures below the freezing point of liquid iron oxide.

Sample Calculations and Applications of Equilibrium Data: Even without activity-composition data on slag and matte solutions, a great variety of calculations and estimates of limiting conditions can be made using the data summarized in table II. The estimations given below are intended only to be illustrative of the methods of using equilibrium data and represent a small fraction of the potentially useful calculations which can be made from the available thermodynamic data. Similar illustrations have been given by Kelley.[1]

Example 1—Estimation of Equilibrium Values of p_{S_2} *and* p_{O_2} *at Various Stages of Copper Smelting:* In fig. 1 were plotted estimates of p_{S_2} and p_{O_2} for various stages of converting and for subsequent oxidation of the blister copper to Cu_2O. The basis of these estimates is given below:

(*a*) *Matte with 25 mol pct* Cu_2S *(75 mol pct FeS):* Since the matte-slag system has a variance of 4, it is necessary to fix values for four independent variables to specify the system. The following four variables can be estimated reasonably well from the known characteristics of the process:

Let temperature = 1300°C = 1573°K

p_{SO_2}, the equilibrium SO_2 pressure, may be taken as 1 atm, as discussed earlier.

a_{FeO} lies between extremes of 0.9 for a slag with no SiO_2 and 0.3 for a slag saturated with both Fe_3O_4 and SiO_2 (see fig. 5). For a first approximation let us take $a_{FeO} = 0.5$.

Taking a_{FeS} = mol fraction FeS in matte = 0.75 seems a reasonable first approximation.

For reaction 1, table II

$$-4.576 \log k_{10} = \Delta F^\circ = 177{,}400 - (1573)(102.22)$$

$$k_{10} = 4.9 \times 10^{-3}$$

$$\frac{a_{FeO}^{10}\ p_{SO_2}}{a_{Fe_3O_4}^{3}\ a_{FeS}} = 4.9 \times 10^{-3}$$

Substituting values given above and solving for $a_{Fe_3O_4}$

$$a_{Fe_3O_4} = 0.64$$

From the data in table II for reaction 3 at 1300°C,

$$k_3 = \frac{a_{Fe_3O_4}}{a_{FeO}^{3}\ p_{O_2}^{1/2}} = 3.1 \times 10^4$$

Substituting the value of $a_{Fe_3O_4}$ just found and the originally assumed value for a_{FeO}, we find

$$p_{O_2} = 2.7 \times 10^{-8} \text{ atm}$$

Now with p_{O_2} and p_{SO_2} both known, the equilibrium constant for reaction 1 can be used to solve for p_{S_2}, to find

$$p_{S_2} = 4.5 \times 10^{-2} \text{ atm}$$

The accuracy of such estimates certainly will be improved by more accurate free-energy data and by data relating a_{FeO} to slag composition and relating a_{FeS} to matte composition. However, when the calculations are repeated with various extreme assumptions, bordering on unreasonableness, the orders of magnitude of p_{O_2} and p_{S_2} are not changed.

(*b*) *Matte with 75 mol pct Cu_2S (25 mol pct FeS):*
Repetition of the above calculations with $a_{FeS} = 0.25$ and the other assumptions unchanged gives

$$a_{Fe_3O_4} = 0.93$$

$$p_{O_2} = 5.6 \times 10^{-8} \text{ atm}$$

$$p_{S_2} = 10^{-2} \text{ atm}$$

(*c*) *Blister-forming stage:*
While blowing Cu_2S to Cu, the converter contains two liquid phases, Cu saturated with Cu_2S and Cu_2S saturated with Cu. In view of the symmetry of the Cu-Cu_2S phase diagram,[12] and lacking better thermodynamic data, the assumption that $a_{Cu} = a_{Cu_2S} = 0.8$ appears to be a reasonable approximation. Finding k_4 at 1300°C from data in table II and substituting these values,

$$p_{S_2} = 2.7 \times 10^{-6} \text{ atm}$$

Then from $p_{SO_2} = 1$ atm and k_1,

$$p_{O_2} = 3.4 \times 10^{-6} \text{ atm}$$

(*d*) *End of oxidation in fire refining:*
When the metal is saturated with Cu_2O, it may be assumed as an approximation that $a_{Cu} = a_{Cu_2O} = 0.9$. From k_7 at 1300°C,

$$p_{O_2} = 4.7 \times 10^{-5} \text{ atm}$$

In the fire-refining procedure the metal approaches equilibrium with an atmosphere in which p_{SO_2} is determined by the fuel used to heat the refining furnace, which might be, for example, 10^{-3} atm.

Table II. Energy Changes in Copper-Smelting Reactions 1100° to 1500°C

No.	Reaction*	ΔH, Cal. per Mol	ΔS°, Cal. per Mol per °K	k at 1300°C (1573°K)	Source of Data†
	A. Formation of Oxides and Sulphides				
1	$\tfrac{1}{2}S_2(g) + O_2 \rightarrow SO_2$	—86,570	— 17.30	1.8 x 10^8	Kelley[1]
2	$Fe(\gamma) + \tfrac{1}{2}O_2 \rightarrow FeO(l)$	—54,890	— 10.55	2.1 x 10^5	Darken and Gurry[6]
2′	$Fe(\gamma) + \tfrac{1}{2}O_2 \rightarrow FeO(s)$	—63,090	— 15.53	2.4 x 10^5	Darken and Gurry
3	$3FeO(l) + \tfrac{1}{2}O_2 \rightarrow Fe_3O_4(s)$	—96,200	— 40.59	3.1 x 10^4	Darken and Gurry
4	$2Cu(l) + \tfrac{1}{2}S_2 \rightarrow Cu_2S(l)$	—25,460	— 3.0	7.6 x 10^2	Kelley‡
5	$Fe(\gamma) + \tfrac{1}{2}S_2 \rightarrow FeS(l)$	—30,260	— 8.3	2.5 x 10^2	Kelley
7	$2Cu(l) + \tfrac{1}{2}O_2 \rightarrow Cu_2O(l)$	—28,920	— 8.26	1.6 x 10^2	Kelley
	B. Copper Smelting Reactions				
6	$2Cu(l) + FeS(l) \rightarrow Cu_2S(l) + Fe(\gamma)$	+ 4,800	+ 5.3	3.1	(4) — (5)
8	$Cu_2O(l) + Fe(\gamma) \rightarrow FeO(l) + 2Cu(l)$	—25,970	— 2.29	1.3 x 10^8	(2) — (7)
9	$Cu_2O(l) + FeS(l) \rightarrow Cu_2S(l) + FeO(l)$	—21,170	+ 3.01	4.0 x 10^8	(2) + (4) — (5) — (7)
10	$3Fe_3O_4(s) + FeS(l) \rightarrow 10FeO(l) + SO_2$	+177,400	+102.22	4.9 x 10^{-3}	(1) + (2) — (5) — 3(3)
11	$Fe(\gamma) + Fe_3O_4(s) \rightarrow 4FeO(l)$	+41,310	+ 30.04	6.7	(2) — (3)
12	$Fe_3O_4(s) + FeS(l) \rightarrow \tfrac{1}{2}S_2 + 4FeO(l)$	+71,570	+ 38.34	2.7 x 10^{-2}	(11) — (5)
13	$Fe_3O_4(s) + FeS(l) + 2Cu(l) \rightarrow 4FeO(l) + Cu_2S(l)$	+46,110	+ 35.34	21	(12) + (4)
14	$Cu_2S(l) + 2Cu_2O(l) \rightarrow 6Cu(l) + SO_2$	— 3,270	+ 2.22	8.7	(1) — (4) — 2(7)

* The data are based on standard states indicated by the abbreviations in parenthesis following the formula: These standard states of unit activity are as follows:
Gaseous reactants, S_2, O_2, SO_2: the gases at 1 atm partial pressure, so $a = p$

$Fe(\gamma)$: solid gamma iron
$FeO(l)$: FeO in pure iron oxide melt of composition saturated with solid gamma iron
$FeO(s)$: FeO in wüstite of composition in equilibrium with solid gamma iron
$Fe_3O_4(s)$: solid magnetite of composition Fe_3O_4
$Cu(l)$: pure liquid copper
$Cu_2S(l)$: pure liquid of composition Cu_2S
$FeS(l)$: pure liquid of composition FeS
$Cu_2O(l)$: pure liquid of composition Cu_2O

† The original data from the sources indicated have been used to calculate ΔH and ΔS° at copper smelting temperatures. In some cases, the standard states have been changed from the original data, and the energy data have been changed accordingly.

‡ Data given for Cu_2S are based on eqs 629 and 630, p. 136 of Kelley's paper.[1]

Substituting this and the value of p_{O_2} just estimated in k_1, we find

$$p_{S_2} = 1.4 \times 10^{-14} \text{ atm}$$

Example 2—Sulphur Dioxide Formation in Reverberatory Smelting: Estimation of p_{SO_2} for the reverberatory smelting step might be based on reaction 10. From data in table II,

$$\begin{aligned} k_{10} &= 10^{-4} \text{ at } 1200° \\ & 4.9 \times 10^{-3} \text{ at } 1300° \\ & 1.5 \times 10^{-1} \text{ at } 1400° \end{aligned}$$

For a 30 pct Cu matte, mol fraction FeS is about 0.75, so assume $a_{FeS} = 0.75$. The slag composition will determine both a_{FeO} and $a_{Fe_3O_4}$, and in turn itself depends on the charge makeup (e.g., a_{FeO} can be decreased by adding more SiO_2; $a_{Fe_3O_4}$ can be increased by more Fe_2O_3 in charge or in returned converter slag; $a_{Fe_3O_4}$ could be reduced by adding scrap Fe to charge). Without these data on slag chemistry, we can still calculate the extreme limits of variation in p_{SO_2} which might be obtained by stoichiometric control of the charge.

The maximum p_{SO_2} will correspond to maximum $\frac{a_{Fe_3O_4}{}^3}{a_{FeO}{}^{10}}$, which will be obtained in a slag saturated with both magnetite and silica. That is $a_{Fe_3O_4} = 1$ and $a_{FeO} = 0.28$ (from fig. 5) at 1300°C. From Darken's data (fig. 3) and values of k_3 it is found similarly that $a_{FeO} = 0.29$ at 1200°C and 0.18 at 1400°C for slag saturated with Fe_3O_4 and SiO_2. Substituting $a_{FeS} = 0.75$, $a_{Fe_3O_4} = 1$, and the values of a_{FeO} just found in the corresponding equations for k_{10}, we find

$$\begin{aligned} p_{SO_2} \max &= 17 \text{ atm at } 1200°\text{C} \\ & 2100 \text{ atm at } 1300°\text{C} \\ & 2.5 \times 10^{6} \text{ atm at } 1400°\text{C} \end{aligned}$$

These extremely high pressures are not of any practical significance beyond the fact that they point to violent evolution of SO_2 if a 30 pct Cu matte is brought into contact with a SiO_2-saturated slag of maximum oxidizing power at any smelting temperature.

The minimum p_{SO_2} in reverberatory smelting, corresponding to minimum $\frac{a_{Fe_3O_4}{}^3}{a_{FeO}{}^{10}}$, will be obtained with a slag saturated with metallic iron and silica. Taking a_{Fe} as 1, using Darken's p_{O_2} data (fig. 3), and values of k_2 and k_3 calculated from table II, we find for Fe and SiO_2-saturated slag:

$$\begin{aligned} &\text{at } 1200°\text{C}: a_{FeO} = 0.46;\ a_{Fe_3O_4} = 1.5 \times 10^{-2} \\ &\text{at } 1300°\text{C}: a_{FeO} = 0.40;\ a_{Fe_3O_4} = 3.8 \times 10^{-3} \\ &\text{at } 1400°\text{C}: a_{FeO} = 0.38;\ a_{Fe_3O_4} = 1.4 \times 10^{-3} \end{aligned}$$

Substituting these values and $a_{FeS} = 0.75$ in k_{10} at these temperatures, $p_{SO_2} = 6.5 \times 10^{-7}$ atm at 1200°C; 2×10^{-6} atm at 1300°C; 4.9×10^{-6} atm at 1400°C

All the above calculations of p_{SO_2} have been for $a_{FeS} = 0.75$. From k_{10} it is apparent that p_{SO_2} is proportional to a_{FeS}, so that p_{SO_2} decreases with increase in grade of matte.

Summarizing, these estimates show that while matte of a given grade is being produced, the equilibrium sulphur dioxide pressure can be varied enormously from subatmospheric to superatmospheric pressure by simply changing the slag composition. A high content of SO_2 in the flue gas, corresponding to rapid evolution of SO_2 from the slag-matte reactions, would be expected with oxidizing slags for which the calculated values of p_{SO_2} are greater than 1 atm. Also, these estimates indicate that for a given matte-slag combination, p_{SO_2} increases sharply with rise in temperature.

Example 3—Magnetite Formation and Dissolution in Slag: Control of magnetite behavior can be an important operating problem. Formation of Fe_3O_4 is deliberately sought in lining the converter, and the converting operation itself gives slags high in Fe_3O_4. On the other hand, dissolution and digestion of magnetite are desired in the reverberatory smelting to avoid bottom buildup and accretion leading to eventual shutdown.

As has been brought out in the preceding discussion, magnetite formation is associated with systems of high oxygen pressure. Fig. 5 shows that at 1300°C Fe_3O_4 will be in equilibrium with iron silicate slags at p_{O_2} values from 2×10^{-8} atm to 2×10^{-6} atm, depending on a_{FeO} in the slag. (See also equilibrium data for reaction 3, table II.) From fig. 1 (also example 1), it is seen that equilibrium p_{O_2} during converting is in and near this range. Moreover, the converter is not at equilibrium, in that the actual oxygen pressure is locally much greater. Thus, the well-known tendency toward magnetite formation in converting is consistent with the thermodynamic data.

The possibility of formation of magnetite by reversal of reaction 10 during converting might be considered. At 1300°C $k_{10} = 4.9 \times 10^{-3}$. Assuming $p_{SO_2} = 0.2$ atm, $a_{Fe_3O_4} = 1$, and taking a_{FeS} near the white-metal stage as 0.01, we find by solving k_{10} that $a_{FeO} = 0.44$. That is, if a_{FeO} is greater than 0.44, reaction 10 will proceed to the left, and FeS will be formed instead of being oxidized; in a sense, this is a reversal of the converting process. In practice a_{FeO} is controlled by addition of SiO_2 which forms a solution with FeO and reduces its activity, thus avoiding any reversal of the converting process. Evidently, then, the siliceous flux added to the converter not only serves to form a fluid, low melting, and manageable slag but also is essential to the completion of the FeS oxidation.

Calculations in example 2 have shown the extremes of variation of $a_{Fe_3O_4}$ possible at equilibrium in iron silicate slags to be from 1.0 in Fe_3O_4-saturated slags down to 10^{-2} to 10^{-3} for Fe-saturated slags. Of course, the slags with $a_{Fe_3O_4} = 1$ are incapable of dissolving more Fe_3O_4, while those with lowest $a_{Fe_3O_4}$ are able to dissolve considerable Fe_3O_4.

Dissolution of magnetite may occur by the following reaction:[16]

$$3\,Fe_3O_4 + FeS \rightleftarrows 10\,FeO + SO_2 \qquad [10]$$

The conditions under which this reaction goes may be considered for two different sites in the reverberatory furnace.

First, at the slag-matte interface, Fe_3O_4 dissolved in slag may react with FeS dissolved in matte to give FeO dissolved in slag. The reaction will proceed only if it develops an SO_2 pressure greater than 1 atm. If the slag is saturated with magnetite and a_{FeO} is, say, 0.4, calculations based on values of k_{10} (from example 2) show that a_{FeS} must be substantially unity for the reaction to proceed at 1200°C, but only 0.02 for the reaction to proceed at 1300°C. Reaction at the slag-matte surface alone would lead to reduction of the dissolved Fe_3O_4 of the slag, so that the slag could dissolve solid magnetite elsewhere in the furnace.

Another possible site of reaction 10 to be considered is the matte, solid magnetite interface (e.g., magnetite on furnace bottom or magnetite suspended in matte). For this site $a_{Fe_3O_4} = 1$ and any FeO formed also must be a separate new phase or in solution in matte since there is no slag, or SiO_2 to form slag, at the site specified. At temperatures from 1200° to 1424°C reduction of magnetite gives solid wüstite which probably is a no more desirable solid product or accretion than magnetite. Wüstite has a variable composition, the melting point decreasing as oxygen content is decreased, but the lowest melting point is 1371°C. Thus, a simple reaction between matte and magnetite to produce solid wüstite and SO_2 does not appear a feasible means for preventing buildup of solid iron oxides on the bottom of the furnace if the bottom temperature is below about 1400°C.

A more reasonable hypothesis for the matte, solid magnetite reaction is that Fe_3O_4 (solid) reacts with FeS in the matte to form FeO dissolved in the matte and SO_2. This hypothesis involves the idea that FeO is soluble in the matte while Fe_3O_4 is not dissolved until it is reduced. Better experimental data on oxides in mattes are needed before any satisfactory appraisal can be made of this possibility.

From the above, it is clear that magnetite behavior represents a complex problem which will require careful analysis not only of the equilibria involved, but also of the kinetics and reaction mechanisms within the converter and reverberatory furnace. The thermodynamic data show that the reaction of magnetite with iron sulphide in the matte is very sensitive to temperature and to FeO activity. A small increase in temperature or a small decrease in FeO activity such as might be obtained by adding SiO_2 to the slag strongly favors the reaction.

Example 4—Iron Content of Blister Copper: An estimate can be made of a_{Fe} during the blister-making step. During this step there should be ample opportunity for formation of Fe_3O_4 from the residual iron, so that as a basis of first approximation equilibrium might be approached in the reaction:

$$3\ Fe + 2\ O_2 \rightleftarrows Fe_3O_4$$

The equilibrium constant for this reaction can be found by algebraically combining data for reactions 2 and 3 (table II). The equilibrium p_{O_2} for the blister-making step was found to be 3.4×10^{-8} atm in example 1c, and $a_{Fe_3O_4}$ is estimated as 1 (max). Thus we can calculate a maximum value for a_{Fe}. At 1300°C a_{Fe} (max) $= 7 \times 10^{-4}$. Reference to the Fe-Cu constitution diagram indicates that Fe dissolved in Cu will have an activity coefficient definitely greater than 1; that is, the activity will be greater than the mol fraction. Hence, we may conclude that blister copper will contain well under 0.07 pct Fe if blown at 1300°C.

Substituting the value of a_{Fe} just calculated and the value of p_{S_2} calculated in example 1c in k_5, we find that $a_{FeS} = 2.7 \times 10^{-4}$ at 1300°C in the blister-making stage. Thus the dissolved iron content of the white-metal phase (being converted to blister) might be on the order of 0.01 pct.

Experimental Program: The foregoing survey has disclosed many gaps in our knowledge of the physical chemistry of copper smelting which can be filled only by experimental work on simple systems under closely controlled conditions. Below is outlined a program of laboratory research that has been planned and started on the basis of the analysis given in the previous sections.

I. Chemistry of the Separate Phases

A. Iron Silicate Slags

Problem 1. Oxidation equilibria for $FeO\text{-}Fe_3O_4\text{-}SiO_2$ melts.

A study of the reaction $CO_2(g) \rightleftarrows O\ (slag) + CO(g)$ over the entire field of melt compositions. The CO_2/CO ratio serves as a convenient yardstick of oxygen pressure.

Problem 2. Determination of liquidus surfaces for $Fe\text{-}O\text{-}SiO_2$ system.

The temperature-composition range for iron silicate slags may be located by extension and modification of Bowen and Schairer's methods, involving bringing the system to equilibrium, quenching, and examination of the quenched solid.

B. Mattes

Problem 3. Sulphur pressure of copper sulphide melts.

A study of the reaction $H_2(g) + Cu_2S(l) \rightleftarrows 2\ Cu\ (dissolved) + H_2S$ from high sulphur melts down to melts saturated with copper. The H_2S/H_2 ratio in the gas is a convenient yardstick of sulphur pressure.

Problem 4. Sulphur pressure of Fe-S and Cu-Fe-S melts.

Study of equilibria for the reactions

$FeS(matte) \rightleftarrows Fe(matte) + \frac{1}{2}\ S_2$

$Cu_2S(matte) \rightleftarrows 2\ Cu(matte) + \frac{1}{2}\ S_2$

C. Liquid Copper (Much of the information needed on solutions of oxygen and sulphur in liquid copper is available, from studies of $H_2O\text{-}H_2$, $CO_2\text{-}CO$, and SO_2 reactions with Cu)

Problem 5. Equilibria for the reaction $H_2S(g) + 2\ Cu(l) \rightleftarrows H_2(g) + Cu_2S$ (dissolved)

II. Solubilities of Cu_2O and Cu_2S in Iron Silicate Slags—Equilibrium studies in slag-metal systems make possible the differentiation between dissolution of Cu_2O and dissolution of Cu_2S, a differentiation difficult to make in a matte-slag system

Problem 6. Cu_2O in iron silicate slags (sulphur-free system).

Reactions: $2\ Cu(l) + O(slag) \rightleftarrows Cu_2O(slag)$

$Cu_2O(slag) \rightleftarrows Cu_2O(metal)$

Problem 7. Cu_2O and Cu_2S in iron silicate slags.

Reactions (in addition to those under 1):

$Cu_2S(slag) \rightleftarrows Cu_2S(metal)$

$Cu_2S(metal) + FeO(slag) \rightleftarrows Cu_2O(slag) + FeS(slag)$

III. Slag-Matte Equilibria

Problem 8. When data from I and II on individual reactions in simple systems are available, it will be possible to deal effectively with the complex relationships of the slag-matte system itself. The experiments will involve matte-slag systems with four independent variables:

temperature, pct SiO_2 in slag, $\frac{N_O}{N_{Fe}}$ in slag,

pct Cu in matte

IV. Solubilities of Oxygen and Oxides in Mattes; the Matte-Magnetite Reactions

Problem 9.

Reactions: $3\ Fe_3O_4(s) + FeS(\text{matte}) \rightleftarrows 10\ FeO(\text{matte}) + SO_2(g)$

$Fe_3O_4(s) + FeS(\text{matte}) \rightleftarrows 4\ FeO(\text{matte}) + \frac{1}{2}\ S_2(g)$

These reactions might be studied by measuring gas pressures of oxygen-containing mattes in magnetite crucibles, accompanied by complete analyses of the mattes.

Work on problems 1, 2, and 5 has been started under a grant by the Research Corp. for the period 1947 to 1949. Work on problem 3 has been started under a fellowship awarded by the International Nickel Co. for the same period.

Summary

In order to plan a program of investigating the fundamentals of copper smelting, a survey of the present status of our knowledge of the thermodynamics of copper smelting has been undertaken. Available thermodynamic data applicable to copper smelting systems are collected and tabulated, and the important gaps are pointed out. A few examples are given of estimations which can be made from the available data.

The simplest matte-slag system has five components: Cu, Fe, O, S and SiO_2. From a narrow equilibrium point of view the operator has four independent controls, no more and no less, which might be temperature and the three stoichiometric variables determined by the charge: grade of matte, silica content of slag, and oxygen/iron ratio $\frac{N_O}{N_{Fe}}$ in slag. Calculations based on recent data by Darken and Gurry show that the equilibrium oxygen pressure for the matte-slag system can be varied over a tremendous range by varying the silica content and more particularly the $\frac{N_O}{N_{Fe}}$ ratio of the slag. It is to be expected that quantitative control of the oxygen pressure (in other words, of the oxidizing or reducing conditions) will have bearing on the practical problems of slag losses and magnetite behavior.

An experimental research program is proposed to supply the thermodynamic data which appear most essential to better quantitative understanding of the chemistry of copper smelting. The proposed program is designed also to shed specific light on the practical problems of slag losses and magnetite behavior.

References

[1] K. K. Kelley: Contributions to the Data on Theoretical Metallurgy. VII. The Thermodynamic Properties of Sulphur and Its Inorganic Compounds. U. S. Bur. Mines. *Bull.* 406 (1937).

[2] P. Y. Huang and C. R. Hayward: Evidence of Formation of Copper Ferrite from Reaction between Cuprous Oxide and Copper Reverberatory Slags. *Trans.* AIME (1949) **182**, 158-176: *Met. Tech.* (April 1947) TP 2140.

[3] A. M. Aksoy: An Investigation of Copper Losses in Copper Reverberatory Slags. M.I.T. Sc.D. Thesis (1943).

[4] E. A. Peretti: An Analysis of the Converting of Copper Matte. Discussions Faraday Soc. (1948) No. 4, 179-184.

[5] L. S. Darken and R. W. Gurry: The System Iron-Oxygen. I. The Wustite Field and Related Equilibria. *Jnl.* Amer. Chem. Soc. (1945) **67**, 1398-1412.

[6] L. S. Darken and R. W. Gurry: The System Iron Oxygen. II. Equilibrium and Thermodynamics of Liquid Oxide and Other Phases. *Jnl.* Amer. Chem. Soc. (1946) **68**, 798-816.

[7] L. S. Darken: Melting Points of Iron Oxides on Silica; Phase Equilibria in the System Fe-Si-O as a Function of Gas Composition and Temperature. *Jnl.* Amer. Chem. Soc. (1948) **70**, 2046-2053.

[8] E. M. Cox, M. C. Bachelder, N. H. Nachtrieb, and A. S. Skapski: The Influence of Temperature on the Affinity of Sulphur for Copper, Manganese, and Iron. *Trans.* AIME, **184**, 27-31; *Jnl. of Met.*, Jan. 1949.

[9] E. Maurer, G. Hammer, and H. Möbius: The Equilibrium between Iron and Hydrogen Sulphide. *Arch. Eisenhutt.* (1942) **16**, 159-165.

[10] A. J. Phillips: The Separation of Gases from Molten Metals. *Trans.* AIME (1947) **171**, 17-46; *Met. Tech.* (June 1947) TP 2208.

[11] N. L. Bowen and J. F. Schairer: The System, FeO-SiO_2. *Amer. Jnl. Sci.* (1932) **24**, 177-213.

[12] Metals Handbook. A.S.M. (1948).

[13] C. B. Carpenter and C. R. Hayward: The Equilibrium Diagram of the System Cu_2S-FeS. *Eng. and Min. Jnl.* Press (1923) **115**, 1055.

[14] O. Reuleaux: Reaktionen und Gleichgewichte in System Cu-Fe-S mit besonderer Berücksichtigung des Kupfersteins. *Met. und Erz.* (1927) **24**, 99-111.

[15] H. E. Merwin and R. H. Lombard: The System Cu-Fe-S. *Econ. Geol.* (1937) **32**, 203-284.

[16] F. S. Wartman and G. L. Oldright: The Reaction Between Magnetite and Ferrous Sulphide. U. S. Bur. Mines. *R.I.* 2901 (1928).

Thermal Segregation: A Mechanism for the Segregation of Hydrogen in Steel

by G. Derge and E. E. Duncan

REVIEW of the literature on hydrogen in steels indicates that inadequate consideration has been given to the influence of temperature gradients on segregation of this element. Even when segregation has been taken into account, the interpretation of the data has been seriously handicapped by incomplete understanding of the mechanism by which it occurred. Recognition of a mechanism which will be described as "thermal segregation" appears to rationalize many of the observed effects so well that it will be reported here with some preliminary experimental evidence. The complete quantitative evaluation of the factors controlling the mechanism will require extensive experimentation.

The operation of the mechanism can be described in relation to fig. 1, which shows the temperature dependence of the solubility of hydrogen in iron at

---

G. DERGE, Member AIME, and E. E. DUNCAN, are associated with the Metals Research Laboratory, Carnegie Institute of Technology, Pittsburgh, Pa.

Technical Note 38 E. Manuscript received Feb. 15, 1950.

gated billet containing a typical amount of hydrogen such as X_1 in fig. 1 from some austenitic temperature to room temperature. The surface will soon reach some low temperature in the α range, T_α, where its hydrogen content is in excess of the solubility limit for the low partial pressure of hydrogen effective at that point. At the same time the center of the billet is at some higher temperature in the γ range, T_γ, where the effective pressure must be very great and the solubility limit is far in excess of the actual hydrogen content. At the same time there will be some intermediate position in the billet at the temperature T_1, which is just at the solubility limit for the effective pressure at this point. The hydrogen in this critical region may now diffuse to the surface and escape or it may diffuse toward the center. The relative influence of these competing opportunities for diffusion will depend upon several factors. Since diffusion rates increase exponentially with temperature, and since the greatest change in solubility is at the γ-α transformation, it is reasonable to expect that under such a temperature gradient the tendency for hydrogen to diffuse to that part of the billet remaining in the γ range will be important. Experimental evidence will be cited which indicates that this "thermal segregation" actually occurs in billets.

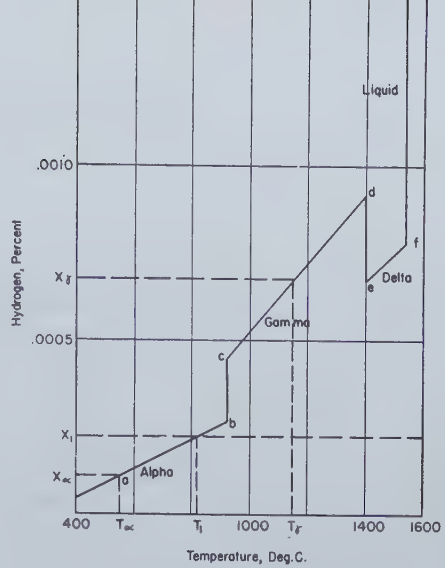

Fig. 1—Solubility of hydrogen in iron at 1 atm pressure.
(Basic Open Hearth Steelmaking. AIME (1944) 469.)

Table I. Hydrogen Segregation in Experimental Ingots

Heat No.	Sample Position	Pct H	Δ H Pct (Center-edge)	Ingot History
Part *A*—Open-hearth Heats				
A_1	Edge Center	0.000225 0.001870	0.00164	4x4 in. Air cooled after pouring.
A_2	Edge Center	0.000110 0.000970	0.00086	4x4 in. Air cooled from soaking pit.
B_1	Edge Center	0.000220 0.001760	0.00154	4x4 in. Air cooled after pouring.
B_2	Edge Center	0.000260 0.000340	0.00008	4x4 in. Water quenched from soaking pit.
Part *B*—Induction Furnace Heats				
C_1	Edge Center	0.000213 0.000300	0.000087	3½x3½ in. Quenched after pouring.
C_2	Edge Center	0.000087 0.000404	0.000317	3½x3½ in. Air cooled after pouring.
D_1	Edge Center	0.000238 0.000328	0.000090	5½x5½ in. Quenched after pouring.
D_2	Edge Center	0.000143 0.000595	0.000452	3½x3½ in. Cooled in sand after pouring.

Consider the four experimental 4x4 in. ingots included in table I *A*. These were teemed directly from the ladle in a basic open-hearth shop. The two ingots A_1 and B_1 which were air cooled from the pouring temperature would have been afforded the greatest opportunity for thermal segregation, and they both show a gradient of about 0.0016 pct H_2 between edge and center. The ingot A_2 which was air cooled from the soaking pit treatment was afforded less opportunity for segregation because the lower initial temperature would have maintained the center in the austenitic condition for a shorter time. The observed segregation was actually about half as great as for those cooled from the pouring temperature. The sample B_2 which was quenched from the soaking pit showed practically no segregation, indicating that the soaking treatment was effective but that the segregation observed in the air-cooled sample occurred after removal from the pit.

Similar experiments were made in the laboratory with induction furnace heats as shown in table I *B*. In both instances the slowly cooled ingots showed greater segregation than those that were quenched. The contrast was greatest in heat *D* where the quenched ingot was larger. In fact, the degree of homogeneity of all quenched ingots was so great that one wonders if any appreciable segregation occurred during solidification. It appears difficult to explain these results by any other mechanism than "thermal segregation."

The absence of segregation in highly alloyed austenitic steels made in the electric furnace has been reported by S. F. Carter.[1] His data were obtained from 4 in. square blocks cast in dry sand. These were compared with similar samples of carbon steels which showed up to eight times as much hydrogen in the center as at the edge. The absence of the γ-α transformation and the large solubility change associated with it would result in little "thermal segregation" during the cooling of the austenitic steels and would explain the difference in behavior of the two types.

If these initial experiments are typical, "thermal segregation" has much more influence on the control of hydrogen in steel than most other processing factors, such as furnace practice. The quantitative evaluation of the factors controlling "thermal segregation" appears to be an essential research problem.

Acknowledgment

This paper has resulted from a research program in the Metals Research Laboratory of the Carnegie Institute of Technology which was sponsored by the Carnegie-Illinois Steel Corporation.

---

[1] S. F. Carter: Effect of Melting Practice on Hydrogen. 7th Annual Elec. Furnace Conf., Iron and Steel Div., AIME. (December 1949.)

Twin Relationships in Ingots of Germanium

by W. C. Ellis

IN an ingot of germanium solidified progressively from the bottom by a method[1] devised by J. H. Scaff and H. C. Theuerer, examination discloses extensive twin relationships. A slice taken about midway in a cylindrical ingot approximately ¾ in. in diameter and 1½ in. in length, after etching and polishing to delineate different orientations, is shown in fig. 1*a*. The orientations of the regions designated with letters were determined by Laue X-ray back-reflection methods and plotted on stereograms. The orientation relationships of the designated components were determined by comparing the values for the nine angles between the three respective cube poles of each orientation with the values calculated in a formal treatment of octahedral multiple twinning in cubic crystals. Germanium, diamond cubic in structure, has the octahedral twinning habit.

I am indebted to K. H. Storks for the calculation of the angular relationships of cube poles in octahedral twinning to four orders. The set of values for the nine angles is distinctive of the order of twinning. Confirmation for a multiple twin relationship is obtained from the determined indices of the mirror planes. These exist for all orders of twinning through the third and for some of the fourth.* If the orientations are not those for twinning, then the nine angles for the cube poles do not correspond in value and distribution to those formally calculated. Since all nine angles must correspond in values and distribution of values to the calculated ones, the Laue method with a precision of one or two degrees is adequate to establish or deny with confidence the existence of multiple twins. Regions of the same orientation can also frequently be identified by the optical reflections. For example, the narrow twin bands in *A* at 2:00 o'clock have orientation B_1.

The interesting twin relationships shown schematically in fig. 1*b* were found for the section in fig. 1*a*. Most of this slice was made up of orientation, *A*, appearing in widely separated regions. Of the four possible first order twins of *A*, three were present in this slice and are designated by *B* with subscripts. Four second order twins of *A* are designated by *C* with subscripts. It is worth emphasizing that two of these, C_4 and C_5, are second orders of *A* through the first order missing in this section. Two regions, designated by *D* with subscripts are third order twins of *A*. D_2 is a sixth order twin of D_4. All orientations found were ascribable to multiple twinning, as if the orientations in this section originated earlier in solidification from a single nucleus.

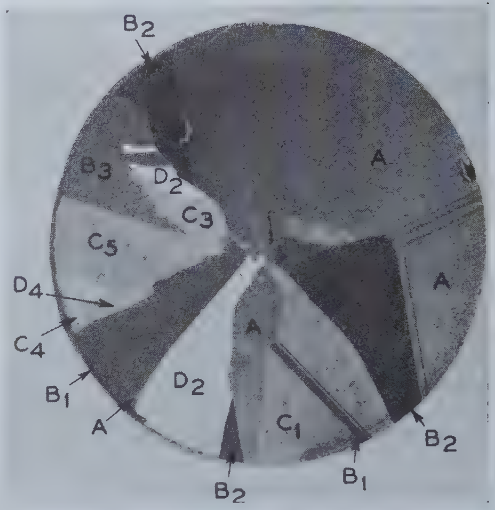

Fig. 1a—Etched transverse section of germanium ingot showing regions of different orientations.
X3.5. Reduced approximately one third in reproduction.

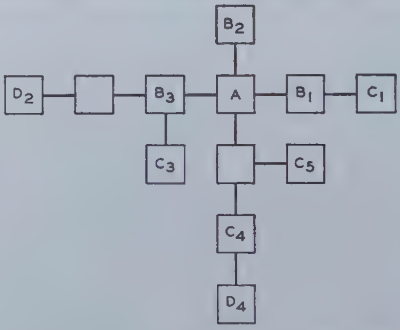

Fig. 1b—Schematic representation of twin relationships in section shown in fig. 1a.

The presence of extensive multiple twinning together with the absence of other orientations appears to be a characteristic result in many instances of solidification of germanium. Fertile conditions for twinning probably exist in the array of atoms in the diamond cubic structure. The high order twins in the section shown, it is reasonable to presume, are the result of progressive octahedral twinning through several generations in the material freezing earlier. Some of these generations do not appear in this section, it is suggested, because their orientations with respect to the growth direction were unfavorable for survival. The extensive twinning is probably promoted during solidification by constraint imposed by volume increase, and to an irregular growth front. Twinning may also be due, in part, to the attempt of the solidifying region to attain the orientation most favorable to the growth direction (maximum thermal gradient). The nucleus for a twinned orientation could have its origin in a "stacking fault" on the close-packed octahedral plane.

Further work is being done in which the course of twinning throughout an ingot is being studied. The results appear to be important in the general theory of solidification.

---

[1] H. C. Torrey and C. A. Whitmer, Crystal Rectifiers. p. 364, 1948. New York. McGraw-Hill Pub. Co.

W. C. ELLIS, Member AIME, is Member of Technical Staff, Bell Telephone Laboratories, Inc., New York, New York.

Technical Note No. 37 E. Manuscript received March 1, 1950.

Activation Energy for

Recrystallization in Rolled Copper

by B. F. Decker and D. Harker

The recrystallization reaction in OFHC and spectroscopically pure copper has been followed by X ray diffraction determinations of the amount of material with the cold-worked and recrystallized textures in specimens which had been given various heat treatments. The heats of activation for recrystallization are found to be: 29.9 kcal per mol for OFHC copper and 22.4 kcal per mol for spectroscopic copper.

Introduction

A reliable and speedy method for measuring the amount of recrystallized material in a piece of rolled metal, together with a new scheme for low temperature heat treatment, have made possible a determination of the activation energy for recrystallization in rolled copper. This method for studying recrystallization rates is different from others reported in the literature.[1]

Oxygen free, high conductivity copper—OFHC copper—of purity 99.98 pct gave an activation energy for recrystallization of 29.9 kcal per mol with recrystallization data taken in the temperature range 208-245°C. Copper of purity 99.999 pct from the American Smelting & Refining Co. gave an activation energy for recrystallization of 22.4 kcal per mol with recrystallization data taken in the temperature range 43-135°C.

The great change in activation energy for recrystallization as the small amount of impurity in the metal is decreased suggests that the motion of grain boundaries is conditioned by the impurities which must be concentrated in them. Thus the OFHC copper recrystallizes with an activation energy of the order of magnitude to be expected for the diffusion of the kind of impurities likely to be present. The high purity copper, on the other hand, recrystallizes with a much lower activation energy, in accord with the notion that the grain boundaries need not wait for the impurities to diffuse with them.

Copper when strongly cold-rolled has a well-defined crystallite texture which can be described by saying that the [111] direction of the face-centered cubic crystals is aligned approximately in the cross-rolling direction and that faces of the form {110} lie approximately in the rolling plane. When such rolled copper is completely annealed the crystallite texture is quite different: the [100] direction is in the cross-rolling direction and faces of the form {100} are in the rolling plane. At intermediate stages of annealing, the copper contains both textures.

If a Geiger counter X ray diffraction spectrometer is set up so as to measure the intensity of the (200) Bragg reflection from the rolled surface of a piece of copper strip, this intensity increases from a very small value in the cold-worked state to a maximum as the specimen is annealed. The same would be true for (200) reflections from planes normal to the rolling or cross-rolling directions. In view of this fact, the amount of material in the copper which has recrystallized can be measured by comparing the intensities of one of these reflections just mentioned with the intensity from a similar specimen after complete annealing. In much the same way the intensity of (111) reflections from planes normal to the cross-rolling direction could be used to measure the amount of unrecrystallized material in the specimen. In the work to be described here the amounts of recrystallized and unrecrystallized material in partly annealed rolled copper specimens were determined in this way.

Experimental Procedure

Samples of oxygen free high conductivity (OFHC) copper, cold-rolled 99.7 pct to 0.002 in. thickness, were subjected to heat treatments for various chosen times at four different temperatures, and high purity copper samples, cold-rolled 98.0 pct to 0.0015 in. thickness, at six different temperatures. Each sample, after treatment, was placed in an orientation sample holder for use with a Geiger counter X ray spectrometer and a reading was taken of the intensity of the (200) reflection from planes perpendicular to

---

B. F. DECKER and D. HARKER, Member AIME, are with the Crystallography Division, Knolls Research Laboratory, General Electric Co., Schenectady, N. Y.

AIME Chicago Meeting, October 1950.

TP 2858 E. Discussion (2 copies) may be sent to Transactions *AIME before Dec. 15, 1950. Manuscript received Nov. 23, 1949.*

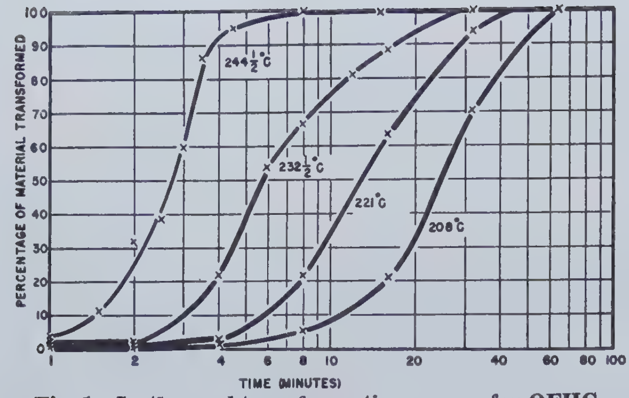

Fig. 1—Isothermal transformation curves for OFHC copper.

the rolling direction for the OFHC copper and of the (111) reflection from planes perpendicular to the cross-rolling direction for the high purity copper. A narrow slit was used at the X ray source and a wide slit at the counter in order to obtain an integrated intensity whatever the line width. Figs. 1 and 2 show the intensities of reflection, expressed as percentages of material transformed, plotted against the logarithm of the time at each temperature. (For the (200) reflection in the rolling direction, maximum intensity corresponds to 100 pct transformation, while, for the (111) reflection in the cross-rolling direction, minimum intensity corresponds to 100 pct transformation). The shape of such a curve is approximately independent of temperature; small variations will be discussed later.

The specimens were heat treated by suspending them in organic liquids boiling under atmospheric pressure. This method provides extremely constant temperatures and allows the specimens to be brought to temperature and quenched rapidly, so that the time at temperature can be well-known. The apparatus is very simple. It consists of a flask for boiling the liquid, surmounted by a water-cooled reflux condenser. Openings fitted with ground glass stoppers are provided. Wires sealed into the stoppers support the specimens in the boiling liquid. A thermometer well allows the exact temperature of the liquid to be read directly.

Table I lists the organic liquids used in this work, the temperatures at which they boiled and the grade of copper treated at these temperatures. (The temperatures are not the boiling points to be found in the literature. They were determined directly in the apparatus just described using a calibrated thermometer).

One set of specimens of high purity copper was given a prolonged heat treatment at 43°C. This treatment was carried out in a constant temperature room in the laboratory of J. F. Eckel of the General Electric Research Laboratory.

Using the isothermal curves, figs. 1 and 2, data were taken to form plots of $\frac{1}{T}$ (T is the absolute temperature in °K) against the logarithm of the time for 50 pct recrystallization. These data fall quite closely on straight lines, as shown in fig. 3. This suggests that the rate of recrystallization is conditioned by a single activation energy which may be obtained from the slope of the straight line plots of fig. 3. If the rate of recrystallization is given by

$$\text{Rate} = A\, e^{\frac{-Q}{RT}}$$

(where Q is an activation energy, R the gas constant, T the absolute temperature and A a constant), then one may write

$$\frac{1}{\tau} = A'\, e^{\frac{-Q}{RT}}$$

where τ is the time for a given amount of recrystallization to take place at T. Then

$$\frac{d\left(\frac{1}{T}\right)}{d(\log \tau)} = \frac{R}{Q}$$

which is an expression for the slopes of the lines in fig. 3. From these slopes it was found that the activation energy for recrystallization is 29.9 kcal per mol for the OFHC copper and 22.4 kcal per mol for the high purity copper.

Table I. Organic Liquids: Boiling Temperatures; Grades of Copper Treated

Liquid	Temperature °C	Grade of Cu
Diethylene Glycol	244.5	OFHC
Diethylene Glycol Monobutyl Ether	232.5	OFHC
Naphthalene	221.0	OFHC
Tetralin	208.0	OFHC
Chlorobenzene	135.2	99.999% pure
Isobutyl Ketone	119.0	99.999% pure
Toluene	112.6	99.999% pure
Water	102.2	99.999% pure
Trichloroethylene	88.2	99.999% pure

Discussion of Results

It was stated above that the rate of recrystallization may be described by a single activation energy. It does not follow that the process of recrystallization is a single process or type of process. In fact

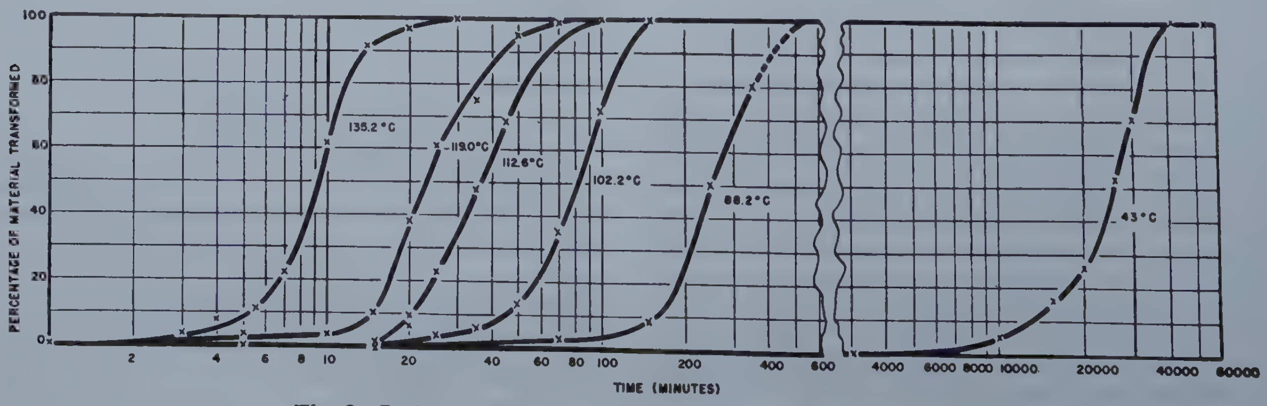

Fig. 2—Isothermal transformation curves for pure copper.

the authors have reason to believe, from application of some of the work of Avrami,[2] that the recrystallized material grows in at least two ways, depending on temperature; and that a transition range of temperature exists in which some combination of the two or perhaps a different mechanism operates. This can be seen from the isothermal curves in figs. 4 and 5, where

$$\log \log \left(\frac{1}{1-v}\right)$$

is plotted against log t. Here v is the fraction of transformed matter at time t. This sort of plot, in effect, magnifies the slight deviations in shape of the curves of figs. 1 and 2. When such a plot is a straight line one may write

$$\log \log \frac{1}{1-v} = \log B + k \log t$$

where log B is the intercept on the axis of abscissas and k is the slope of the line, or

$$v = 1 - e^{-Bt^k}$$

which is the expression derived by Avrami[3] for grain growth. The value of k indicates the type of growth occurring. If k lies between 2 and 3, the growing grains are plate-like; if k lies between 3 and 4, they are polyhedral. The reader will note that straight lines occur in figs. 4 and 5, but in both figures, there is a region between the $k < 3$ and $k > 3$ ranges, where the lines are not straight, and the process cannot be described by Avrami's expression. Since some straight lines are obtained, Avrami's assumptions—among them that both nucleation and growth processes have activation energies equal to Q—are compatible with these data. It is quite plausible that at lower temperatures the growth of recrystallized material may be plate-like, since the specimens used were very thin and the concentration of nuclei initiating growth could conceivably be so small that the growing grains would become large compared to the thickness of the sample in the early stages of the reaction. At high temperatures, on the other hand, the concentration of nuclei could be large enough to make the size of a grain small compared to the thickness of the specimen, and the polyhedral growth law would apply. The transition region possibly would be some mixture of these two types of growth. The discussion just given should not be taken as a definite explanation, but only as a plausible one.

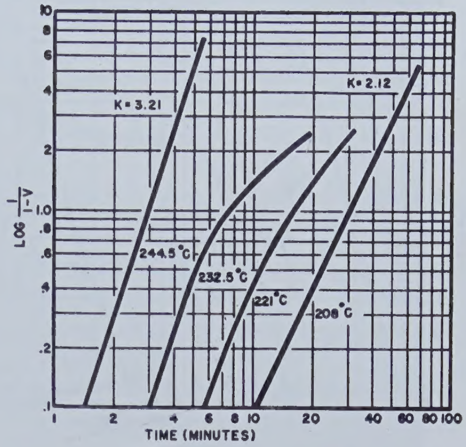

Fig. 4—Isothermal transformation curves for OFHC copper (Avrami plot; V = fraction recrystallized).

It is to be expected that impurities concentrate in the boundaries between the grains, whether worked or not. Since the recrystallized and cold-worked crystals have such different orientations, the boundaries between them must be particularly well-defined, and, therefore, should contain a distinctly higher impurity concentration than the interiors of the crystals themselves. If we assume that a grain boundary, as it moves, cannot escape from the impurities originally contained in it, then the rate of grain boundary motion should have about the activation energy of the rate of impurity diffusion.[4] The recrystallization process consisting, as it does, of the growth of relatively perfect crystals at the expense of cold-worked material, takes place by

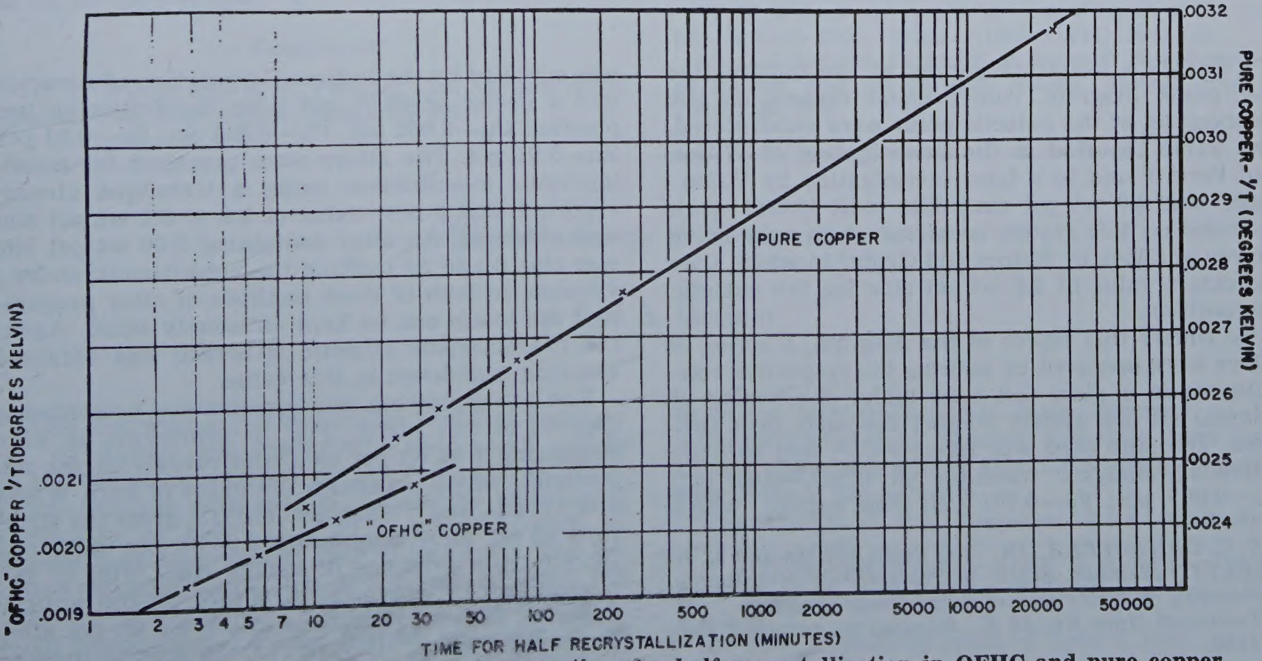

Fig. 3—Reciprocal of absolute temperature vs. time for half recrystallization in OFHC and pure copper.

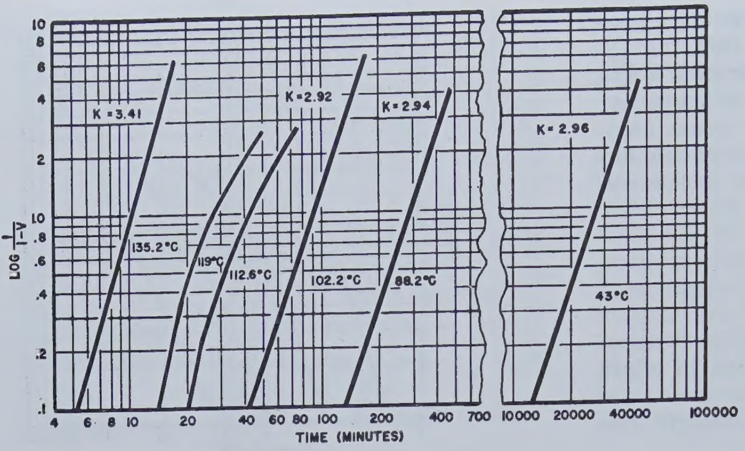

Fig. 5—Isothermal transformation curves for pure copper (Avrami plot; V = fraction recrystallized).

grain boundary motion and should, therefore, be conditioned by impurity diffusion in the manner just outlined. On the other hand, perfectly pure metal should allow grain boundary motion at a rate depending on the smaller activation energy necessary for the slight atomic displacements which take place when material in one crystal becomes material in a grain boundary or in another crystal. From this point of view it is not surprising that the very pure copper recrystallizes with a much lower activation energy than does the OFHC copper.

References

[1] J. K. Stanley and R. F. Mehl: Recrystallization of Silicon Ferrite in Terms of Rate of Nucleation and Rate of Growth. *Trans.* AIME (1942) **150**, 260. Also W. A. Anderson and R. F. Mehl: Recrystallization of Aluminum in Terms of the Rate of Nucleation and the Rate of Growth. *Trans.* AIME (1945) **161**, 140.

[2] Melvin Avrami: Kinetics of Phase Change. II. Transformation-time Relations for Random Distribution of Nuclei. *Jnl. Chem. Phys.* (1940) **8**, 212.

[3] Ibid. p. 220.

[4] R. M. Barrer: Some Aspects of Diffusion in Solids. *Proc.* Phys. Soc. (London) **52**, 58-70.

Metallographic Re-evaluation of the

Indium-Zinc Eutectic Composition

by

S. C. Carapella, Jr.

and

E. A. Peretti

DURING a literature survey of the indium-zinc phase diagram, controversial reports on the composition of the eutectic point were encountered. The value reported in the investigation of Wilson and Peretti[1] and in a later investigation by Valentiner[2] was 4.0 wt pct zinc. The most recent work recorded on this system consisted of an exhaustive survey of alloys by Rhines and Grobe[3] in which they indicate a value of 2.8 wt pct zinc for the eutectic composition.

To clarify this aspect of the diagram, a series of alloys were prepared by melting the respective constituents in a glass test tube under a covering of mineral oil and slowly cooling the melt in a furnace. The zinc used was Baker's C.P. and had the following analysis: insoluble in H_2SO_4—0.01 pct; Pb—0.001 pct; Fe—0.001 pct. The indium, which was supplied by the Indium Corporation of America, had a purity of 99.97 pct with the following impurities: Cu—0.002 pct; Pb—0.006 pct; Sn—0.01 pct; Zn—0.01 pct. The alloys were prepared for metallographic examination using a technique already reported[4] and a new value of 2.0 ± 0.1 wt pct zinc was observed. An alloy containing 2.00 wt pct zinc was also made by melting the constituents under a vacuum. In both of these methods of alloy preparation the losses can be kept extremely small. Again, the characteristic eutectic structure was obtained, assuring confidence in this value.

The accompanying micrographs are presented in support of this point. Fig. 1*a* represents an alloy containing 4.00 wt pct zinc, and reveals excess zinc particles, which precludes the value of both Wilson and Peretti, and Valentiner. Fig. 1*b*, gives the structure of an alloy containing 2.2 wt pct zinc, also showing the presence of excess zinc. Fig. 1c is a micrograph of a typical structure of the eutectic observed in several sections of the 2.0 wt pct alloy. In the 1.8 pct zinc alloy, fig. 1*d*, the definite presence of the primary indium can be noted. From these re-

---

S. C. CARAPELLA, JR., is O'Brien Fellow and E. A. PERETTI, Member AIME, is Professor of Metallurgy, University of Notre Dame, Notre Dame, Indiana.

Technical Note No. 36 E. Manuscript received Feb. 8, 1950.

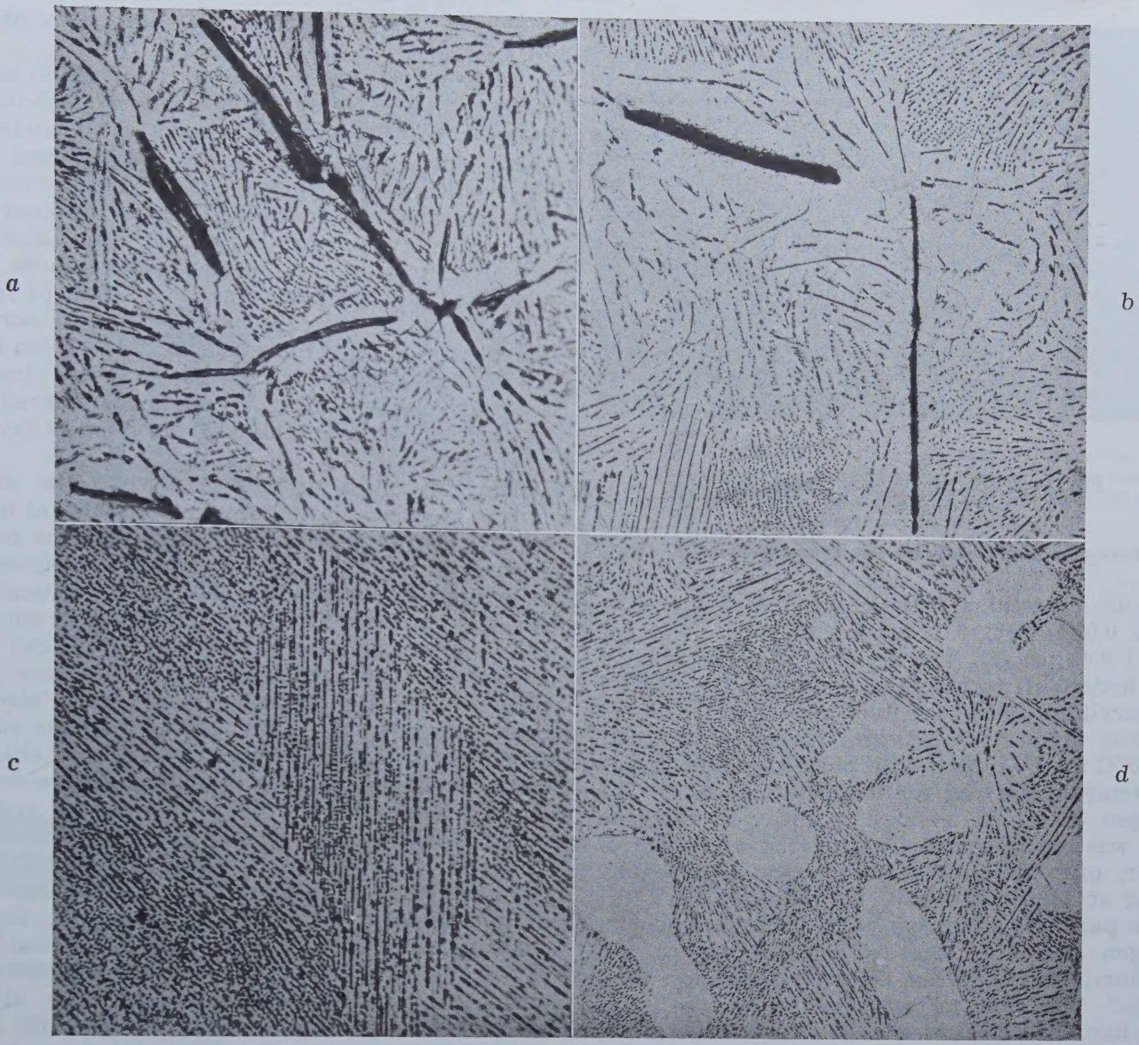

Fig. 1—*a*. **4 pct Zn, 96 pct In, as cast.**
b. **2.2 pct Zn, 97.8 pct In, as cast.**
c. **2.0 pct Zn, 98.0 pct In, as cast.**
d. **1.8 pct An, 98.2 pct In, as cast.**

Etched with Villela's Reagent. X100.

sults, the value reported by Grobe and Rhines seems to be too high in zinc.

References

[1] C. L. Wilson and E. A. Peretti: Zinc-Indium Alloy System. *Ind. Eng. Chem.* (1936) **28**, 204.

[2] S. Valentiner: Uber die Systeme Indium-Zink und Indium-Kadmium. *Ztsch. Metallkunde* (1943) **35**, 250.

[3] F. N. Rhines and A. Grobe: Constitution of the System Indium-Zinc. *Trans.* AIME (1944) **156**, 253.

[4] S. C. Carapella, Jr. and E. A. Peretti: Metallography of Indium and Indium-rich Alloys. *Metals Progress* (1949) **56**, 666.

Slip Markings in Chromium

by Earl S. Greiner

THE hot working of chromium was first reported by Hunter and Jones,[1] who used small pellets of the material obtained by the reduction of chromium chloride with sodium. Later, the working of chromium at 600° to 1100°C was reported by Marden and Rich,[2] and at 1250°C by Kroll.[3] The hot rolled material[3] had a Brinell hardness of about 150 (62.5 kg, 2.5 mm ball, 1 min) and was brittle at room temperature. Except for that associated with hardness indentations, no plastic flow in chromium at room temperature has been reported to the author's knowledge. Studies described here have shown slip markings in chromium after deformation at room temperature.

The specimen was prepared from electrolytic

E. S. GREINER, Member AIME, is Member of Technical Staff, Bell Telephone Laboratories, Inc., New York, N. Y.

TN 39 E. Manuscript received April 6, 1950.

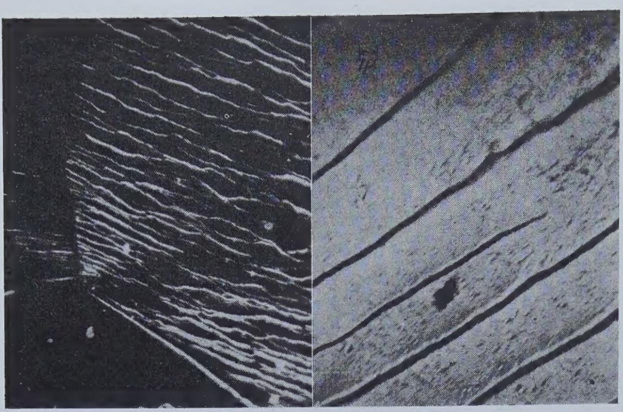

a b

Fig. 1—Slip markings in chromium.
a. Dark field illumination. X800.
b. Electron micrograph. X6000.

Reduced approximately five-eighths in reproduction.

chromium containing 0.04 pct Fe, 0.01 pct C, 0.01 pct Cu, 0.01 pct Pb, 0.02 pct S, 0.02 pct H_2, 0.01 pct N_2, and 0.45 pct O_2. The material was first melted under hydrogen (oxygen-free, and dried at —195°C) in a beryllium oxide crucible and, after solidification, was further treated with hydrogen at 1500° to 1600°C for 1 hr, then with purified helium at the same temperature and for the same duration. The hydrogen contained a small quantity of nitrogen which was not removed. The ingot was crushed to powder, pressed into a compact, and sintered by heating at 1300° to 1400°C in hydrogen for 1 hr, then in purified helium for ½ hr. The treatment in hydrogen decreased the oxygen content of the chromium;[4] that in helium partially decomposed the nitrides.[5] The compact was then compressed between hardened steel blocks, at room temperature, from a thickness of 0.235 to 0.165 in.; annealed alternately in hydrogen and helium at 1300°C; further compressed to a thickness of 0.139 in. and re-annealed in the purified atmospheres at 1300°C. A surface of the specimen was mechanically polished for metallographic examination and the sample then compressed (between steel blocks) from 0.139 to 0.123 in. (11.5 pct reduction) with the polished surface being placed so that it was parallel to the axis of compression.

The slip markings developed on the polished face by compression, as observed at X800 with dark field illumination, are shown in fig. 1*a*. Greater detail is revealed in fig. 1*b*, an electron micrograph (X6000) obtained by the silica replica method.[6] The markings, after elimination by polishing, were not restored by etching.

The wavy markings in fig. 1*a* suggest that more than one slip plane is operative in chromium at room temperature. These planes have not been identified. A multiplicity of slip planes has been observed in alpha iron[7] which has the same structure (body-centered cubic) as chromium.

It is conceivable that the slip markings, fig. 1*b*, are a group of slip lines which were not resolved in the orientation of the silica replica used for this electron micrograph. Slip lines having a separation distance of about 100 atom diameters were observed in aluminum by Heidenreich.[8]

The method of deformation, compression between hardened steel blocks, was probably important in relation to the result obtained. The surfaces of these blocks were smooth but not polished. Thus, the resulting stress system consisted of the compressive stress normal to the surfaces of the steel blocks in contact with the chromium, and also compressive stresses parallel to these surfaces in the vicinity of the contact faces, as a result of friction. The effect is to decrease the tensile stress normal to the shear planes in the region of flow. Even though the critical normal stress for fracture (cohesive strength) in chromium may be low compared to the critical shear stress, this circumstance is favorable to shear flow.

The brittleness of chromium, and the author's failure to effect plastic flow in the material by rolling at room temperature indicate that the resolved normal stress, at this temperature, exceeds the critical value for fracture before the critical shear stress is attained. On the other hand, the successful rolling of chromium at 1250°C by Kroll[3] and by the author at 1300°C suggests that, at these higher temperatures, the critical resolved shear stress has been reduced to a greater extent than the cohesive strength. This might be attributed to a change in operative slip system, or to a temperature-sensitive effect of impurities on the critical normal and shear stresses. The behavior may be analogous to that of alpha iron, for which the ratio of the critical normal stress for fracture to the critical shear stress decreases with decreasing temperature; thus accounting for the low-temperature brittleness.[9]

The results of the present investigation show that chromium can be deformed plastically at room temperature by compression combined with hydrostatic pressure, to reduce the tensile component normal to the slip planes, as has been done with cast bronze, cast iron, marble, and sandstone.[10]

Acknowledgments

The author is indebted to E. E. Thomas for supplying the micrograph and to K. H. Storks for the electron micrograph.

References

[1] M. A. Hunter and A. Jones: *Trans.* Amer. Elec. Soc. (1923) **44**, 23.

[2] J. W. Marden and M. N. Rich: U. S. Pat. No. 1760367 (1930).

[3] W. Kroll: *Ztsch. anorg. allgem. Chem.* (1936) **226**, 23.

[4] C. G. Maier: U. S. Bur. Mines. *Bull.* 436 (1942) 17.

[5] C. G. Maier: *loc. cit.*, 15.

[6] R. D. Heidenreich and V. G. Peck: *Jnl. Appl. Phys.* (1943) **14**, 23.

[7] H. J. Gough: *Proc.* A.S.T.M. (1933) **33, Pt. 2,** 3.

[8] R. D. Heidenreich: Cold Working of Metals. Amer. Soc. Met. (1948) **57**.

[9] E. Maurer and R. Mailänder: *Stahl u. Eisen* (1925) **45**, 409; obtained from C. S. Barrett: Structure of Metals. 322. 1943. New York. McGraw-Hill Book Co.

[10] M. Gensamer: Strength of Metals Under Combined Stresses. Amer. Soc. Met. (1940) 13.

Correction

In the April 1950 issue: TP 2838 C. *Experimental Operation of A Basic-lined Surface-blown Hearth for Steel Production* by C. E. Sims and F. L. Toy. P. 702: The second line of the caption of fig. 4 should read in part, "First slag removed after blowing 2 min." P. 704: The fifteenth line in the first column should read in part, "240 fps as in Heat No. 19, fig. 4."